INSIGHT INTO THE PHYSIOLOGIC IMPACT OF RIGHT-TO-LEFT INTRAPULMONARY AND INTRACARDIAC SHUNT IN HEALTHY HUMANS

by

JONATHAN E. ELLIOTT

A DISSERTATION

Presented to the Department of Human Physiology
and the Graduate School of the University of Oregon
in partial fulfillment of the requirements
for the degree of
Doctor of Philosophy

September 2014

DISSERTATION APPROVAL PAGE

Student: Jonathan E. Elliott

Title: Insight into the Physiologic Impact of Right-to-Left Intrapulmonary and Intracardiac Shunt in Healthy Humans

This dissertation has been accepted and approved in partial fulfillment of the requirements for the Doctor of Philosophy degree in the Department of Human Physiology by:

Dr. Andrew T. Lovering	Chairperson
Dr. John R. Halliwill	Core Member
Dr. Hans Dreyer	Core Member
Dr. Michael K. Stickland	Core Member
Dr. J. Josh Snodgrass	Institutional Representative

and

J. Andrew Berglund	Dean of the Graduate School

Original approval signatures are on file with the University of Oregon Graduate School.

Degree awarded September 2014.

DISSERTATION ABSTRACT

Jonathan E. Elliott

Doctor of Philosophy

Department of Human Physiology

September 2014

Title: Insight into the Physiologic Impact of Right-to-Left Intrapulmonary and Intracardiac Shunt in Healthy Humans

Large diameter intrapulmonary arteriovenous anastomoses (IPAVA) have been known to exist in humans for >60 years, and the prevalence of patent foramen ovale (PFO) is ~35-40% in the general population. However, respiratory physiologists have largely ignored the presence of a PFO and only recently begun to appreciate IPAVA. Reasons some remain critical of IPAVA to be physiologically relevant is due to the relatively undefined role for blood flow through IPAVA to contribute to pulmonary gas exchange efficiency and the unknown and mechanism(s) regulating blood flow through IPAVA.

In Chapter IV the role for blood flow through IPAVA to contribute to pulmonary gas exchange efficiency ($A\text{-}aDO_2$) was investigated using an experimental paradigm minimizing contributions from alveolar ventilation-to-perfusion inequality and diffusion limitation to the $A\text{-}aDO_2$. The increase in blood flow through IPAVA corresponded to an increase in the $A\text{-}aDO_2$ and an increase in total venous admixture of ~2% of the cardiac output. Bronchial shunt was estimated to be ~1%, which suggests blood flow through IPAVA and Thebesian blood flow constitute the remaining ~1% of the cardiac output during intravenous infusion of epinephrine. We originally proposed to quantify blood

flow through IPAVA during the conditions in Chapter IV using radiolabeled macroaggregated albumin; however, ongoing studies demonstrated the need to validate this technique when breathing hyperoxia.

In Chapter V the effect of sildenafil, nifedipine, and acetazolamide on blood flow through IPAVA during exercise breathing room air and 100% O_2 was investigated, and no effect was observed. These pharmacologic interventions act through mechanisms with the potential to prevent or reduce the hyperoxia-mediated reduction in blood flow through IPAVA. Nifedipine and acetazolamide may prevent or limit pulmonary vascular smooth muscle contraction, while sildenafil may augment relaxation of pulmonary vascular smooth muscle.

Lastly, in Chapter VI it was demonstrated that after acclimatization to hypobaric hypoxia in healthy humans, blood flow through IPAVA was reduced, and subjects with a PFO have impaired pulmonary gas exchange efficiency and a reduced degree of ventilatory acclimatization.

This dissertation includes previously unpublished co-authored material.

CURRICULUM VITAE

NAME OF AUTHOR: Jonathan E. Elliott

GRADUATE AND UNDERGRADUATE SCHOOLS ATTENDED:

University of Oregon, Eugene

DEGREES AWARDED:

Doctor of Philosophy, Human Physiology, 2014, University of Oregon
Master of Science, Human Physiology, 2010, University of Oregon
Bachelor of Science, Human Physiology, 2008, University of Oregon

AREAS OF SPECIAL INTEREST:

Intrapulmonary Arteriovenous Anastomoses
Patent Foramen Ovale
Pulmonary Vascular Physiology
Pulmonary Gas Exchange
Exercise Physiology

PROFESSIONAL EXPERIENCE:

Graduate Research Fellow, Department of Human Physiology, University of Oregon, June 2012 – June 2014

Graduate Teaching Fellow, Department of Human Physiology, University of Oregon, September 2008 – June 2012

Certified Personal Trainer, Carpe Diem, 2008 – 2009

Physical Therapy Aide, Out Patient Rehab, Sacred Heart Hospital, 2006 – 2008

Physical Therapy Aide, In Patient Rehab, Sacred Heart Hospital, 2007 – 2008

Certified Personal Trainer, 24hr Fitness, 2004 – 2006

GRANTS, AWARDS, AND HONORS:

Young Investigator Award, Society of Experimental Biology & Medicine, February 2014

Eugene & Clarissa Evonuk Memorial Graduate Fellowship in Environmental Physiology, College of Arts and Sciences, June 2013

Lung Health Dissertation Grant, Funded – returned, American Lung Association, July 2012 – June 2014

Predoctoral Fellowship, Funded – accepted, American Heart Association, July 2012 – June 2014

Clarence and Lucille Dunbar Scholarship, College of Arts and Sciences, University of Oregon, June 2012

Jan Broekhoff Graduate Scholarship, Department of Human Physiology, University of Oregon, June 2012, 2014

PUBLICATIONS:

Lovering AT, Duke JW, Elliott JE. Intrapulmonary arteriovenous anastomoses in humans – regulation by, and response to, exercise and the environment. *J Physiol,* 2014. (In Review)

Duke JW, Elliott JE, Laurie SS, Beasley KM, Yang X, Gust CE, Mangum TS, Gladstone IM. Breathing hypoxic gas during exercise does not excessively widen the alveolar-to-arterial oxygen difference in adults with bronchopulmonary dysplasia. *J Appl Physiol,* 2014. (In Review)

Lovering AT, Elliott JE, Laurie SS, Beasley KM, Yang X, Gust CE, Mangum TS, Gladstone IM. Expiratory flow limitation and dynamic hyperinflation in adult survivors of bronchopulmonary dysplasia. *Annals of ATS,* 2014. (In Review)

Subudhi AW, Bourdillon N, Bucher J, Davis C, Elliott JE, Eutermoster M, Evero O, Fan JL, Jameson-Van Houton S, Julian CG, Kark J, Kark S, Kayser B, Kern JP, Kim S, Lathan C, Laurie SS, Lovering AT, Paterson R, Polaner DM, Ryan BJ, Spira JL, Tsao JW, Wachsmuth NB, Roach RC. AltitudeOmics: The integrative physiology of human acclimatization to hypobaric hypoxia and its retention on reascent. *PLoS One*, e92191, 2013.

Lovering AT, Laurie SS, Elliott JE, Beasley KM, Yang X, Gust CE, Mangum TS, Goodman RD, Hawn JA, Gladstone IM. Normal pulmonary gas exchange

efficiency and absence of exercise-induced arterial hypoxemia in adults with bronchopulmonary dysplasia. *J Appl Physiol,*115:1150-1156, 2013.

Elliott JE, Nigam MS, Laurie SS, Beasley KM, Goodman RD, Hawn JA, Gladstone IM, Chesnutt MS, & Lovering AT. Prevalence of the transpulmonary passage of saline contrast in healthy young humans at rest breathing room air. *Resp Physiol Neuro,* 188: 71-78, 2013.

Laurie SS, Elliott JE, Goodman RD, & Lovering AT. Catecholamine-induced opening of intrapulmonary arteriovenous anastomoses in healthy humans at rest. *J Appl Physiol,* 113: 1213-1222, 2012

Elliott JE, Choi Y, Laurie SS, Yang X, Gladstone IM, & Lovering AT. To the Editor: Reply to "Sonic echocardiography: what does it mean when there are no bubbles in the left ventricle?" *J Appl Physiol,* 110: 296-297, 2011.

Elliott JE, Choi Y, Laurie SS, Yang X, Gladstone IM, & Lovering AT. Effect of initial gas bubble composition on detection of inducible intrapulmonary arteriovenous shunt during exercise in normoxia, hypoxia or hyperoxia. *J Appl Physiol,* 110: 35-45, 2011.

Lovering AT, Elliott JE, Beasley KM, & Laurie SS. Pulmonary pathways and mechanisms regulating transpulmonary shunting into the general circulation: an update. *Injury, Int. J. Care Injured,* 41(S2): S16-S23, 2010.

Laurie SS, Yang X, Elliott JE, Beasley KM, & Lovering AT. Hypoxia-induced intrapulmonary arteriovenous shunting at rest in healthy humans. *J Appl Physiol,* 109: 1072-1079, 2010.

ACKNOWLEDGMENTS

The road to this point in time has neither been smooth nor easy, but it has been an incredible journey that has truly transformed myself, not only as a scientist, but as a person. Although there are many people deserving of recognition, I owe a particularly significant *thank you* to my advisor, mentor, and friend, Dr. Andrew Lovering. Without his guidance, mentorship, and belief in me, I would not be where I am today. I would like to express my sincere appreciation to Dr. John Halliwill and Dr. Hans Dreyer, who have been integral to my dissertation and have been indispensible mentors over the years. The final two members of my dissertation, Dr. Michael Stickland and Dr. Josh Snodgrass have also been valuable resources and incredibly helpful. In addition to my dissertation committee, I would like to express my sincere appreciation to Dr. Robert Roach for his continued mentorship, guidance and support.

I owe a huge thank you to Dr. Steve Laurie who has been a tremendous resource and source of support throughout my graduate education, and to Dr. JJ Duke for his support and guidance, especially in navigating the world of statistics. I would also like to thank Dr. Igor Gladstone who has truly been an inspiration over the years and has taught me many valuable life lessons. Dr. Jerold Hawn, has been an integral part of my dissertation and member of the Cardiopulmonary and Respiratory Physiology Lab. Additionally, Randall Goodman and Eben Futral, who have not only provided unparalleled ultrasonography expertise but have been wonderful friends. Of course, I owe an enormous thank you to the entire Human Physiology Department, and particularly to my fellow graduate students, especially Kara Beasley, Steven Romero, Vienna Brunt, Austin Hocker and Christopher Banek.

Finally, I would like to communicate a very special thank you to my mother Polly Shannon, brother Matt Elliott, and sister Hanna Elliott. All of you have always been there for me, providing unconditional love and support, and have had complete faith in everything that I do. I love you all, and will also, always be there for you.

TABLE OF CONTENTS

Chapter Page

I. INTRODUCTION 1
Historical Perspective 4
Background and Significance 12
Pulmonary Gas Exchange Efficiency 12
Regulation of Blood Flow Through IPAVA: Hyperoxia 16
Pulmonary Gas Exchange Efficiency After Acclimatization to Hypobaric Hypoxia in Subjects With and Without a Patent Foramen Ovale 18
Statement of Problem 21
Purpose and Hypotheses 21
Aim #1: Determine Whether or Not Blood Flow Through Intrapulmonary Arteriovenous Anastomoses Contributes to Pulmonary Gas Exchange Efficiency 22
Aim #2: Determine the Effect of Sildenafil, Nifedipine, and Acetazolamide on Blood Flow Through Intrapulmonary Arteriovenous Anastomoses During Exercise Breathing 100% O_2 23
Aim #3: Characterize Pulmonary Gas Exchange Efficiency in Healthy Humans With and Without a Patent Foramen Ovale in Acute and After Acclimatization to Hypobaric Hypoxia 24

II. REVIEW OF THE LITERATURE 26
Introduction 26
Patent Foramen Ovale 26
Intrapulmonary Arteriovenous Anastomoses 32
Pulmonary Gas Exchange 36
Pulmonary Diffusion 38
Alveolar Ventilation-to-Perfusion 42
Right-to-Left Shunt 47
Classical Paradigm 50
Pulmonary Gas Exchange During Exercise at Sea Level 51
Pulmonary Gas Exchange During Exercise in Acute Hypoxia 56
Pulmonary Gas Exchange After Acclimatization to Hypobaric Hypoxia 58
Regulation of Blood Flow Through Intrapulmonary Arteriovenous Anastomoses 60
Exercise 61
Normobaric Hypoxia 63
Hypobaric Hypoxia 64
Alveolar Hyperoxia 65

Chapter Page

III. METHODS 69
Informed Consent 69
Echocardiographic Screening 69
Detection of Patent Foramen Ovale 70
Pulmonary Artery Systolic Pressure 73
Left Ventricular Outflow Tract 74
Lung Function Testing 75
Forced Vital Capacity 75
Slow Vital Capacity 77
Whole-Body Plethysmography 77
Diffusion Capacity for Carbon Monoxide 79
Subject Instrumentation 80
Intravenous Catheterization 80
Arterial Catheterization 81
Measures of Core Body Temperature 83
Peripheral Oxygen Saturation and Heart Rate 84
12-Lead Echocardiogram 85
Echocardiography Measurements 86
Transthoracic Saline Contrast Echocardiography 86
Pulmonary Artery Systolic Pressure 87
Cardiac Output 87
Open Circuit Acetylene Uptake 88
Delivery of Inspired Gas Mixtures 89
Measurement of Arterial Blood Gases 90
Arterial Blood Draw and Analysis 90
Tonometry 92
AltitudeOmics 93
Subject Recruitment and Screening 93
Timeline 94

IV. INCREASED CARDIAC OUTPUT, NOT PULMONARY ARTERY SYSTOLIC PRESSURE, INCREASES INTRAPULMONARY SHUNT IN HUMANS BREATHING ROOM AIR AND 40% O_2 97
Introduction 97
Methods 100
Subjects 101
Instrumentation 101
Protocol 102
Measurements 104
Calculations 106
Statistical Analyses 108
Results 108

Chapter Page

Transpulmonary Passage of Saline Contrast and Pulmonary Gas Exchange Efficiency 109
Cardiac Output and Pulmonary Artery Systolic Pressure 114
Discussion 114
Experimental Design 115
Pulmonary Gas Exchange Efficiency During the I.V. Infusion of Epinephrine 118
Reconciling Anatomic and Gas Exchange Dependent Data 122
Cardiac Output and Pulmonary Artery Systolic Pressure 123
Limitations 124
Summary 127

V. PHARMACOLOGIC INVESTIGATIONS INTO THE MECHANISTIC REGULATION OF INTRAPULMONARY ARTERIOVENOUS ANASTOMSES 130
Introduction 130
Methods 132
Subjects 133
Protocol 133
Detection of Blood Flow Through Intrapulmonary Arteriovenous Anastomoses 134
Respiratory Variables 134
Cardiac Output and Pulmonary Artery Systolic Pressure 135
Statistics 135
Results 136
Subject Characterization and Pulmonary Function 136
Hemodynamic and Ventilatory Effects of Pharmacologic Interventions 137
Transpulmonary Passage of Saline Contrast 140
Discussion 142
Sildenafil 143
Nifedipine 144
Acetazolamide 145
Limitations 146
Conclusions 147

VI. ALTITUDEOMICS: IMPAIRED PULMONARY GAS EXCHANGE EFFICIENCY AND VENTILATORY ACCLIMATIZATION AFTER 16 DAYS AT 5260M IN HUMANS WITH PATENT FORAMEN OVALE 149
Introduction 149
Methods 151
Subject Recruitment and Screening 152
Spirometry, Diffusion Capacity, and Lung Volumes 152

Chapter Page

Echocardiographic Screening 152
Acute Normobaric Hypoxia 154
Timeline 155
Subject Instrumentation and Exercise Protocol 155
Pulmonary Artery Systolic Pressure and Cardiac Output 156
Arterial Blood Gases, Body Temperature and Blood Lactate....156
Calculations....157
Statistical Analyses 158
Results.... 159
Overview....159
Anthropometric, Exercise, Hematologic, and Pulmonary Function Data....163
Sea Level (SL) 163
Acute Ascent to 5260m (ALT1) 166
Acclimatization to 5260m (ALT16) 168
Discussion.... 171
Pulmonary Gas Exchange Efficiency in PFO− and PFO+ Subjects at SL 171
Pulmonary Gas Exchange Efficiency in PFO− and PFO+ Subjects at ALT1 173
Pulmonary Gas Exchange Efficiency and Ventilatory Acclimatization in PFO− and PFO+ Subjects at ALT16 174
Acclimatization and Left-Sided Contrast in PFO− and PFO+ Subjects....179
Summary 181

VII. CONCLUSIONS 183
Main Findings.... 183
Summary and Future Directions.... 184

REFERENCES CITED.... 191

LIST OF FIGURES

Figure Page

3.1. AltitudeOmics Overview Timeline 95

4.1. Protocol Schematic 104

4.2. Bubble Scores and Pulmonary Gas Exchange Efficiency 113

4.3. Cardiac Output and Pulmonary Artery Systolic Pressure 115

5.1. Bubble Scores During Exercise Breathing Room Air and 40% O_2 141

6.1. Pulmonary Gas Exchange and Arterial Blood Gases 165

6.2. Effect of PFO Size on Pulmonary Gas Exchange Efficiency 165

6.3. Bubble Scores at Rest Breathing Room Air and 14% O_2 166

6.4. Bubble Scores at Rest and During Exercise 167

6.5. Ventilatory Acclimatization 168

6.6. Calculated Change in Venous Admixture 169

6.7. Pulmonary Gas Exchange Efficiency, Group 178

LIST OF TABLES

Table Page

4.1. Anthropometric and Pulmonary Function Data 109

4.2. Cardiopulmonary and Respiratory Data Breathing Room Air, During the I.V. Infusion of EPI With and Without Atropine 110

4.3. Cardiopulmonary and Respiratory Data Breathing 40% O_2, During the I.V. Infusion of EPI With and Without Atropine 111

4.4. Difference in $\dot{Q}_{VA}/\dot{Q}_T$ With I.V. EPI and During Conditions of Iso-Alveolar Ventilation Without I.V. EPI 122

5.1. Anthropometric and Pulmonary Function Data 136

5.2. Hemodynamic and Ventalitory Data During Exercise Beathing Room Air 138

5.3. Hemodynamic and Ventalitory Data During Exercise Beathing 100% O_2 139

6.1. Anthropometric, Exercise, Hematologic and Pulmonary Function Data 160

6.2. Cardiopulmonary and Arterial Blood Gas Data at Rest in the PFO− and PFO+ Groups at Sea level (SL), Acute Hypoxia (ALT1) and After Acclimatization to High-Altitude (ALT16) 161

6.3. Cardiopulmonary and Arterial Blood Gas Data During Exercise in the PFO− and PFO+ Groups at Sea level (SL), Acute Hypoxia (ALT1) and After Acclimatization to High-Altitude (ALT16) 162

LIST OF EQUATIONS

Equation Page

2.1. Alveolar Ventilation 36

2.2. Conversion Factor, *K* 37

2.3. Alveolar Gas Equation 37

2.4. Fick's First Law of Diffusion 38

2.5. Roughton-Forster Equation 39

2.6. Rate of Rise in Pulmonary Capillary PO_2 40

2.7. Oxygen Content Equation 40

2.8. Hill Equation 41

2.9. $\dot{V}_A/\dot{Q}$ Ratio for O_2 42

2.10. $\dot{V}_A/\dot{Q}$ Ratio for CO_2 42

2.11. Retention/Excretion of Inert Gas 43

2.12. Bohr Dead Space Equation 47

2.13. Berggren Shunt Equation 48

2.14. Modified Bernoulli Equation 74

2.15. Boyles Law 78

CHAPTER I

INTRODUCTION

The primary function of the lung is to facilitate movement of oxygen into the body and remove carbon dioxide out of the body, a critical process that is collectively referred to as pulmonary gas exchange. A second, less appreciated, function of the lung is to filter the incoming venous blood and prevent thrombi from reaching the arterial circulation and manifesting as emboli. Obligatory to efficiently performing both of these tasks is directing blood flow through the pulmonary capillary network. However, large diameter (15-750 μm) intrapulmonary arteriovenous anastomoses (IPAVA), which have been known to exist in healthy human lungs for over 60 years, offer a vascular conduit for blood flow to bypass the pulmonary capillary network (171, 188, 225, 228, 262). Thus, by acting as a collateral pathway, blood flow through these pathways could theoretically compromise both functions of the lung; impairing pulmonary gas exchange efficiency as a right-to-left shunt as well as providing thrombi a pathway to circumvent the pulmonary capillary filter.

Despite the anatomic data demonstrating the existence of IPAVA, respiratory physiology and medicine have only recently begun to appreciate these vessels and their potential clinical impact. One reason some remain critical of IPAVA to be physiologically or pathophysiologically relevant, is due to the relatively undefined role that blood flow through IPAVA has in contributing to pulmonary gas exchange efficiency and some types of stroke (2). Secondarily, the mechanisms regulating blood flow through IPAVA remain unclear. Currently little is known other than conditions that increase blood flow through IPAVA (i.e., during exercise, in acute normobaric hypoxia, and

during the intravenous infusion of catecholamines), and conditions that decrease blood flow through IPAVA (i.e., with alveolar hyperoxia). Accordingly, the overarching purpose of this dissertation is to establish the role that blood flow through IPAVA has on pulmonary gas exchange efficiency and to begin to investigate the potential mechanistic regulation of these vessels; thereby helping to define the physiologic relevance of IPAVA in healthy humans.

In addition to blood flow through IPAVA, the presence of a functionally patent foramen ovale (PFO) also provides a 'collateral pathway', albeit one that is much more direct, which impairs both the filtering ability of the lung and pulmonary gas exchange efficiency. As a requisite right-to-left shunt in the fetal cardiopulmonary circulation, the foramen ovale is patent in 100% of healthy humans in utero. After birth, the reversal of pressure gradients between the right and left atria result in the septum primum covering, and therefore functionally closing, the foramen ovale within the septum secundum (71, 82, 118). Over time, fusion of the septum primum/secundum occurs in the majority of infants (i.e., permanent anatomical closure of the foramen ovale) preventing blood flow through the foramen ovale. However, recent work using transthoracic saline contrast echocardiography (TTSCE) has revealed ~35-40% of adult humans continue to have a PFO (55, 156, 266). Although right-to-left blood flow through a PFO would be expected to be intermittent and variable in volume (64), recent work by Lovering *et al.* has shown that subjects with a PFO can have significantly worse pulmonary gas exchange efficiency at rest breathing either room air or in acute normobaric hypoxia (12% O_2) (145). Thus, not only is the prevalence of PFO in the general population more common than previously reported (~25-35%) from prior autopsy studies (82), these subjects possess an

additional source of right-to-left shunt resulting in a measureable decrement in pulmonary gas exchange efficiency determined via arterial blood gas analysis, compared to subjects without a PFO. Remarkably, past work that has set the foundation for our current understanding of pulmonary gas exchange efficiency has presumably been carried out in subjects with and without a PFO. Included in this prior work, is work that was designed to understand human acclimatization to high-altitude. Accordingly, it remains unknown how our current understanding of pulmonary gas exchange, either at sea level or high-altitude, may differ when taking into consideration the presence of a PFO.

The first objective addressed in Chapter IV, was to demonstrate that blood flow through IPAVA participated relevantly in pulmonary gas exchange and contributes to the efficiency of this process in healthy humans. We had originally proposed to quantify blood flow through IPAVA during the conditions in Chapter IV using radiolabeled macroaggregated albumin; however, ongoing studies demonstrated the need to validate this technique when breathing hyperoxia. The second objective, addressed in Chapter V, was to investigate the impact of several pharmacologic interventions targeting blood flow through IPAVA during exercise breathing 100% O_2 and provide potential insight into the mechanistic regulation of these vessels. The third objective, addressed in Chapter VI was two fold; A) to characterize human acclimatization to high-altitude (i.e., after acclimatization to 5260m) in healthy humans with and without a PFO, with pulmonary gas exchange as a key element, and B) to explore the long-term regulation of blood flow through IPAVA after acclimatization after acclimatization to high-altitude.

HISTORICAL PERSPECTIVE

The historical perspective provided herein is based largely off of two comprehensive historical reviews, provided by Dr. Andrew Lumb (149) and Dr. John West (254). Respiratory physiology has a unique and particularly colorful history in the context of pulmonary gas exchange that is also, as alluded to earlier, intimately linked to high-altitude physiology. Atmospheric pressure provides the driving pressure that ultimately determines the inspired PO_2, which in part regulates alveolar PO_2 (PAO_2) and consequently arterial PO_2 (PaO_2); hence, pulmonary gas exchange. Establishing that barometric pressure provides this driving pressure and that it decreases with increasing altitude represented a key advance in respiratory physiology. Evangelista Torricelli is credited with inventing the mercury barometer in 1644, remarking, that, *"We live submerged at the bottom of an ocean of the element air, which by unquestioned experiments is known to have weight…"* Although speculated by Torricelli, experimental evidence that barometric pressure falls with increasing altitude was provided by Blaise Pascal in 1648, however it would be another 200 years before the significance of this finding was realized.

Progress in respiratory physiology slowed during the mid 1700's until the profound scientific breakthrough of the characterization of respiratory gases. However, leading up to this point there had been several similar, yet unique hypotheses describing air. As far back as 570 BC early Greek philosophers, including Hippocrates and Anaximenes recognized that air, or 'pneuma' as it was referred to at the time, was essential to life. Erasistratus believed that air was taken up by the lung and converted into a 'vital-spirit' within the heart. Interestingly, this vital spirit was also thought to be

further converted into 'animal spirit' in the brain that was transmitted via the nervous system to muscles. Much of this early speculation was investigated by Claudius Galen in the 2nd and 3rd century. He too shared Erasistratus's belief that pneuma was instilled in the blood within the lung and was converted to vital spirit in the heart; however, Galen also proposed that some blood passed through invisible pores within the interventricular septum of the heart, an idea that would persist for another 1400 years. Challenging Galen's theory of invisible interventricular pores was first done by the prolific Arabic scientist, Ibn Al Nafis in the 13th century (258), later by Servetus in the 16th century (who's work was deemed heretical by the Catholic church, and with it he was burned at the stake), and shortly thereafter again by Realdus Colombo. In the 17th century several Oxford physiologists, namely Robert Boyle, Robert Hooke, Richard Lower and John Mayow, made major contributions to respiratory physiology. Together they demonstrated, by pumping air out of a closed container, that flames were extinguished and animals perished, confirming the presence of a vital component present in air. Mayow later described the vital component of air as 'nitro-aerial spirit' in 1674. Although air was still recognized as "vital", the theory of phlogiston was put forth by George Ernst Stah. Phlogiston was thought to be released during the process of combustion and therefore was not sustainable for life. In contrast, 'dephlogisticated air' was sustainable for life and was identified as such by Joseph Priestly in the late 18th century. His work involved burning mercuric oxide and noting that candles burned with *"a remarkably vigorous flame"* in this 'pure air' and that mice could respire and live much longer than in 'common air'. Of course, mercuric oxide has the chemical composition HgO, which releases oxygen on combustion, although Priestly was unaware

of this at the time. Shortly thereafter, Carl Scheel also inadvertently produced oxygen in his experiments and drew similar conclusions as Priestly, although rather than dephlogisticated air, Scheel refered to it as 'fire air'. Finally, it was Antoine-Laurent Lavoisier, a French scientist who in 1777 discovered that 'eminently respirable air' was not a pneuma, a vital spirit, a nitro-aerial spirit, dephlogisticated air, pure air, or fire air, but was actually a chemical element, namely oxygen. In fact Lavoisier actually described all three respiratory gases (although carbon dioxide was discovered earlier by Joseph Black) described in a passage of his work: *"Eminently respirable air (oxygen) that enters the lung, leaves it in the form of chalky aeriform acids (carbon dioxide) in almost equal volume…Respiration acts only on the portion that is eminently respirable…the excess, that is its mephitic portion (nitrogen), is a purely passive medium which enters and leaves the lung…without change or alteration. The respirable portion of air has the property to combine with blood and its combination results in its red color."*

Around this same time with the advent of man-carrying balloons either by hot air or helium, the ill effects of high-altitude and the 'effects of (low) air pressure' were being explored. These balloonists were enticed with the desire to ascend higher and higher, reaching altitudes in excess of 10,000m although, not surprisingly, they would often return partially paralyzed, unconscious, or even dead. Less extreme and rapid of high-altitude ascents have taken the form of mountaineering with many accounts in the 19th century on the deleterious effects of high-altitude and the imminent development of mountain sickness, physical weakness, and of course breathlessness. However, it was the French environmental physiologist Paul Bert who effectively married the two fields of respiratory physiology and high-altitude physiology. Not surprisingly, Bert is also known

as the father of modern high-altitude physiology, with his landmark contribution *La Pression Barométric* published in 1878 (17). It was Bert who elucidated the deleterious effects of high-altitude (low pressure) being attributable to reduced PO_2. In fact, prior to a tragic balloonist ascent, Bert sent caution by way of a letter to the balloonist team when he learned they had planned for too little supplemental oxygen. Unfortunately, the letter arrived too late.

By this time it was clear oxygen was not only necessary for life but it was metabolically 'consumed'. John Dalton published his law of partial pressures in the early 19^{th} century (43), and later that century additional traction was gained describing the presence of oxygen and carbon dioxide in the blood. Much of this work was spearheaded by German chemists; Gustav Magnus demonstrated that oxygen and carbon dioxide was present in arterial and venous blood but oxygen was most abundant in arterial blood, while Lothar Meyer demonstrated that oxygen was not *only* dissolved in blood by way of its non-linear extraction profile. Hemoglobin was soon identified as the compound in blood that gave it is characteristic red color, and Hüfner characterized the affinity for hemoglobin with oxygen showing that 1.34 ml of oxygen can bind to 1 g of hemoglobin. Hüfner used crystallized hemoglobin and showed that the relationship between the prevailing PO_2 and hemoglobin saturation was a rectangular hyperbola. Credit to the first description that the so called 'oxygen-hemoglobin dissociation curve' was sigmoidal and not rectangular, is to the Danish physiologist, Christian Bohr, due to his experimental approach resembling that of Hüfners except rather than using crystallized hemoglobin, Bohr used whole human blood (21).

In the 20th century expeditions to high-altitude were becoming increasingly popular (257), not only from personal intrigue but for medical and physiological research, often centering on respiratory physiology as the measurement of the partial pressure of oxygen in arterial blood had become possible. One of the first expeditions was led by Nathan Zuntz with Joseph Barcroft and C. Gordon Douglas in 1906. Data collected on this expedition indicated that in one subject exercising, his $\dot{V}O_2$ was 1.52 L/min, while his PAO_2 was 57 mm Hg. Bohr had recently described a numerical procedure to calculate the change in PO_2 throughout the time course along the pulmonary capillary, and using these data from Zuntz he calculated PaO_2 to exceed PAO_2. Based on his fundamental algorithm now known as the 'Bohr Integration', and these data from Zuntz, Bohr's interpretation was that the lungs may actively secrete oxygen (23). John Haldane, was a prominent respiratory physiologist who rigorously investigated the oxygen secretion theory using his own methodological approach. This involved taking three small blood samples from the subject, 1) under the experimental conditions, 2) after breathing a small percentage of carbon monoxide, and 3) one that was saturated with carbon monoxide using coal-gas. To the 2nd blood sample, a standard solution of carmine was added in 0.5-1.0 ml increments until the 'pink hue' matched the 1st vial, the volume was recorded and the addition of carmine continued until the hue matched the 3rd vial, and again the volume was recorded. Then, the ratio of the volume of carmine required to match the hue of the 2nd vial to the 1st vial compared the total volume (carmine + blood sample), was divided by the ratio of the final volume of carmine necessary for the hue to match the 3rd vial compared to the final total volume of blood/carmine (83, 84). Clearly there was a very subjective component to this method, and that is qualitatively comparing the pink hues in

each vial. Furthermore, a correction factor had to be employed because when the carmine-blood samples were exposed to daylight, the color was diminished or very difficult to distinguish compared to analyzing the sample in a dark setting. Through these experiments the average PaO_2 was determined by Haldane to be ~200 mm Hg, notably higher than even the inspired PO_2 at sea level (~150 mm Hg), and therefore Haldane became a strong supporter of Bohr's oxygen secretion theory.

Together Bohr and Haldane championed the oxygen secretion theory until a Danish couple, August and Marie Krogh investigated the matter further, as described in the historical account offered by Albert Gjedde (74). August Krogh was a pupil a Bohr's, and by way of inventing a microtonometer, determined that PaO_2 measured in a rabbit was always lower than PAO_2 (121). The publication of this initial report was intentionally delayed by Krogh in an attempt to resolve the controversy privately first, however, for uncertain reasons Bohr was unwavering. Subsequently, the Kroghs published six additional papers, all in series, that centered around dismantling the oxygen secretion theory. The second paper in this installment ruled out the possibility that oxygen may be being converted to carbon dioxide, and thus impacting the PO_2 measurement (123). The third paper investigated the possibility that the vagus nerve was capable of actually secreting gas, which Krogh disproved using turtles showing that severing the vagus nerve reduced gas exchange by way of increases in flow rather than inhibiting oxygen secretion (124). The fourth paper (125) showed that oxygen tensions cannot be accurately calculated using the carbon monoxide approach of Haldane and Douglas (52, 84). The fifth paper in this series demonstrated that the solubility of oxygen was much greater than that measured by Bohr (126). The sixth paper provided evidence that Bohr's previous

calculations of diffusion coefficients with the help from Haldane were erroneously low and based on arbitrary assumptions (122). Finally the seventh paper in this series summarized the main findings from the prior six publications (127). Collectively these manuscripts refuted the oxygen secretion theory and instead paved the way for the 'passive diffusion' theory and, although Bohr was perhaps more relenting to his prior hypothesis, he passed away at his desk in 1911, while Haldane was steadfastly committed until his death in 1936.

The following year, 1911, after publication of the 7 part series from the Kroghs, an important high-altitude expedition took place on the summit of Pikes Peak in Colorado at 4300m. The expedition was led by Haldane and published by Douglas (51), which reports many influential observations, including the hyperventilation following ascent, periodic breathing during sleep, and polycythemia accompanying acclimatization. Interestingly the oxygen secretion hypothesis was revisited during this expedition, not surprisingly considering whom the leader of the expedition was. It was reported that Douglas achieved a $\dot{V}O_2$ during exercise of 2.195 L/min and had an PAO_2 of ~60 mm Hg, and an PaO_2 that was again measured erroneously to be above PAO_2. The authors then used Krogh's own calculations of the diffusion capacity of the lung, determined to be ~38 ml/min/mm Hg, to determine that the gradient between alveolar PO_2 and that in the mixed venous blood would need to be 58 mm Hg if the diffusion theory were true. Of course this meant the $P\bar{v}O_2$ was only 2 mm Hg, and unlikely to be physiologically possible. Approximately 2 years later Marie Krogh refuted these calculations by determining that the diffusing capacity of the lung increased with exercise by as much as 20-40% (128). Thus, the diffusing capacity of the lung in Douglas was likely greater than

~38 ml/min/mm Hg, which allowed for a more reasonable PO_2 gradient and cardiac output ($\dot{Q}_T$), that was likely possible by way of passive diffusion and therefore without oxygen secretion.

Concluding the historical context surrounding the feud between the Kroghs pushing the diffusion theory and Bohr and Haldane pushing the oxygen secretion theory, are data obtained in 1923 by another classical high-altitude expedition to Cerro de Pasco, Peru by Joseph Barcroft (7). Barcroft noted that the measured PaO_2 was always lower than the calculated value for PAO_2. Although Haldane would not let go the oxygen secretion theory, it is fitting that the final report providing evidence against this pervasive theory in the history of respiratory physiology came from a high-altitude expedition. The next major advancement in respiratory physiology pertaining to pulmonary gas exchange surrounded the matching between alveolar ventilation and pulmonary blood flow. Much of this work stemmed from World War II and was initially founded by Wallace Fenn, Hermann Rahn, and Arthur Otis (259). Compared to the historical context surrounding diffusion, that of alveolar ventilation-to-perfusion matching is quite dull. However it is no less important, and will be expanded upon in Chapter II. Intermingled in this era is another substantial body of work, that pertaining to arteriovenous connections existing in multiple vascular beds, including the lungs. This work would later become the foundation for that which we now know represents intrapulmonary arteriovenous anastomoses (IPAVA). Again, the historical context of work surrounding the description of IPAVA is not exactly colorful, but fundamental to this dissertation and will also be expanded upon in Chapter II.

Collectively, this historical perspective is intended to provide an initial starting point describing the turbulent and exciting history of respiratory physiology. Particularly the fascinating origins of how we have come to understand the importance of the air we breathe and the remarkable link between respiratory physiology and high-altitude physiology. Lastly, the controversy surrounding the oxygen secretion vs. diffusion theories was expanded upon to illustrate that, as is common in science, theories are only theories until proven wrong. Secondarily, methodological limitations such as those experienced by Haldane in measuring PaO_2 represented the crux of some of these issues. As will be described, some potential interesting parallels may be drawn from this historical review and the current state of our working knowledge of pulmonary gas exchange.

BACKGROUND AND SIGNIFICANCE

Pulmonary Gas Exchange Efficiency

Although the lung serves multiple important functions, a major role is to exchange gases between the atmosphere and blood. Pulmonary gas exchange is a deceptively complex process, that is dependent upon many factors, including the diffusion capacity of the blood-gas barrier (Dm), pulmonary capillary blood volume (Vc), pulmonary blood flow, the gradient between alveolar (PAO_2) and mixed venous PO_2 ($P\bar{v}O_2$) the non-linear O_2 dissociation curve that is also impacted by body temperature, acid-base status, and PCO_2, the rate at which O_2 combines with hemoglobin that is also non-linear and is a function of the prevailing O_2 saturation (θ), and the fact that O_2 is also transported dissolved in the plasma. The efficiency of this process is ultimately defined

by the difference between PAO_2 and arterial PO_2 (PaO_2), termed the alveolar-to-arterial PO_2 difference (A-aDO_2). An A-aDO_2 of 0 mm Hg reflects perfect pulmonary gas exchange, while impairments in this process manifest as an A-aDO_2 >0 mm Hg. Three factors can theoretically contribute to impairments in pulmonary gas exchange efficiency; alveolar ventilation-to-perfusion ($\dot{V}_A/\dot{Q}$) inequality, incomplete equilibration between end-capillary PO_2 ($Pc'O_2$) and PAO_2 (diffusion limitation), and right-to-left shunt. The normal mammalian lung at rest is remarkably efficient at exchanging gases between the alveolar air and capillary blood, because all of these factors are not problematic at rest. However, during conditions that challenge the lungs ability to exchange gases (i.e., during exercise or breathing hypoxic gas mixtures), the efficiency of this process decreases. Thus, the matching between alveolar ventilation ($\dot{V}_A$) and pulmonary blood flow may deteriorate, pulmonary capillary transit time may decrease and be insufficient for complete O_2 equilibration, and the contribution of right-to-left shunt may increase due to the reduction in $P\bar{v}O_2$.

Over the last century, considerable work has been done to investigate the relative contribution that each of the three aforementioned factors has in explaining the measured A-aDO_2 at rest and during exercise at sea level and high-altitude. Although technically very challenging, several techniques have been developed to partition the contribution of these factors apart and much of our current understanding of pulmonary gas exchange efficiency has come from this work. The multiple inert gas elimination technique (MIGET) was developed to quantify $\dot{V}_A/\dot{Q}$ inequality based on the retention and excretion of 6 inert gases of varying solubility (236). In theory, the MIGET can also quantify the contribution of intrapulmonary right-to-left shunt due to the fact that blood

flow through an intrapulmonary right-to-left shunt represents a $\dot{V}_A/\dot{Q}$ ratio of 0. Thus, any portion of the A-aDO_2 not explained by $\dot{V}_A/\dot{Q}$ inequality and intrapulmonary right-to-left shunt determined using the MIGET is attributed to the effects of diffusion limitation and postpulmonary right-to-left shunt via the bronchial and Thebesian circulations (229). With a quantification of $\dot{V}_A/\dot{Q}$ inequality and intrapulmonary shunt using the MIGET, partitioning the remainder of the A-aDO_2 between diffusion limitation and postpulmonary shunt can be done using the 100% O_2 technique (196). The 100% O_2 technique is based on the principle that with the removal of alveolar N_2, as occurs when breathing a fraction of inspired O_2 (FIO_2) = 1.0, the PAO_2 in all lung units must increase to that of the inspired PO_2 less alveolar PCO_2 ($PACO_2$). There is then little discrepancy in PAO_2 between lung units, regardless of their respective V_A/Q ratios, and how poorly ventilated they may be. Furthermore, when breathing a FIO_2 = 1.0, $P\bar{v}O_2$ is only marginally increased (to ~50 mm Hg) compared to breathing room air at sea level and therefore, not only is the driving gradient between PAO_2 and $P\bar{v}O_2$ maximally increased, but the slope of the O_2 dissociation curve between those points reduced. It follows then that when breathing a FIO_2 = 1.0 $\dot{V}_A/\dot{Q}$ inequality and diffusion limitation are eliminated as potential contributing factors to the A-aDO_2, leaving only right-to-left shunt. In combination, the MIGET and 100% O_2 technique then theoretically allow for the quantification and separation between $\dot{V}_A/\dot{Q}$ inequality (from the MIGET), all sources of right-to-left shunt (from the 100% O_2 technique), and diffusion limitation (from the remainder of the A-aDO_2 not explained by $\dot{V}_A/\dot{Q}$ inequality and right-to-left shunt). Furthermore, by subtracting intrapulmonary right-to-left shunt (from the MIGET) from

all sources of right-to-left shunt (from the 100% O_2 technique), the contribution of postpulmonary right-to-left shunt can be obtained.

Of course, the above partitioning assumes these gas exchange dependent techniques are accurately measuring each factor; specifically, the contribution of right-to-left shunt from the MIGET and 100% O_2 technique. Non-capillary gas exchange has been documented in humans (108, 109, 209) and cats (40) and therefore may result in an underestimation of intrapulmonary right-to-left shunt using the MIGET. Breathing a FIO_2 = 1.0 during exercise has been shown to prevent or reduce blood flow through IPAVA detected using saline contrast echocardiography (54, 144), and therefore right-to-left shunt measured during exercise breathing a FIO_2 = 1.0 would not include contributions from blood flow through IPAVA. Interestingly, the classical understanding of pulmonary gas exchange efficiency described by data obtained using the MIGET and 100% O_2 technique emphasizes the relative importance of $\dot{V}_A/\dot{Q}$ inequality and diffusion limitation while suggesting a minimal contribution of right-to-left shunt from all sources.

The idea that blood flow through IPAVA contributes relevantly to pulmonary gas exchange efficiency as a source of right-to-left shunt (24, 143, 216) is not supported by prior work using the MIGET or 100% O_2 technique. Pooling data from several studies using the MIGET (101, 112, 175, 185, 195), intrapulmonary shunt averages 0.2 ± 0.7% of the $\dot{Q}_T$ during exercise ($\dot{V}O_2$ = 3.7 ± 0.7 L/min) breathing room air at sea level. Work by Vogiatzis *et al*. (233) reports right-to-left shunt measured during exercise in subjects breathing a FIO_2 = 1.0 to average 0.5 ± 0.5% of the $\dot{Q}_T$. In contrast to these data obtained using the MIGET and 100% O_2 technique, data obtained using solid microspheres and radiolabeled macroaggregates of albumin (MAA) reports appreciably higher values of

intrapulmonary right-to-left shunt. Intravenously injected 25 and 50 μm microspheres in exercising dogs confirms that blood flow through IPAVA does occur during exercise and was calculated to be 1.4% (range 0.2 to 3.1 %) of the $\dot{Q}_T$ (215). Studies in healthy humans using Technetium 99m-labelled MAA (^{99m}Tc-MAA) and gamma camera imaging measured blood flow through IPAVA to be 1.3% (range −0.3 to 2.7%) of the $\dot{Q}_T$ during maximal exercise (141). These studies used MAA with a mean diameter of 20–40 μm and 90% of MAA between 10 and 90 μm in size. Work prior to this used ^{99m}Tc albumin microspheres with a size range of 7-25 um in diameter and an increase in shunt of 2.4% of the $\dot{Q}_T$ was reported in 5 normal subjects during exercise, with a range of -2.4 to 5.9% (261).

Accordingly, there appears to be a discrepancy between intrapulmonary shunt measured using the MIGET and right-to-left shunt measured using the 100% O_2 technique compared to blood flow through IPAVA determined using large diameter ^{99m}Tc-MAA and solid microspheres. As previously mentioned this discrepancy is not without precedence (72, 245). All prior work investigating the potential contribution of blood flow through IPAVA to pulmonary gas exchange efficiency has been done in humans during conditions where the relative contribution of $\dot{V}_A/\dot{Q}$ inequality and diffusion limitation cannot be rigorously excluded. For this reason, blood flow through IPAVA has only been correlated with impairments in pulmonary gas exchange efficiency (24, 143, 216).

Regulation of Blood Flow Through IPAVA: Hyperoxia

In addition to the physiological relevance of blood flow through IPAVA being unclear with respect to pulmonary gas exchange efficiency, the mechanistic regulation of

blood flow through IPAVA remains unclear as well. Conditions known to increase blood flow through IPAVA (exercise, breathing hypoxic gas mixtures, and the intravenous (i.v.) infusion of catecholamines) are all associated with increases in $\dot{Q}_T$ and pulmonary arterial systolic pressure (PASP). One attractive hypothesis to regulating blood flow through IPAVA is that it responds passively to this increase in $\dot{Q}_T$ and PASP (133, 216). However, during exercise breathing a $FIO_2 = 1.0$ blood flow through IPAVA is prevented or significantly reduced despite $\dot{Q}_T$ only decreasing by ~10% for a given $\dot{V}O_2$ and no change in PASP (80). How then can we explain the hyperoxia-mediated reduction in blood flow through IPAVA? One possible explanation is that a distinctly different mechanism underlying the hyperoxia-mediated reduction in blood flow through IPAVA exists, which is presumably an active, but selective, vasoconstriction of pulmonary vascular smooth muscle. Indeed, breathing a $FIO_2 = 0.40$ has been shown to cause significant redistributions in pulmonary blood flow within as short as 10 min as demonstrated in sheep using 15 μm microspheres (162). Similarly, the absolute $\dot{V}_A/\dot{Q}$ ratio is increased in anesthetized pigs ventilated with a $FIO_2 = 0.50$ measured using 15 μm microspheres (93).

Thus, these data demonstrate that hyperoxia is capable of acutely and dynamically altering the pulmonary vasculature. Although vascular smooth muscle tone is affected by a multitude of vasoactive substances, a common theme is the necessity to increase or decrease intracellular calcium levels in order to elicit a vasoconstrictor or vasodilator response, respectively. Considering the possibility that IPAVA are lined with vascular smooth muscle raises the potential to pharmacologically target these vessels during exercise breathing a $FIO_2 = 1.0$. Pharmacologically reversing the hyperoxia-mediated

reduction in blood flow through IPAVA during exercise breathing a FIO_2 = 1.0 would suggest a potential mechanistic regulatory pathway controlling blood flow through IPAVA. Alternatively, if IPAVA are unresponsive to these pharmacologic interventions, it can be determined that the pathways involved may not be obligatory to regulating blood flow through IPAVA during exercise in hyperoxic conditions. This work represents the first pharmacological investigation into this area.

Pulmonary Gas Exchange Efficiency After Acclimatization to Hypobaric Hypoxia in Subjects With and Without a Patent Foramen Ovale

It is well established that pulmonary gas exchange progressively worsens in a workload dependent manner during exercise at sea level (48). This impairment in pulmonary gas exchange efficiency during exercise is exacerbated in acute hypoxia, such that for any given $\dot{V}O_2$, the alveolar-to-arterial PO_2 difference ($A\text{-}aDO_2$) is greater compared to exercise in normoxia (235). Following acclimatization to hypobaric hypoxia, pulmonary gas exchange efficiency is thought to improve compared to acute hypoxia (88, 203). Seminal work from Dempsey *et al*. (47) reported a trend for an increased $A\text{-}aDO_2$ during treadmill walking after 4 days at 3100m compared to sea level, and a partial normalization during the same exercise protocol following 21 days at 3100 m compared to that obtained after 4 days. Bebout *et al*. (13) subsequently demonstrated that, compared to acute normobaric hypoxia, acclimatization to 3800m for 2 weeks resulted in an ~3 mm Hg reduction in the $A\text{-}aDO_2$ during submaximal cycle ergometer exercise. Calbet *et al*. (28) subsequently reported that, compared to acute normobaric hypoxia, acclimatization to 5260m for 9-10 weeks resulted in an ~9 mm Hg reduction in the $A\text{-}aDO_2$ during submaximal cycle ergometer exercise. Collectively, these data suggest that pulmonary

gas exchange efficiency in non-acclimatized individuals improves with acclimatization to high-altitude compared to acute hypoxia.

The initial impairment in pulmonary gas exchange efficiency in acute hypoxia is likely explained by an increase in diffusion limitation secondary to the reduction in PAO_2, and increase in $\dot{Q}_T$ (i.e., decreased pulmonary capillary transit time) for a given $\dot{V}O_2$ compared to exercise breathing room air at sea level (183, 184, 229). After acclimatization, the improvement in pulmonary gas exchange efficiency is also thought to result from a comparatively lessened degree of diffusion limitation; secondary to, not only an increase in PAO_2 and decreased $\dot{Q}_T$ for a given $\dot{V}O_2$ compared to exercise in acute hypoxia (28, 29, 31) but also to, potential improvements in pulmonary diffusing capacity (3). Additional rationale for the emphasis on initial impairments and subsequent improvements in diffusion limitation explaining the initial impairment and subsequent improvement in pulmonary gas exchange efficiency during exercise at high-altitude is that the contributions of $\dot{V}_A/\dot{Q}$ inequality and right-to-left shunt to the A-aDO_2 decrease as the level of hypoxia increases (255, 256).

However, the prior work describing this paradigm is: 1) based off of data collected using functional gas exchange dependent methods, (i.e., the MIGET and 100% O_2 technique) that may not include the contribution of blood flow through IPAVA to the A-aDO_2; and, 2) has presumably been carried out in subjects with and without a PFO. Yet, individuals with a PFO have an additional source of right-to-left shunt, via the foramen ovale, compared to individuals without a PFO. Lovering *et al*. (145) has demonstrated that pulmonary gas exchange efficiency at rest (but not during exercise) in subjects with a PFO is significantly worse when breathing room air at sea level and in

acute normobaric hypoxia ($FIO_2 = 0.12$) compared to subjects without a PFO. As mentioned earlier, the contributions of $\dot{V}_A/\dot{Q}$ inequality and right-to-left shunt to the A-aDO_2 decrease as the level of hypoxia increases; however, a hallmark of acclimatization to high-altitude is an increase in PaO_2. Therefore, for the same reason that the effect of a given volume of right-to-left shunt to the A-aDO_2 is less in acute hypoxia (due to the difference between $P\bar{v}O_2$ and PaO_2 decreasing), the effect of this same volume of right-to-left shunt to the A-aDO_2 is greater after acclimatization (due to the difference between $P\bar{v}O_2$ and PaO_2 increasing). Of course, the increase in PaO_2 after acclimatization to high-altitude is only secondary to an increase in alveolar ventilation. Meaning for the same volume of pulmonary blood flow, there will be an overall increase in the $\dot{V}_A/\dot{Q}$ ratio that should correspond to a reduction in the extent of heterogeneity in PO_2 between alveoli (31, 63, 204).

In summary, the improvement in pulmonary gas exchange efficiency after acclimatization is likely driven by a lessened degree of diffusion limitation, however the contribution of right-to-left shunt to the A-aDO_2 is also increased; and individuals with a PFO have an additional source of right-to-left shunt. Furthermore the prevalence of PFO in the general population is ~35-40% (55, 156, 266). Accordingly, it remains possible that after acclimatization to high-altitude, pulmonary gas exchange efficiency may only be improved in individuals without a PFO. Similarly, other physiologic adaptations accompanying acclimatization to high-altitude also have never been investigated in subjects with and without a PFO, specifically blood flow through IPAVA and ventilatory acclimatization.

STATEMENT OF PROBLEM

Pulmonary gas exchange is a complex process that can be impaired by several factors (i.e., $\dot{V}_A/\dot{Q}$ inequality, diffusion limitation and right-to-left shunt). Partitioning the relative contribution from each factor from the measured A-aDO_2 has technical challenges, but in order to draw conclusions on one contributor (i.e., right-to-left shunt) the others must be eliminated (i.e., $\dot{V}_A/\dot{Q}$ inequality and diffusion limitation). To date, the contribution of blood flow through IPAVA on pulmonary gas exchange efficiency has not been evaluated in an experimental setting that eliminates contributions from $\dot{V}_A/\dot{Q}$ inequality and diffusion limitation. Therefore, whether or not blood flow through IPAVA contributes to pulmonary gas exchange efficiency remains controversial. Secondarily, the mechanisms regulating blood flow through IPAVA remain speculative, particularly those mediating the hyperoxia-mediated reduction in blood flow through IPAVA during exercise. Lastly, although blood flow though IPAVA has been demonstrated to increase in acute normobaric hypoxia, the long-term regulation of blood flow through IPAVA during chronic hypoxia at rest and during exercise has not been investigated. Moreover, prior work characterizing human acclimatization to high-altitude has been carried out in subject populations with and without PFO.

PURPOSE AND HYPOTHESES

The primary purpose of this dissertation is three fold; 1) to investigate the contribution of blood flow through IPAVA on pulmonary gas exchange efficiency with $\dot{V}_A/\dot{Q}$ inequality and diffusion limitation eliminated; 2) investigate the potential effect of pharmacologic interventions regulating this; and 3) to describe pulmonary gas exchange

efficiency in healthy humans with and without a PFO in acute hypobaric hypoxia and after acclimatization to hypobaric hypoxia.

Aim #1: Determine Whether or Not Blood Flow Through Intrapulmonary Arteriovenous Anastomoses Contributes to Pulmonary Gas Exchange Efficiency

To establish IPAVA as physiologically relevant, we intend to demonstrate the potential for blood flow through IPAVA to impair pulmonary gas exchange efficiency. Previous work addressing this question was completed during conditions in which the role for IPAVA to be unequivocally involved in pulmonary gas exchange efficiency could not be determined (24, 143, 216). Accordingly, it remains unknown whether or not blood flow through IPAVA impairs pulmonary gas exchange efficiency. However, confirming that blood flow through IPAVA does contribute to pulmonary gas exchange efficiency could result in a paradigm shift in how we understand pulmonary gas exchange. As outlined in this dissertation we have developed a novel experimental design capable of isolating blood flow through IPAVA and all sources of right-to-left shunt, as the only contributing factor to pulmonary gas exchange efficiency. Thus, the first aim of this dissertation will be to utilize this experimental design and confirm or refute the potential for blood flow through IPAVA to contribute to pulmonary gas exchange efficiency.

Aim #2: Determine the Effect of Sildenafil, Nifedipine, and Acetazolamide on Blood Flow Through Intrapulmonary Arteriovenous Anastomoses During Exercise Breathing 100% O_2

During exercise breathing room air, blood flow through IPAVA is known to increase (53, 54, 115, 143, 216), which has been quantified using nuclear imaging techniques (141). However, during exercise breathing a $FIO_2 = 1.0$ blood flow through IPAVA is prevented or significantly reduced (54, 144). As previously described, the explanation for this hyperoxia-mediated reduction in blood flow through IPAVA is presumably via an active regulation of IPAVA. Suggesting the involvement of alterations in the tone of pulmonary vascular smooth muscle associated with IPAVA. Therefore, pharmacologic interventions known to act on pulmonary vascular smooth muscle, and specifically cause vasodilation and/or prevent vasoconstriction may be capable of preventing this hyperoxia-mediated reduction in blood flow through IPAVA. If so, knowledge of the pharmacologic mechanism of action may shed light on the potential regulation of IPAVA. Accordingly, the pharmacologic interventions utilized in this dissertation were sildenafil, nifedipine, and acetazolamide. Together these medications operate through unique cellular pathways, and either promote pulmonary vasodilation via augmenting the activity of nitric oxide (sildenafil), inhibiting vasoconstriction via blocking L-type calcium channels (nifedipine), or preventing an increase in intracellular calcium through a non L-type calcium channel mechanism (acetazolamide). Therefore, these pharmacologic interventions act through mechanisms with the potential to prevent or reduce the hyperoxia-mediated reduction in blood flow through IPAVA (9). Thus, the second aim of this dissertation is to investigate the effect of sildenafil, nifedipine, and

acetazolamide on the reduction in blood flow through IPAVA during exercise breathing a $FIO_2 = 1.0$.

Aim #3: Characterize Pulmonary Gas Exchange Efficiency in Healthy Humans With and Without a Patent Foramen Ovale in Acute and After Acclimatization to Hypobaric Hypoxia

Pulmonary gas exchange efficiency at rest and during exercise is impaired in healthy humans in acute hypoxia compared to when breathing room air at sea level, and is improved following acclimatization to hypobaric hypoxia compared to acute hypoxia. The mechanism explaining this initial impairment, and subsequent improvement in pulmonary gas exchange efficiency is likely driven by initial impairments, and subsequent improvements, in diffusion limitation. However, this prior work has presumably been done in subjects with and without a PFO, and as described, humans with a PFO have an additional source of right-to-left shunt that results in a measureable decrement in pulmonary gas exchange efficiency (145). Accordingly, it remains unknown how pulmonary gas exchange efficiency after acclimatization differs in humans with and without a PFO. Furthermore, although blood flow through IPAVA increases in acute normobaric hypoxia (134), it unknown if blood flow through IPAVA is altered following acclimatization to hypobaric hypoxia. Thus, the third aim of this dissertation is to characterize pulmonary gas exchange efficiency in healthy humans in acute, and after acclimatization to, hypobaric hypoxia; and secondarily to investigate effect of acclimatization to hypobaric hypoxia on blood flow through IPAVA.

Chapter IV is in review with the *Journal of Physiology* and Joseph W. Duke, Jerold A. Hawn, John R. Halliwill, and Andrew T. Lovering are co-authors. I performed the experimental work, led the project, and the writing is entirely my own; Joseph W. Duke provided technical and editorial assistance; Jerold A. Hawn placed all radial artery catheters; and John R. Halliwill and Andrew T. Lovering helped develop the protocol, and provided guidance and editorial assistance.

Chapter V is in review with *Respiration Physiology & Neurobiology* and Joel E. Futral, Randall D. Goodman, and Andrew T. Lovering are co-authors. I performed the experimental work, led the project, and the writing is entirely mine; Joel E. Futral and Randall D. Goodman provided technical assistance with performing echocardiography during exercise; and Andrew T. Lovering helped develop the protocol, and provided guidance and editorial assistance.

Chapter VI is in review with the *Journal of Applied Physiology* and Steven S. Laurie, Julia P. Kern, Kara M. Beasley, Randall D. Goodman, Bengt Kayser, Andrew W. Subudhi, Robert C. Roach, and Andrew T. Lovering are co-authors. The data presented in this chapter come from a very large, multinational, field based project entitled "AltitudeOmics." However, I performed the experimental work, led this aspect of AltitudeOmics, and the writing is entirely mine; Steven S. Laurie, Julia P. Kern, and Kara M. Beasley provided technical and editorial assistance; Randall D. Goodman provided technical assistance with performing echocardiography during exercise; and Bengt Kayser, Andrew W. Subudhi, Robert C. Roach, and Andrew T. Lovering helped develop the protocol, and provided guidance and editorial assistance.

CHAPTER II

REVIEW OF THE LITERATURE

INTRODUCTION

This review of the pertinent literature will track sequentially with Chapters IV, V, and VI with regard to the overall topic of each. However, areas of research that are pertinent across all Chapters are those pertaining to the presence of a patent foramen ovale and blood flow through IPAVA. Accordingly, I will begin by reviewing both of these subject areas. Following these sections, the subject matter will transition to pulmonary gas exchange efficiency, which represents a focal feature of this dissertation and is most pertinent to Chapters IV and VI. The factors related to pulmonary gas exchange efficiency will be reviewed, followed by the work that has developed our current understanding of these areas. Transitioning from pulmonary gas exchange will be to the regulation of blood flow through IPAVA including the reduction in blood flow through IPAVA during exercise breathing an $FIO_2 = 1.0$.

PATENT FORAMEN OVALE

Embryologic development of the fetal heart begins as a single common cavity that eventually separates into four distinct chambers (181). In doing so one-way valves develop that separate the right and left atria from the right and left ventricle, with the purpose being to permit uni-directional blood flow through them. In contrast, separation between the right and left atria and the right and left ventricle takes the form of a septal wall, with the purpose being to prevent blood flow across between them. However, crucial to the developing fetus is a non-fully formed septal division, particularly between

the right and left atria (71). Gas exchange occurs in utero at the level of the placenta, by way of the mother, and because of this, it is advantageous that blood flow to the developing pulmonary circulation be minimal. Maintaining an opening between the right and left atria allows blood flow to bypass the developing pulmonary circulation by flowing directly from the right-to-left atrium. This opening, called the foramen ovale, develops as the septum primum and septum secundum (named based their sequential appearance) develop (181). After birth, gas exchange in the infant occurs in the lung and no longer via the placenta, and thus, pulmonary blood flow increases from ~20% in utero to 100% of the $\dot{Q}_T$ (191). This increase in pulmonary blood flow is associated with a fall in pulmonary vascular resistance, while systemic vascular resistance gradually increases (58). Once systemic vascular resistance exceeds pulmonary vascular resistance, the foraman ovale functionally closes by way of the septum primum being pushed against the septum secundum (71). Over time the septum secundum forms a permanent anatomic seal over the foramen ovale by fusing to the septum secundum (36). A fascinating description of the fetal atria from Claudius Galen was included in a review by Bradley Patten, originally from John Dalton's text 'Doctrine of the Circulation' (44), providing an uncanny description of what we now know as the foramen ovale:

"*There is a kind of orifice or fenestra common to both…at this orifice there is attached a membrane, like a lid or cover opening toward the pulmonary vessel [left atrium] so that it will yield to the influx of blood from the vena cava, but will prevent its regurgitation into that vessel. …Soon after birth, either within a day or two, or, in some animals after four or five days or a little longer, you will find the membrane at the foramen coalescing but not yet fully adherent. Looking at the same place in the adult*

animal, you would say there had never been a time when it was open; and, on the other hand, in a foetus, before or immediately after birth when this membrane is attached so to speak, only by it's root, the rest of it hanging free in the vascular cavity, you would hardly believe in it's ever becoming agglutinated." – (Opera Omnia, vol. IV, p.243; translation by Dalton, 1884, p.69 (44) – and quoted from (180))

However, nearly 2 millennia have passed since Galen's observation and we now know permanent anatomical closure of the foramen ovale fails to occur after birth in some individuals, and therefore remains 'patent' throughout life and is referred to as a patent foramen ovale (PFO). Studies examining the prevalence of PFO in the general population also have an interesting history and as described by Bradely Patten;

"*Publications dealing with the failure of the foramen ovale to close have been appearing for more than three centuries* (181)*." - Bradley M. Patten, 1938*

According to this report, summarizing data obtained on autopsy from 9 studies dating from 1837 – 1934, the presence of a PFO was identified in 864 out of the combined 4083 cases. The prevalence of PFO in these 9 studies ranged from 15% to 43%, and averaged ~21% (181). Nevertheless, the publication generally cited as the classical reference for the prevalence of PFO is that by Hagen *et al*., (82) also determined on autopsy. This manuscript offers the additional details that describe the size of detected PFO that ranged from 1-19 mm and also suggested the prevalence of PFO declined from ~35% in humans <29 years old to ~25% in humans >30 years old. However, more recent work has utilized a different, more sensitive technique (saline contrast echocardiography, described in Chapter III), in detecting the presence of a PFO and determined the

prevalence to be 35-40% (55, 266), including one report in humans up to ~60 years old (156).

The right-to-left shunt provided by a PFO has been recognized clinically as a potential explanation for neurological insult, including stroke and particularly those that are otherwise unexplained i.e., cryptogenic. Lechat *et al*. (135) reported that the prevalence of PFO was significantly higher (40%) in patients with stroke compared to patients without stroke (10%). Furthermore, these data also reported that out of the patients with stroke, there was a 54% prevalence of PFO in patients with cryptogenic stroke. Webster *et al*. (248) also reported data suggesting the presence of a PFO may be an under recognized cause of stroke. In this study there was a 50% prevalence of PFO in patients with stroke while only a 15% prevalence of PFO in patients without stroke. Homma *et al.* (99) made the observation that patients with a PFO were at a significantly increased risk for cryptogenic stroke compared to subjects with a small PFO. Since these studies, the association between PFO and stroke has appeared many times in the literature (49, 50, 98, 99, 132, 178, 190, 211).

Nevertheless, there have also been several studies demonstrating the presence of recurrent paradoxical embolism in patients who have undergone surgical treatment for PFO closure. Messé *et al.* (165) reviewed several comprehensive publications in this area (20, 99, 157), and concluded that the risk of recurrent cryptogenic stroke in patients with a PFO, was no different than the risk for cryptogenic stroke in patients without a PFO. A similar conclusion was also reached by Meier *et al.* (160) in a recent superiority trial across 29 clinical centers in Europe, Canada, Brazil, and Australia, where closure of a PFO did not result in a significant reduction in the risk of recurrent embolic events. In a

study by Windecker *et al.* (264) 78 patients with a PFO who had a documented neurologic insult underwent surgical intervention for PFO closure, and 8 patients suffered recurrent paradoxical embolic events within the first year post-PFO closure. It was noted by these authors that the presence of 'postprocedural shunt' was a strong predictor for recurrent paradoxical embolic events. Postprocedural shunt is the presence of left-sided contrast using saline contrast echocardiography, after surgically closing the PFO, suggesting an alternative explanation for left-sided contrast. One plausible explanation for postprocedural shunt is blood flow through IPAVA, which has recently been suggested to be a potentially unrecognized cause of ischemic stroke and transient ischemic attack (TIA). Abushora *et al.* (2) demonstrated that the transpulmonary passage of saline contrast was an independent predictor, on the same order of magnitude as hypertension and hyperlipidemia, for stroke and/or TIA.

Furthermore, as reviewed by Kerut *et al*. (116) PFO has been implicated in several more pathologic process in addition to stroke, including decompression sickness in divers (73, 91, 168) and pilots (41), and may exacerbate arterial hypoxemia in patients with and chronic lung disease (81, 210). Lastly, it has been hypothesized that individuals with PFO may be at an increased risk for the development of high-altitude pulmonary edema (HAPE). Right-to-left intracardiac shunt across the PFO is dependent on right atrial pressure exceeding left atrial pressure, which can occur transiently during normal respiration (64), and is exacerbated during conditions of elevated pulmonary pressures. Exaggerated pulmonary hypertension is a hallmark of HAPE, and previous work has suggested the prevalence of PFO is >4 times higher in HAPE susceptible than HAPE resistant individuals (4). In this theory, the acute increase in pulmonary arterial pressure

associated with ascent to high-altitude facilitates right-to-left shunt across the PFO, thereby worsening arterial hypoxemia, resulting in a vicious downward spiral of increased shunt, leading to increased hypoxemia, leading to increased pressure, and the cycle continues (10).

Despite the presence of a PFO being recognized since the time of Galen and its appreciation in clinical disorders such as stroke, transient ischemic attack, migraine, decompression sickness and HAPE, its appreciation to contribute to pulmonary gas exchange efficiency is less widely accepted. Although previous research has suggested a role for PFO to explain the occurrence of systemic arterial oxygen desaturation or exaggerated arterial oxygen desaturation in patients with lung disease (81, 210), these studies do not have measures of pulmonary gas exchange efficiency. Lovering *et al*. (145) did investigate the effect of a PFO on pulmonary gas exchange efficiency and demonstrated that subjects with a PFO have an increased A-aDO_2 at rest breathing room air and a $FIO_2 = 0.12$. However, no difference was observed in the A-aDO_2 between subjects with and without a PFO during exercise, which the authors reasoned, to be due to the possibility that the volume of blood flow through the PFO remained constant from rest to exercise. Interestingly, in light of recent work demonstrating that the degree of left-sided contrast visualized on release of a Valsalva maneuver correlates to the size of the PFO (64), of the 8 subjects with a PFO in the study by Lovering *et al*., 6 would be classified as having a 'small' PFO and 2 would be classified as having a 'large' PFO. Strictly speaking the size or diameter of the PFO is less important than the volume of blood flow across it, yet intuitively a larger PFO should confer a larger volume of right-to-left shunt compared to a smaller PFO. This is illustrated both by the greater degree of

left-sided contrast visualized from a large PFO in the work by Fenster *et al*. (64) and by our data in Chapter VI. As will be described, those subjects with a large PFO (n = 6) had an increased A-aDO_2 compared to those subjects with a small PFO (n = 5) at rest and throughout exercise at 70, 100, 130, and 160 Watts **(Figure 6.2)**.

In summary, the prevalence of PFO in the general population is ~35-40% and blood flow across the PFO is an undisputed source of right-to-left shunt. Despite the appreciation of PFO pertaining to clinical disorders, the contribution of a PFO to pulmonary gas exchange efficiency is underappreciated. Interestingly, the prior work that has characterized the basis for our current understanding of pulmonary gas exchange efficiency has been carried out in subjects with and without a PFO. Thus, a priority in Chapter IV and V was to screen and exclude subjects for PFO, as the presence of a PFO would cloud our interpretation of blood flow through IPAVA using TTSCE as well as our interpretation of pulmonary gas exchange efficiency. In Chapter VI, per the study design, subjects with and without a PFO were included and the data analysis was separated for those with and without a PFO.

INTRAPULMONARY ARTERIOVENOUS ANASTOMOSES

Pre-capillary arteriovenous anastomoses form a direct connection between the arterial and venous circulation, and have been documented in the pulmonary circulation of the infant (226, 262) and adult human (225, 228), as well as in birds, dogs, cats, rabbits, and rats (12, 171, 179, 186, 188, 215). With the exception of the work done by Rahn, Stroud and Tobin in 1952, the remaining aforementioned studies used large diameter (15-500 μm) glass or synthetic microspheres to demonstrate the presence of

intrapulmonary arteriovenous anastomoses (IPAVA). This anatomic-based technique operates on the principle that anything larger than the diameter of the largest pulmonary capillary (≤13 μm) is filtered out and prevented from reaching the pulmonary venous circulation (75). Thus, microspheres injected into the pulmonary arterial circulation can only be recovered within the pulmonary venous effluent if a large diameter IPAVA, which bypasses the pulmonary capillary bed, is present and allows blood to flow through it. Criticism toward the majority of this seminal, anatomic-based work using large diameter microspheres has been due to the non-physiologic conditions the isolated lung models or animal preparations were studied under. However, more recently, Lovering *et al*. confirmed the presence of IPAVA using 25 and 50 μm microspheres in isolated healthy human and baboon lungs which were ventilated and perfused with physiologic pressures (146).

For ethical and medical reasons it is not possible to inject solid, non-biodegradable microspheres into human subjects. However, gas-filled microbubbles (saline contrast), which pose no risk for permanent embolization of the lung, can be used in human subjects and are the basis for a technique called transthoracic saline contrast echocardiography (TTSCE). TTSCE is considered the gold standard, minimally invasive anatomic-based technique for detecting blood flow through IPAVA in humans (14, 30, 71, 94, 128). Saline contrast is created by agitating saline and air together, which is then injected into a peripheral vein while the heart is visualized in the apical, four-chamber view using transthoracic ultrasound. Once injected, this microbubble replete blood very quickly opacifies the right-side of the heart, appearing as a “cloud of echos,” where it is then pumped through the pulmonary circulation (78, 79). Similar to microspheres, the

pulmonary microcirculation functions as a biological sieve to filter out bubbles >13 μm in diameter and prevent their appearance in the left heart (163, 164). Additionally, due to the physical properties governing the *in vivo* dynamics of gas-filled bubbles, those bubbles that are smaller than 13 μm rapidly dissolve before reaching the left heart (269, 270). Accordingly, the appearance of saline contrast in the left heart, in subjects without a PFO post peripheral venous injection demonstrates blood flow through IPAVA (25, 26, 46, 60, 94-96, 159, 189, 198, 231, 269-273).

Using TTSCE we have shown that ~30% of the general healthy population do not demonstrate blood flow through IPAVA at rest breathing room air, while ~40% have a PFO, and the remaining ~30% demonstrate no left-sided contrast (55). However, breathing hypoxic gas mixtures at rest (134) results in the recruitment of IPAVA and the transpulmonary passage of saline contrast. Data from Niden and Aviado in 1956 support these findings by demonstrating that in intact, anesthetized dogs using an over embolization model, the number of large diameter (60-420 μm) glass microspheres recovered from the pulmonary venous effluent increased during ventilation of hypoxic gas (FIO_2 = 0.10) compared to room air (171). More recent work by Bates *et al*. in 2012 demonstrates that in intact spontaneously breathing rats, the number of 15-70 μm microspheres that escape pulmonary filtration is significantly increased when breathing hypoxic gas (FIO_2 = 0.08) compared to breathing room air (12).

Similarly, during exercise breathing room air IPAVA are also recruited and allow for the transpulmonary passage of saline contrast (53, 54, 115, 143, 173, 216). These data are supported by work done by Stickland, Lovering & Eldridge in 2007 which demonstrated that 25 μm microspheres escaped pulmonary filtration in 5/6 exercising

dogs, whereas at rest the pulmonary capillary bed prevented the transpulmonary passage of microspheres in 8/8 dogs (215). Furthermore, Lovering *et al*. in 2009 demonstrated that in healthy humans, exercise resulted in an increase in the transpulmonary passage of large diameter (15-105 μm) technetium-99m labeled macroaggregated albumin particles (141).

In contrast to exercise breathing room air, during exercise breathing 100% O_2, IPAVA remain closed and the transpulmonary passage of saline contrast is prevented or significantly reduced (54, 144). Previous work by Niden and Aviado in 1956 also supports these data by demonstrating in intact, anesthetized dogs using an over embolization model, the number of large diameter (60-420 μm) glass microspheres recovered from the pulmonary venous effluent decreased during ventilation of 100% O_2 (171). Moreover, recent work from our lab using nuclear imaging techniques quantifies the reduction in blood flow through IPAVA during exercise breathing a $FIO_2 = 1.0$ (Duke, Elliott, *et al*., *In Preparation*).

To summarize, over the past 60 years a significant body of anatomic-based evidence has been collected to support the existence of large diameter IPAVA. In fact, Sirsi and Bucher stated in 1953 that, "It is now generally accepted that arteriovenous anastomoses exist in the lungs" (208). Additionally, these *ex-vivo* microsphere data are supported by *in-vivo* work done in healthy humans using TTSCE and macroaggregated albumin. Thus, not only is it clear that IPAVA exist using TTSCE, the general conditions in which blood flow through these vascular conduits occurs (i.e., during exercise, breathing hypoxic gas mixtures, and during the i.v. infusion of catecholamines) and is prevented (i.e., during conditions of alveolar hyperoxia) have now been described.

Nevertheless, the physiologic significance of blood flow through IPAVA remains controversial largely due to, 1) the undefined role for blood flow through IPAVA to contribute to pulmonary gas exchange efficiency by providing a source of right-to-left shunt, and 2) the undefined mechanistic regulation of blood flow through IPAVA. Both of these points will be expanded upon in the proceeding sections and Chapters.

PULMONARY GAS EXCHANGE

Pulmonary gas exchange describes the transfer of gas between the atmosphere and pulmonary capillary blood, with a particular emphasis on the transfer of O_2 from the alveolar air to the pulmonary capillary blood and the elimination of metabolically produced CO_2 from the pulmonary capillary blood to the alveolar air. Fundamental to this process is adequately ventilating the alveolar air space, i.e., alveolar ventilation ($\dot{V}_A$). This differs from the more general term, minute ventilation ($\dot{V}_E$), by subtracting the volume of anatomic dead space from the tidal volume (149). In addition to anatomic dead space, if portions of the lung are ventilated but not receiving blood flow, these portions would also reflect physiologic dead space. As will be described later, these areas reflect an alveolar ventilation-to-perfusion ($\dot{V}_A/\dot{Q}$) ratio equal to infinity (∞). The measurement of gas flow, i.e. $\dot{V}_E$, using modern equipment is relatively straightforward, and determining $\dot{V}_A$ can be calculated as described in the classic text by Hermann Rahn and Wallace Fenn (187):

$$V_A = \frac{(VCO_2 \times K)}{PACO_2}$$

Equation 2.1. Alveolar Ventilation

where $\dot{V}CO_2$ represents the volume of CO_2 produced, and *K* is a correction factor. In practice, $PaCO_2$ can be used as a surrogate for $PACO_2$, assuming complete end-capillary CO_2 equilibration; an assumption with relatively minor error associated with it, particularly in healthy humans at rest (242). The correction factor *K* corrects $\dot{V}CO_2$ to body temperature and pressure:

$$K = \left[(273 + T_B) \times \frac{760}{273}\right]$$

Equation 2.2. Conversion Factor, *K*

where T_B is body temperature, 760 mm Hg is barometric pressure (P_B) at sea level, and 273 Kelvin is 0℃. At sea level and 37℃, K is equal to 863 mm Hg.

Alveolar ventilation at a given metabolic rate ultimately regulates PAO_2, which is also a function of the inspired PO_2. Direct measures of PAO_2 are not possible, yet PAO_2 can be calculated with knowledge of P_B, FIO_2, $PACO_2$, and $\dot{V}CO_2/\dot{V}O_2$. Of course the accuracy of this calculation depends on the accuracy of all of these measurements, and again, in practice $PaCO_2$ can be used as a surrogate for $PACO_2$ while P_B should be corrected for water vapor pressure and body temperature, especially during exercise (196):

$$PAO_2 = \left[(P_B - e^{0.05894809 \times T_B + 1.689589}) \times FIO_2\right] - PaCO_2 \times \left[FIO_2 + \frac{(1 - FIO_2)}{RER}\right]$$

Equation 2.3. Alveolar Gas Equation

Finally, PaO_2 can be directly measured using a blood gas analyzer (described further in Chapter III) and ultimately, the difference between PAO_2 and PaO_2, reflects the efficiency of pulmonary gas exchange for O_2. This is referred to as the alveolar-to-arterial PO_2 difference ($A\text{-}aDO_2$), where an $A\text{-}aDO_2$ = 0 mm Hg reflects perfect pulmonary gas

exchange efficiency and anything >0 mm Hg reflects an impairment in this process. In theory the A-aDO_2 can never be <0 mm Hg, however in practice due to the aforementioned errors inherent to calculating PAO_2 negative values are not uncommon in the literature, particularly when subjects are 'resting' before beginning exercise (112, 142, 175, 216, 234). Potential factors that can impair pulmonary gas exchange efficiency are, 1) incomplete end-capillary O_2 equilibration (diffusion limitation), 2) alveolar ventilation-to-perfusion ($\dot{V}_A/\dot{Q}$) inequality, and 3) right-to-left shunt. Sources of right-to-left shunt include, 1) postpulmonary shunt via the bronchial and Thebesian circulations, which drain the lungs and heart, respectively, 2) intracardiac shunt via the PFO, and 3) intrapulmonary shunt.

Pulmonary Diffusion

Pulmonary O_2 diffusion is a complex process mediated by several factors, including the gradient between PAO_2 and capillary PO_2 (PcO_2) and the oxygen diffusing capacity of the lungs (DLO_2). The oxygen diffusing capacity of the lungs is defined as the amount of oxygen transferred per minute ($\dot{V}O_2$) divided by the difference between PAO_2 and capillary PO_2 (PcO_2). Which rearranges to form the familiar equation of Fick's First Law of Diffusion when applied to pulmonary gas exchange that was first conceptualized by Bohr (23):

$$\mathrm{VO_2}(t) = \mathrm{DLO_2}[\mathrm{PAO_2} - \mathrm{PcO_2}(t)]$$

Equation 2.4. Fick's First Law of Diffusion

Therefore, this process is not instantaneous and based off of this principle it is clear that this process can be impaired if the mean pulmonary capillary erythrocyte transit time is insufficient to allow full equilibration between end-capillary PO_2 ($Pc'O_2$) and

PAO_2. Furthermore, complete equilibration between $Pc'O_2$ and PAO_2 can be impacted by the partial pressure gradient between PAO_2 and PcO_2. As previously described, PAO_2 is chiefly impacted by the inspired PO_2 as well as the degree of alveolar ventilation ($\dot{V}_A$) and prevailing metabolic rate. Pulmonary capillary PO_2 initially reflects mixed venous PO_2 ($P\bar{v}O_2$), and the gradient between $P\bar{v}O_2$ and PAO_2 plays a significant role in the rate at which O_2 diffuses and binds with hemoglobin. Of note, although generally speaking a larger gradient confers a more rapid diffusion of O_2, what is most important for determining the rate of O_2 equilibration is the slope of the O_2 dissociation curve (βO_2) between the particular PAO_2 and $P\bar{v}O_2$ under study (182, 242, 243).

Finally, DLO_2 can be separated into two distinct but related processes; 1) the diffusion of O_2 across the blood gas barrier and through the plasma (i.e., the membrane component, Dm), and 2) the diffusion of O_2 into the red cell and combining with hemoglobin (i.e., the red cell component, θ) (200). The membrane component is treated as applicable to the entire lung, however, for the same to be true of θ, it must be multiplied by the entire pulmonary capillary blood volume (Vc). Accordingly, the resistance to diffusion of O_2 in the lung is the inverse of DLO_2. Analogous to electrical theory (Ohms law), resistances are additive when in series and therefore the inverse of Dm and θ are additive to produce the entire resistance to diffusion of O_2 in the lung. This relationship was derived rigorously by Roughton and Forster in 1957 (200):

$$\frac{1}{\mathrm{DLO_2}} = \frac{1}{\mathrm{DmO_2}} + \frac{1}{(\theta \times \mathrm{Vc})}$$

Equation 2.5. Roughton-Forster Equation

These two fundamental relationships form the basis of the current working "Bohr Integration" for calculating the rate of rise in PO_2 of a 'slug' of blood moving through a

pulmonary capillary. Although a comprehensive review of the mathematical derivation is beyond the scope of this dissertation, it is worthwhile to briefly review the process as it still employed today to describe pulmonary capillary diffusion equilibration. Re-expressing the left and right hand side of **Equation 2.4** for O_2 concentrations at time *t*, and incorporating **Equation 2.5**, respectively, produces the first order differential equation describing the rate of O_2 diffusion as a function of time (240, 242):

$$\frac{\partial \mathrm{CcO_2}}{\partial t} = \frac{100}{\mathrm{Vc}} \times \left[\frac{1}{\frac{1}{\mathrm{DmO_2}} + \frac{1}{\mathrm{V_c} \times \theta}} \right] \times (\mathrm{PAO_2} - \mathrm{PcO_2})$$

Equation 2.6. Rate of Rise in Pulmonary Capillary PO_2

where $\partial \mathrm{CcO_2}/\partial t$ is the O_2 content in the pulmonary capillary blood at time *t* and is a function of the previously defined terms. Content is expressed as ml O_2 per dL of blood as described by the content equation:

$$\mathrm{O_2\ Content} = \left[1.39 \times \mathrm{Hb} \times \left(\frac{\mathrm{SO_2}}{100} \right) \right] + (0.003 \times \mathrm{PO_2})$$

Equation 2.7. Oxygen Content Equation

Due to the non-linearity of the O_2 dissociation curve and the fact that θ varies as a function of PcO_2 (i.e., O_2 saturation) this equation cannot be directly integrated and therefore must be numerically solved. This is accomplished using 4th order Runge-Kutta method of numerical integration that is optimized for a 'large' (in the computing sense) time step that maintains accuracy while reducing computing time. Doing so using previously published computer algorithms (240, 243) solves this equation for 'small' (in the physiological sense) time steps (0.001 sec). Where the number of necessary solutions depends on the pulmonary capillary transit time [(i.e., Vc/pulmonary blood flow)*60] which is 0.75 sec assuming pulmonary blood flow equals 6 L/min and Vc equals 75 ml.

The value for DmO_2 is usually 40 ml O_2/min/mm Hg, and that of θ depends on the initial PcO_2 which is solved as a callable unit within **Equation 2.6** according to Staub *et al*. (212, 213). In the previously published computer algorithms implementing this Bohr Integration, computing the corresponding PcO_2 from the CcO_2 for a given time step is done using a regula falsi in three dimensions method of iteration (177). Indeed, computing the PcO_2 that corresponds to a given CcO_2 is much more complicated than the reverse, which can be done using the callable unit described by Kelman (114). However, another way to convert CcO_2 into PcO_2 is to determine the O_2 saturation (neglecting dissolved PO_2) that would yield the given CcO_2 using the first half of **Equation 2.7**. Then by way of assuming a value for the P_{50}, the corresponding PO_2 can be computed using the Hill equation (90):

$$SO_2 = \frac{PO_2^n}{PO_2^n + P_{50}^n}$$

Equation 2.8. Hill Equation

where SO_2 is the hemoglobin-O_2 saturation corresponding to the calculated PO_2, and corresponding P_{50} (i.e., the PO_2 which results in a SO_2 of 50%). The superscript 'n' is the Hill coefficient, which is equal to 2.7 in humans. By way of the Hill equation as described, I have recapitulated this Bohr Integration procedure described by Dr. Peter Wagner and Dr. John West using MatLab. However, through personal communication with Dr. Peter Wagner (email: 4/9/2013), the original Fortran code was provided to me, which can be easily implemented after building a Fortran compiler. The mathematical modeling of the rate of rise in pulmonary capillary PO_2 was originally carried out using our MatLab code, and verified using the more rigorous Fortran version.

According to this analysis complete $Pc'O_2$ equilibration occurs within ~0.3 sec when PAO_2 equals 100 mm Hg and $P\bar{v}O_2$ equals 40 mm Hg, well below the mean pulmonary capillary transit time of 0.75 sec (described above). It should be appreciated that not all lung units will have this 'mean' transit time and some will be slower and some will be more rapid. Accordingly, it remains possible that the pulmonary capillary transit time in some lung units may be faster than 0.75 sec and if sufficient, there is the potential for a diffusion limitation to exist in that lung unit. Experimentally, it is not possible to directly measure diffusion limitation, and as described previously it is inferred based off of the portion of the A-aDO_2 not explained by $\dot{V}_A/\dot{Q}$ inequality and right-to-left shunt.

Alveolar Ventilation-to-Perfusion

As mentioned in Chapter II, significant advancements in the study of $\dot{V}_A/\dot{Q}$ inequality came from the work of Wallace Fenn, Arthur Otis, and Hermann Rahn during the World War II era (259) and stemmed from the development of the O_2-CO_2 diagram (187). The foundation behind understanding $\dot{V}_A/\dot{Q}$ relationships is that when at *steady state*, pulmonary gas exchange follows the principles of mass conservation (246). The $\dot{V}_A/\dot{Q}$ ratio for O_2 and for CO_2 can then be calculated and approximated using the following equations:

$$V_A/Q = 8.63 \times \frac{(Cc'O_2 - CvO_2)}{(PIO_2 - PAO_2)}$$

Equation 2.9. $\dot{V}_A/\dot{Q}$ Ratio for O_2

$$V_A/Q = 8.63 \times \frac{(CvO_2 - Cc'O_2)}{(PAO_2 - PICO_2)}$$

Equation 2.10. $\dot{V}_A/\dot{Q}$ Ratio for CO_2

As described by Dr. Peter Wagner, although these equations are seemingly straightforward they are remarkably difficult to solve and obtain an actual PO_2 value based off a specific $\dot{V}_A/\dot{Q}$ ratio (241, 246). Many of the same mathematical complexities encountered in the Bohr Integration surface here as well, namely the issue of processing the Kelman equation in reverse. However, when they are applied to an inert gas the complexity is dramatically reduced, because no longer must we consider a non-linear O_2 dissociation curve and the other confounding variables encountered in the Bohr Integration analysis (256). In doing so the fraction of inert gas that is retained in the capillary blood (i.e., not excreted via the lung), or vice versa, is a function of its blood-gas partition coefficient (λ). Thus, the fraction of gas excreted by the lung, or retained in the blood, can be calculated using the following equation and is the foundation for the MIGET (236-238):

$$\frac{P_{A_{IG}}}{P_{v_{IG}}} = \frac{\lambda}{\lambda + \frac{V_A}{Q}} = \frac{P_{c'_{IG}}}{P_{v_{IG}}}$$

Equation 2.11. Retention/Excretion of Inert Gas

where the subscript IG denotes 'inert gas', the left hand side is the fraction of inert gas excreted by the lung, while the right hand side is the fraction of inert gas retained in the blood. As a reminder, this relationship in its simplistic description is only valid assuming the alveolar and end-capillary concentrations of all gases are identical, i.e., complete end-capillary inert gas diffusion equilibration. Nevertheless, considering inert gases are expected to equilibrate within a few hundredths of a second, this assumption seems reasonable.

The MIGET employs this principle and based on the λ for any gas, the retention of that gas will fall (i.e., more will be excreted) as the $\dot{V}_A/\dot{Q}$ ratio increases. Just as arterial blood can be collected and analyzed, so can mixed-expired air, and thus the retention (via the arterial blood sample) and excretion (via the mixed expired air sample) allow the measurement of the fraction of inert gas that is both retained and excreted. In theory, information about one yields information about the other; however, just as the retention of inert gases reflects the distribution of perfusion, the excretion of inert gases reflects the distribution of ventilation.

There are approximately 100,000 primary lobules or acini within the lung (249) and therefore, there are theoretically 100,000 different possible $\dot{V}_A/\dot{Q}$ ratios. Meaning that in order to measure each, 100,000 different gases with a unique λ would be necessary (176). However, it is argued that sufficient resolution in the MIGET is obtained by the use of 6 inert gases, each with varying solubility's, molecular weights and λ (sulfur hexafluoride, ethane, cyclopropane, halothane, diethyl ether, and acetone) (62). Sulfur hexafluoride has the lowest solubility, 0.0009 ml gas/dL blood/mm Hg and $\lambda = 0.005$, while acetone is the most soluble, 40 ml gas/dL blood/mm Hg and $\lambda = 300$. Based on these parameters the limits imposed by the MIGETs computer algorithm can detect $\dot{V}_A/\dot{Q}$ ratios as low as 0.005 and as high as 100 (238). Additional assumptions required are for gas exchange in the lung to be in steady state, for ventilation and perfusion to be non-pulsatile, complete diffusion equilibration between capillary blood and alveolar air, and for different lung compartments to function independently (97). Based on the retention and excretion of the 6 inert gases, the MIGET computer algorithm uses a 50-compartment model, meaning it calculates the $\dot{V}_A$ and $\dot{Q}$ distributions across these 50

compartments optimized for a logarithmic scale. Controversy around the MIGET expressing $\dot{V}_A/\dot{Q}$ ratios on a logarithmic scale has previously been an issue, with the proposed superior scale being one that is linear (223). Nevertheless, using these distributions, the MIGET provides a measure of 'global' $\dot{V}_A/\dot{Q}$ inequality, while the $logSD_{\dot{Q}}$ and $log\ SD_{\dot{V}}$ are the standard deviation of the perfusion and ventilation distributions, respectively, providing an index of 'dispersion' for each parameter. Therefore, a larger value for either reflects greater dispersion. However, the values for $logSD_{\dot{Q}}$ and $log\ SD_{\dot{V}}$ explicitly do not take into account shunt ($\dot{V}_A/\dot{Q} = 0$) and dead space ventilation ($\dot{V}_A/\dot{Q} = \infty$) due the log of 0 and ∞ being undefined values. However, shunt and dead space ventilation are generally thought of as separate issues from $\dot{V}_A/\dot{Q}$ inequality (69).

Determination of shunt from MIGET only includes that from intrapulmonary and intracardiac shunt, and excludes right-to-left shunt from the bronchial and Thebesian circulations. Shunt is determined predominantly from the retention of sulfur hexafluoride (the least soluble gas), by extrapolation to a $\dot{V}_A/\dot{Q}$ ratio (or λ) from 0.005 to 0. Therefore, any potential error or reason for the retention of sulfur hexafluoride to be underestimated will equate to an underestimation of shunt, while simultaneously an overestimation of perfusion to low $\dot{V}_A/\dot{Q}$ units. As described by Hlastala, (97) without this mathematical extrapolation if shunt was determined based on the retention of sulfur hexafluoride alone, shunt would be overestimated because the λ of sulfur hexafluoride is high enough to be influenced by low and even normal $\dot{V}_A/\dot{Q}$ units. The same issue of extrapolation to a $\dot{V}_A/\dot{Q}$ from 100 to ∞ for the determination of dead space ventilation also exists. Importantly, shunt measured by the MIGET includes intracardiac shunt via the PFO, and

excludes postpulmonary shunt via the bronchial and Thebesian circulations. As will be discussed in a proceeding section, in addition to the MIGETs inherent limitations and assumptions it "has never been validated against an independent technique" (as stated by Teplick *et al*., ref #223) over the past 40 years of practice. Perhaps one of the most difficult to reconcile findings is that there has never been one report of detecting a PFO using the MIGET. Yet, as has been pointed out, the prevalence of PFO in the general population is 35-40% and results in a measureable impact on pulmonary gas exchange efficiency detected via arterial blood gas analysis (145) a finding that has been replicated and extended in Chapter VI of this dissertation.

Despite the limitations in the MIGET it remains a very powerful tool for analyzing pulmonary gas exchange and is the current gold standard for quantifying global $\dot{V}_A/\dot{Q}$ inequality. In theory measurement of the alveolar-to-arterial PN_2 difference would solely reflect $\dot{V}_A/\dot{Q}$ inequality (244), yet the use of this measurement is technically very difficult and not commonly employed (32). An alternative means to obtain a crude (compared to the MIGET) estimate of $\dot{V}_A/\dot{Q}$ inequality is from the arterial-to-alveolar PCO_2 difference (a-$ADCO_2$). The theory is that with only $\dot{V}_A/\dot{Q}$ inequality and no right-to-left shunt or diffusion limitation there is predominantly an increase in *both* the a-$ADCO_2$ and A-aDO_2. While without $\dot{V}_A/\dot{Q}$ inequality, and only right-to-left shunt and/or diffusion limitation, there is predominantly *only* an increase in the A-aDO_2 with very little change in the a-$ADCO_2$. Accordingly, in theory if one were to measure an increase in the A-aDO_2 while simultaneously detecting right-to-left shunt (e.g., using TTSCE), and no change was observed in the A-aDCO_2, this would *suggest* that $\dot{V}_A/\dot{Q}$ inequality was not significantly contributing to the increased A-aDO_2. Importantly, at that point

there is still the problem of distinguishing between right-to-left shunt and diffusion limitation. Additionally, accurately measuring $PACO_2$ is problematic, however in healthy humans at rest, end-tidal PCO_2 ($P_{ET}CO_2$) provides a good approximation of $PACO_2$ (138, 148, 232). Furthermore, it has been shown that the a-$ADCO_2$ correlates well with dead space ventilation (V_D/V_T), which is calculated using the Bohr equation (22) modified by Enghoff (59):

$$\frac{V_D}{V_T} = \frac{PACO_2 - P\bar{E}CO_2}{PACO_2}$$

Equation 2.12. Bohr Dead Space Equation

where, $PACO_2$ is alveolar PCO_2 and $P\bar{E}CO_2$ is mixed expired PCO_2. In practice, $PaCO_2$ can be used as a surrogate for $PACO_2$ although it should be clear that the two are not necessarily interchangeable. Thus, measures of both the a-$ADCO_2$ and V_D/V_T, should be linearly related and in the presence of significant $\dot{V}_A/\dot{Q}$ inequality, both will increase.

Right-to-Left Shunt

According to Riley and Cournand shunt is defined as blood flow that does not participate in gas exchange, therefore in the context of pulmonary gas exchange, shunt is blood flow that does not participate in *pulmonary* gas exchange (196). The 'direction' of shunt determines its role in impairing pulmonary gas exchange efficiency, where only a right-to-left shunt, meaning venous-to-arterial blood flow, will lower PaO_2 (in contrast to a left-to-right shunt). As previously described, sources of right-to-left shunt include postpulmonary shunt via the bronchial and Thebesian circulations from the lungs and heart, intracardiac shunt (e.g., blood flow through a PFO), and intrapulmonary shunt (potentially including blood flow through IPAVA). Accordingly, all humans have this anatomic postpulmonary shunt resulting from the bronchial and Thebesian circulations

returning their venous blood directly to the left side of the heart (6, 192, 227). Intracardiac shunt is most commonly thought of as blood flow through a PFO, though can also stem from defects in the atrial and ventricular septum and other congenital cardiac abnormalities. Intrapulmonary shunt is defined as an area of the lung with a $\dot{V}_A/\dot{Q}$ ratio = 0, though in practical terms is technically difficult to distinguish between areas of the lung with a $\dot{V}_A/\dot{Q}$ ratio >0 but still being very low. For this reason issue with the semantics of 'shunt' have arisen in the literature with a elegant review of this provided by Eugene Robins (197). In Robins editorial, 'shunt' may reflect *true* shunt (i.e., mixed venous blood), blood flow through areas of very low $\dot{V}_A/\dot{Q}$, or blood flow through vascular conduits that are diffusion limited. Accordingly, a term commonly used to reflect not only *true* shunt, but $\dot{V}_A/\dot{Q}$ inequality and diffusion limitation is 'venous admixture' (5, 149, 260). Calculation of the fraction of $\dot{Q}_T$ that represents shunt ($\dot{Q}_S/\dot{Q}_T$) and venous admixture ($\dot{Q}_{VA}/\dot{Q}_T$) is identical as described by the Berggren shunt equation (14):

$$\frac{Q_S}{Q_T} = \frac{(Cc'O_2 - CaO_2)}{(Cc'O_2 - CvO_2)} = \frac{Q_{VA}}{Q_T}$$

Equation 2.13. Berggren Shunt Equation

The classical method for quantifying right-to-left shunt from all sources is the 100% O_2 technique (196). When breathing 100% O_2 alveolar N_2 is eliminated and therefore the PAO_2 in all lung units must rise to that of the inspired PO_2 less water vapor pressure and $PACO_2$. There is then, theoretically, little discrepancy in PAO_2 between ventilated lung units. Furthermore the driving gradient for O_2 diffusion, and the slope between PAO_2 and $P\bar{v}O_2$ is optimized, and eliminates contributions from $\dot{V}_A/\dot{Q}$ inequality and diffusion limitation (196). Based on this principle only right-to-left shunt quantified

using the 100% O_2 technique will be referred to as $\dot{Q}_S/\dot{Q}_T$ in this dissertation, and all other measures of pulmonary gas exchange efficiency will have the related $\dot{Q}_{VA}/\dot{Q}_T$ parameter. However, when breathing 100% O_2 accurately measuring and calculating PaO_2 and PAO_2, respectively, presents with additional technical challenges. Errors in the measured PaO_2 can only result in a reduction in the PaO_2 measured by the PO_2 electrode, and can stem from room air bubbles forming in the sample syringe, heparin equilibrated with room air that has been added to the sample syringe, diffusion of O_2 out of the syringe, consumption of O_2 by white blood cells and the PO_2 electrode itself. Thus, this technique always underestimates PaO_2 and therefore, will likely overestimate the measured A-aDO_2.

As has been mentioned and will be described further in Chapter V, during exercise when breathing a $FIO_2 = 1.0$, blood flow through IPAVA is prevented or significantly reduced. Therefore, any potential venous admixture that could result from blood flow through IPAVA during exercise breathing room air or hypoxic gas mixtures, would go undetected when breathing 100% O_2. Critics of this finding had postulated that the lack of left-sided contrast observed during exercise breathing 100% O_2 was actually a function of altered *in vivo* gas-bubble dynamics due to the altered external partial pressure environment (i.e., significantly reduced PN_2) compared to breathing room air (i.e., PN_2 equilibrated with room air). In this view, the injected microbubbles would rapidly collapse and not survive long enough to reach the left heart. However, this concern was refuted in a study we performed in 2011, demonstrating that the lack of left-sided contrast observed during exercise breathing 100% O_2 is not a function of potentially altered *in vivo* gas-bubble dynamics (54).

Accordingly and as detailed in Chapter IV, we propose that breathing an FIO_2 >0.21 but <1.0 has the potential to not significantly reduce the transpulmonary passage of microbubbles (i.e., blood flow through IPAVA) but still be sufficiently high to minimize contributions from $\dot{V}_A/\dot{Q}$ inequality and diffusion limitation. For example, according to Forster (65), the 'venous admixture' component of $\dot{V}_A/\dot{Q}$ inequality will become trivial once PAO_2 reaches ~250 mm Hg, equal to an FIO_2 of ~0.40. Implementing the previously described Bohr Integration the time required for complete end-capillary PO_2 equilibration when breathing an $FIO_2 = 0.40$ is reduced to <0.1 sec, and is therefore approaching the rate of inert gas equilibration. Finally, recent work in our lab has demonstrated that the degree of left-sided contrast observed during exercise breathing an $FIO_2 = 0.40$ is not different from room air (Davis, Elliott, *et al. In Preparation*). In summary, compared to breathing 100% O_2, when breathing an FIO_2 that elevates PAO_2 to the mid-200 range (i.e., 40% O_2), accurate measures of PaO_2 are more reliable, metabolic rate can be directly measured using commercial metabolic acquisition systems, $\dot{V}_A/\dot{Q}$ and diffusion limitation can be minimized/eliminated, and blood flow through IPAVA is qualitatively unchanged.

CLASSICAL PARADIGM

The preceding sections have described the theory and primary methods used to quantify each of the factors capable of impairing pulmonary gas exchange efficiency. Data collected with these methods, predominantly the functional gas exchange dependent ones (MIGET and 100% O_2 technique) has shaped our current understanding of pulmonary gas exchange. The proceeding sections will now summarize the pertinent

literature relating to pulmonary gas exchange during exercise, in acute normobaric hypoxia, and after acclimatization to hypobaric hypoxia.

Pulmonary Gas Exchange During Exercise at Sea Level

It has been well established that pulmonary gas exchange efficiency, although minimally impaired at rest ($A\text{-}aDO_2$ = ~5 mm Hg) worsens with increasing exercise intensity, reaching a maximal value at $\dot{V}O_{2max}$. The normal resting $A\text{-}aDO_2$ has almost always been entirely attributed to $\dot{V}_A/\dot{Q}$ inequality from past studies using the MIGET (34, 69, 85, 102, 195, 229). From these data, although postpulmonary shunt via the bronchial and Thebesian circulations is present in 100% of humans, the contribution of this source of shunt has been considered to be small or non-detectable (236). Other attempts to quantify postpulmonary shunt using the 100% O_2 technique report values ranging from 0.18-2.2% of the $\dot{Q}_T$ (85, 229, 235). Cardús *et al*. (34) reports data using the MIGET from 64 subjects at rest (18-71 years old) and shows that in 90% of subjects ~0.75% of the $\dot{Q}_T$ was estimated to flow through areas of very low $\dot{V}_A/\dot{Q}$ (<0.1). In this study, 7 of the 64 subjects (10%) had a higher value, ranging from 1-3% of the $\dot{Q}_T$. Interestingly, the individual data are plotted and there are 18 (28%) subjects with ~0.5% or greater of the $\dot{Q}_T$ estimated to flow through areas of very low $\dot{V}_A/\dot{Q}$ (<0.1). It is tempting to speculate that these subjects may have an unidentified PFO. Despite these MIGET data, Robb Glenny has commented that the entire normal resting $A\text{-}aDO_2$ can be accounted for by postpulmonary shunt (76).

It is generally taught from data obtained through the use of the MIGET that $\dot{V}_A/\dot{Q}$ inequality contributes to the majority of the $A\text{-}aDO_2$ at rest through submaximal exercise ($\dot{V}O_2$ <2.0 L/min) at sea level, while at higher levels of exercise intensity diffusion

limitation predominates. In this paradigm, right-to-left shunt does not significantly contribute to the A-aDO_2 during exercise. Torre-Beuno *et al.* (229) demonstrated that during exercise at sea level the predicted A-aDO_2 (i.e., that explainable by $\dot{V}_A/\dot{Q}$ inequality) *exceeded* the measured A-aDO_2 (i.e., that explainable by all sources of venous admixture) up to a $\dot{V}O_2$ of ~3.0 L/min, and no statistical differences were observed between the measured and predicted A-aDO_2. In the companion paper by Gale *et al*. (69) there was also no statistical differences in the mean $LogSD_{\dot{Q}}$ and $LogSD_{\dot{V}}$ (indexes of dispersion), and no statistical differences in the dispersion of inert gas retention ($DISP_R$), excretion ($DISP_E$), or the difference in these parameters ($DISP_{R-E}$). Briefly, $DISP_R$, $DISP_E$, and $DISP_{R-E}$ are derived directly from the inert gas retention/excretion data. $DISP_R$ and $DISP_E$ reflect the root-mean square difference between measured values of retention and excretion and those for a homogenous lung (with no $\dot{V}_A/\dot{Q}$ inequality), and $DISP_{R-E}$ is the root-mean square difference between $DISP_R$ and $DISP_E$. Only the slope of the individual regression lines for $DISP_R$ was found to be statistically different during exercise (up to a $\dot{V}O_2 = 2.71 \pm 0.53$) at sea level. Hammond *et al*. (85) followed up on the studies by Gale *et al.* and Torre-Bueno *et al.* that suggested a trend for increasing $\dot{V}_A/\dot{Q}$ inequality at higher levels of exercise intensity. In this study the predicted A-aDO_2 exceeded the measured A-aDO_2 up to a $\dot{V}O_2$ of ~2.0 L/min, where thereafter the measured A-aDO_2 was statistically greater than the predicted at a $\dot{V}O_2 = 3$ and 4 L/min. Wagner *et al*. (235) also reported data in 8 subjects during exercise at sea level and demonstrated no significant changes in the $LogSD_{\dot{Q}}$, $LogSD_{\dot{V}}$, $DISP_R$, $DISP_E$, and $DISP_{R-E}$, yet the measured A-aDO_2 did exceed that of the predicted during exercise at a $\dot{V}O_2$ >35 ml/kg/min. Of note only when these data from Wagner *et al*., ($n = 8$) were combined with

those data from Gale *et al*., (n = 8) significant differences in all indexes of $\dot{V}_A/\dot{Q}$ inequality were observed. Hopkins *et al*. (102) contributed to this body of work by reporting data obtained using the MIGET in 10 highly trained endurance athletes. In this study the measured A-aDO_2 only exceeded the predicted A-aDO_2 at a $\dot{V}O_2$ = 5.0 L/min, and only $LogSD_{\dot{Q}}$ was shown to increase. The authors comment that at maximal exercise areas of low $\dot{V}_A/\dot{Q}$ (<0.1) accounted for ~1% of the blood flow, although intrapulmonary shunt was not observed. They also comment on the fact that during exercise ventilation increases out of proportion to $\dot{Q}_T$ (in this study ~20 fold increase in $\dot{V}_E$, and ~6 fold increase in $\dot{Q}_T$), and because of this, the effects of $\dot{V}_A/\dot{Q}$ inequality on the A-aDO_2 are minimized. Reeves *et al.,* (193) have also made the comment that because of the 20 fold increase in $\dot{V}_E$ and 6 fold increase in $\dot{Q}_T$, the overall $\dot{V}_A/\dot{Q}$ ratio increases from ~1 at rest to as high as 5 or 6 at maximal exercise, and therefore even the lowest $\dot{V}_A/\dot{Q}$ region during maximal exercise is higher than the highest $\dot{V}_A/\dot{Q}$ region at rest. This fits with the data from Hopkins *et al.,* (102) which report an improvement in $LogSD_{\dot{V}}$ from rest to exercise, and no difference during exercise. In contrast, Hopkins *et al*. (102) do report an increase in $LogSD_{\dot{Q}}$ at a $\dot{V}O_2$ of ~4.3 and ~5.1 L/min, yet only a significant difference between the measured and predicted A-aDO_2 at the higher $\dot{V}O_2$. Rice *et al.* (195) investigated difference in $\dot{V}_A/\dot{Q}$ inequality using the MIGET in high level endurance athletes with documented history of exercise-induced arterial hypoxemia (EIAH), and in controls subjects without EIAH. Although no difference was observed in the $LogSD_{\dot{Q}}$ and $LogSD_{\dot{V}}$, the measured A-aDO_2 did exceed the predicted A-aDO_2 at a $\dot{V}O_2$ of ~3.5 and 4.5 L/min.

To summarize, Torre-Beuno *et al.* demonstrated no increase in $\dot{V}_A/\dot{Q}$ inequality and no evidence of diffusion limitation up to a $\dot{V}O_2$ of 3.5 L/min at sea level. Gale *et al.* found no significant differences in any index of dispersion up to a $\dot{V}O_2$ of 2.7 L/min at sea level. Hammond *et al.* showed evidence of a diffusion limitation at a $\dot{V}O_2$ of 3 and 4 L/min and a corresponding increase in $\dot{V}_A/\dot{Q}$ inequality, resulting from predominantly an increase in $LogSD_{\dot{V}}$ at a $\dot{V}O_2$ of 3 L/min and an increase in both $LogSD_{\dot{Q}}$ and $LogSD_{\dot{V}}$ at a $\dot{V}O_2$ of 4 L/min. Wagner *et al*. reported no increase in $\dot{V}_A/\dot{Q}$ inequality or any index of dispersion from rest to a $\dot{V}O_2$ of ~3.7 L/min, and evidence of a diffusion limitation at a $\dot{V}O_2$ of ~2.7 and ~3.7 L/min. Hopkins *et al*. showed an increase in $\dot{V}_A/\dot{Q}$ inequality at a $\dot{V}O_2$ of ~2, 4, and 5 L/min and evidence of a diffusion limitation only at a $\dot{V}O_2$ of ~5 L/min, while $LogSD_{\dot{V}}$ decreased and $LogSD_{\dot{Q}}$ increased, from rest to exercise at sea level. Rice *et al*. reported no increase in $\dot{V}_A/\dot{Q}$ inequality, $LogSD_{\dot{Q}}$, or $LogSD_{\dot{V}}$, from rest to exercise (up to $\dot{V}O_2$ of ~4.5 L/min) and evidence of a diffusion limitation at a $\dot{V}O_2$ of ~3.5 and ~4.5 L/min.

Thus, from data using the MIGET during exercise up to a $\dot{V}O_2$ of ~5 L/min the results are somewhat inconsistent; with $\dot{V}_A/\dot{Q}$ inequality and various indexes of dispersion increasing in some, and either not changing or decreasing in others. Of the studies by Hammond *et al*. and Hopkins *et al*. that demonstrate an increase in $\dot{V}_A/\dot{Q}$ inequality up to a $\dot{V}O_2$ of ~5 L/min, $\dot{V}_A/\dot{Q}$ inequality may account for 25-40% of the measured $A\text{-}aDO_2$ (i.e., 5-10 mm Hg of the measured 25-30 mm Hg). Regardless of whether or not a diffusion limitation is developing at this high-intensity exercise, this increase in $A\text{-}aDO_2$ due to $\dot{V}_A/\dot{Q}$ inequality can easily be accounted for by a ~1% shunt (140, 214). As a reminder, the MIGET theoretically provides a measure of $\dot{V}_A/\dot{Q}$

inequality and intrapulmonary shunt, with the remaining portion of the A-aDO_2 not explained by these factors being attributed to diffusion limitation. Therefore, diffusion limitation is never directly measured and always inferred by process of elimination. Clearly, this is only a limitation inasmuch as the MIGETs accuracy in measuring the other factors. Physiologically, the likelihood of a diffusion limitation developing even during heavy exercise seems improbable. As previously discussed (*Pulmonary Diffusion, p.* 43) complete end-capillary O_2 diffusion equilibration occurs in ~0.3 sec of the ~0.75 sec mean pulmonary capillary transit time. During exercise the increase in pulmonary blood flow and potential reduction in mean pulmonary capillary transit time is offset by a simultaneous increase in Vc owing to an increase in left-atrial pressure. Pulmonary capillary blood volume can increase ~3x, from ~70 to 210 ml, meaning that even when $\dot{Q}_T$ is ~25 L/min, mean pulmonary capillary transit time is still ~0.5 sec. However, it should be appreciated that in elite athletes capable of attaining very high levels of exercise (i.e., $\dot{V}O_2$ ~5 L/min and $\dot{Q}_T$ ~35 L/min), mean pulmonary capillary transit time would approach 0.35 sec, and therefore some degree of diffusion limitation would be expected. Data from Hsia *et al*. provide evidence against the possibility for a diffusion limitation, albeit in exercising foxhounds, demonstrating that with pneumonectomy of 42% of their lung, a plateau in diffusing capacity is never reached and diffusion equilibration is maintained even at maximal exercise (104-106).

Importantly, when interpreting the data suggesting an increase in diffusion limitation during high intensity exercise, it is important to remember that it may not be mean pulmonary capillary transit time that is the defining factor. Instead it should be appreciated that there is likely a spectrum of pulmonary capillary transit times throughout

the lung and those that are sufficiently rapid may comprise the volume of blood necessary to explain the development of a diffusion limitation.

Pulmonary Gas Exchange During Exercise in Acute Hypoxia

As previously described, hypoxia represents a useful tool for respiratory physiologists as it provides yet another means to challenge the pulmonary system for performing adequate gas exchange. Lilienthal *et al.* (137) measured a similar increase in the A-aDO_2 in men during exercise at sea level and breathing an FIO_2 equivalent to 13000ft. The conclusions reached by these authors was that during exercise at sea level, shunt predominantly explains the measured A-aDO_2 while at 'altitude', diffusion limitation predominantly explains the measured A-aDO_2. Asmussen and Neilsen (5) studied pulmonary gas exchange efficiency during exercise breathing room air, an FIO_2 = 0.12, and 1.0. Their interpretation applied the entire shunt measured during exercise breathing an FIO_2 = 1.0 to the other FIO_2s, and concluded that diffusion limitation had no measurable impact on the A-aDO_2, during exercise breathing any FIO_2. Following the advent of the MIGET technique, Gale *et al.* (69) report measures of dispersion during exercise at 5000, 10,000, and 15,000ft with only $LogSD_{\dot{Q}}$ and the related $DISP_R$ index increasing during heavy exercise at 10,000 and 15,000ft (no differences were observed at 5000ft). These data track with the companion paper by Torre-Bueno *et al.* (229) where the development of a diffusion limitation was inferred during exercise at 10000 and 15000ft. Wagner *et al*. followed up on these studies, by collecting data in more subjects at rest and during exercise at 10000 and 15000ft. At rest, there was no increase in $\dot{V}_A/\dot{Q}$ inequality or any index of dispersion, although during exercise overall $\dot{V}_A/\dot{Q}$ inequality increased at 10000 and 15000ft. Specifically due to increases in $LogSD_{\dot{Q}}$ and $DISP_R$,

while no differences were observed in $LogSD_{\dot{V}}$ and $DISP_E$. Furthermore, an increase in diffusion limitation was detected at lower levels of exercise intensity compared to exercise at sea level. In contrast to the lack of an effect in $LogSD_{\dot{V}}$ and $DISP_E$ noted by Wager *et al.,* (235) in the study by Hammond *et al.* (86) all of the indexes of dispersion increased during exercise breathing an $FIO_2 = 0.11$. However again, significant diffusion limitation was detected during exercise. In the seminal work from 'Operational Everest II' by Wagner *et al.* (239) overall $\dot{V}_A/\dot{Q}$ inequality increased during exercise as the altitude increased, although significant differences in indexes of dispersion were predominantly observed when $P_B = 282$ ($n = 5$), and 240 mm Hg ($n = 5$) and were constrained only to $LogSD_{\dot{Q}}$ and $DISP_R$. Again, diffusion limitation was detected during exercise, which occurred at lower exercise intensities as the altitude increased.

Although overall increases in $\dot{V}_A/\dot{Q}$ inequality, particularly from perfusion dispersion are present in the literature it should be remembered that the contribution of $\dot{V}_A/\dot{Q}$ inequality to the $A\text{-}aDO_2$ decreases as the level of hypoxia increases (214, 239). The rationale for this is similar to why the effect of a given volume of right-to-left shunt on the $A\text{-}aDO_2$ also decreases as the level of hypoxia increases. Just as the PaO_2 becomes closer to $P\bar{v}O_2$ (diminishing the effect of shunt) the $\dot{V}_A/\dot{Q}$ ratios of individual lung regions are positioned on the steep portion of the O_2 dissociation curve. Furthermore, $\dot{V}_A$ increases even more out of proportion to $\dot{Q}_T$ during exercise in hypoxia compared to exercise at sea level, further right-shifting the lung to an overall *higher* $\dot{V}_A/\dot{Q}$ ratio. As described by Calbet *et al*. (31) the fact that $\dot{V}_A$, V_T, and flow are all increased for a given VO_2 compared to exercise at sea level, this should further reduce ventilatory inhomogeneities and result in improved $\dot{V}_A/\dot{Q}$ matching.

Rationale for an increase in diffusion limitation during exercise in hypoxia seems more plausible than at sea level with PAO_2 being decreased and $\dot{Q}_T$ being increased. Thus, for a given $\dot{V}O_2$, mean pulmonary capillary transit time is likely less than at sea level (100) despite the potential for the further recruitment of pulmonary capillaries (33). Furthermore, although DLO_2 increases in hypoxia the effective slope between PAO_2 and PvO_2 increases which will function to reduce the rate of O_2 uptake, as described by Piiper and Scheid (183, 184). Nevertheless Calbet *et al*. present an interesting interpretation of this theory, where according to the model of Piiper and Scheid (183) and data from Wagner *et al*. (229, 235) the increase in A-aDO_2 for a given $\dot{Q}_T$ should be more pronounced in hypoxia than when breathing room air at sea level, i.e., the slope of the A-aDO_2 vs. $\dot{Q}_T$ relationship should be steeper. However, Calbet *et al*. (31) demonstrate that contrary to this expected relationship, the slope is only shifted upward, meaning for a given $\dot{Q}_T$ the A-aDO_2 is proportionally higher in hypoxia than breathing room air at sea level. Calbet *et al*. (30) have also demonstrated that after increasing $\dot{Q}_T$ (by ~2 L/min) via hemodilution, no change was observed in the A-aDO_2, which they use as further evidence that $\dot{Q}_T$ may not be limiting pulmonary gas exchange in hypoxia. Together, these data suggest the possibility that the prevailing paradigm put forth by Piiper and Scheid may not entirely describe the measured response to pulmonary gas exchange efficiency during exercise in hypoxia.

Pulmonary Gas Exchange After Acclimatization to Hypobaric Hypoxia

It is well established that pulmonary gas exchange progressively worsens in a workload dependent manner during exercise at sea level (48). This impairment in pulmonary gas exchange efficiency during exercise is exacerbated in acute hypoxia, such

that for any given $\dot{V}O_2$, the A-aDO_2 is greater compared to exercise in normoxia (235). Following acclimatization to hypobaric hypoxia, pulmonary gas exchange efficiency is thought to improve compared to acute hypoxia (88, 203). The classic study from Dempsey *et al.* (47) reported a trend for an increased A-aDO_2 during treadmill walking after 4 days at 3100 m compared to sea level, and a partial normalization during the same exercise protocol following 21 days at 3100m compared to that obtained after 4 days. Bebout *et al.* (13) subsequently demonstrated that, compared to acute normobaric hypoxia, acclimatization to 3800m for 2 weeks resulted in an ~3 mm Hg reduction in the A-aDO_2 during submaximal cycle ergometer exercise. Calbet *et al.* (28) subsequently reported that, compared to acute normobaric hypoxia, acclimatization to 5260m for 9-10 weeks resulted in an ~9 mm Hg reduction in the A-aDO_2 during submaximal cycle ergometer exercise. Collectively, these data suggest that pulmonary gas exchange efficiency in non-acclimatized individuals improves with acclimatization to high-altitude compared to acute hypoxia.

Acclimatization to hypobaric hypoxia is characterized by a multitude of physiologic adaptations, notably a time-dependent increase in ventilation (250). Compared to acute hypoxia, ventilatory acclimatization helps to increase CaO_2 by increasing PAO_2 and the driving gradient for O_2 diffusion at the alveolar-capillary interface, subsequently increasing PaO_2 and therefore, SaO_2. Consequently, compared to acute hypoxia the further increase in $\dot{V}_A$, and therefore PAO_2 with acclimatization would theoretically reduce the relative contributions from $\dot{V}_A/\dot{Q}$ inequality and diffusion limitation while increasing the relative contribution of right-to-left shunt on the A-aDO_2. Indeed, as is the case in acute hypoxia, the greater increase in $\dot{V}_A$ should equate to a

greater right-shifted mean $\dot{V}_A/\dot{Q}$ ratio, thereby lessening potential disparities in the PO_2 between alveoli (63, 193, 204). Diffusion limitation would theoretically also be reduced compared to acute hypoxia by way of an increased driving gradient for O_2 diffusion (243), increased $P\bar{v}O_2$, and a potential improvement in diffusing capacity for O_2 (3). Lastly, a given volume of right-to-left shunt would have a greater effect on the A-aDO_2 due to the difference between $P\bar{v}O_2$ and PaO_2 increasing after acclimatization compared to acute hypoxia. However, this possibility has not been directly investigated.

REGULATION OF BLOOD FLOW THROUGH INTRAPULMONARY ARTERIOVENOUS ANASTOMOSES

In contrast to functional gas exchange dependent techniques, which do not report significant intrapulmonary shunt during exercise, there are several 'anatomic based' techniques that have been used to demonstrate blood flow through large diameter IPAVA, during various conditions (described below). These anatomic based techniques are based on the assumption that the lung provides a biological sieve and receives 100% of the $\dot{Q}_T$; therefore particles injected [microspheres, microbubbles or radiolabeled macroaggregates of albumin (MAA)] into the venous circulation will be filtered be the sieve action of the pulmonary capillaries, which have a mean diameter of 7-10 μm (75, 199). However, these particles can escape pulmonary filtration if they bypass the pulmonary capillaries and flow through a large diameter vascular conduit, i.e., IPAVA. Thus, the transpulmonary passage of these particles demonstrates blood flow through IPAVA. It is worth mentioning that data collected using, either microspheres,

microbubbles or radiolabeled MAA, all report very consistent findings, as outlined below.

Exercise

Blood flow through IPAVA, although trivial or absent at rest, was demonstrated to increase during exercise in the classic studies by Stickland *et al.* (216) and Eldridge *et al.* (53). Kennedy *et al.* (115) demonstrated that the transpulmonary passage of saline contrast during exercise was not different between men and women. While others have demonstrated the transpulmonary passage of saline contrast during exercise breathing room air (54, 115, 130, 131, 143), it should be noted that in the work by La Gerche *et al.* (130) and Lalande *et al.* (131) subjects were not screened for PFO. Neglecting to screen for PFO introduces the possibility that the appearance of left-sided contrast is due to blood flow across the PFO, in addition to blood flow through IPAVA.

The aforementioned data using TTSCE provide evidence of blood flow through IPAVA, but this technique does not quantify the volume of blood flow through IPAVA, nor does it provide us with information about the size/diameter of IPAVA. However, intravenously injected 25 and 50 μm microspheres in exercising dogs confirms that blood flow through IPAVA does occur during exercise and was calculated to be 1.4% (range 0.2 to 3.1 %) of the $\dot{Q}_T$ (215). Interestingly, the observation of increased blood flow through IPAVA in the exercising dog was less in the isolated dog lung preparation (<0.02% of the $\dot{Q}_T$). This suggests the possibility that either some blood borne factor or innervation to the lung is responsible for increasing blood flow through IPAVA. Studies in healthy humans using ^{99m}Tc-MAA and gamma camera imaging measured blood flow through IPAVA to be 1.3% (range −0.3 to 2.7%) of the $\dot{Q}_T$ during maximal exercise

(141). These studies used MAA with a mean diameter of 20–40 μm and 90% of MAA between 10 and 90 μm in size. Studies prior to these used ^{99m}Tc albumin microspheres with a size range of 7-25 um in diameter and these authors found an increase in shunt to 2.4% (range -2.4 to 5.9%) of $\dot{Q}_T$ in 5 normal subjects during exercise (261). Furthermore, recent work from our laboratory demonstrates using ^{99m}Tc-MAA and gamma camera imaging that ~1.4% of the $\dot{Q}_T$ flows through IPAVA during exercise in healthy humans (n = 10).

To summarize these data, the finding that ~2% of the $\dot{Q}_T$ flows through IPAVA during exercise appears to be a reproducible and consistent finding. The extent of the variability that exists in this area of the literature pertain to factors such as the exercise intensity where subjects begin to demonstrate blood flow through IPAVA, and the volume of blood flow through IPAVA. Nevertheless, using either microspheres, microbubbles or radiolabeled MAA, healthy human subjects demonstrate blood flow through IPAVA during exercise that is quantitatively and qualitatively very similar. The mechanisms regulating blood flow through IPAVA during exercise at sea level are unknown, although a recurring hypothesis is that blood flow through IPAVA may be responding passively to the increases in $\dot{Q}_T$ and/or PASP (15, 216). In this way, IPAVA may serve a functional role of minimizing excessive increases in pulmonary pressure, however if this were true PASP would be expected to increase during exercise breathing a FIO_2 = 1.0 when blood flow through IPAVA is prevented, and this finding has not been observed.

Normobaric Hypoxia

Compared to breathing room air at rest at sea level, where blood flow through IPAVA is trivial or non-detectable (55), breathing hypoxic gas at sea level (normobaric hypoxia) is known to increase blood flow through IPAVA at rest (134). During exercise in normobaric hypoxia qualitatively there is an increased degree of blood flow through IPAVA in healthy humans that occurs at lower workloads compared to breathing room air at sea level (54, 143). These data are supported from work by Niden and Aviado (171) demonstrating the number of large diameter microspheres recovered in the pulmonary venous effluent increased in intact dogs ventilated with a $FIO_2 = 0.10$. More recently, Bates *et al.* (12) also demonstrated the transpulmonary passage of microspheres in intact rats ventilated with a $FIO_2 = 0.08$. Interesting, similar to the work by Stickland *et al.* (215) using isolated dog lungs, Bates *et al.* (12) reports blood flow through IPAVA is minimal in the isolated rat lung preparation. Unpublished observations from our lab also demonstrate an increase in blood flow through IPAVA in healthy humans at rest breathing an $FIO_2 = 0.12$, and report that ~1.3% of the $\dot{Q}_T$ flows through IPAVA (Duke, Elliott, *et al. In Preparation*). Nevertheless, the mechanism(s) regulating hypoxia-induced blood flow through IPAVA remain unknown.

Compared to exercise, hypoxia-induced blood flow through IPAVA occurs at lower $\dot{Q}_T$ and before significant increases in PASP (<30-45 min). Therefore, it is possible the hypoxia-induced increase in blood flow through IPAVA is regulated differently. Work by Laurie *et al.* (134) showed a correlation between decreasing SpO_2 and increases in blood flow through IPAVA. However to date, no study has investigated the effects of decreases in PaO_2 independently of CaO_2 (or vice versa) on the regulation of blood flow

through IPAVA. An attractive hypothesis is the reduction in PO_2 secondary to breathing hypoxic gas mixtures, stimulates the release of ATP via red blood cells (56, 57, 77), which function as a vasodilatory signal for IPAVA. Arterial hypoxemia is also a sympathetic stimulant that increases levels of circulating catecholamines (61). However, data from Laurie *et al.* (134) show that in healthy humans breathing an $FIO_2 = 0.12$, blood flow through IPAVA is unaffected after β-adrenergic receptor blockade via i.v. propranolol. Accordingly, the mechanisms responsible for hypoxia-induced blood flow through IPAVA remain elusive.

Hypobaric Hypoxia

Few studies investigating blood flow through IPAVA in hypobaric hypoxia are present in the literature. Using transcranial Doppler, Imry *et al.* (107) investigated the occurance of emboli detected in the cerebral circulation post the peripheral venous injection of agitated saline contrast at rest and during exercise on acute ascent to 3450m and after 8 days at 3450m. Of the 8 subjects without PFO, no subjects demonstrated cerebral microbubbles at rest at altitude before or after acclimatization. During exercise, 5/8 subjects demonstrated cerebral microbubbles on acute ascent to 3450m and no subjects did after acclimatization. More recent field studies to a higher altitude of 5050m using TTSCE to detect blood flow through IPAVA have also been carried out by Foster *et al.* (67). This work was done after 21 days of acclimatization to 5050m and demonstrated that in healthy sea level inhabitants after acclimatization to high-altitude blood flow through IPAVA at rest was qualitatively reduced compared to normobaric hypoxia. The authors speculated that several possibilities might explain the lower than expected blood flow through IPAVA including pulmonary vascular remodeling and/or

reduced $\dot{Q}_T$ with acclimatization compared to acute normobaric hypoxia. Additionally, it remains possible that the *in vivo* microbubble dynamics of saline contrast are altered in hypobaric environments, a topic expanded upon in Chapter VI.

Alveolar Hyperoxia

Of particular interest in this field are the studies in healthy humans breathing 100% O_2 demonstrating that blood flow through IPAVA is either prevented or qualitatively reduced as detected using TTSCE (144). One criticism of these findings is that the reduced appearance of left-sided contrast is due to changing the external partial pressure of the environment of the intravenously injected bubbles, but this criticism was experimentally refuted (54). These findings using TTSCE are also supported from work by Niden and Aviado (171) which demonstrate the reduction in large diameter microspheres collected in the pulmonary venous effluent in dogs ventilated with a FIO_2 = 1.0. Potential criticism with this work is that blood flow through IPAVA was increased secondary to pulmonary embolization.

The mechanism(s) responsible for the hyperoxia-mediated reduction in blood flow through IPAVA during exercise at sea level are unknown. Entertaining the hypothesized mechanism of exercise-induced blood flow through IPAVA being due to increases in $\dot{Q}_T$ and PASP, it is likely that an alternative mechanism regulating the hyperoxia-mediated reduction in blood flow through IPAVA exists. This is because, during exercise breathing a FIO_2 = 1.0 for any given $\dot{V}O_2$, $\dot{Q}_T$ is reduced by ~10%. Yet blood flow through IPAVA during maximal exercise breathing a FIO_2 = 1.0 is still less than blood flow through IPAVA during submaximal exercise breathing room air, when $\dot{Q}_T$ is no different or even higher.

The effect of oxygen tension on regulating blood flow through IPAVA is particularly provocative as these data suggest that some of the pulmonary vasculature may be regulated opposite that of the conventional pulmonary circulation, e.g. hypoxia increases, whereas hyperoxia reduces blood flow through IPAVA. However, this resemblance to the regulation of the systemic circulation is also present in the regulatory pathways controlling the vascular tone of the ductus arteriosus (251). Considering the ductus arteriosus is an important vessel in the fetal cardiopulmonary circulation, and that right-to-left shunt is an important factor for development in utero, it has been hypothesized by us and others that IPAVA may represent remnant vessels of the fetal circulation (134, 158). Interestingly, work by McMullan *et al.* (158) showed that blood flow through IPAVA occurred in developing sheep, but was reduced in the adult sheep. Therefore, it seems logical to speculate potential mechanism(s) regulating blood flow through IPAVA when breathing a $FIO_2 = 1.0$ may resemble those that are known to regulate the tone of the ductus arteriosus.

Expansion on this theory and potential regulatory pathways is provided in Chapter V. However, contraction of the ductus arteriosus is stimulated by an increase in oxygen tension from fetal to neonatal levels, causing the inhibition of potassium (K_v) channels within ductus smooth muscle cells, membrane depolarization, and subsequent calcium entry via voltage gated L-type calcium channels (230). Pharmacologic blockade of L-type calcium channels via calcium channel blockers (e.g., nifedipine) may prevent the necessary increase in intracellular calcium for constriction of IPAVA. However, intracellular calcium levels may also be increased independently by calcium release from the sarcoplasmic reticulum and from non voltage gated calcium channels (252).

Nevertheless, nifedipine has been shown to reduce or prevent the increase in pulmonary artery pressure associated with acute hypoxia (207).

Endothelium-derived nitric oxide (NO) is a major endogenous agent regulating pulmonary vascular tone, which is primarily regulated by increases in cGMP via soluble guanylyl cyclase activation and subsequent activation of protein kinase G. The three isoforms of NO synthase, neuronal (nNOS), inducible (iNOS) and eNOS have all been identified in the lung (71). Breathing hyperoxia is also associated with an increase in reactive oxygen species (ROS), predominantly from cytochrome c oxidase subunit III in the electron transport chain, but also potentially from NADPH oxidase (252). This increase in ROS associated with hyperoxia has been demonstrated to attenuate endothelial mediated vasodilation in human skin (268). Additionally, hyperoxia has been shown to increase forearm vascular resistance, a finding that is abolished after high-dose i.v. ascorbic acid (153). Collectively, these data lend support that hyperoxia may reduce production of and/or bioavailability of NO and therefore, contribute to the hyperoxia-mediated reduction in blood flow through IPAVA.

Another attractive hypothesis is the involvement of 20-hydroxyeicosatetraenoic acid (20-HETE), an ω-hydroxylation product of arachadonic acid from cytochrome P450. Interestingly, 20-HETE has been demonstrated to not only be a potent constrictor of multiple vascular beds (renal, cerebral and skeletal muscle), it has been shown to be produced in an O_2-dependent fashion (89, 129, 167). Across a physiologic range of PO_2, from 20 to 160 mm Hg, 20-HETE formation increases nearly linearly with the increasing PO_2 (89). However, to my knowledge studies investigating the formation of 20-HETE in increasingly hyperoxic conditions have not been done. Moreover, there are many

isoforms of the cytochrome P450 enzyme with different families and subtypes predominating in different vascular beds, and a selective inhibitor for the ω-hydroxylation arachadonic acid (i.e., the formation of 20-HETE) is not approved for human use (17-Octadecynoic acid) (167, 170).

CHAPTER III

METHODS

INFORMED CONSENT

The University of Oregon Institutional Review Board via Research Compliance Services and the Committee for Protection of Human Subjects formally approved the studies and protocols that constitute this dissertation (Chapters IV-VI). However, in Chapter VI, in addition to the University of Oregon, the institutional review boards from the University of Colorado Denver and the U.S. Department of Defense also formally approved the protocols therein. Prior to all studies, I verbally discussed procedures and risks with every subject and written informed consent was obtained from all subjects prior to participation.

ECHOCARDIOGRAPHIC SCREENING

Through collaboration with the Oregon Heart & Vascular Institute one of two highly skilled (a combined 40+ years of experience) registered diagnostic cardiac sonographers works in our laboratory twice a week, and have performed all ultrasonography for the work in this dissertation (Randy Goodman, RDCS, BS, and Eben Futral, RDCS, MBA). All subjects underwent a comprehensive echocardiographic screening, performed by Randy Goodman or Eben Futral and overseen by myself. A three-lead electrocardiogram is placed and subjects are positioned in the left lateral decubitus position in a reclining chair with head resting on their left arm. This position not only allows the heart to move anteriorly and laterally against the subject's ribcage, but also allows the ribs to spread apart and facilitate obtaining a clear apical, four

chamber view of the heart. For convenience and due to the ultrasound probe and required gel, male subjects are asked to go shirtless and female subjects are provided a scrub top.

The process begins with the sonographer thoroughly inspecting cardiac structures to rule out potential cardiac abnormalities. Including the right ventricular outflow tract to identify signs of obstruction, and the pulmonary artery and aorta for signs of stenosis. Left-ventricular function and all valves are inspected to rule out signs of congenital heart disease, and the pericardium is inspected to rule out signs of pericardial effusion. Once normal cardiac function and signs of heart disease are ruled out, the next step is identification of a PFO.

Detection of Patent Foramen Ovale

The foramen ovale is a critical right-to-left shunt in the fetal cardiopulmonary circulation and is patent in 100% of healthy humans in utero. At birth, the reversal of pressure gradients between the right and left atria result in the septum primum covering, and therefore functionally closing, the foramen ovale within the septum secundum (71, 82, 118). Over time fusion of the septum primum/secundum occurs in most infants (i.e., permanent anatomical closure of the foramen ovale); however, it has long been recognized that the foramen ovale does not permanently close in some adult humans and remains patent. The classic study by Hagen *et al*. (82) reported a prevalence patent foramen ovale (PFO) of 25-35% identified using a probe during autopsy (n = 965). In these humans the septum primum/secundum offers a functional closure, rather than anatomical closure, but only when left atrial pressure exceeds right atrial pressure. In this condition blood flow across the foramen ovale is either prevented or allowed to flow from the left atrium to the right atrium, however when right atrial pressure exceeds left

atrial pressure blood in the right atrium flows directly into the left atrium. Identification of PFO in healthy, living humans is accomplished by exploiting the pressure dependence of right-to-left blood flow through the PFO using a technique called saline contrast echocardiography, and using this technique recent work has revealed ~35-40% of adult humans have a PFO (55, 156, 266).

Performing saline contrast echocardiography involves first placing an intravenous catheter (see Subject Instrumentation) in the antecubital fossa that is connected to an extension set and a three way stopcock. Attached to the stopcock are two 10 ml syringes, one with 3 ml of saline and one with 1 ml of air. This saline-air mixture is agitated back and forth, vigorously, for 10-15 sec creating a microbubble suspension that is then injected into the peripheral vein. With the subject breathing normally, the microbubbles are rapidly visualized as a "cloud of echoes" that opacify the right heart after traveling via the venous blood to the right heart. With the heart visualized in the apical, four-chamber view, the left heart can be simultaneously monitored and the appearance of contrast in the left heart within 3 cardiac cycles is evidence for the presence of a PFO. Although past work has suggested that visualizing left heart contrast up to 5 cardiac cycles post right heart opacification is evidence for a PFO (267), recent work has demonstrated that the optimal timing of contrast appearing in the left heart is within 4 cardiac cycles (18).

The rationale for concern over the optimal number of cardiac cycles for PFO detection is that there is a second mechanism by which microbubbles can enter the left heart, via flowing through the pulmonary circulation. In healthy humans at rest mean pulmonary (whole lung) transit time is ~9 sec (100), meaning for someone with a resting

heart rate of 40 bpm, 6 cardiac cycles must occur before contrast that has traveled through the pulmonary circulation can appear in the left heart. Thus, observing contrast in the left heart in ≤4 cardiac cycles is fairly conclusive evidence for a PFO, yet observing contrast in the left heart in >4 cardiac cycles is inconclusive for a PFO because it could have reached the left heart after flowing through the pulmonary circulation. As previously described this is most likely to occur by traversing the pulmonary circulation via large diameter IPAVA.

In order to conclusively identify the presence of a PFO, saline contrast injections are repeated in coordination with a Valsalva maneuver. The Valsalva maneuver is designed to transiently elevate right atrial pressure and create conditions that are optimal for detecting blood flow through the PFO. Performing a Valsalva maneuver is very simple, although proper coaching of the subjects is critical in order to accurately identify PFO. Subjects are instructed to take a small breath, "bear down" and exhale against a closed glottis, creating increased intra-abdominal pressure and preventing blood flow from returning to the right side of the heart via the inferior vena cava. This increase in pressure is maintained for ~15 sec, where just before release the agitated saline contrast is injected. Upon release of the Valsalva maneuver, the saline contrast microbubble suspension is immediately visualized in the right heart in coordination with the previously restricted, and therefore increased volume of blood. Right atrial pressure is then transiently elevated above that in the left atrium and any blood flow across the PFO will be accompanied by microbubbles that can be visualized in the left heart. This procedure is not only a very reliable method of detecting PFO but it has been recently demonstrated to correlate with the size of PFO as determined using intracardiac

echocardiography (64). Although not part of this dissertation we have recently published data on 176 subjects that have been screened within our laboratory that reports a 38% prevalence for PFO (55). These data are also in agreement with similar work using transthoracic saline contrast echocardiography that also demonstrate a 35-38% prevalence of PFO in the general population (156, 266).

Pulmonary Artery Systolic Pressure

The next step in the echocardiographic screening process is the determination of pulmonary artery systolic pressure (PASP). This represents the peak blood pressure developed during systole in the pulmonary artery and can be estimated by measuring the peak velocity of retrograde blood flow across the tricuspid valve during systole. When the right ventricle contracts the tricuspid valve is forced closed, preventing blood flow into the right atrium, however a small volume of blood leaks past the tricuspid valve with every cardiac cycle in almost all individuals. The velocity of this blood flow is proportional to the pressure gradient between the right ventricle and right atrium that is in turn, dependent on the pressure within the pulmonary artery. All things equal, a higher pulmonary artery pressure will correspond to an increased peak velocity of blood flow across the tricuspid valve. Using Doppler ultrasound the sonographer carefully aligns the probe so as to direct the signal across the tricuspid valve and the resulting tricuspid regurgitate is visualized as inverted waveforms, representing the velocity of blood flow. The peak of each waveform corresponds to the peak velocity (v) of blood flow and an average of ≥3 measurements is taken. Right atrial pressure (P_{RA}) is then estimated based on the collapsibility of the inferior vena cava as well as the diameter of the inferior vena cava. Collapsibility is determined by imaging the inferior vena cava in coordination with

subjects taking a quick inspiration. Right atrial pressure was determined to be: 3 mm Hg if the inferior vena cava collapses >50% and the diameter being ≤2.1 cm; 15 mm Hg if the inferior vena cava collapses <50% and the diameter is >2.1 cm, and; 8 mm Hg if either of these parameters is indeterminate. These values are then applied to the modified Bernoulli equation (202):

$$\mathrm{PASP} = 4v^2 + P_{RA}$$

Equation 2.14. Modified Bernoulli Equation

The gold standard method of measuring pulmonary pressure is via right heart catheterization and directly measuring pulmonary artery pressure. Doing so allows one to obtain *mean* pulmonary artery pressure, rather than *peak systolic* pulmonary artery pressure, and is subject to fewer limitations, however, prior work has demonstrated a very strong correlation between measurements of PASP and direct right heart catheterization (92, 275). Potential limitations in measuring PASP via echocardiography stem from this technique actually measuring the peak systolic pressure generated within the right ventricle. Thus, this is one prominent reason why we screen subjects for right ventricular outflow tract obstruction in the initial echocardiographic screening process. If present, the pressure generated in the right ventricle would be greater than the pressure in the pulmonary artery distal to the obstruction, and therefore, our measure of PASP would be erroneously high.

Left Ventricular Outflow Tract

The final step in the echocardiographic screening process is the measurement of the diameter of the left ventricular outflow tract. While subjects were in the left lateral decubitus position, the left ventricular outflow tract diameter was measured using 2-

dimensional echocardiography in triplicate and the average was used to determine the cross sectional area. Knowing the cross sectional area of the left ventricular outflow tract allows one to determine stroke volume based on the velocity of blood flow through the outflow tract determined using pulsed wave Doppler ultrasound. This estimate of stroke volume is then multiplied by heart rate determined via lead II of the 3-lead ECG to determine $\dot{Q}_T$. The left ventricular outflow tract diameter is assumed constant, and not to have changed through the duration of the studies and from rest to exercise.

LUNG FUNCTION TESTING

The next step in the screening process, after we have completed the echocardiographic screening is to perform a series of pulmonary function tests. Collectively these tests are performed to ensure that all subjects have normal pulmonary function and no signs of lung disease are present. All tests are conducted according to the American Thoracic Society/European Respiratory Society (ATS/ERS) guidelines (152, 166, 247).

Forced Vital Capacity

The forced vital capacity (FVC) maneuver is designed to determine the maximal volume of air exhaled from a maximal inspiration, performed with a maximally forced expiratory effort. Subject instrumentation consists of a nose-clip and a low resistance mouthpiece, which is fitted over a MedGraphics PreVent pneumotach connected to one of two primary pieces of equipment in our laboratory capable of performing spirometry: (the MedGraphics Ultima CardiO_2 or Elite Series Plethysmograph). With subjects seated upright they are instructed to breathe quietly through the mouthpiece with their feet flat

on the floor and their hands on their knees. The maneuver begins when, at the end of a normal tidal inspiration, subjects are instructed to exhale all the air in their lungs and continue until reaching residual volume (RV). At that point in time subjects are then instructed to take a maximal inspiration, to total lung capacity (TLC), at which point they maximally exhale "blast" all of the air in their lungs to residual volume once again for ≥6 sec. The resulting flow-volume loop recorded represents their *forced* vital capacity, and further analysis of this recording yields information pertaining to other important parameters.

The main secondary parameter is the volume of air exhaled during the first second of their maximal expiration from a maximal inspiration, the forced expiratory volume in 1 sec (FEV_1). In healthy, young individuals the ratio of this volume to their FVC (i.e., FEV_1/FVC ratio) should be ~0.80. A reduced FEV_1 and therefore FEV_1/FVC ratio <0.80 is one indication for air flow limitation/obstruction, which could be due to age or pathology (e.g., chronic obstructive pulmonary disease or asthma). Similar to FEV_1 is the expiratory flow rate between 25% and 75% of their maximal expiration (i.e., FEF_{25-75}). This middle portion of the expiratory volume is effort independent and offers an assessment of small airway reactivity and/or obstruction. In subjects with a reduced FEF_{25-75}, the expiratory portion of the FVC maneuver will be curvilinear in this FEF_{25-75} region and therefore can contribute to a reduced FEV_1.

The ATS/ERS has clear guidelines on determining the validity and reproducibility of the FVC maneuver and requires a minimum of 3 successful trials. Acceptable repeatability is achieved when the difference between the largest and next largest FVC and FEV_1 is ≤0.150 L. Each of these parameters also has defined predicted values based

on subjects age, sex and height. Subjects in this dissertation had no spirometric variable, particularly FVC, FEV_1 and FEV_1/FVC ratio, <90% predicted.

Slow Vital Capacity

The slow vital capacity (SVC) is performed after the FVC maneuver and is essentially the same maneuver performed in a slow and controlled fashion with the intent to measure subject's vital capacity. Performing a SVC begins with subjects positioned in the same manner as during the FVC. They are encouraged to breathe quietly at normal functional residual capacity (FRC), in some cases allowing subjects to relax by taking a sigh facilitates breathing at FRC. Subjects are required to take ≥4 tidal breaths at a constant FRC, at which point at the end of the next tidal expiration subjects are instructed to inhale slowly to TLC. This inhalation should not be forced, but also not unduly slow and verbal encouragement to fully reach TLC is imperative. Once at TLC subjects are instructed to relax and exhale passively from the natural recoil of the chest wall, again in a natural and not forced manner. Eventually effort is required to continue expiration at which point verbal encouragement to fully exhale to RV is similarly imperative. Performing the vital capacity in a slow manner reduces the rate of small airway collapse and therefore typically allows for a slightly larger vital capacity measurement when comparing to the FVC. Repeatability requirements for the SVC are similar to the FVC, ≥3 SVC maneuvers with the largest and next largest being ≤0.150 L apart.

Whole-Body Plethysmography

Spirometric variables are clinically very useful for detecting and quantifying the severity of lung disease, although the FVC and SVC maneuvers do not yield measurements of absolute lung volumes, specifically, TLC, FRC, and RV. Although

these are not clinically irrelevant, they technically more challenging to obtain, which limits their use in clinical practice outside of specialty pulmonology clinics. Nevertheless, whole body plethysmography is the gold standard method to measure lung volumes and is based on Boyle's Law:

$$P_1V_1 = P_2V_2$$

Equation 2.15. Boyles Law

which states that under isothermal conditions, when a constant mass of gas is compressed or decompressed, the gas volume decreases or increases, and the gas pressure changes such that the product of pressure and volume are constant. The pressure within, and volume of, subject's thoracic cavity is then related to the pressure within, and volume of, the plethysmograph. The procedure for this test begins similar to that for the SVC maneuver where subjects are instructed to take ≥4 tidal breaths at a constant FRC, and again, subjects are encouraged to sigh to facilitate breathing at FRC. Once the subject reaches end-expiration, the subject is instructed to begin a series of gentle pants, which are essentially very shallow breaths that correspond to a specific mouth pressure generated by the panting maneuver and box pressure generated by the chest wall movement. The rate at which this panting maneuver is performed is important and must be between 70-90 pants per min. Once at the correct panting rate, the shutter within the mouthpiece closes for ~2-3 sec and 3-5 satisfactory panting maneuvers are recorded, which should appear almost superimposable on the pressure volume plot. The shutter then re-opens and the subject is instructed to perform a slow inspiratory vital capacity maneuver followed by an expiratory vital capacity maneuver. This procedure allows for the determination of the volume of gas within the thoracic cavity at FRC which when

subtracted from expiratory reserve volume will yield RV. Similarly, TLC can be computed by adding RV to the measured vital capacity. Repeatability is obtained when the measured values of FRC agree to within 5%, and ≥3 successful trials have been performed.

Diffusion Capacity for Carbon Monoxide

Although there are several methods for determining the lungs diffusion capacity for carbon monoxide (e.g., steady state, intra-breath, and rebreathing techniques), the method used in our laboratory is the single-breath, breath hold technique. The procedure begins with subjects seated upright within the MedGraphics Elite Series Plethysmograph breathing normally through the mouthpiece with a nose-clip in place. Subjects are encouraged to breathe naturally and relaxed at a constant end expiratory volume, and after ≥4 breaths with a stable FRC, subjects exhale to RV in an unforced fashion. Once at RV there is an audible "clicking" noise from within the apparatus signifying that the expiratory outlet is pinched shut. Subjects are then quickly instructed to take a full breath in, all the way to TLC, which is delivered from the test gas cylinder (0.3% carbon monoxide, 21% oxygen, 0.5% neon, balanced nitrogen). Critical to accurate interpretation of the test results is that subjects inhale to >85% of their predicted TLC. The single-breath of test gas is held for 8 sec, after which the expiratory outlet opens signified by an audible "click" and subjects are instructed to exhale in a rapid but unforced fashion. A sample of this exhaled alveolar gas is then directed through a column of diatomaceous earth that allows for the separation of gases based on their size and is analyzed using a gas chromatograph. Neon serves as the tracer gas that is biologically inert, and is used to determine the initial alveolar carbon monoxide fraction, and the

alveolar volume at which carbon monoxide uptake is occurring. The computer then compares the volume of carbon monoxide delivered relative to the volume of carbon monoxide in the exhaled alveolar sample to calculate the volume of carbon monoxide that diffused from the alveolar air into the blood. This volume is standardized to the time of the breath hold (111), and presented as both an absolute diffusing capacity (DL_{CO}) and a diffusing capacity relative to the calculated alveolar volume (DL_{CO}/V_A) determined during the test. Although differences in DL_{CO} can arise from differences in lung volumes, based on differences in height and sex, these can be corrected for by comparing the DL_{CO}/V_A values across subjects.

SUBJECT INSTRUMENTATION

Intravenous Catheterization

On all studies involving the peripheral injection of agitated saline contrast, I placed an intravenous catheter (i.v.) in a peripheral vein in the antecubital fossa. For studies that also involved the i.v. infusion of epinephrine, a secondary i.v. was placed in the opposite arm. Briefly, a tourniquet is applied to the upper arm and subjects are instructed to squeeze a piece of foam to facilitate engorging the venous circulation in their forearm. If this process does not result in sufficient venous distension to visualize and/or feel a vein adequate for catheterization, a hot damp towel was laid over the area to further promote dilation. Once an adequate vein had been identified, an 18-22G 1.25" i.v. (ProtectIV Safety i.v. Catheter - radiopaque) was placed and connected to an extension set and one 3-way stopcock. Saline from a prefilled 10 ml syringe was used to ensure proper placement and adequate flushing of saline. Care was taken to pinch off the

extension set and turn the stopcock to the off position. Finally, a piece of tegaderm (2.75 x 3.25 in) was set over the i.v. and extension set to maintain its placement.

Arterial Catheterization

Arterial catheterization is a technically involved procedure and a critical piece of this dissertation, as the proper analysis of arterial blood is a fundamental skill set of respiratory physiologists that is essential to measuring pulmonary gas exchange efficiency. For the studies in this dissertation arterial catheterization was performed in the radial artery of all subjects. Due to the invasiveness and risk associated with procedure, radial artery catheters were placed in the subjects in Chapter IV by a licensed cardiologist (Dr. Jerold Hawn) and for the subjects in Chapter VI radial arterial catheters were placed by the physician currently on site (Drs. Christopher Davis, Morgen Eutermoser, and David Polaner). Prior to the placement of radial artery catheters an Allen's test was conducted to ensure adequate collateral circulation in the hand. For all subjects in this dissertation, both hands were required to pass the Allen's test in order to proceed with this procedure. Assessing adequate collateral circulation is important due to the rare but possible risk of occluding blood flow via the radial artery. Blood flow to the hand comes from two primary arteries, the radial and ulnar, and these two arteries anastomose in the palm. In some subjects the connection is very thorough, and both arteries supply sufficient blood flow to the hand on their own. However, in some subjects the connection is less thorough or relatively nonexistent, and in these subjects arterial catheterization carries the risk of preventing adequate blood flow to the hand. Thus, the Allen's test is conducted by manually occluding blood flow via both the ulnar and radial arteries with the forefingers of both hands, and instructing the subject to firmly open and close their

fist. This causes their hand to become very pale, at which point they are instructed to open their hand and we then release pressure on the ulnar artery and count the number of seconds required for color to fully return to their hand, which must be in ≤7 sec. We preferentially chose to catheterize the non-dominate hand for subjects in Chapter IV, however for subjects in Chapter VI, arterial catheters were placed on three separate occasions, which necessitated using both wrists. Although I screened all subjects using the Allen's test, the physician on site performed the test as well and always had the final decision.

All radial artery catheters (20G x 1.75" Arrow International, Reading, PA, USA) were placed under aseptic conditions following sterile techniques and under local anesthesia using 1% lidocaine with 2% by volume nitroglycerin (5 mg/ml) to minimize vasospasm. Subjects were positioned supine with their arm laid over a table covered in sterile drapes and their wrist in a support keeping it in an extended position. A secondary sterile drape with a 3" circular access hole was positioned with subject's radial artery in the center of this access hole and unfolded to cover their arm. A 20G needle was used to gain access the radial artery, after which a guide wire was threaded through the needle into the radial artery. The needle was then removed and the catheter was threaded onto the guide wire and into the radial artery. Finally, the guide wire was removed and an extension set with 3-way stopcock that was pre-flushed with heparinized saline (1 unit/ml) was connected to the catheter and proper placement was ensured by flushing the catheter with heparinized saline. This circuit was then connected to a pressurized flush system of heparinized saline that continuously and slowly dripped to maintain patency of

the catheter. Thereafter, arterial blood samples could be drawn for direct measurement of arterial PO_2, PCO_2, pH, SaO_2, hemoglobin, hematocrit and lactate.

Measures of Core Body Temperature

An important step in accurately measuring the true *in vivo* arterial PO_2 and PCO_2 is to correct the arterial blood sample for subject's core body temperature. When analyzed in the arterial blood gas machine, the temperature at the electrode interface is 37 ℃, and therefore, the PO_2/PCO_2 of the sample will be reflective of 37℃. If subject's body temperature is lower or higher than 37℃, the measured PO_2/PCO_2 will be lower or higher, respectively, compared to the true in vivo PO_2/PCO_2. It follows then that accurately measuring core body temperature is most important during conditions when body temperature would be expected to deviate from 37℃, such as during exercise.

Although various methods exist for measuring body temperature (tympanic, sublingual, rectal, esophageal, and via an ingestible pill) studies in this dissertation used the ingestible pill and esophageal method. For all visits in Chapter VI, the ingestible pill (HQinc., CoreTemp, Palmetto, FL, USA) was used and subjects were instructed to take the pill ~3 hours prior to the start of exercise. The pill is activated prior to ingestion by removing a magnetic connection and the correct serial number is entered into the wireless receiving device. With the handheld receiver near subject's abdominal area, temperature recordings are transmitted and displayed to the nearest hundredth. Serial measures in at least triplicate were always taken and the average temperature was recorded.

For subjects in Chapter IV measures of esophageal temperature were primarily used, and I placed all of the temperature probes (Mon-a-therm General Purpose Probe, 7-french). Subjects were positioned seated upright on the counter such that while standing,

I could see directly into their mouths using a headlight to assist with visualizing the back of the throat. The self-administration of 2 ml of 2% Lidocaine gel into the nasal cavity, was generally sufficient to temporarily anesthetize the area and back of the throat. However, an additional 1-2 sprays of HurriCaine spray (20% Benzocaine oral anesthetic) was used to further anesthetize the back of the throat and dampen subject's gag reflex if necessary. The esophageal temperature probe was then inserted in the nasal cavity via nasal intubation and advanced until visualized in the back of the throat. At which point subjects were provided a glass of water with a straw, and instructed to take small sips of water in a consistent rhythmic order. With each sip of water, the probe was advanced another 1-2 inches until at the appropriate point estimated to be at the level of the atria based off of subjects sitting height (161). Four subjects in Chapter IV could not tolerate the placement of the temperature probe and instead were given an ingestible temperature pill ~2-3 hours prior to beginning data collection.

Peripheral Oxygen Saturation and Heart Rate

A forehead pulse oximeter (Nellcor N600x, Covidien, Dublin, Ireland) was used to record peripheral estimates of arterial oxygen saturation (SpO_2) and heart rate, which were continuously fed into our metabolic data acquisition system. The pulse oximeter is a adhesive oval shape with one red light emitting diode (LED) and another infrared LED, that when placed directly above the pupil record estimates of hemoglobin saturation. The wavelength of the red (660 nm) and infrared light (940 nm) are reflected differently based on the state of the hemoglobin molecule, i.e. bound or unbound. Although normally >97% of hemoglobin is bound with oxygen (HbO_2) some hemoglobin, usually <2% is bound with carbon monoxide (HbCO) or is methemoglobin, which is interpreted via

pulse oximetry as bound (i.e. oxygenated) hemoglobin. Accordingly pulse oximetry provides an estimate that is usually ~2% higher than true *in vivo* HbO_2. The gold standard method of measuring HbO_2 is via CO-oximetry described in the *arterial blood draw and analysis section.* The pulsatile changes in color determined using pulse oximetry also provide an estimate of heart rate, however heart rate was also measured via lead II of either a 3-lead ECG (Chapters V and VI) or a 12-lead ECG (Chapter IV).

12-Lead Echocardiogram

For all subjects in Chapter IV a 12-lead ECG was placed to continuously monitor electrical activity of the heart. Atrial through ventricular depolarization and repolarization is recorded via electrical impulses from electrodes on the skin and generates a waveform displayed real time ($CardiO_2$, Mortara, MedGraphics). The placement of three limb leads, one on the left shoulder, right shoulder and left iliac crest give rise to the three bipolar limb leads (lead I, II, and III) and the three augmented unipolar limb leads (aVR, aVL, and aVF) that analyze the heart in the frontal place. The placement of six unipolar chest leads (V1, V2, V3, V4, V5 and V6) analyze the heart in the transverse plane with V1-3 positioned in front of the heart to analyze posterior/anterior activity, and V4-6 positioned around the side of the chest to analyze right/left/lateral activity. The placement of V4 was repositioned ~2 in inferiorly to allow room for the ultrasound probe to reach the necessary location (139).

ECHOCARDIOGRAPHY MEASUREMENTS

Transthoracic Saline Contrast Echocardiography

The detection of blood flow through intrapulmonary arteriovenous anastomoses (IPAVA) was done using transthoracic saline contrast echocardiography (TTSCE) in the same manner as was described in the echocardiographic screening procedure section. For subjects in Chapter V and VI subjects were positioned seated upright on a stationary cycle ergometer, and for subjects in Chapter IV, subjects were reclined in the left lateral decubitus position. In all cases, the sonographer (Randy Goodman or Eben Futral) obtained an apical, four-chamber view and individually adjusted the receiver settings for all subjects and for every injection to optimize the image. Care was taken to emphasize the image and optimize it on the left ventricle in a non-foreshortened view. Saline (3 ml) and air (1 ml) was agitated between two 10 ml syringes connected in series by two 3-way stopcocks. Connected to the first stopcock was a 250-1000 ml bag of saline via a solution set, and connected to the second stopcock was the extension set of the i.v. catheter. In this way saline could be easily and rapidly filled into the syringe. Saline and air were agitated together for ~15 sec for all injections, and after injection, the sonographer recorded the subsequent 20 cardiac cycles at >30 frames/sec post appearance of contrast in the right ventricle. Each injection was analyzed by individually advancing the recording frame-by-frame and identifying the single frame with the greatest number and/or spatial distribution of microbubbles in the left ventricle. Based on this single frame, a 0-5 score was assigned; 0 = 0 microbubbles, 1 = 1-3 microbubbles, 2 = 4-12 microbubbles, 3 = >12 microbubbles appearing as a bolus, 4 = >12 microbubbles heterogeneously filling the left ventricle, and 5 = >12 microbubbles homogenously filling the left ventricle. This scoring

system was first published in 2008 (144) and has subsequently been published in other work from our group (54, 55, 133, 134) and is not without precedent (11).

The sonographers were the primary scorers of each saline contrast injection, however we have previously reported very good agreement between bubble scores obtained when analyzed by a licensed cardiologist blinded to the conditions. In an effort to further validate reproducibility of this scoring system, the cardiologist reviewed 57 echocardiogram recordings. There was 100% agreement on whether there was or was not contrast in the left ventricle, and 93% agreement on the bubble score between the sonographer and cardiologist. Of the 4 recordings with disparate scores, disagreement was between whether or not they should be scored a 0 or 1. Accurately identifying a single microbubble takes a very skilled eye, y*et al*so represents in all likelihood a trivial, insignificant volume of blood flow through IPAVA.

Pulmonary Artery Systolic Pressure

As described previously, PASP was determined by measuring the peak velocity (v) of the tricuspid regurgitation jet and estimating right atrial pressure (P_{RA}) based on the collapsibility of the inferior vena cava, and applying these to the modified Bernoulli equation; see **Equation 2.14** (42, 92, 202, 275).

Cardiac Output

Cardiac output ($\dot{Q}_T$) was estimated using echocardiography and determined at the level of the left ventricular outflow tract (LVOT). Previously during the screening visit, subjects LVOT diameter had been determined and recorded. This value was used to estimate the cross sectional area of the outflow tract. Pulsed wave Doppler ultrasound was used in all studies to determine the LVOT velocity time integral ($LVOT_{VTI}$) of blood

flow through the outflow tract. Measures of the $LVOT_{VTI}$ were recorded in triplicate and the average was multiplied by the previously determined cross sectional area of the LVOT. The product of the $LVOT_{VTI}$ and LVOT cross sectional area equals the stroke volume, which multiplied by heart rate provides an estimate of $\dot{Q}_T$.

Other echocardiographic methods exist to determine $\dot{Q}_T$, such as the modified Simpson's method, however previous pilot work conducted in our laboratory has shown the modified Simpson's method to be unreliable when heart rate is elevated. This was demonstrated by measuring $\dot{Q}_T$ using modified Simpson's and LVOT during exercise and comparing the measured $\dot{Q}_T$ values to the predicted $\dot{Q}_T$ based off of the measured $\dot{V}O_2$ (8). Measured values using the modified Simpson's method plateaued after ~10-12 L/min, whereas measured values using LVOT tracked very well to the predicted values.

OPEN CIRCUIT ACETYLENE UPTAKE

In Chapter IV $\dot{Q}_T$ was also measured using the open circuit acetylene washin method as developed by Stout *et al*. (217), modified by Gan *et al*. (70), and subsequently validated in humans against the direct Fick approach (110). Subjects breathed through a non-rebreathing Hans-Rudolph mouthpiece connected to an automatic three-way sliding valve allowing rapid and non-interruptive transitions (i.e., during subjects expiration) between two different inspiratory ports. When breathing room air, one inspiratory port was open to room air and the other was connected to a normoxic acetylene gas mixture (0.6% acetylene, 9.0% helium, 20.9% O_2, balance N_2). When breathing 40% O_2, one inspiratory port was connected to a hyperoxic gas mixture (40% O_2, balance N_2) and the other was connected to a hyperoxic acetylene gas mixture (0.6% acetylene, 9.0% helium,

40% O_2, balance N_2). During the washin phase, breath-by-breath acetylene and helium uptake was measured by a respiratory mass spectrometer (Marquette MGA 1100, MA Tech Services) and tidal volume was measured by a pneumotach (Hans Rudolph 3700) linearized by the method of Yeh *et al*. (274) and calibrated using test gas between before each study. Finally, it should be clear that the fundamental limitation of open circuit acetylene uptake is that blood flow through intrapulmonary right-to-left shunts is not detected using this method.

DELIVERY OF INSPIRED GAS MIXTURES

In all studies in Chapters IV-VI, subjects breathed through a low resistance, non-rebreathing mouthpiece and they expired to room air. When subjects inspired room air, the inspiratory port was also open to room air. However when the FIO_2 was manipulated, and subjects either breathed 40% O_2 (Chapter IV) and 100% O_2 (Chapter V) the inspiratory port was connected to a non-diffusing Mylar Douglas bag. This Douglas bag was connected to a compressed gas blender that is connected to two compressed gas cylinders; medical grade room air, and medical grade 100% O_2. By adjusting the blender the appropriate FIO_2 could be obtained and verified using our metabolic data acquisition system. The gas analyzer in our metabolic data acquisition system is a zirconia O_2 cell that we calibrate prior to all studies using a known gas mixture. In series between the hosing that delivers gas to the Douglas bag and the gas blender, is a flow regulator that can be adjusted to manipulate the flow rate into the bag based off of subject's minute ventilation.

In Chapter IV the mouthpiece subject breathed through was a custom built two-way non-rebreathing mouthpiece with a pneumatic sliding valve allowing rapid and non-interruptive transitions (i.e., during subjects expiration) between two different inspiratory ports. When breathing room air, one inspiratory port was open to room air and the other was connected to a normoxic acetylene gas mixture (0.6% acetylene, 9.0% helium, 20.9% O_2, balance N_2). When breathing 40% O_2, one inspiratory port was connected to a hyperoxic gas mixture (40% O_2, balance N_2) and the other was connected to a hyperoxic acetylene gas mixture (0.6% acetylene, 9.0% helium, 40% O_2, balance N_2).

MEASUREMENT OF ARTERIAL BLOOD GASES

Arterial Blood Draw and Analysis

Although analyzing arterial blood is a technically straightforward procedure, substantial care must be taken to obtain accurate measures, particularly when subjects are breathing >21% O_2. As described in the *arterial catheterization* section, patency of arterial catheters was maintained using a pressurized flush system of heparinized saline, and connected in series to this circuit, between the solution set and extension set, were two 3-way stopcocks. Arterial blood samples were obtained by first wasting ~1 ml of blood because the extension set and stopcock have a combined dead space of ~0.5 ml. A new, heparinized 3 ml syringe was then connected to the stopcock and arterial blood was withdrawn over an ~15 sec window. Care was taken to include several respiratory cycles when subjects were resting, however this was less of a concern during conditions of elevated ventilation (i.e., during exercise or the i.v. infusion of epinephrine). Additionally the precise duration of the blood draw was noted, from start to finish, so as to accurately

align the blood draw with metabolic data. The arterial sample was withdrawn in such a way as to keep any small air bubble at the tip of the syringe, which was immediately expelled after passing the sample to the investigator in charge of analyzing the samples. During the analysis investigators were careful to maintain a positive pressure on the sample syringe during the analysis to pre-emptively prevent the production of an air bubble. Additionally, all arterial samples were held with a firm seal over the tip of the syringe, rocked back and forth to facilitate mixing, and prior to their immediate analysis a small volume of blood near the tip of the syringe was wasted to continually rid the sample of blood that is most at risk for room air contamination. All arterial blood samples analyzed in Chapters IV and VI were done using a Siemens RAPIDLab248 containing a Clarke electrode for measurement of PO_2 and a Severinghaus electrode for measurement of PCO_2. After obtaining the arterial sample, the investigator in charge of monitoring the arterial catheter resumed the pressurized flush system of heparinized saline to flush the arterial catheter. The blood gas analyzer requires ~60 sec to analyze each sample, and during this period, the sample was analyzed using CO-oximetry via a Radiometer OSM3 to determine arterial O_2 saturation and hemoglobin concentration. Arterial blood samples were analyzed in duplicate and triplicate if time permitted or if the difference between the first two measurements exceeded 5%. After which the arterial blood was analyzed for hematocrit using the microcapillary tube centrifugation method, and for lactate concentration (YSI 1500 Sport).

All arterial blood samples were corrected for body temperature and were collected using a blood gas analyzer calibrated daily using tonometered whole human blood (see below).

Tonometry

The process of tonometry is similar, but superior, to using standard quality control methods in that it allows for the correction of day-to-day fluctuations and inherent errors in measuring the exact PO_2 and PCO_2. Samples of whole human blood are positioned within a heated block (37 ℃) and equilibrated for ~120 min with gases of known concentrations of O_2 and CO_2 that are anticipated to reflect the expected arterial PO_2 and PCO_2. These samples are then analyzed in duplicate and triplicate if the difference between the first to measurements exceeds 5%. A correction factor based off of the inverse slope of the measured versus predicted values was applied to the measured values in this dissertation.

For Chapter IV, the gases chosen were expected to span the range of arterial PO_2 and PCO_2 anticipated in subjects breathing room air and 40% O_2 at rest (PO_2 = 100, 210, and 245 mm Hg; PCO_2 = 21, 35, 48 mm Hg). Consistent inherent errors with handling and analyzing blood with PaO_2 in the 220-230 mm Hg range are also present during the process of tonometry, and therefore this correction factor will help offset these.

For Chapter VI, the gases chosen were expected to span the range of arterial PO_2 and PCO_2 anticipated in subjects at rest and during exercise breathing room air in Eugene, OR (130m, P_B = 750 mm Hg) and on Mt. Chacaltaya, Bolivia (5260m, P_B = 410 mm Hg). For data collected at sea level the gases chosen spanned arterial PO_2 = 40, 70, 110 mm Hg and arterial PCO_2 = 15, 35, 50 mm Hg. For data collected at altitude the gases chosen spanned arterial PO_2 = 25 and 50 mm Hg, and PCO_2 = 15 and 30 mm Hg. Only two tonometry gases were used at altitude due to the extreme difficulty and cost associated with obtaining these gases and transporting them to the research lab.

ALTITUDEOMICS

AltitudeOmics represents a very large, multinational collaborative research expedition investigating human acclimatization to hypoxia with the ultimate goal to marry the physiological adaptations to high-altitude with the accompanying genomic, proteomic, metabalomic, and epigenetic changes. Much of the prior methodological descriptions apply to this part of the AltitudeOmics project that represents Chapter VI of this dissertation, however considering the size and scope of this project a more detailed description is warranted that has largely been paraphrased from our recent publication describing the overview of this project (218).

Subject Recruitment and Screening

All subjects were recruited from Eugene, OR (130m, P_B = ~750 mm Hg) and only screened if they met the following exclusion criteria; born at >1500m, having traveled to altitudes >1000m in the past three months (including air travel), using prescription medications, smoking, pregnant, having a history of serious head injury, personal or familial history of migraine, cardiovascular or respiratory disease, hematologic abnormalities such as sickle cell trait, pulmonary function of diffusing capacity for carbon monoxide <90% predicted, or failing to meet the requirements of the army physical fitness test (push-ups, sit-ups, and 2 mi run). After excluding subjects for the aforementioned criteria, a total of 79 subjects were screened, that included additional testing identifying the presence of a PFO, a $\dot{V}O_{2max}$ test and short bout of breathing 14% O_2 to determine the baseline level of left-sided contrast at this level of acute normobaric hypoxia. The final group of 24 subjects that met the combined screening criteria

participated in the study, however two subjects dropped out for non-medical reasons, and one subject suffered from a non-altitude related gastrointestinal illness such that this subject was never fully healthy. These three subjects were excluded from the data analysis and the remaining 21 subjects participated in the project.

Timeline

Baseline testing occurred in our Cardiopulmonary and Respiratory Physiology lab in the Spring of 2012. However, prior to the experimental study visit, all subjects completed a familiarization visit, in which a mock study visit was carried out. In both the familiarization protocol and experimental study visit (i.e., sea level testing, **Figure 3.1**), two subjects were completed each day. Experimental study visits were ~14 hour work days for investigators and occurred over a 14 day period, with a two day 'break' between the first 6 (12 subjects) and last 6 (12 subjects) experimental study days. Approximately one month later, study investigators (including myself) traveled to La Paz, Bolivia, to prepare/improve the housing conditions and laboratory setting.

Due to our laboratory equipment being held in Bolivian customs until the day prior to the first study visit, we set-up the entire laboratory for physiologic testing and laboratory space for omics analyses that night (before the first subjects); a process that took ~7 days to complete for baseline testing at sea level (SL). From this day forward, subjects traveled to Bolivia in pairs, on successive days (i.e., two subjects arrived each day). Upon arrival in El Alto, subjects were escorted from the airport at 4300m to Coroico at 1525m where they rested for ~48 hours. After this, subjects traveled in pairs from Coroico, via car, while breathing supplemental O_2 to Mt. Chacaltaya at 5260m, an elevation gain of 3735m. The first subject immediately began instrumentation after being

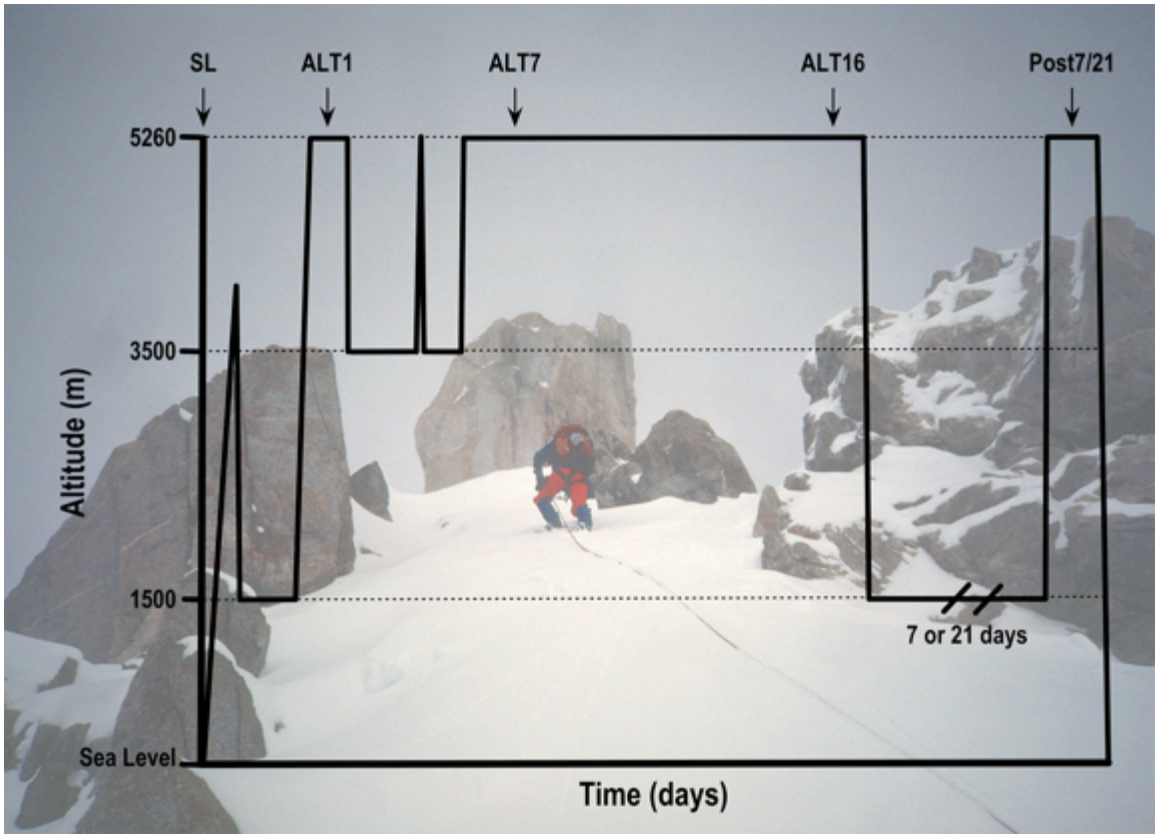

Figure 3.1. AltitudeOmics Overview Timeline
As published in the project overview paper of this series (218) *the time course for each subject with respect to altitude. Arrows indicated experimental study days. Data in Chapter VI comes from experiments at SL, ALT1 and ALT16.*

removed from supplemental O_2, while the second subject remained breathing supplemental O_2. After the first subject was almost done with the physiologic testing protocol, the second subject was removed from supplemental O_2 and began instrumentation, after which the physiologic protocol was repeated again. This study visit occurring after acutely and rapidly being transported to 5260m was referred to as ALT1 (the first day at 5260m, **Figure 3.1**). These two subjects then slept overnight at 5260m breathing supplemental O_2, with an emergency medicine physician in the same room. The following morning, these subjects completed a 3.2km field 'run', after which they descended to La Paz at 3800m where they remained for 3 days. On the fourth day in

Bolivia (ALT4) subjects returned to Mt. Chacaltaya for ~6 hours to promote acclimatization, and then returned to La Paz, after which they returned again to Mt. Chacaltaya on ALT5 where they remained for the following 12 days. This process was repeated for all 24 subjects, such that the number of residents on Mt. Chacaltaya increased by 2 per day, until all 24 subjects resided on Mt. Chacaltaya.

After the 11 day period of acclimatization spent at 5260m, the first subjects who arrived were the first subjects to be tested on ALT16 (**Figure 3.1**). These subjects then spent one last night on Mt. Chacaltaya before performing the 3.2km field run again and afterwards descending to Coroico for either 7 (n = 14) or 21 (n = 7) days. The same physiologic protocol was carried out at ALT16 as was done at ALT1 and SL. After the first study visit for ALT1, there were 12 sequential study visits, with a one day break in the middle, allowing investigators to descend to La Paz to shower and replenish snacks. Thus, there was also a ~2 day break before the first ALT16 study visit.

The general experimental protocol for SL, ALT1 and ALT16 (**Figure 3.1**) was to first instrument subjects with a radial artery and antecubital vein catheter, have subjects complete a series of cognitive function tests, perform a series of blood draws for analyses of omics data, and perform a muscle biopsy of the vastus lateralis. Subjects remained seated upright and ventilatory responses to different CO_2 levels were recorded, they then performed a cycle ergometer VO_{2peak} test and a 5km time trial.

CHAPTER IV

INCREASED CARDIAC OUTPUT, NOT PULMONARY ARTERY SYSTOLIC PRESSURE, INCREASES INTRAPULMONARY SHUNT IN HUMANS BREATHING ROOM AIR AND 40% O_2

This chapter is in review at the *Journal of Physiology* and Joseph W. Duke, Jerold A. Hawn, John R. Halliwill, and Andrew T. Lovering are co-authors. I performed the experimental work, led the project, and the writing is entirely my own; Joseph W. Duke provided technical and editorial assistance; Jerold A. Hawn placed all radial artery catheters; and John R. Halliwill and Andrew T. Lovering helped develop the protocol, and provided guidance and editorial assistance. All co-authors formally approved this manuscript for submission.

INTRODUCTION

In healthy humans without a patent foramen ovale (PFO), blood flow through intrapulmonary arteriovenous anastomoses (IPAVA) can be detected using saline contrast echocardiography (159, 163, 198). Although blood flow through IPAVA is absent or trivial at rest (55), blood flow through IPAVA increases during exercise (53, 54, 143, 216), while breathing hypoxic gas mixtures at rest (134), and during the intravenous (i.v.) infusion of inotropic drugs (24, 133). The physiological significance of these findings remains controversial (103) but it has been hypothesized that blood flow through IPAVA could provide a source of venous admixture and impair pulmonary gas exchange efficiency, i.e. increase the alveolar-to-arterial difference in PO_2 ($A\text{-}aDO_2$) (143, 216).

Bryan *et al*. (24) demonstrated that during the i.v. infusion of dobutamine and dopamine in healthy humans at rest breathing room air, the degree of left-sided contrast increased, yet the A-aDO_2 remained unchanged (24). However, in accordance with the Fick principle of mass balance, this necessitates an increase in the calculated shunt fraction ($\dot{Q}_S/\dot{Q}_T$) due to an increase in mixed venous O_2 content ($C\overline{v}O_2$) secondary to an increased Q_T and constant whole body $\dot{V}O_2$. In that study, increases in left-sided contrast, which never exceeded intermittent boluses of contrast in the left ventricle, corresponded to increases in $\dot{Q}_T$ that increased by ~50% above resting values. Similar work by Laurie *et al*. (133) without measurements of the A-aDO_2, has demonstrated in healthy humans without a PFO that at rest breathing room air during the i.v. infusion of epinephrine (EPI) blood flow through IPAVA is increased. In that study the highest dose of EPI (320 ng/kg/min) corresponded to an ~2-fold increase in $\dot{Q}_T$ and pulmonary artery systolic pressure (PASP) the qualitative degree of left-sided contrast ranged from intermittent boluses to heterogeneous filling of the left ventricle. Accordingly, the data from Bryan *et al*. support the potential that blood flow through IPAVA may provide a source of venous admixture, yet in light of the work by Laurie *et al*., it remains possible that higher $\dot{Q}_T$ and PASP would have corresponded to greater degrees of left-sided contrast and therefore, potentially more blood flow through IPAVA resulting in a measurable increase in the A-aDO_2.

In addition to potential contributions from blood flow through IPAVA, pulmonary gas exchange efficiency may also be impaired by alveolar ventilation-to-perfusion ($\dot{V}_A/\dot{Q}$) inequality, incomplete end-capillary O_2 diffusion equilibration (diffusion limitation), and right-to-left shunt via the bronchial and Thebesian circulations.

Determination of the A-aDO_2 via arterial blood gas analysis and calculation of alveolar PO_2 (PAO_2) does not yield information concerning the relative contribution of each of these factors. This is particularly relevant during interventions known to increase blood flow through IPAVA (e.g., during exercise, breathing hypoxic gas mixtures, or the i.v. infusion of catecholamines) where the pulmonary capillary transit time required for complete end-capillary O_2 equilibration, mixed venous PO_2, and driving gradient for O_2 across the alveolar-capillary interface may vary considerably. As a result, contributions from $\dot{V}_A/\dot{Q}$ inequality, diffusion limitation, and shunt may differ during these different interventions, and thus obscure the ability to draw conclusions regarding the potential contributions from each on the A-aDO_2 unless some of these contributions are held constant.

Accordingly, an experimental paradigm that would eliminate $\dot{V}_A/\dot{Q}$ inequality and diffusion limitation while increasing blood flow through IPAVA in healthy humans at rest would be optimal to determine if blood flow through IPAVA contributed to pulmonary gas exchange efficiency. Elevating PAO_2 via breathing 100% O_2 at sea level theoretically eliminates $\dot{V}_A/\dot{Q}$ inequality and diffusion limitation (196), however, blood flow through IPAVA during exercise and the i.v. infusion of EPI has been shown to be significantly reduced or eliminated when breathing 100% O_2 (24, 54, 133, 144). Thus, breathing 100% O_2 isolates the contribution of right-to-left shunt, but this would not include the contribution of blood flow through IPAVA, and therefore may not represent the same volume of right-to-left shunt when breathing room air. Instead, breathing <100% O_2 but, >21% O_2 has the potential to sufficiently elevate PAO_2 such that the contributions of $\dot{V}_A/\dot{Q}$ inequality and diffusion limitation are minimized or prevented, yet

still permits blood flow through IPAVA. According to theoretical analyses describing the rate of O_2 uptake across the alveolar-capillary interface (240) and unpublished observations in our laboratory (Davis *et al*.), breathing 40% O_2 satisfies both of these requirements. Compared to breathing room air, when breathing 40% O_2, blood flow through IPAVA is qualitatively unchanged, PAO_2 is increased >2 fold, and mean end-capillary O_2 equilibration time is reduced to ~0.1 sec.

The purpose of the current study was to investigate the potential for blood flow through IPAVA to provide a source of venous admixture and impair pulmonary gas exchange. To this end, we employed the aforementioned experimental paradigms by quantifying the A-aDO_2 in healthy humans at rest, breathing room air and 40% O_2 during the i.v. infusion of EPI. Additionally, to increase $\dot{Q}_T$ with lower doses of i.v. EPI, this protocol was repeated following vagal blockade via atropine. We hypothesized that the A-aDO_2 would increase during the i.v. infusion of EPI when breathing room air, and the resulting increase in A-aDO_2 would not be ameliorated during the i.v. infusion of EPI when breathing 40% O_2.

METHODS

The University of Oregon Office for Protection of Human Subjects approved this project and all subjects provided verbal and written informed consent prior to participation. All studies were performed in accordance with the *Declaration of Helsinki*.

Subjects

Nine subjects (4 female) volunteered to participate in this study, all of which were healthy, young, non-smoking and without a history of cardiopulmonary or respiratory disease.

According to the American Thoracic Society and European Respiratory Society standards (ATS/ERS) all subjects demonstrated normal pulmonary function, lung volumes and capacities, and diffusion capacity for carbon monoxide. Pulmonary function was assessed using computerized spirometry (MedGraphics Ultima CardiO_2, St. Paul, MN, USA) and involved forced and slow vital capacity manoeuvres (166). Lung volumes and capacities were determined using whole body plethysmography (MedGraphics Elite Plethysmograph) (247). Lung diffusion capacity for carbon monoxide (DL_{CO}) was determined by the single-breath, breath hold method (119, 152) using the Jones and Meade method for timing (111).

All subjects underwent a comprehensive echocardiographic screening procedure performed by a registered diagnostic cardiac sonographer in both adult and paediatric echocardiography with 25 years of experience (Philips iE33, The Netherlands). The purpose of this screening procedure was to confirm that subjects were without cardiac abnormalities, including a PFO. To this end, subjects were rigorously screened using transthoracic saline contrast echocardiography (TTSCE) as described previously (55, 139) and did not have a PFO.

Instrumentation

Following local anesthesia [1% lidocaine, 2% by volume nitroglycerine (5 mg/ml) to minimize vasospasm] a 20 Ga x 1.75 in radial artery catheter (Arrow International,

Reading, PA, USA) was placed under aseptic conditions by a board certified cardiologist. Patency of the arterial catheter was maintained using a pressurized flush system of normal saline. Intravenous catheters (i.v.) (18-22 Ga) were placed in the antecubital fossa of each arm, one for the injection of agitated saline contrast and one for the infusion of epinephrine and atropine. All catheters were connected to an extension set (7.0 inch, 0.3 mL volume) followed by a three-way stopcock. Measures of core body temperature were made using an esophageal temperature probe (Mon-A-Therm), which was inserted via nasal intubation following the application of an anesthetic gel (2 mL of 2% lidocaine gel) into the nasal cavity. In subjects who could not tolerate the esophageal temperature probe placement (4/9 subjects), an ingestible core temperature pill (HQInc) was used. Unpublished observations from our laboratory demonstrate that temperature obtained using esophageal and the core temperature pill is in good agreement at rest ($R^2 = 0.85$). Lastly, a 12-lead ECG (MedGraphics, Mortara, CardiO_2) was placed with V4 repositioned ~5 cm inferiorly as described previously (139).

Protocol

Subjects reported to the laboratory at 0700 hours and after familiarization with the study procedure began instrumentation. Thereafter, subjects were repositioned in a reclining chair in the left lateral decubitus position, and remained in this position for the duration of the protocol. The first set of measurements **(Figure 4.1A)** were made breathing room air and 40% O_2 before and during the i.v. infusion of epinephrine (EPI). The second set of measurements **(Figure 4.1B)** were made breathing room air and 40% O_2 following vagal blockade via atropine (ATR) before and during the i.v. infusion of epinephrine. In both sets of measurements, before and after ATR, the order of breathing

room air or 40% O_2 was done in a random and balanced fashion. However, measurements with ATR always occurred second due to the ½ life of ATR being ~120 min.

Epinephrine was diluted in sterile saline to 4,000 ng/mL and depending on subjects body weight, was delivered at a constant rate for 5 min, using a continuous infusion syringe pump (Harvard Apparatus, Pump 22) as described previously (133). In the first set of measurements, before vagal blockade, EPI was infused at 320 ng/kg/min (320 EPI). In the second set of measurements, after vagal blockade, EPI was infused at 80 ng/kg/min (ATR+80 EPI). Vagal blockade was accomplished via the i.v. infusion of 2 mg of atropine, diluted in 10 mL of sterile saline, at a constant rate of 1 mL/min for 10 min.

In both sets of measurements, before and after ATR, subjects were allowed ~20 min for EPI to be metabolized and a final measurement without i.v. EPI was made. In this measurement, subjects reproduced the respiratory rate and tidal volume they had during the i.v. infusion of EPI. Respiratory rate was coached using a metronome and tidal volume was coached by verbal feedback while observing real time ventilatory data.

Thus, the first set of measurements (**Figure 4.1A**) were made breathing room air and 40% O_2 at baseline (Pre EPI), during the i.v. infusion of EPI at 320 ng/kg/min (320 EPI) and subsequently while reproducing the ventilation ($\dot{V}_A$) they had at 320 EPI ($\dot{V}_A$ @ 320 EPI). Following vagal blockade, the second set of measurements (**Figure 4.1B**) were made breathing room air and 40% O_2 at baseline (Pre EPI (ATR)), during the i.v. infusion of EPI at 80 ng/kg/min (ATR+80 EPI) and subsequently while reproducing the ventilation they had at ATR+80 EPI ($\dot{V}_A$ @ ATR+80 EPI).

A. Pre vagal blockade

Room Air					40% O_2				
Pre EPI	320 EPI	20 min break	V_A (320 EPI)	20 min break	15 min Pre-breathe	Pre EPI	320 EPI	20 min break	V_A (320 EPI)

B. Post vagal blockade, 2 mg atropine

Room Air					40% O_2				
Pre EPI (ATR)	ATR + 80 EPI	20 min break	V_A (ATR + 80 EPI)	20 min break	15 min Pre-breathe	Pre EPI (ATR)	ATR + 80 EPI	20 min break	V_A (ATR + 80 EPI)

Figure 4.1. Protocol Schematic
Schematic of the overall protocol, with dark grey boxes indicating the time points where measurements were made (see below). EPI, epinephrine; ATR, atropine; 320 EPI, 320 ng/kg/min epinephrine; $\dot{V}_A$ (320 EPI), iso-alveolar ventilation after break from 320 EPI; ATR+80 EPI, 80 ng/kg/min of epinephrine with atropine; $\dot{V}_A$ (ATR+80 EPI), iso-alveolar ventilation after break from ATR+80 EPI.

Measurements

Respiratory Variables. Breath-by-breath metabolic data was collected (MedGraphics, CardiO_2) and presented as the mid 5 of 7 (i.e., the moving average of five breaths excluding the low and high). In this way continuous measures of pulmonary $\dot{V}O_2$, $\dot{V}CO_2$, minute ventilation ($\dot{V}_E$), and associated parameters, including end tidal and mixed expired PO_2 and PCO_2 values, were collected. Gases with known O_2 and CO_2 concentrations were used to calibrate the gas analyzer before every test and change from breathing room air or 40% O_2.

Cardiac Output and Pulmonary Artery Systolic Pressure. Cardiac output was measured using the open circuit acetylene washin method developed by Stout *et al*. (217), modified by Gan *et al*. (70), and subsequently validated in humans using direct Fick (110). Subjects breathed through a non-rebreathing Hans-Rudolph mouthpiece connected to an automatic three-way sliding valve allowing rapid and non-interruptive transitions (i.e., during subjects expiration) between two different inspiratory ports. When breathing

room air, one inspiratory port was open to room air and the other was connected to a normoxic acetylene gas mixture (0.6% acetylene, 9.0% helium, 20.9% O_2, balance N_2). When breathing 40% O_2, one inspiratory port was connected to a hyperoxic gas mixture (40% O_2, balance N_2) and the other was connected to a hyperoxic acetylene gas mixture (0.6% acetylene, 9.0% helium, 40% O_2, balance N_2). During the washin phase, breath-by-breath acetylene and helium uptake was measured by a respiratory mass spectrometer (Marquette MGA 1100, MA Tech Services) and tidal volume was measured by a pneumotach (Hans Rudolph 3700) linearized by the method of Yeh *et al*. (274) and calibrated using test gas before each study.

Pulmonary artery systolic pressure was determined by measuring the peak velocity (v) of the tricuspid regurgitation jet and estimating right atrial pressure (P_{RA}) based on the collapsibility of the inferior vena cava, and applying these to the modified Bernoulli equation $4v^2 + P_{RA}$ (42, 92, 202, 275).

Blood Flow Through Intrapulmonary Arteriovenous Anastomoses. Transthoracic saline contrast echocardiography (TTSCE) was used to detect blood flow through IPAVA as before (133). Briefly, agitated saline contrast was produced by combining 3 ml room air with 1 ml of normal saline and agitating for ~15 sec prior to injecting. Each agitated saline contrast injection was visualized in the apical, four-chamber view and recorded at >30 frames per second for 20 cardiac cycles post-appearance of saline contrast in the right ventricle. The single frame within the 20 cardiac cycle recording with the greatest density and spatial distribution of contrast was qualitatively assessed using a previously published scoring system (144) similar to others (11); 0 = no bubbles, 1 = 1-3 bubbles, 2

= 4-12 bubbles, 3 = >12 bubbles appearing as a bolus, 4 = >12 bubbles heterogeneously filling the left ventricle, and 5 = >12 bubbles homogeneously filling the left ventricle.

Arterial Blood Gas Analysis. Arterial blood (3 mL) was drawn anaerobically via the radial artery over 10-15 sec into a heparinized syringe and immediately analyzed in duplicate (and triplicate if necessary) for arterial PO_2 (PaO_2), arterial PCO_2 ($PaCO_2$), and pH. The blood-gas analyzer (Siemens RAPIDLab 248, Germany) was calibrated daily with tonometered whole human blood by equilibrating three 6 ml samples of human blood, positioned within a heated block (37 ℃), with gases of known concentrations of O_2 and CO_2 for ~120 min. The gases were chosen to span the expected range of PaO_2 and $PaCO_2$ anticipated in subjects breathing room air and 40% O_2 at rest (PO_2 = 100, 210, and 245 mm Hg; PCO_2 = 21, 35, 48 mm Hg). Each sample was run in triplicate, and the values were used to create a predicted versus measured slope. A correction factor based off of the inverse slope of this relationship was applied to measured values in this study. Arterial blood gases were also corrected for body temperature (48, 113, 205). Arterial O_2 saturation (SaO_2) and hemoglobin (Hb) were measured with CO-oximetry (Radiometer OSM3, Copenhagen, Denmark). Hematocrit was analyzed using the microcapillary tube centrifugation method (M24 Centrifuge, LW Scientific, Lawrenceville, GA, USA). Blood lactate was analyzed in duplicate using an electrochemical analyzer (YSI 1500 Sport, Yellow Springs, OH, USA).

Calculations

Alveolar PO_2 (PAO_2) was calculated using the ideal gas equation, using temperature/tonometry corrected $PaCO_2$, and a respiratory quotient (RER) from a 15 sec

average of breath-by-breath metabolic data corresponding to the time and duration of the arterial blood draw:

$$PAO_2 = [(P_B - e^{0.05894809 \times T_B + 1.689589}) \times FIO_2] - PaCO_2 \times \left[FIO_2 + \frac{(1 - FIO_2)}{RER}\right]$$

Equation 2.3. Alveolar Gas Equation

where T_B is core body temperature for temperature correction of water vapor pressure, RER is the respiratory exchange ratio ($\dot{V}CO_2/\dot{V}O_2$), and P_B is barometric pressure measured daily using a solid-state transducer barometer (7400 series Perception II, Davis Instruments). Pulmonary gas exchange efficiency (A-aDO_2) was then determined at rest and during i.v. infusion of EPI with and without ATR by subtracting the temperature/tonometry corrected PaO_2 from the corresponding calculated PAO_2.

Measures of O_2 content were calculated from the standard content equation:

$$O_2 \text{ Content} = \left[1.39 \times Hb \times \left(\frac{SO_2}{100}\right)\right] + (0.003 \times PO_2)$$

Equation 2.7. Oxygen Content Equation

using an O_2 carrying capacity of 1.39 ml O_2/g Hb and subjects directly measured corresponding Hb (g Hb/dL). For arterial O_2 content (CaO_2) SO_2 represents CO-oximetry measured arterial O_2 saturation (SaO_2) and temperature/tonometry corrected PaO_2. For end-capillary O_2 content ($Cc'O_2$) SO_2 represents calculated end-capillary O_2 saturation ($Sc'O_2$) via the Kelman equation (114) assuming end-capillary PO_2 ($Pc'O_2$) was equal to PAO_2. Mixed venous O_2 content was calculated using the Fick equation ($\dot{V}O_2 = \dot{Q}_T \times (CaO_2 - C\bar{v}O_2)$) and rearranging such that, $C\bar{v}O_2 = CaO_2 - (\dot{V}O_2/Q_T)$.

Total venous admixture (Q_{VA}/Q_T) required to account for the entirety of the $AaDO_2$ was calculated from the shunt equation using the previously calculated O_2 contents:

$$\frac{Q_{VA}}{Q_T} = \frac{Cc'O_2 - CaO_2}{Cc'O_2 - C\bar{v}O_2}$$

Equation 2.13. Berggren Shunt Equation

Alveolar ventilation ($\dot{V}_A$) was calculated using the directly measured $\dot{V}CO_2$ and temperature corrected $PaCO_2$:

$$V_A = \frac{(VCO_2 \times 863)}{PaCO_2}$$

Equation 2.1. Alveolar Ventilation

Statistical Analyses

Statistical analyses using GraphPad Prism (v. 5.0d) were done using a one-way analysis of variance comparing measured and calculated variables within an FIO_2 (room air or 40% O_2) without and with ATR. A Tukey's multiple comparison post hoc test was used to determine specific pairwise differences within variables. Non-parametric analyses (bubble scores) were done using a Friedman's test with a Dunn's multiple comparison post-hoc test. All comparisons were determined *a priori* and significance was set to $p < 0.05$.

RESULTS

Subject anthropometric and pulmonary function data are presented in **Table 4.1**. Cardiopulmonary and respiratory data when breathing room air are presented in **Table 4.2,** and when breathing 40% O_2 are presented in **Table 4.3**.

Table 4.1. Anthropometric and Pulmonary Function Data

	Absolute	% Predicted
Age, yr	24.6 ± 4.9	
Height, cm	172 ± 11	
Weight, kg	73.3 ± 11.2	
FVC, L	5.12 ± 1.09	(103.6 ± 5)
FEV_1, L	4.19 ± 0.86	(101.5 ± 6.9)
FEV_1/FVC, %	82 ± 5	(97 ± 5)
FEF_{25-75}	4.18 ± 1.2	(95.4 ± 6.4)
SVC, L	5.43 ± 1.1	(111.4 ± 6.7)
TLC, L_{pleth}	6.55 ± 1	(106 ± 7.3)
DL_{CO}, mL · min^{-1} · $mmHg^{-1}$	36.56 ± 7.46	(122.5 ± 17.9)
DL_{CO}/V_A, mL · min^{-1} · $mmHg^{-1}$	5.69 ± 0.62	(117.1 ± 15.6)

Values are mean ± standard deviation. FVC, forced vital capacity; FEV1, forced expiratory volume in 1 s; SVC, slow vital capacity; FEF_{25-75}, forced expiratory flow from 25 to 75% of FVC; TLC, total lung capacity; DL_{CO}, uncorrected diffusion capacity for carbon monoxide; DL_{CO}/V_A, DL_{CO} per alveolar volume;

Transpulmonary Passage of Saline Contrast and Pulmonary Gas Exchange Efficiency

When breathing room air, from Pre EPI to 320 EPI, the transpulmonary passage of saline contrast increased **(Figure 4.2A)** concomitant with an increase in the A-aDO_2 **(Figure 4.2B)** that corresponded with an increase in calculated $\dot{Q}_{VA}/\dot{Q}_T$ **(Figure 4.2C)**. Similarly, when breathing 40% O_2, from Pre EPI to 320 EPI, the transpulmonary passage of saline contrast increased **(Figure 4.2D)** concomitant with an increase in the A-aDO_2 **(Figure 4.2E)** that corresponded with an increase in calculated $\dot{Q}_{VA}/\dot{Q}_T$ **(Figure 4.2F)**. As expected, when breathing 40% O_2 the magnitude of the increase in A-aDO_2 was greater compared to breathing room air, however, importantly, calculated $\dot{Q}_{VA}/\dot{Q}_T$ increased to the same extent and averaged 2 ± 1%.

Table 4.2. Cardiopulmonary and Respiratory Data Breathing Room Air, During the I.V. Infusion of EPI With and Without Atropine

	Pre EPI	320 EPI	V_A @ 320 EPI	Pre EPI (ATR)	ATR+80 EPI	V_A @ ATR+80 EPI
$\dot{V}_E$, L · min^{-1}	10.5 ± 2.2	16.4 ± 2.9*	15.5 ± 2.8*	11.4 ± 2.1	15.7 ± 3.2*	15.5 ± 2.9*
$\dot{V}_A$, L · min^{-1}	5.9 ± 1.7	9.5 ± 3.1*	9.4 ± 2.6*	5.5 ± 1.3	8.4 ± 2.1*	8.0 ± 1.6*
RR	14.3 ± 3.6	19.3 ± 2*	17.5 ± 4	18.2 ± 3.7	21.6 ± 3.4	20.6 ± 3.8
V_T, mL	764 ± 158	851 ± 141	937 ± 384	640 ± 112	730 ± 104	757 ± 117
V_D/V_T	0.44 ± 0.09	0.43 ± 0.08	0.39 ± 0.08	0.51 ± 0.07	0.47 ± 0.05	0.48 ± 0.05
$\dot{V}O_2$, L · min^{-1}	0.32 ± 0.08	0.35 ± 0.08	0.34 ± 0.06	0.30 ± 0.06	0.33 ± 0.09	0.31 ± 0.06
$\dot{V}CO_2$, L · min^{-1}	0.28 ± 0.08	0.41 ± 0.10*	0.39 ± 0.08	0.27 ± 0.07	0.38 ± 0.09*	0.35 ± 0.07
RER	0.87 ± 0.04	1.21 ± 0.22*	1.15 ± 0.28*	0.89 ± 0.05	1.17 ± 0.1*	1.13 ± 0.14*
HR, bpm	63 ± 6	80 ± 16*	73 ± 10	82 ± 15	97 ± 20	83 ± 13
PaO_2, mm Hg	99 ± 4	107 ± 7	110 ± 8*	101 ± 4	107 ± 2*	110 ± 5*
$PaCO_2$, mm Hg	41 ± 4	38 ± 5	36 ± 4	41 ± 4	39 ± 3	37 ± 3
PAO_2, mm Hg	99 ± 5	113 ± 7*	112 ± 8*	99 ± 4	111 ± 3*	112 ± 5*
SaO_2, %	96.9 ± 0.4	97.2 ± 0.4	97.4 ± 0.3	96.9 ± 0.3	97.2 ± 0.3	97.4 ± 0.2
CaO_2, ml O_2 · dL^{-1}	17.46 ± 1.62	18.47 ± 1.69	17.51 ± 1.8	17.2 ± 1.77	18.07 ± 1.84	17.72 ± 1.93
pH	7.392 ± 0.017	7.402 ± 0.028	7.418 ± 0.023	7.387 ± 0.018	7.391 ± 0.01	7.405 ± 0.015
Hct, %	39 ± 3	41 ± 3	40 ± 4	39 ± 5	40 ± 4	41 ± 3
Hb, g · dL^{-1}	13.2 ± 1.3	13.9 ± 1.3	13.2 ± 1.4	13 ± 1.4	13.6 ± 1.4	13.3 ± 1.5
Core Temp, °C	36.8 ± 0.3	36.7 ± 0.3	36.8 ± 0.3	36.9 ± 0.3	36.7 ± 0.3	36.7 ± 0.3
Lactate, mmol · L^{-1}	0.94 ± 0.32	1.59 ± 0.38*	1.28 ± 0.34	1.12 ± 0.3	1.35 ± 0.32	1.42 ± 0.3

Values are mean ± standard deviation. $\dot{V}_A$, minute ventilation, $\dot{V}_A$, alveolar ventilation; RR, respiratory rate; V_T, tidal volume; V_D/V_T, dead space to tidal volume ratio; a-$P_{ET}CO_2$, arterial-to-end tidal PCO_2 difference; $\dot{V}O_2$, volume of O_2 consumed; $\dot{V}CO_2$, volume of CO_2 produced; RER, respiratory exchange ratio; HR, heart rate; PaO_2, arterial PO_2; $PaCO_2$, arterial PCO_2; PAO_2, alveolar PO_2; SaO_2, arterial oxygen saturation; CaO_2, arterial oxygen content; Hct, hematocrit; Hb, hemoglobin. *, $p < 0.05$, Pre EPI compared to 320 EPI and $\dot{V}_A$ @ 320 EPI; *, $p < 0.05$, Pre EPI (ATR) compared to ATR+80 EPI and $\dot{V}_A$ @ ATR+80 EPI.

Table 4.3. Cardiopulmonary and Respiratory Data Breathing 40% O_2, During the I.V. Infusion of EPI With and Without Atropine

	Pre EPI	320 EPI	V_A @ 320 EPI	Pre EPI (ATR)	ATR+80 EPI	V_A @ ATR+80 EPI
$\dot{V}_E$, L・min^{-1}	10.4 ± 2.5	15.6 ± 4.7*	14.6 ± 4.2	11.3 ± 2.1	15 ± 3	14.9 ± 4.5
$\dot{V}_A$, L・min^{-1}	5.3 ± 1.3	10.9 ± 9.0	9.9 ± 8.0	5.4 ± 1.2	8.8 ± 2.5	7.7 ± 3.1
RR	15.9 ± 3.8	19.2 ± 5.5	18.2 ± 5	18.2 ± 2.8	21.6 ± 4.4	20.3 ± 4.6
V_T, mL	656 ± 59	830 ± 221	840 ± 294	620 ± 62	702 ± 78	740 ± 177
V_D/V_T	0.48 ± 0.05	0.45 ± 0.05	0.46 ± 0.08	0.53 ± 0.06	0.43 ± 0.06	0.49 ± 0.08
$\dot{V}O_2$, L・min^{-1}	0.30 ± 0.08	0.33 ± 0.08	0.31 ± 0.09	0.28 ± 0.07	0.31 ± 0.07	0.27 ± 0.09
$\dot{V}CO_2$, L・min^{-1}	0.26 ± 0.06	0.39 ± 0.12*	0.35 ± 0.10	0.26 ± 0.06	0.37 ± 0.09	0.34 ± 0.14
RER	0.86 ± 0.1	1.16 ± 0.21*	1.05 ± 0.14*	0.93 ± 0.12	1.24 ± 0.13*	1.25 ± 0.19*
HR, bpm	58.2 ± 7.6	81.3 ± 22.2*	72.1 ± 11.3	83.2 ± 23.6	92.2 ± 24.2	81 ± 18.2
PaO_2, mm Hg	223 ± 12	222 ± 8	232 ± 11	220 ± 9	225 ± 4	230 ± 11
$PaCO_2$, mm Hg	42 ± 5	37 ± 9	36 ± 9	42 ± 4	38 ± 4	39 ± 3
PAO_2, mm Hg	235 ± 10	245 ± 8	245 ± 12	230 ± 6	243 ± 8*	241 ± 9*
SaO_2, %	98.01 ± 0.29	97.93 ± 0.27	98 ± 0.24	97.96 ± 0.2	97.96 ± 0.19	98.03 ± 0.2
CaO_2, ml O_2・dL^{-1}	18.1 ± 1.84	18.92 ± 1.77	18.21 ± 1.7	18.02 ± 1.95	18.59 ± 2.05	18.07 ± 1.94
pH	7.388 ± 0.017	7.400 ± 0.026	7.406 ± 0.04	7.386 ± 0.015	7.384 ± 0.014	7.407 ± 0.018†
Hct, %	40 ± 4	41 ± 4	40 ± 4	40 ± 3	41 ± 4	39 ± 3
Hb, g・dL^{-1}	13.3 ± 1.4	13.9 ± 1.4	13.3 ± 1.3	13.2 ± 1.5	13.7 ± 1.6	13.2 ± 1.5
Core Temp, °C	36.7 ± 0.2	36.8 ± 0.3	36.8 ± 0.2	36.8 ± 0.2	36.7 ± 0.3	36.8 ± 0.2
Lactate, mmol・L^{-1}	0.83 ± 0.19	1.54 ± 0.4*	1.42 ± 0.32†	1.03 ± 0.32	1.28 ± 0.21	1.28 ± 0.29

Values are mean ± standard deviation. See Table 4.2 for definitions of abbreviations and symbols.

When breathing room air, from Pre EPI (ATR) to ATR+80 EPI, the transpulmonary passage of saline contrast increased **(Figure 4.2A)** concomitant with an increase in the A-aDO_2 **(Figure 4.2B)** that corresponded with an increase in calculated **(Figure 4.2C)**. When breathing 40% O_2, from Pre EPI (ATR) to ATR+80 EPI, the transpulmonary passage of saline contrast increased **(Figure 4.2D)** concomitant with an increase in the A-aDO_2 **(Figure 4.2E)** that corresponded with an increase in calculated $\dot{Q}_{VA}/\dot{Q}_T$ **(Figure 4.2F)**. Similarly, as expected when breathing 40% O_2 the magnitude of the increase in A-aDO_2 was greater compared to breathing room air, however, importantly, calculated $\dot{Q}_{VA}/\dot{Q}_T$ increased to the same extent and averaged 2 ± 1%. Therefore, both before and after ATR, the i.v. infusion of EPI at either 320 or 80 ng/kg/min corresponded to an impairment in pulmonary gas exchange efficiency and an increase in calculated $\dot{Q}_{VA}/\dot{Q}_T$ that all averaged 2 ± 1%.

The respiratory rate and tidal volume, and therefore $\dot{V}_A$, subjects had during 320 EPI was reproduced for the $\dot{V}_A$ @ 320 EPI measurement. Accordingly, per experimental design there was no difference in $\dot{V}_A$ or dead space ventilation (V_D/V_T) between 320 EPI and $\dot{V}_A$ @ 320 EPI when breathing room air and 40% O_2 **(Table 4.2 and 4.3)**. Prior to the $\dot{V}_A$ @ 320 EPI measurement, EPI from the preceding infusion (i.e., 320 EPI) was allowed time to be metabolized and as such the transpulmonary passage of saline contrast was reduced to Pre EPI values at this time point when breathing room air **(Figure 4.2A)** and 40% O_2 **(Figure 4.2D)**. Similarly, at $\dot{V}_A$ @ 320 EPI the A-aDO_2 was reduced to Pre EPI values when breathing room air **(Figure 4.2B)** and 40% O_2 **(Figure 4.2E)** which also corresponded to calculated $\dot{Q}_{VA}/\dot{Q}_T$ being reduced to Pre EPI values when breathing room air **(Figure 4.42C)** and 40% O_2 **(Figure 4.2F).**

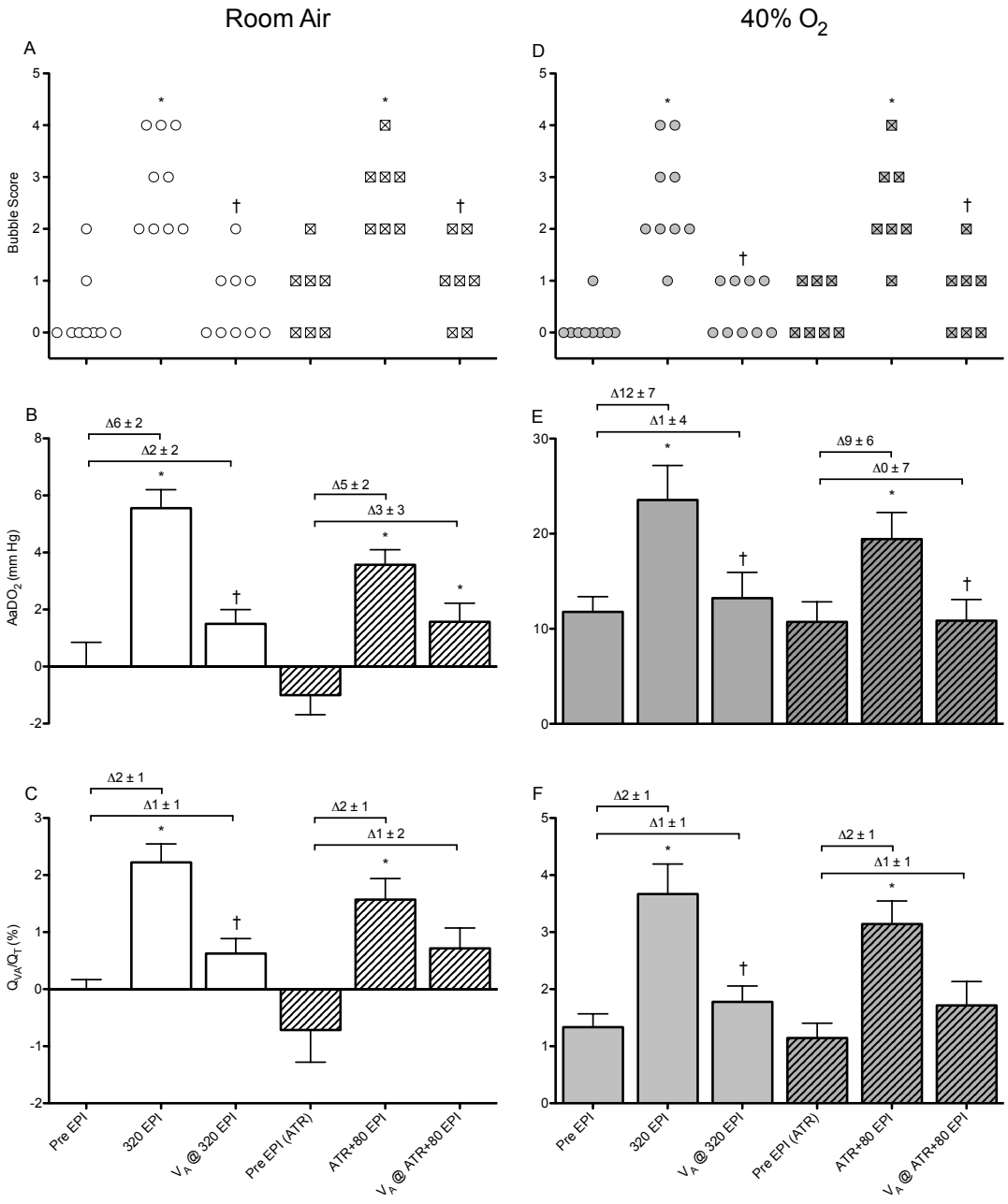

Figure 4.2. Bubble Scores and Pulmonary Gas Exchange Efficiency
*The transpulmonary passage of saline contrast (bubble scores, panel A and B), pulmonary gas exchange efficiency (A-aDO_2, panel C and D) and calculated venous admixture ($\dot{Q}_{VA}/\dot{Q}_T$, panel E and F) before (non-hatched) and after (hatched) vagal blockade breathing room air (open symbols) and 40% O_2 (shaded symbols). * = Pre EPI compared to 320 EPI and $\dot{V}_A$ @ 320 EPI; Pre EPI (ATR) compared to ATR+80 EPI and $\dot{V}_A$ @ ATR+80 EPI. † = 320 EPI compared to $\dot{V}_A$ @ 320 EPI; ATR+80 EPI compared to $\dot{V}_A$ @ ATR+80 EPI.*

When breathing room air, during $\dot{V}_A$ @ ATR+80 EPI the transpulmonary passage of saline contrast was reduced to Pre EPI (ATR) values **(Figure 4.2A)**, corresponding to a reduction in calculated $\dot{Q}_{VA}/\dot{Q}_T$ to Pre EPI (ATR) values **(Figure 4.2C)**. When breathing 40% O_2, from ATR+80 EPI to $\dot{V}_A$ @ ATR+80 EPI, the transpulmonary passage of saline contrast was reduced to Pre EPI (ATR) values **(Figure 4.2D)** corresponding to a reduction in the A-aDO_2 **(Figure 4.2E)** and calculated $\dot{Q}_{VA}/\dot{Q}_T$ **(Figure 4.2F)** to Pre EPI (ATR) values.

Cardiac Output and Pulmonary Artery Systolic Pressure

When breathing room air and 40% O_2, $\dot{Q}_T$ increased during 320 EPI and ATR+80 EPI, however there was no difference between 320 EPI and ATR+80 EPI **(Figure 4.3A and 4.3B)**. Pulmonary artery systolic pressure (PASP) increased during 320 EPI **(Figure 4.3C and 4.3D)** when breathing room air and 40% O_2. However, PASP was not increased during ATR+80 EPI when breathing room air and 40% O_2 **(Figure 4.3C and 4.3D)**.

DISCUSSION

The main finding of this study was that the i.v. infusion of EPI in healthy humans resulted in an increase in the transpulmonary passage of saline contrast and a concomitant increase in the A-aDO_2 and calculated $\dot{Q}_{VA}/\dot{Q}_T$; when breathing room air and 40% O_2. Neither the transpulmonary passage of saline contrast, nor the calculated $\dot{Q}_{VA}/\dot{Q}_T$ differed during the i.v. infusion of EPI when breathing room air and 40% O_2. The increase in A-aDO_2 observed during the i.v. infusion of EPI before or after vagal blockade was not due to the associated increase in ventilation. Furthermore, these findings were present during

the i.v. infusion of EPI at 320 ng/kg/min before vagal blockade, and during the i.v. infusion of EPI at 80 ng/kg/min after vagal blockade. Lastly, these data lend support that blood flow through IPAVA is mediated primarily by increases in $\dot{Q}_T$.

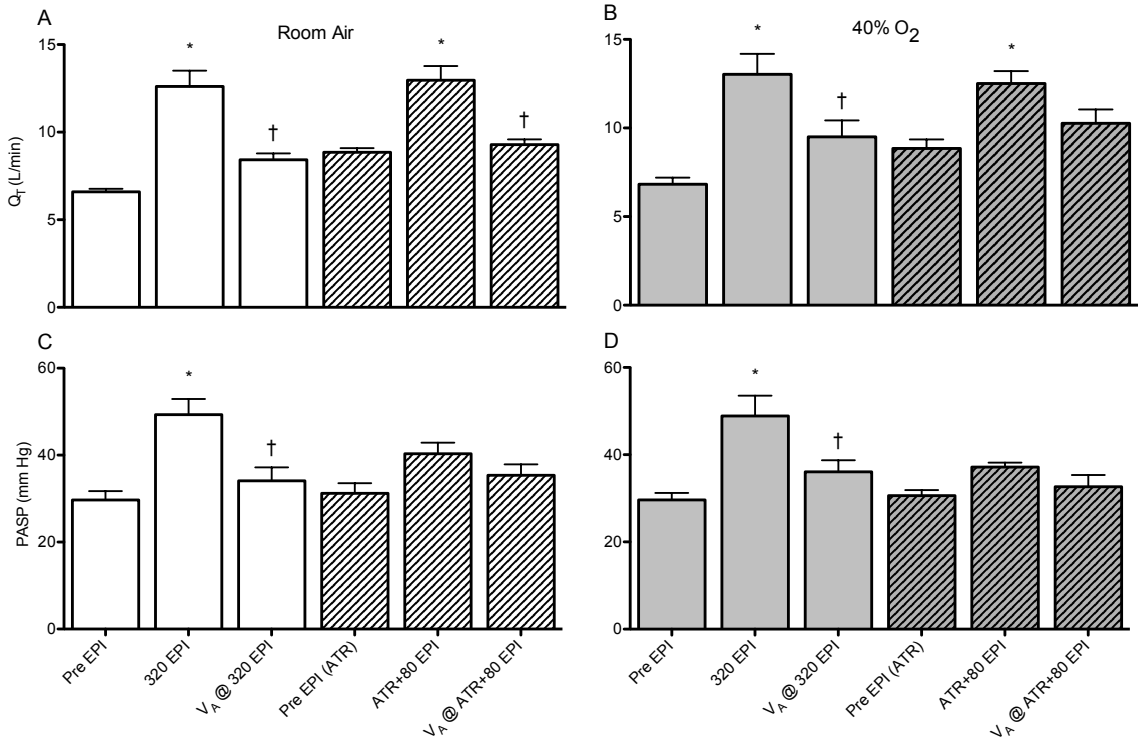

Figure 4.3. Cardiac Output and Pulmonary Artery Systolic Pressure
*Cardiac output (Panel A and B) and pulmonary artery systolic pressure (PASP, panel C and D) before (non-hatched) and after (hatched) vagal blockade breathing room air (open symbols) and 40% O_2 (shaded symbols). * = Pre EPI compared to 320 EPI and $\dot{V}_A$ @ 320 EPI; Pre EPI (ATR) compared to ATR+80 EPI and $\dot{V}_A$ @ ATR+80 EPI. † = 320 EPI compared to $\dot{V}_A$ @ 320 EPI; ATR+80 EPI compared to $\dot{V}_A$ @ ATR+80 EPI.*

Experimental Design

Pulmonary gas exchange efficiency is defined and quantified by the A-aDO_2 where an A-aDO_2 >0 mm Hg reflects imperfect pulmonary gas exchange that could be caused by three distinct mechanisms; 1) incomplete end-capillary O_2 diffusion equilibration (diffusion limitation), 2) alveolar ventilation-to-perfusion ($\dot{V}_A/\dot{Q}$) inequality,

and 3) right-to-left shunt. Importantly, subjects in the current study were rigorously screened and did not have an intracardiac shunt (i.e., a PFO). Therefore, sources of right-to-left shunt present in subjects in the current work are postpulmonary shunt (e.g., venous blood from the bronchial and Thebesian circulations) and intrapulmonary shunt. Previous work has hypothesized that blood flow through IPAVA, inferred from the transpulmonary passage of saline contrast, provides a source of intrapulmonary shunt (24, 143, 216). However, this remains a controversial topic (103) and therefore was the focus of the current investigation.

As outlined in the introduction, the experimental paradigm used to address this question was to increase blood flow through IPAVA in healthy humans at rest when breathing room air and 40% O_2. When breathing 40% O_2 the potential contributions from diffusion limitation and $\dot{V}_A/\dot{Q}$ inequality to the A-aDO_2 are prevented, and therefore, the contribution of postpulmonary and intrapulmonary shunt will be the only remaining factor capable of explaining an increase in the A-aDO_2 and calculated $\dot{Q}_{VA}/\dot{Q}_T$.

Effect of breathing 40% O_2 on diffusion limitation. Compared to breathing room air, when breathing 40% O_2 PAO_2 increased from ~100 mmHg to ~235 mm Hg, corresponding to an increase in calculated mixed venous PO_2 ($P\bar{v}O_2$) of ~40 mm Hg when breathing room air, to ~45 mm Hg when breathing 40% O_2. Accordingly, the partial pressure gradient of O_2 across the alveolar-capillary interface was ~60 mm Hg when breathing room air, which increased >3 fold to ~190 mm Hg when breathing 40% O_2. The result of this increased driving gradient for the diffusion of O_2 across the alveolar-capillary interface is a markedly increased rate of end-capillary O_2 equilibration. Using a computer algorithm implementing a Bohr integration for the lung, similar to

previously published work (240, 243), the rate of O_2 uptake across the alveolar-capillary interface can be model-predicted. According to this model, in subjects at rest breathing room air, complete end-capillary O_2 equilibration is predicted to occur within ~0.4 sec, whereas when breathing 40% O_2 complete end-capillary O_2 equilibration is predicted to occur within ~0.1 sec. Importantly, in these same conditions, mean pulmonary capillary transit time is predicted to be ~0.7 sec, which is unchanged between breathing room air and 40% O_2. Although on average complete end-capillary O_2 equilibration is expected to occur when breathing room air at rest (235), it remains possible that some lung units might have a pulmonary capillary transit time <0.4 sec, such that these lung units would potentially be diffusion limited. However, this possible scenario is much less likely when breathing 40% O_2 considering the pulmonary capillary transit time in a diffusion limited lung unit would need to be <0.1 sec. Therefore, when breathing 40% O_2, the potential contribution from diffusion limitation to the A-aDO_2 is minimized compared to breathing room air.

Effect of breathing 40% O_2 on $\dot{V}_A/\dot{Q}$ inequality. When breathing 40% O_2, the potential contribution from $\dot{V}_A/\dot{Q}$ inequality on the A-aDO_2 would also be expected to be minimized compared to breathing room air, based on the same principles as those which define the 100% O_2 technique. With the removal of alveolar N_2, as occurs when breathing 100% O_2, the PAO_2 in all lung units must increase to that of the inspired PO_2 less $PACO_2$. There is then, very little discrepancy in PAO_2 between lung units, regardless of their respective $\dot{V}_A/\dot{Q}$ ratios, and how poorly ventilated they may be. Following this same logic, although alveolar N_2 is not eliminated when breathing 40% O_2, it's further reduced compared to breathing room air and the venous admixture component of $\dot{V}_A/\dot{Q}$ inequality

is nearly eliminated when PAO_2 reaches ~250 mm Hg (65). Although regional atelectasis resulting in $\dot{V}_A/\dot{Q}$ inequality may be a concern when breathing a high FIO_2, prior work in humans breathing 40% O_2 has been shown to not be associated with an increase in $\dot{V}_A/\dot{Q}$ inequality (45).

Effect of breathing 40% O_2 on blood flow through IPAVA. The effect of breathing 40% O_2 on blood flow through IPAVA has not been directly investigated and more extensive work in this area would be of interest. However, it is known that breathing 100% O_2 during exercise (54, 144) and during the i.v. infusion of catecholamines (24, 133) significantly reduces, or eliminates the transpulmonary passage of saline contrast. This has been demonstrated to not be a product of O_2 breathing altering the *in vivo* dynamics of saline contrast (54) and is also in agreement with work using solid microspheres to detect a reduction in blood flow through IPAVA in anesthetized dogs ventilated with 100% O_2 (171). Conversely, bubble scores during 320 EPI and ATR+80 EPI were not different between breathing room air and 40% O_2 **(Figure 4.2A and 4.2B)** yet bubble scores have been shown to be reduced or eliminated during 320 EPI when breathing 100% O_2 (133). Thus, our experimental paradigm allows for blood flow through IPAVA while preventing contributions from $\dot{V}_A/\dot{Q}$ inequality and diffusion limitation.

Pulmonary Gas Exchange Efficiency During the I.V. Infusion of Epinephrine

When breathing room air the A-aDO_2 increased by 6 mm Hg at 320 EPI compared to Pre EPI, which corresponded to an increase in calculated $\dot{Q}_{VA}/\dot{Q}_T$ of 2%. This 2% increase in calculated $\dot{Q}_{VA}/\dot{Q}_T$ necessary to explain the measured A-aDO_2 could in theory include contributions from diffusion limitation, $\dot{V}_A/\dot{Q}$ inequality, and right-to-

left shunt. When breathing 40% O_2 the A-aDO_2 increased by 12 mm Hg at 320 EPI compared to Pre EPI, which corresponded to a similar increase in calculated $\dot{Q}_{VA}/\dot{Q}_T$ of 2%. However, unlike when breathing room air, this 2% increase in calculated $\dot{Q}_{VA}/\dot{Q}_T$ when breathing 40% O_2 is only explained by an increase in right-to-left shunt. Prior work in dogs has also demonstrated an increase in intrapulmonary shunt during the i.v. infusion of EPI using microspheres (172) to detect blood flow through IPAVA and by arterial blood gas analysis to determine the impact on pulmonary gas exchange efficiency; a finding that was also demonstrated to be eliminated in dogs ventilated with 100% O_2 (16) demonstrating that 100% O_2 prevented blood flow through IPAVA as we have suggested occurs in humans (54, 144).

During the i.v. infusion of EPI at either 320 EPI or ATR+80 EPI, $\dot{Q}_T$ was similarly increased by ~2 fold above Pre EPI values. Assuming no change in pulmonary capillary blood volume, this should correspond to a decrease in mean pulmonary capillary transit time from ~0.7 sec to ~0.35 sec. As previously discussed, when breathing room air and 40% O_2 complete end-capillary O_2 equilibration is expected to occur within ~0.4 sec and ~0.1 sec, respectively. Therefore, if pulmonary capillary blood volume remained constant, some degree of diffusion limitation would be possible when breathing room air, although breathing 40% O_2 should sufficiently minimize this potential. That said, it seems unlikely that pulmonary capillary blood volume would not increase to some degree in response to the ~2-fold increase in pulmonary blood flow and any increase in pulmonary capillary blood volume would mitigate reductions in mean pulmonary capillary transit time. Furthermore, as expected based on the Fick principle of mass balance, calculated $P\bar{v}O_2$ increased secondary to the ~2 fold increase in $\dot{Q}_T$ and constant

whole body $\dot{V}O_2$. Specifically, calculated $P\bar{v}O_2$ would have increased from ~40 mm Hg at Pre EPI to ~50 mm Hg at 320 EPI when breathing room air, and from 45 mm Hg at Pre EPI to ~55 mm Hg at 320 EPI when breathing 40% O_2. In both cases, the ~10 mm Hg increase in $P\bar{v}O_2$ would help to accelerate end-capillary O_2 equilibration (243).

The potential that $\dot{V}_A/\dot{Q}$ inequality was increased during the i.v. infusion of EPI at 320 EPI or at ATR+80 EPI cannot be excluded, although as discussed it would likely be minimized when breathing 40% O_2 compared to room air. Prior work investigating the effect of inotropic drugs on $\dot{V}_A/\dot{Q}$ inequality in healthy humans is lacking. However, in 4 patients admitted to the intensive care unit for acute respiratory failure from pulmonary embolism, Manier and Castaing (154) showed a non-significant decrease in mean $\dot{V}_A/\dot{Q}$ for blood flow distribution (0.67 to 0.57) and non-significant decrease in Log SD_Q (1.19 to 1.11) during the i.v. infusion of dobutamine at 10 μg/kg/min. In 2 of these patients shunt ($\dot{V}_A/\dot{Q} = 0$) increased, one of which was also assessed during the i.v. infusion of dobutamine when breathing 40% O_2 and shunt was unchanged compared to breathing room air. In another study, Rennotte *et al*. (194) studied 10 patients admitted to the intensive care unit for a variety of reasons and found a significant increase in log SD_Q during the i.v. infusion of dopamine, but not during the i.v. infusion of dobutamine (both drugs at 5 μg/kg/min). Work in dogs with pulmonary edema secondary to oleic acid infusion, has demonstrated that an increase in $\dot{Q}_T$ via the i.v. infusion of isoproterenol (136) and dopamine (151) resulted in a significant increase in shunt. Of note, in the work by Lynch *et al*., the changes in shunt occurred whether $\dot{Q}_T$ was pharmacologically or mechanically altered. Therefore, as concluded by these authors, the increase in shunt from pharmacologically increased $\dot{Q}_T$ is likely not due to vasoconstrictor or vasodilator

activity of these drugs as the increase in shunt is observed when $\dot{Q}_T$ is increased via mechanical means as well. The current study in healthy humans lends support to this conclusion, by demonstrating the same increase in shunt in response to the same increase in $\dot{Q}_T$ during both 320 EPI and ATR+80 EPI.

If it is accepted that diffusion limitation and $\dot{V}_A/\dot{Q}$ inequality are likely not significantly contributing to the measured A-aDO_2 in healthy humans breathing room air and 40% O_2 during 320 EPI and ATR+80 EPI, one possibility other than an increase in intrapulmonary shunt remains; an increase in postpulmonary shunt. The chronotropic and inotropic effects of EPI, and chronotropic effects of ATR may increase Thebesian blood flow, and similarly the increase in ventilation may increase bronchial blood flow. In an attempt to control for the potential confounding effects of increased ventilation, measurements were made in iso-alveolar ventilation conditions after EPI had been allowed time (~20 min) to be metabolized [i.e., $\dot{V}_A$ @ 320 EPI and $\dot{V}_A$ @ ATR+80 EPI]. At these time points, tidal volume and respiratory rate were matched to their respective, preceding condition during the i.v. infusion of EPI **(Table 4.2 and 4.3)**. Accordingly, the increase in calculated Q_{VA}/Q_T during $\dot{V}_A$ @ 320 EPI and $\dot{V}_A$ @ ATR+80 EPI may serve as a measure of predominantly bronchial shunt. Therefore, subtracting the increase in $\dot{Q}_{VA}/\dot{Q}_T$ during $\dot{V}_A$ @ 320 EPI and $\dot{V}_A$ @ ATR+80 EPI, from 320 EPI and ATR+80 EPI, respectively, would yield the increase in total right-to-left shunt less the contribution from bronchial blood flow. Doing so reveals an ~1% increase in $\dot{Q}_{VA}/\dot{Q}_T$ during 320 EPI breathing room air and 40% O_2, and an ~1% increase in $\dot{Q}_{VA}/\dot{Q}_T$ during ATR+80 EPI breathing room air and 40% O_2 **(Table 4.4)**, of which could be either Thebesian and/or intrapulmonary shunt.

Table 4.4. Difference in $\dot{Q}_{VA}/\dot{Q}_T$ With I.V. EPI and During Conditions of Iso-Alveolar Ventilation Without I.V. EPI

		Q_{VA}/Q_T		Q_{VA}/Q_T
Room Air	320 EPI	2%	ATR+80 EPI	2%
	$\dot{V}_A$ @ 320 EPI	1%	$\dot{V}_A$ @ ATR+80 EPI	1%
	Difference =	**1%**	Difference =	**1%**
40% O_2	320 EPI	2%	ATR+80 EPI	2%
	$\dot{V}_A$ @ 320 EPI	1%	$\dot{V}_A$ @ ATR+80 EPI	1%
	Difference =	**1%**	Difference =	**1%**
	Mean =	**1%**	Mean =	**1%**

Reconciling Anatomic and Gas Exchange Dependent Data

Neither work using the multiple inert gas elimination technique nor the 100% O_2 technique, both gas exchange dependent methods, have reported detecting significant intrapulmonary right-to-left shunt in healthy humans during exercise. Pooling data from several studies using the MIGET (101, 112, 175, 195), intrapulmonary shunt averages 0.2 ± 0.7% of the $\dot{Q}_T$. Work by Vogiatzis *et al*. (233) reports right-to-left shunt from all sources measured during exercise in subjects breathing 100% O_2 to average 0.5 ± 0.5%. Data from the current study, particularly when breathing 40% O_2, challenges these data by reporting a calculated $\dot{Q}_{VA}/\dot{Q}_T$ of 2% during conditions of increased blood flow through IPAVA while contributions from diffusion limitation and $\dot{V}_A/\dot{Q}$ inequality are minimized. However, breathing 100% O_2 has been demonstrated to reduce or eliminate blood flow through IPAVA as detected using TTSCE (24, 54, 133, 144). If true, then the impact of blood flow through IPAVA on pulmonary gas exchange efficiency would be minimal when breathing 100% O_2. However, when breathing 40% O_2 blood flow through

IPAVA can be detected using TTSCE, and there is also a significant and measureable impact on pulmonary gas exchange efficiency.

Cardiac Output and Pulmonary Artery Systolic Pressure

Cardiac output and PASP have previously been hypothesized as potential mechanisms responsible for regulating blood flow through IPAVA (24, 130, 133, 173, 216). The primary purpose of the ATR+80 EPI measurement was to facilitate increasing $\dot{Q}_T$ to a similar extent as 320 EPI, with a lower dose of EPI. However, it has also been shown that the chronotropic effects of ATR are associated with no change in mean pulmonary artery pressure measured using right heart catheterization in patients with asthma and emphysema at rest (263) and in a different group of patients (1). In support of these observations, although in healthy human subjects, PASP in the current study was unchanged during Pre EPI (ATR) compared to Pre EPI, despite $\dot{Q}_T$ increasing by ~2 L/min when breathing room air and 40% O_2 **(Figure 4.3)**. Furthermore, unlike during 320 EPI which resulted in an ~20 mm Hg increase in PASP, during ATR+80 EPI, PASP only increased by ~10 mm Hg when breathing room air and 40% O_2 **(Figure 4.3)**. In both conditions, 320 EPI and ATR+80 EPI, $\dot{Q}_T$ was not different (~12.5 L/min) when breathing room air and 40% O_2 **(Figure 4.3)**. Therefore, both 320 EPI and ATR+80 EPI produced similar increases in $\dot{Q}_T$, yet PASP was less during ATR+80 EPI, and there was no difference in bubble scores during 320 EPI and ATR+80 EPI **(Figure 4.2)**. Although bubble scores do not represent a means to quantify blood flow through IPAVA and are a semi-quantitative, non-distributed variable, the calculated $\dot{Q}_{VA}/\dot{Q}_T$ was ~2% during both 320 EPI and ATR+80 EPI when breathing room air and 40% O_2. These data suggest that

blood flow through IPAVA is more dependent on increases in pulmonary blood flow, rather than increases in pulmonary artery systolic pressure.

Limitations

Saline contrast echocardiography. The detection of blood flow through IPAVA using TTSCE is based on the rationale that the pulmonary circulation functions as a biological sieve, filtering out bubbles that are larger than the diameter of a pulmonary capillary. Although the size of the injected bubbles remains unknown, it is estimated that based on the minimum size necessary for bubbles to be stable enough to survive the pulmonary transit time, their initial diameter would need to be >60 μm (53). To date, there is no direct evidence that either pulmonary capillaries or corner vessels can distend to diameters >20 μm, even under pulmonary pressures that are supra-physiologic for humans. For example at pulmonary pressures up to 73 mm Hg in isolated greyhound lungs the mean capillary diameter was found to be 6.5 μm and the maximum capillary diameter measured was 13 μm (75, 199). Thus, the transpulmonary passage of bubbles larger than the diameter of a pulmonary capillary indicates these bubbles have escaped pulmonary capillary filtration by traversing the pulmonary circulation via large diameter IPAVA. However, this technique *does not* quantify the volume of blood flow through IPAVA; therefore, the bubble scoring system which is not without precedent (11), offers a qualitative assessment of the degree and spatial distribution of left-sided contrast.

In subjects without a PFO, the alternative explanation for observing left-sided saline contrast is the possibility that bubbles are, by some means, travelling through pulmonary capillaries and/or corner vessels. In this way, left-sided contrast would not reflect blood flow through IPAVA. However, this possibility should be considered with

several points in mind. First, bubbles small enough to traverse pulmonary capillaries (<10 μm) have an estimated survival time of 180-550 msec (164, 269, 270) and in healthy humans at rest, mean pulmonary transit time is ~9 sec, that decreases to ~3 sec at maximal exercise with $\dot{Q}_T$ in excess of 30 L/min (100). Second, Roelandt *et al*. (198) demonstrated that an injection pressure of 300 mm Hg through a firmly wedged pulmonary artery catheter was needed to observe left-sided contrast, by forcing bubbles to deform and squeeze through pulmonary capillaries. Third, pulmonary capillary disruption, not distension has been predicted to be the more likely result of pulmonary capillary pressures sufficient to distend pulmonary capillaries to >20 μm in diameter (253).

Although we cannot definitely rule out the possibility that microbubbles are, by some means, traversing pulmonary capillaries, the transpulmonary passage of 25 and 50 μm microspheres has been demonstrated in isolated human lungs ventilated and perfused with physiologic pressures (146). And work in animals during exercise (215) and breathing hypoxic gas at rest (12) demonstrate the transpulmonary passage of >25 μm and 70 μm microspheres, respectively. Importantly, the transpulmonary passage of non-deformable, large diameter microspheres can only be explained by blood flow through IPAVA, and for these aforementioned studies using microspheres, studies using saline contrast microbubbles demonstrate the same findings (54, 134, 143).

Accurately Measuring Arterial PO_2 >200 mm Hg. Accurate measurements of PaO_2 are critically important to the interpretation of these data, and several precautions were taken to ensure very high standards. When breathing room air PaO_2 at Pre EPI was ~100 mm Hg (Eugene, OR; 130 m above sea level), which increased to ~220 mm Hg when

breathing 40% O_2. During 320 EPI and ATR+80 EPI when $\dot{V}_A$ was doubled, PaO_2 increased to ~110 mm Hg and ~230 mm Hg when breathing room air and 40% O_2, respectively. Accordingly, this >2-fold increase in PaO_2 when breathing 40% O_2 amplifies several potential sources of error compared to when breathing room air, all of which can only decrease the measured PO_2, and therefore, increase the measured A-aDO_2. Perhaps the most significant error is that air bubbles within the sampling syringe, will be composed of room air, and thus contain a PO_2 of ~150 mm Hg, ~70 to 80 mm Hg lower than PaO_2 when breathing 40% O_2. This was minimized by withdrawing all arterial blood samples in such a way as to keep any small air bubble at the top of the sample, which was immediately expelled, and by maintaining a positive pressure on the sample syringe during the analysis to pre-emptively prevent the production of an air bubble.

Additional potential issues are, 1) the possible diffusion of O_2 from the sample through the syringe, 2) the consumption of O_2 by white blood cells, and 3) the consumption of O_2 by the PO_2 electrode during the analysis. The impact of the first two concerns increases over time, and therefore, we minimized this by immediately analyzing each sample. All of these concerns can also, at least partially, be corrected for by calibrating the blood gas analyzer on each study day using tonometered human blood, as before (142). This practice is similar, but superior, to using standard quality control methods in that it allows for the correction of day-to-day fluctuations and inherent errors in measuring the exact PO_2 and PCO_2, of which, include aforementioned concerns. Consistent inherent errors with handling and analyzing blood with PaO_2 in the 220-230 mm Hg range are also present during tonometry, and therefore this correction factor will help offset these. After correcting PaO_2 and $PaCO_2$ for core body temperature, the

tonometry correction resulted in an average increase in PaO_2 of <1 mm Hg and <2 mm Hg when breathing room air and 40% O_2, respectively. The minimal change in PaO_2, particularly when breathing 40% O_2 is reflective of our careful handing and immediate analysis of all arterial blood samples.

Lastly, although potential errors related to measuring PaO_2 can result in large errors in the measured A-aDO_2, these are less of a concern in the calculation of $\dot{Q}_{VA}/\dot{Q}_T$. As described in the methods, $Cc'O_2$ is calculated assuming complete end-capillary O_2 equilibration with PAO_2 that is calculated using the ideal alveolar gas equation, and from this the Kelman equation is used to compute $Sc'O_2$. Therefore, the calculation of PAO_2 is independent of the measured PaO_2 and is instead dependent on accurate measures of metabolic rate, the fraction of inspired O_2, and $PaCO_2$. In contrast, calculation of CaO_2 is affected by the measured PaO_2 inasmuch as the dissolved concentration of PO_2 contributes, which corresponds to <0.5 and <1 ml O_2/dL of blood or ~2% and ~4% of the CaO_2, when breathing room air and 40% O_2, respectively. Without direct measures of mixed venous blood, $C\bar{v}O_2$ is calculated using measured CaO_2, $\dot{V}O_2$, and Q_T according to the Fick principle of mass balance [$C\bar{v}O_2 = CaO_2 - (\dot{V}O_2/\dot{Q}_T)$]. Therefore, although CaO_2 is directly affected by errors in the measured PaO_2, $C\bar{v}O_2$ is affected to an equal magnitude in the same direction, which all else being equal, will offset error in the measured PaO_2 on the calculation of $\dot{Q}_{VA}/\dot{Q}_T$.

Summary

The current study investigated the potential that blood flow through IPAVA provides a source of venous admixture that can contribute relevantly to pulmonary gas exchange efficiency. These data demonstrate that during the i.v. infusion of EPI (i.e.,

during conditions of elevated pulmonary blood flow) the transpulmonary passage of saline contrast is increased concomitant with an increase in calculated $\dot{Q}_{VA}/\dot{Q}_T$ and A-aDO_2. Furthermore, this impairment in pulmonary gas exchange efficiency was present to the same extent, with $\dot{Q}_{VA}/\dot{Q}_T$ averaging ~2% during 320 EPI and ATR+80 EPI, not only when breathing room air, but also when breathing 40% O_2 when contributions from $\dot{V}_A/\dot{Q}$ inequality and diffusion limitation were minimized. When the potential contribution from predominately bronchial shunt is subtracted from this total, the average $\dot{Q}_{VA}/\dot{Q}_T$ is again similar between breathing room air and 40% O_2 and averages 1% which may be the result of Thebesian shunt and/or blood flow through IPAVA. The current paradigm describing mechanisms of impaired pulmonary gas exchange efficiency does not include blood flow through IPAVA, particularly during exercise. However, the transpulmonary passage of saline contrast is also observed during exercise and thus, blood flow through IPAVA during exercise may also provide a source of venous admixture.

Although during exercise breathing 40% O_2 blood flow through IPAVA is not reduced, during exercise breathing 100% O_2, blood flow through IPAVA is reduced. This has been repeatedly demonstrated using TTSCE, radiolabeled MAA, and microspheres. However, the explanation for this remains unknown and the purpose of the next chapter was to investigate the pharmacologic effect of sildenafil, nifedipine and acetazolamide, on the hyperoxia-mediated reduction in blood flow through IPAVA. This study marks the first investigation into this area.

CHAPTER V

PHARMACOLOGIC INVESTIGATIONS INTO THE MECHANISTIC REGULATION OF INTRAPULMONARY ARTERIOVENOUS ANASTOMSES

This chapter is in review with *Respiration Physiology & Neurobiology* and Joel E. Futral, Randall D. Goodman, and Andrew T. Lovering are co-authors. I performed the experimental work, led the project, and the writing is entirely mine; Joel E. Futral and Randall D. Goodman provided technical assistance with performing echocardiography during exercise; and Andrew T. Lovering helped develop the protocol, and provided guidance and editorial assistance.

INTRODUCTION

Blood flow through intrapulmonary arteriovenous anastomoses (IPAVA) is trivial or non-detectable in healthy humans at rest breathing room air (55), yet increases during exercise and the intravenous (i.v.) infusion of catecholamines when breathing room air as detected by the transpulmonary passage of saline contrast (24, 53, 54, 133, 143, 216). However, blood flow through IPAVA is prevented or significantly reduced during exercise and the i.v. infusion of catecholamines when breathing 100% O_2 (24, 54, 133, 144). This particular finding is controversial, in that it implies blood flow through the pulmonary circulation can be regulated by the fraction of inspired O_2 (FIO_2), and that IPAVA appear to be regulated opposite of the conventional pulmonary circulation. Specifically, IPAVA respond to changes in the FIO_2 similar to the systemic circulation and constrict in response to hyperoxia. However, previous work supports this supposition by demonstrating an active regulation of the pulmonary circulation as measured by an

increase in perfusion heterogeneity using 15 μm microspheres, in sheep ventilated with a FIO_2 = 0.4 (162) and pigs ventilated with a FIO_2 = 0.5 (93) compared to room air. Additionally, the transpulmonary passage of solid microspheres has been demonstrated to decrease in anesthetized dogs ventilated with 100% O_2 compared to room air (171). Furthermore, considering previous work demonstrating IPAVA dilate in response to hypoxia (134), the regulation of IPAVA bears a striking resemblance to the fetal cardiopulmonary circulation; and although patent in fetal sheep, blood flow through IPAVA decreases in juvenile sheep and is absent in adult sheep (158).

Regulated similar to IPAVA, constricting and dilating in response to increases and decreases in O_2 tension, respectively, is the ductus arteriosus that is also a vital component of the fetal cardiopulmonary circulation. Closure of the ductus arteriosus at birth is initiated by an increase in O_2 tension, a process regulated by O_2 sensitive potassium channels that are inhibited by increases in O_2 tension, leading to membrane depolarization and a subsequent increase in intracellular calcium through L-type voltage-gated calcium channels (230). In utero the tone of the ductus arteriosus is reflective of competing vasodilator and vasoconstrictor influences, with the primary vasodilating mechanisms being the production of endothelium-derived nitric oxide and prostaglandin E2 (37, 38). Accordingly, the mechanistic regulation of IPAVA may also resemble that of the ductus arteriosus. Specifically, the reduction in blood flow through IPAVA during exercise breathing a FIO_2 = 1.0, presumably via vasoconstriction of IPAVA, may also in part be regulated by L-type calcium channels or reductions in the bioavailability of nitric oxide. If so, pharmacologic interventions known to block L-type calcium channels (nifedipine) and augment the action of nitric oxide (sildenafil) may reduce or prevent the

potential O_2 mediated constriction of IPAVA and thereby allow for the transpulmonary passage of saline contrast during exercise breathing a $FIO_2 = 1.0$. Regardless of the mechanism, constriction of vascular smooth muscle is dependent on an increase in intracellular calcium and acetazolamide has been shown to prevent intracellular calcium from increasing in pulmonary vascular smooth muscle cells by a non L-type voltage-gated calcium channel mechanism (206). Thus, acetazolamide may also prevent the potential O_2 mediated constriction of IPAVA, and allow blood flow through IPAVA during exercise breathing a $FIO_2 = 1.0$.

Therefore, the purpose of this study was to investigate the independent effects of sildenafil, nifedipine, and acetazolamide on the regulation of blood flow through IPAVA during exercise breathing a $FIO_2 = 1.0$. To this end we studied 8 healthy human subjects at rest and during submaximal exercise breathing room air and a $FIO_2 = 1.0$, at baseline without any pharmacologic intervention, with a single dose of sildenafil (100 mg, p.o), with a single dose of nifedipine (20 mg, p.o), and after acetazolamide (250 mg, p.o., t.i.d for 3 days).

METHODS

The University of Oregon Office for Protection of Human Subjects approved this project and all subjects provided verbal and written informed consent prior to participation. All studies were performed in accordance with the *Declaration of Helsinki*.

Subjects

Eight subjects (2 female) volunteered to participate in this study, all of which were healthy, young, non-smoking and without a history of cardiopulmonary or respiratory disease.

According to the American Thoracic Society and European Respiratory Society standards (ATS/ERS) all subjects demonstrated normal spirometry, lung volumes and capacities, and diffusing capacity for carbon monoxide. Pulmonary function was assessed using computerized spirometry (MedGraphics Ultima CardiO_2, St. Paul, MN, USA) and involved forced and slow vital capacity maneuvers (166). Lung volumes and capacities were determined using whole body plethysmography (MedGraphics Elite Plethysmograph) (247). Lung diffusion capacity for carbon monoxide (DL_{CO}) was determined by the single-breath, breath hold method (119, 152) using the Jones and Meade method for timing (111).

All subjects underwent a comprehensive echocardiographic screening procedure performed by a registered diagnostic cardiac sonographer in both adult and pediatric echocardiography with 25 years of experience (Philips iE33, The Netherlands). The purpose of this screening procedure was to confirm that subjects were without cardiac abnormalities, including a patent foramen ovale (PFO). To this end, subjects were rigorously screened using transthoracic saline contrast echocardiography (TTSCE) as described previously (55, 139) and did not have a PFO.

Protocol

For each visit, subjects performed two bouts of cycle ergometer exercise (Lode Excalibur), separated by a 30 min rest period, at 50, 100, 150, 200, and 250 W for 3 min

each, breathing room air and 100% O_2. All subjects completed the aforementioned exercise protocol on four separate visits separated by >5 days; 1) without pharmacologic intervention (i.e., baseline); 2) with a single dose of 100 mg p.o. sildenafil, 3) with a single dose of 20 mg p.o. nifedipine, and 4) after 3 days of 250 mg p.o. acetazolamide, every 8 hours t.i.d. The order of pharmacologic intervention, as well as the order of exercise bouts breathing room air and 100% O_2, were randomized.

Detection of Blood Flow Through Intrapulmonary Arteriovenous Anastomoses

Transthoracic saline contrast echocardiography (TTSCE) was used to detect blood flow through IPAVA as before (133). However, briefly, agitated saline contrast was produced by combining 3 ml room air with 1 ml of normal saline and agitating for ~15 sec prior to injecting. Each agitated saline contrast injection was visualized in the apical, four-chamber view with subjects on the cycle ergometer in the forward leaning aerobar position, and recorded at >30 frames per second for 20 cardiac cycles post-appearance of saline contrast in the right ventricle. The single frame within the 20 cardiac cycle recording with the greatest density and spatial distribution of contrast was qualitatively assessed using a previously published scoring system (144) similar to others (11); 0 = no bubbles, 1 = 1-3 bubbles, 2 = 4-12 bubbles, 3 = >12 bubbles appearing as a bolus, 4 = >12 bubbles heterogeneously filling the left ventricle, and 5 = >12 bubbles homogeneously filling the left ventricle.

Respiratory Variables

Breath-by-breath metabolic data was collected (MedGraphics, CardiO_2) and presented as the mid 5 of 7 (i.e., the moving average of five breaths excluding the low and high). In this way continuous measures of pulmonary $\dot{V}O_2$, $\dot{V}CO_2$, minute ventilation

($\dot{V}_E$), and associated parameters, including end tidal PO_2 and PCO_2 values, were collected. Gases with known O_2 and CO_2 concentrations were used to calibrate the gas analyzer before every exercise test.

Cardiac Output and Pulmonary Artery Systolic Pressure

Cardiac output was estimated using echocardiography and determined at the level of the left ventricular outflow tract (LVOT). Previously during the screening visit, subjects LVOT diameter had been determined and recorded. This value was used to estimate the cross sectional area of the outflow tract. Pulsed wave Doppler ultrasound was used in all studies to determine the LVOT velocity time integral ($LVOT_{VTI}$) of blood flow through the outflow tract. Measures of the $LVOT_{VTI}$ were recorded in triplicate and the average was multiplied by the previously determined cross sectional area of the LVOT. The product of the $LVOT_{VTI}$ and LVOT cross sectional area equals the stroke volume, which multiplied by heart rate, provides an estimate of cardiac output.

Pulmonary artery systolic pressure was determined as before (133, 134) by measuring the peak velocity (v) of the tricuspid regurgitation jet and estimating right atrial pressure (P_{RA}) based on the collapsibility of the inferior vena cava, and applying these to the modified Bernoulli equation; $4v^2 + P_{RA}$ (42, 92, 202, 275).

Total pulmonary resistance (TPR) was calculated as previously described (120), by pulmonary artery systolic pressure divided by cardiac output, and has been previously published by our group (173).

Statistics

Statistical analyses were done using GraphPad Prism (v5.0d) and all comparisons were determined *a priori*. Comparisons of data from rest to exercise, within an FIO_2 and

pharmacologic intervention, were done using a one-way analysis of variance with a Tukey's multiple comparison post-hoc test. Comparisons of data at rest and during exercise within an FIO_2, with and without pharmacologic intervention were done using a paired t-test with alpha adjusted for the number of comparisons made. The aforementioned analyses were done for non-parametric data (i.e., bubble scores) using a Kruskal Wallis one-way analysis of variance and a Mann-Whitney t-test.

RESULTS

Subject Characterization and Pulmonary Function

Anthropometric, pulmonary function, lung volumes/capacities, and diffusion capacity for carbon monoxide are presented in **Table 5.1**. All subjects demonstrated normal pulmonary function, and were ≥85% predicted on all parameters.

Table 5.1. Anthropometric and Pulmonary Function Data

	Absolute	% Predicted
Age, yr	24.5 ± 5.5	
Height, cm	162.5 ± 39.6	
Weight, kg	72.6 ± 10.1	
FVC, L	5.1 ± .08	(94.7 ± 7)
FEV_1, L	4.1 ± 0.6	(94.1 ± 3.9)
FEV_1/FVC, %	81.1 ± 6.6	(97 ± 7.9)
FEF_{25-75}	3.9 ± 1.0	(95.6 ± 10)
SVC, L	5.2 ± .7	(102.3 ± 9.4)
TLC, L_{pleth}	6.9 ± 1.1	(105.1 ± 6.6)
DL_{CO}, $mL \cdot min^{-1} \cdot mmHg^{-1}$	39.1 ± 7.2	(123.6 ± 21.5)
DL_{CO}/V_A, $mL \cdot min^{-1} \cdot mmHg^{-1}$	5.9 ± 0.9	(122.5 ± 23.9)

Values are mean ± standard deviation. FVC, forced vital capacity; FEV_1, forced expiratory volume in 1 s; SVC, slow vital capacity; FEF_{25-75}, forced expiratory flow from 25 to 75% of FVC; TLC, total lung capacity; DL_{CO}, uncorrected diffusion capacity for carbon monoxide; DL_{CO}/V_A, DL_{CO} per alveolar volume;

Hemodynamic and Ventilatory Effects of Pharmacologic Interventions

Room air: The hemodynamic and ventilatory response to exercise was not different during exercise at baseline and with all pharmacologic interventions, with the exceptions noted below **(Table 5.2)**. However, with nifedipine, cardiac output was significantly elevated at rest and during exercise at 50 W, concomitant with an increased heart rate at rest and throughout exercise compared to baseline. Although no difference was observed at rest with sildenafil, similar to nifedipine, heart rate was increased during exercise compared to baseline. Despite the peripheral circulatory hemodynamic changes associated with sildenafil and nifedipine, no significant ventilatory changes were observed. In contrast, no significant hemodynamic changes were observed with acetazolamide, however, minute ventilation was increased at rest and during exercise.

100% O_2: During The hemodynamic and ventilatory response to exercise was not different during exercise at baseline and with all pharmacologic interventions, with the exceptions noted below **(Table 5.3)**. However, similar to exercise breathing room air, nifedipine resulted in an increased $\dot{Q}_T$ at rest and during exercise at 50 and 100 W. Similarly, compared to baseline, heart rate was increased at rest and during exercise with nifedipine. This increase in $\dot{Q}_T$ was also accompanied with an increase in pulmonary artery systolic pressure, yet total pulmonary vascular resistance was not different compared to baseline. Unlike when breathing room air, with sildenafil no significant hemodynamic changes were measured. However, the augmented ventilation at rest and during exercise with acetazolamide was also present when breathing 100% O_2 and no significant hemodynamic changes were observed.

Table 5.2. Hemodynamic and Ventalitory Data During Exercise Beathing Room Air

		Rest	50 W	100 W	150 W	200 W	250 W
$\dot{Q}_T$, L min	Baseline	4.3 ± 0.9	7.3 ± 1.5*	9.8 ± 2.1*	10.8 ± 2.4*	12.5 ± 2.2*	15 ± 2.4*†
	Sildenafil	4.5 ± 1.2	7.7 ± 1.9	9.9 ± 2.6*	11.7 ± 3.5*	13.3 ± 4.2*	15.1 ± 4.1*
	Nifedipine	5.6 ± 1.3†	8.2 ± 1.9†	10.2 ± 2.9*	10.5 ± 2.9*	13 ± 3.6*	15.1 ± 4.2*
	Acetazolamide	4.6 ± 1.2	7.9 ± 1.5	9.7 ± 1.6*	11.9 ± 2.2*	15.3 ± 2.8*	16.5 ± 1.5*
SV, mL	Baseline	69 ± 13	76 ± 22	85 ± 25	82 ± 27	83 ± 22	90 ± 22
	Sildenafil	60 ± 16†	76 ± 21	78 ± 22	84 ± 31	85 ± 30	90 ± 28
	Nifedipine	68 ± 20	78 ± 22	83 ± 27	74 ± 25	82 ± 27	89 ± 27
	Acetazolamide	69 ± 18	76 ± 15	85 ± 20	86 ± 18	96 ± 17	97 ± 8
HR, bpm	Baseline	65 ± 18	99 ± 15*	117 ± 15*	137 ± 19*	153 ± 19*	165 ± 16*
	Sildenafil	75 ± 15	103 ± 18*†	128 ± 23*†	145 ± 22*†	159 ± 18*†	171 ± 15*
	Nifedipine	86 ± 18†	108 ± 22*	126 ± 25*	146 ± 23*†	162 ± 18*†	172 ± 18*†
	Acetazolamide	71 ± 15	105 ± 13*	118 ± 20*	140 ± 20*	160 ± 15*	170 ± 13*
SpO_2, %	Baseline	98.4 ± 1.7	98.1 ± 2.2	97.5 ± 2.7	97.3 ± 2.1	96.7 ± 2.4	94.5 ± 2.4
	Sildenafil	98.5 ± 1.8	98.1 ± 1.9	97.9 ± 2.2	98.3 ± 1.5	98 ± 1.4	96.1 ± 1.4
	Nifedipine	98.7 ± 0.9	99 ± 0.9	98.6 ± 0.8	98.8 ± 0.8	98.7 ± 0.8	97 ± 1.3
	Acetazolamide	98.7 ± 1.2	98.8 ± 1.3	98.8 ± 1.3	98.4 ± 1.5	97.5 ± 1.6	96.3 ± 1.5
PASP, mm Hg	Baseline	27.9 ± 6.7	40 ± 5.7	43.2 ± 8*	49.4 ± 10.1*	55.2 ± 11.3*	56.6 ± 9.2*
	Sildenafil	27.4 ± 6	38.4 ± 7.9	46.4 ± 13.1*	51.3 ± 8.4*	56.3 ± 8.8*	58.4 ± 8.8*
	Nifedipine	31.5 ± 6.2	40.2 ± 9.2	44.6 ± 11.7	51.6 ± 13.2*	58 ± 10*	60.3 ± 12.5*
	Acetazolamide	29.5 ± 7.2	37.8 ± 9.1	40.7 ± 6.6	45.6 ± 8.8*	48.9 ± 8.8*	57.1 ± 4.4*
TPR, mm Hg/L/min	Baseline	6.7 ± 2.3	5.7 ± 1.4	4.5 ± 1*	4.7 ± 1.1	4.5 ± 0.9*	3.9 ± 1.3*
	Sildenafil	6.5 ± 2.1	5.3 ± 1.9	4.8 ± 1	4.9 ± 2.2	4.6 ± 1.6	4.2 ± 1.6
	Nifedipine	5.7 ± 1	5 ± 1.1	4.5 ± 1.2	5.1 ± 1.4	4.8 ± 1.5	4.2 ± 1.2
	Acetazolamide	6.9 ± 2	5 ± 0.8*	4.2 ± 0.5*	3.9 ± 0.6*	3.3 ± 1*	3.5 ± 0.4*
$\dot{V}_E$, L min	Baseline	11.4 ± 2.2	25.7 ± 4.4*	35.9 ± 5.2*	49.8 ± 5.2*	66.5 ± 8.7*	88.2 ± 14.8*
	Sildenafil	11.9 ± 1.4	25.3 ± 2.7*	38.3 ± 4.2*	52.7 ± 5*	71.2 ± 10.5*	92.1 ± 14.2*
	Nifedipine	13.1 ± 3.7	27.5 ± 3.4*	37.2 ± 6.4*	54.6 ± 11.7*	72.6 ± 12.7*	89.8 ± 18.6*
	Acetazolamide	14.7 ± 1.6†	32.7 ± 4.7*†	46.9 ± 7.2*†	63.8 ± 9.4*†	81.1 ± 11.4*†	105.2 ± 17.9*†

Values are mean ± standard deviation. $\dot{Q}_T$, cardiac output; SV, stroke volume; HR, heart rate; SpO_2, peripheral arterial O_2 saturation; PASP, pulmonary artery systolic pressure; TPR, total pulmonary resistance; RR, respiratory rate; V_T, tidal volume; $\dot{V}_E$, minute ventilation. *, significantly different from rest within a given pharmacologic condition; †, significantly different from baseline without pharmacologic intervention for that specified workload.

Table 5.3. Hemodynamic and Ventalitory Data During Exercise Beathing 100% O_2

		Rest	50 W	100 W	150 W	200 W	250 W
$\dot{Q}_T$, L min	Baseline	4.9 ± 0.7	6.9 ± 1.9	9 ± 2.5*	10.9 ± 2.2*	13.1 ± 2.8*	13.7 ± 2.2*
	Sildenafil	4.4 ± 1.3	7.2 ± 1.6	8.5 ± 2.2*	11.7 ± 2.5*	12.8 ± 3.1*	15 ± 3.4*†
	Nifedipine	6.3 ± 1.4†	8.8 ± 1.5†	11.1 ± 2.1*†	11.7 ± 2.7*	13.2 ± 3*	15.5 ± 5*
	Acetazolamide	4.4 ± 1.4	7.7 ± 2	10.2 ± 2.2*	12.4 ± 2.7*	14.2 ± 2.7*	17.5 ± 2.3*
SV, mL	Baseline	63 ± 14	73 ± 20	79 ± 31	83 ± 26	88 ± 25	84 ± 20
	Sildenafil	59 ± 15	79 ± 17	79 ± 19	94 ± 24*	90 ± 23*	96 ± 20*
	Nifedipine	66 ± 19	78 ± 18	87 ± 24	82 ± 23	84 ± 23	93 ± 29
	Acetazolamide	60 ± 16	78 ± 18	87 ± 23	92 ± 24*	93 ± 21*	106 ± 14*
HR, bpm	Baseline	81 ± 19	97 ± 27*	118 ± 16*	136 ± 21*	152 ± 19*	166 ± 16*
	Sildenafil	75 ± 16	93 ± 22*	108 ± 25*	129 ± 23*	145 ± 22*	156 ± 18*
	Nifedipine	99 ± 19†	116 ± 25*†	132 ± 22*†	145 ± 22*†	160 ± 19*†	168 ± 18*
	Acetazolamide	75 ± 17	87 ± 35*	120 ± 17*	138 ± 19*	154 ± 18*	166 ± 16*
SpO_2, %	Baseline	99.3 ± 0.7	99.3 ± 0.7	98.9 ± 0.5	99.2 ± 0.7	99.1 ± 1.1	99 ± 0.8
	Sildenafil	99.4 ± 0.5	99.2 ± 0.4	99.7 ± 0.4	99.5 ± 0.4	99.6 ± 0.4	99.5 ± 0.5
	Nifedipine	99.3 ± 0.3	99.5 ± 0.5	99.3 ± 0.4	99.5 ± 0.4	99.5 ± 0.5	99.5 ± 0.5
	Acetazolamide	99.3 ± 0.6	99.6 ± 0.4	99.5 ± 0.4	99.5 ± 0.4	99.7 ± 0.5	99.2 ± 0.7
PASP, mm Hg	Baseline	27.6 ± 4.8	35 ± 5.8	42.5 ± 4.6*	43.2 ± 8.8*	51.8 ± 7.7*	55.4 ± 11.1*
	Sildenafil	27.6 ± 7.5	35.7 ± 8.4	41.6 ± 10.3*	49.4 ± 10.4*	51.1 ± 8*	58.6 ± 6.3*
	Nifedipine	31 ± 7.2	45.6 ± 15.3†	48.9 ± 11.1*	55.1 ± 10.8*	55.4 ± 7.5*	61.9 ± 11.9*
	Acetazolamide	26.2 ± 4.8	31.5 ± 2.6	39.7 ± 2.2*	44.5 ± 8.1*	49 ± 7.4*	56.7 ± 9*
TPR, mm Hg/L/min	Baseline	5.8 ± 1.5	5.9 ± 4	5.1 ± 1.5	4 ± 0.6	4.2 ± 1.2	4.1 ± 0.8
	Sildenafil	6.6 ± 1.8	5.1 ± 1.2	5 ± 1.1	4.5 ± 1.7*	4.2 ± 1.3*	4 ± 0.6*
	Nifedipine	5.1 ± 1.6	5.2 ± 1.9	4.5 ± 1.1	5.1 ± 1.9	4.4 ± 1	4.6 ± 1.7
	Acetazolamide	6.2 ± 1.1	4.3 ± 1	3.8 ± 0.8	3.7 ± 1	3.6 ± 0.8	3.3 ± 0.7
$\dot{V}_E$, L min	Baseline	13.4 ± 2.8	23.7 ± 4.4*	35.7 ± 3.6*	47.8 ± 3.7*	61.6 ± 4.3*	79.3 ± 11.7*
	Sildenafil	12.8 ± 2.8	24.6 ± 2.1*	36.7 ± 3*	50.3 ± 6.8*	63.2 ± 8.9*	81.1 ± 15.3*
	Nifedipine	13.5 ± 2.4	13.1 ± 3.7*	27.5 ± 3.4*	37.2 ± 6.4*	54.6 ± 11.7*	72.6 ± 12.7*
	Acetazolamide	17.2 ± 3.3†	30.8 ± 3.6*	44.8 ± 5.1*†	59.2 ± 10.7*†	75.8 ± 11.9*†	91 ± 22*

Values are mean ± standard deviation. See Table 5.2 for definitions of terms and acronyms.

100% O_2: During exercise at baseline and with all pharmacologic interventions, the expected hemodynamic and ventilatory response occurred to similar degrees **(Table 5.3)**. However, similar to exercise breathing room air, nifedipine resulted in an increased $\dot{Q}_T$ at rest and during exercise at 50 and 100 W. Similarly, compared to baseline, heart rate was increased at rest and during exercise with nifedipine. This increase in $\dot{Q}_T$ was also accompanied with an increase in pulmonary artery systolic pressure, yet pulmonary vascular resistance was not different compared to baseline. Unlike when breathing room air, no significant hemodynamic changes were associated with sildenafil. However, the augmented ventilation at rest and during exercise with acetazolamide was also present when breathing 100% O_2 and no significant hemodynamic changes were observed.

Transpulmonary Passage of Saline Contrast

Room air: During exercise at baseline and with all pharmacologic interventions, the transpulmonary passage of saline contrast progressively increased and was significantly elevated during exercise at 150, 200, and 250 W **(Figure 5.1A)**. Bubble scores during exercise with sildenafil **(Figure 5.1C)** and acetazolamide **(Figure 5.1G)** were similar compared to baseline. Although not statistically different from baseline, mode bubble scores were the highest during exercise with nifedipine from rest through 200 W **(Figure 5.1E)**. Furthermore, consistent with the elevated $\dot{Q}_T$ at rest and 50 W with nifedipine, there was a trend ($p = 0.08$) for bubble scores to be higher compared to baseline.

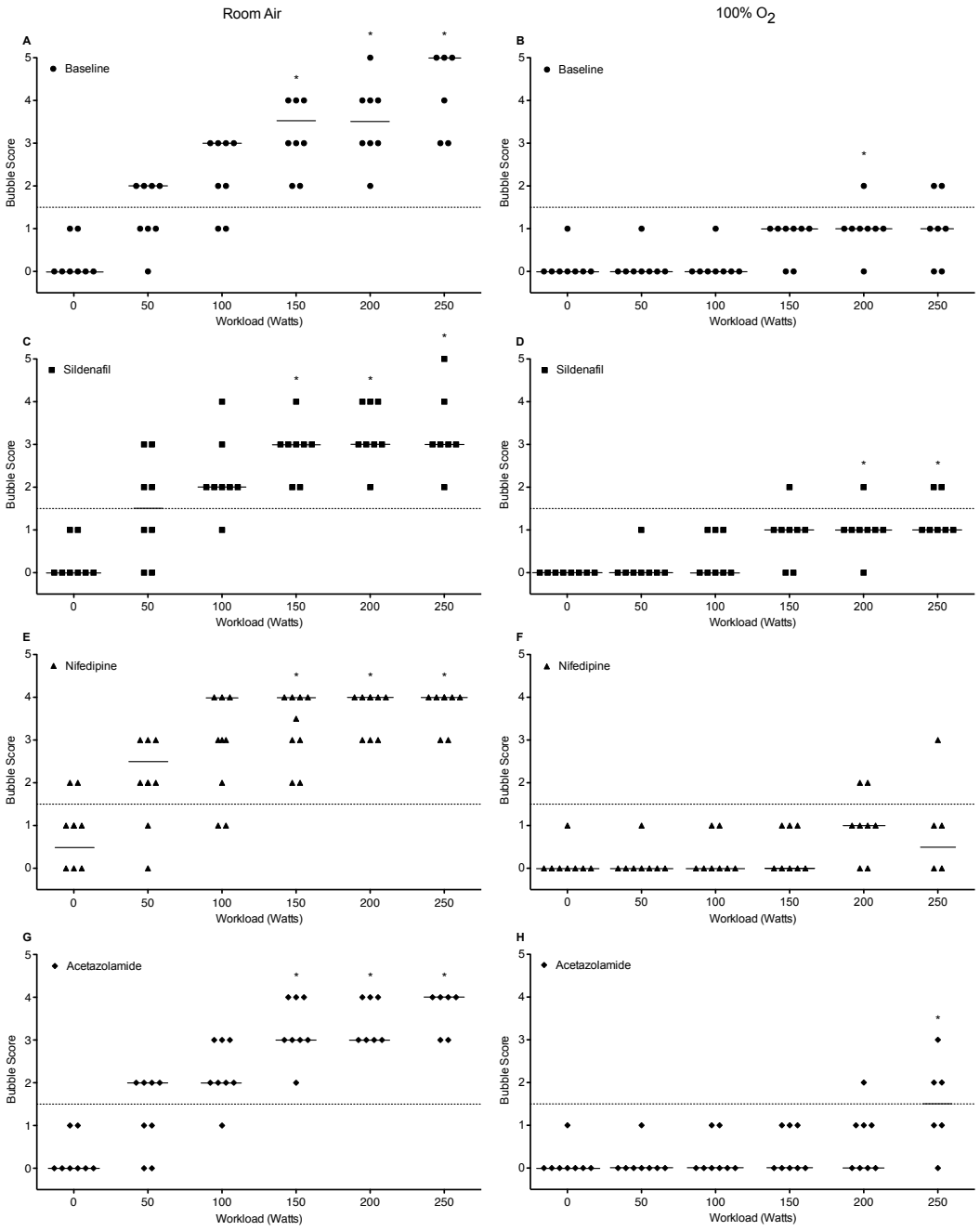

Figure 5.1. Bubble Scores During Exercise Breathing Room Air and 40% O_2
Bubble scores during exercise breathing room air and 100% O_2; at baseline without pharmacologic intervention (A and B), after 100 mg p.o. Sildenafil (C and D), after 20 mg p.o. nifedipine (E and F), and after three days of 250 mg p.o. t.i.d. acetazolamide (G and H).

100% O_2: As expected, the transpulmonary passage of saline contrast was trivial during exercise at baseline and only significantly increased from rest breathing a FIO_2 = 1.0 during exercise at 200 W. During exercise with sildenafil, nifedipine, and acetazolamide, the transpulmonary passage of saline contrast was not different compared to baseline. Similar to baseline without pharmacologic intervention, significant increases in bubble scores were only observed at 200 and 250 W.

DISCUSSION

The current study investigated the pharmacologic influence of sildenafil, nifedipine, and acetazolamide on the regulation of blood flow through IPAVA during exercise in healthy humans breathing a FIO_2 = 1.0. The primary finding of the current study was that the general absence of blood flow through IPAVA during exercise breathing a FIO_2 = 1.0 was not significantly altered following administration of a single dose of sildenafil (100 mg, p.o), a single dose of nifedipine (20 mg, p.o), or after acetazolamide (250 mg, p.o., t.i.d. for 3 days).

We have previously shown that during exercise breathing a FIO_2 = 1.0 blood flow through IPAVA is prevented or significantly reduced. The current study found similar results during exercise breathing a FIO_2 = 1.0 with pharmacologic interventions that are known modulators of pulmonary vascular tone. All of these pharmacologic interventions act through mechanisms with the potential to prevent or reduce the O_2 induced constriction of IPAVA (9). Nifedipine and acetazolamide have the potential to prevent or limit pulmonary vascular smooth muscle contraction, while sildenafil augments the potential relaxation of pulmonary vascular smooth muscle. The increase and decrease in

blood flow through IPAVA during exercise breathing room air and a $FIO_2 = 1.0$, may at least partially be a result of IPAVA vasodilation and vasoconstriction, respectively. Accordingly, by preventing the potential vasoconstriction of IPAVA or augmenting the vasodilation of IPAVA, these pharmacologic interventions could have allowed blood flow through IPAVA to occur during exercise breathing a $FIO_2 = 1.0$, as occurs during exercise breathing room air. However, this was not the case and potential explanations for this are discussed below.

Sildenafil

Endothelium derived or exogenous nitric oxide (NO) promotes smooth muscle relaxation by activation of soluble guanylate cyclase and the subsequent production of cyclic guanosine monophosphate (cGMP), and via activation of protein kinase G, decreased intracellular calcium levels. The type-5 phosphodiesterase (PD-5) isoform, located primarily in the penis and lungs, rapidly degrades cGMP and thereby limits the NO mediated relaxation. Sildenafil citrate inhibits PD-5, prolonging the survival cGMP, and thus promotes vascular relaxation by allowing the effects of NO to persist longer, rather than increasing the bioavailability of NO.

Previous work has demonstrated a correlation between increases in blood flow through IPAVA when breathing room air and increases in $\dot{Q}_T$ (24, 133, 216) that may be in part due to the associated increase in sheer stress and increased release of NO. If so, the possibility that blood flow through IPAVA is NO mediated should be interpreted in light of recent work demonstrating the i.v. infusion of nitroglycerin in healthy humans at rest did not increase the transpulmonary passage of saline contrast (147). However, the

i.v. infusion of nitroglycerin did not increase $\dot{Q}_T$, and therefore, it remains possible that IPAVA were open but the transpulmonary passage of saline contrast did not occur due to potential factors such as mean pulmonary transit time being to long for *in vivo* microbubbles to survive. Furthermore, prolonging the action of cGMP with sildenafil ingestion did not significantly change the transpulmonary passage of saline contrast during exercise breathing room air. Nevertheless, it remains possible that during exercise breathing room air, IPAVA are open without augmenting the vasodilatory effects of NO with sildenafil.

During exercise breathing a $FIO_2 = 1.0$ with sildenafil, also did not result in an increase in the transpulmonary passage of saline contrast. The explanation for this may be due to an increase in the production of reactive oxygen species, known to occur during O_2 breathing, which may limit the bioavailability of NO (201). Thus, the vasodilatory effects of NO during exercise breathing a $FIO_2 = 1.0$ may be diminished, similar to hyperoxia attenuating endothelial mediated vasodilation in peripheral vascular beds (268). However, these data suggest that even when augmenting the action of NO that is present, no significant increase in blood flow through IPAVA is detected.

Nifedipine

Nifedipine is a dihydropyridine that blocks the activation of voltage gated (L-type) calcium channels (207), that when open allow for the influx of calcium down the concentration gradient (2 mM extracellular vs. 100 nM intracellular). L-type calcium channels are critical to the control of vascular tone and have been demonstrated to be integral in facilitating the O_2 induced constriction of the ductus arteriosus (230). Additionally, and also via blockade of L-type calcium channels, nifedipine has been

shown to prevent hypoxic pulmonary vascoconstriction using the same dosage (20 mg, p.o.) as the current study (10, 174). Accordingly, considering the pervasive influence of L-type calcium channels in regulating vascular tone and their documented role in mediating both O_2 induced constriction of the ductus arteriosus and hypoxic pulmonary vasoconstriction it seemed plausible that IPAVA may be similarly regulated. Nevertheless, no effect was observed during exercise breathing a $FIO_2 = 1.0$ with nifedipine, suggesting that the O_2 induced constriction of IPAVA is not primarily mediated via L-type calcium channels.

Acetazolamide

Acetazolamide is a carbonic anhydrase inhibitor, most commonly known for it's utility in preventing acute mountain sickness (66) owing to it's respiratory stimulating properties secondary to renal excretion of bicarbonate (i.e., metabolic acidosis) and carbonic anhydrase inhibition in central chemoreceptors (155, 221). However, a secondary property of acetazolamide is a reduction/prevention of increases in pulmonary artery pressure in acute hypoxia (222). The mechanism explaining the prevention of hypoxic pulmonary vasoconstriction via acetazolamide has been shown to not be a result of intracellular acidification or changes in membrane potential and is independent of carbonic anhydrase inhibition (206). Accordingly, acetazolamide prevents increases in intracellular calcium via a non L-type calcium channel mechanism. Importantly, the dosage used in the current study (250 mg, p.o. every 8 hours, t.id.) has also been shown to prevent hypoxic pulmonary vasoconstriction in acute hypoxia (224). Despite the efficacy of acetazolamide in preventing hypoxic pulmonary vasoconstriction, these data

suggest that the O_2 induced constriction of IPAVA is not mediated by a similar mechanism.

Limitations

Blood flow through IPAVA was detected using transthoracic saline contrast echocardiography, and previous work has discussed the associated limitations (24, 53, 54, 134, 216). However, particularly pertinent to the current study is addressing the potential concern that blood flow through IPAVA is not detected during exercise breathing a FIO_2 = 1.0 due to O_2 breathing altering the partial pressure environment of *in vivo* microbubbles and destabilizing them (103). In this way, blood flow through IPAVA may be occurring during exercise breathing a FIO_2 = 1.0 yet the failure to observe significant left-sided contrast reflects the failure for saline contrast to survive long enough, to reach the left heart. Previous work by our group has demonstrated this theory to not be experimentally valid and therefore, saline contrast created from room air is appropriate to use in subjects breathing a FIO_2 = 1.0 to detect blood flow through IPAVA (54). The bubble scoring system used in the current study, although not without precedence (11), and previously published (54, 55, 133, 134, 144), is a qualitative approach intended to characterize the degree of left sided contrast. This bubble scoring system does not represent a means to quantify blood flow through IPAVA. Yet, considering O_2 breathing does not affect the *in vivo* dynamics of saline contrast created from room air it is likely that the reductions in bubble score during exercise breathing a FIO_2 = 1.0 truly reflect a reduction in blood flow through IPAVA. Of note, to validate the reproducibility of our bubble scoring system, previous work from our lab has demonstrated very good agreement with bubble scores assigned by one of two expert sonographers (combined

>40 years experience) and cardiologist blinded to the conditions. In one of these studies, a cardiologist reviewed 57 saline contrast recordings and reported 100% agreement on whether there was or was not left heart contrast, and 53 (93%) were assigned the same score (55).

Conclusions

As expected, at baseline without pharmacologic intervention the transpulmonary passage of saline contrast occurred during exercise breathing room air and was prevented or reduced during exercise breathing a $FIO_2 = 1.0$. These findings were not significantly altered following the administration of sildenafil (100 mg, p.o), nifedipine (20 mg, p.o), and after acetazolamide (250 mg, p.o., t.i.d for 3 days). Of particular interest is that none of these pharmacologic interventions resulted in blood flow through IPAVA during exercise breathing a $FIO_2 = 1.0$, despite these drugs being well-known modulators of pulmonary vascular tone (9). However, rather than IPAVA being regulated similar to the ductus arteriosus or fetal cardiopulmonary circulation, there regulation may be more similar to the systemic circulation which is also known to dilate in response to low O_2 tensions and constrict in response to high O_2 tensions. Accordingly, and also like the systemic circulation, it remains possible that IPAVA are not mediated by these mechanisms and/or there are redundant mechanisms facilitating O_2 induced IPAVA constriction, similar to those redundant mechanisms regulating peripheral blood flow (35).

Up until this point, Chapter IV and V included subjects without a PFO, as the purpose was to either demonstrate that blood flow through IPAVA, 1) contributed to pulmonary gas exchange efficiency, 2) was reduced during exercise breathing 100% O_2, and was potentially regulated by various pharmacologic interventions. However, I shift now to including both subjects with and without a PFO to investigate the effect of human acclimatization to hypobaric hypoxia. All prior studies investigating human acclimatization to hypobaric hypoxia have presumably been done in subjects with and without a PFO and therefore it is unknown to what extent PFO influences acclimatization to hypobaric hypoxia.

CHAPTER VI

ALTITUDEOMICS: IMPAIRED PULMONARY GAS EXCHANGE EFFICIENCY AND VENTILATORY ACCLIMATIZATION AFTER 16 DAYS AT 5260M IN HUMANS WITH PATENT FORAMEN OVALE

This chapter is in review with the *Journal of Applied Physiology* and Steven S. Laurie, Julia P. Kern, Kara M. Beasley, Randall D. Goodman, Bengt Kayser, Andrew W. Subudhi, Robert C. Roach, and Andrew T. Lovering are co-authors. The data presented in this chapter come from a very large, multinational, field based project entitled "AltitudeOmics". However, I performed the experimental work, led this aspect of AltitudeOmics, and the writing is entirely mine; Steven S. Laurie, Julia P. Kern, and Kara M. Beasley provided technical and editorial assistance; Randall D. Goodman provided technical assistance with performing echocardiography during exercise; and Bengt Kayser, Andrew W. Subudhi, Robert C. Roach, and Andrew T. Lovering helped develop the protocol, and provided guidance and editorial assistance.

INTRODUCTION

It is well established that pulmonary gas exchange progressively worsens in a workload dependent manner during exercise at sea level (48). This impairment in pulmonary gas exchange efficiency during exercise is exacerbated in acute hypoxia, such that for any given $\dot{V}O_2$, the alveolar-to-arterial PO_2 difference ($A\text{-}aDO_2$) is greater compared to exercise in normoxia (235). Following acclimatization to hypobaric hypoxia, pulmonary gas exchange efficiency is thought to improve compared to acute hypoxia (88, 203). Seminal work from Dempsey *et al*. (47) reported a trend for an increased $A\text{-}aDO_2$

during treadmill walking after 4 days at 3100 m compared to sea level, and a partial normalization during the same exercise protocol following 21 days at 3100 m compared to that obtained after 4 days. Bebout *et al*. (13) then demonstrated that, compared to acute normobaric hypoxia, acclimatization to 3800 m for 2 weeks resulted in an ~3 mm Hg reduction in the A-aDO_2 during submaximal cycle ergometer exercise. Calbet *et al*. (28) subsequently reported that, compared to acute normobaric hypoxia, acclimatization to 5260m for 9-10 weeks resulted in an ~9 mm Hg reduction in the A-aDO_2 during submaximal cycle ergometer exercise. Collectively, these data suggest that pulmonary gas exchange efficiency in non-acclimatized individuals improves with acclimatization to high-altitude compared to acute hypoxia.

Recently, our group has explored the consequences of an intracardiac right-to-left shunt via a patent foramen ovale (PFO) in healthy humans during exercise breathing room air and in acute hypoxia. In the course of these investigations it became apparent that the presence of a PFO could be critical to the interpretation of work where pulmonary gas exchange efficiency is a key element and, to our knowledge, prior work investigating human acclimatization to high-altitude have not considered the effect of a PFO. The classic study by Hagen *et al*. (82) reported a PFO prevalence of 25-35% identified using a probe during autopsy (n = 965). Recent work from several research groups using saline contrast echocardiography (n = 104-1162) report that ~40% of adult humans have a PFO (55, 156, 266). Therefore, according to the multiplication rule for conditional probability and using a 35% prevalence of PFO, there is a <5% chance that the aforementioned studies on pulmonary gas exchange efficiency after acclimatization would randomly select all subjects without PFO. Right-to-left blood flow through a PFO

occurs when right atrial pressure exceeds left atrial pressure, which can occur transiently during normal respiration (64). Thus, right-to-left blood flow through a PFO is likely intermittent and variable in volume, however it does result in a measureable impact on pulmonary gas exchange efficiency. Lovering *et al*. (145) found that subjects with a PFO have an increased A-aDO_2 at rest, breathing either room air at sea level or a normobaric hypoxic gas mixture (12% O_2).

The primary purpose of this study was to investigate pulmonary gas exchange efficiency at rest and during exercise in subjects with and without a PFO after acclimatization to hypobaric hypoxia. We hypothesized that subjects with a PFO would have worse pulmonary gas exchange efficiency after acclimatization to high-altitude compared to subjects without a PFO. To test this hypothesis, healthy male and female lowlanders, with and without a PFO, were studied at rest and during exercise at sea level, after being acutely transported to 5260m, and after living at 5260m on Mt. Chacaltaya, Bolivia, for 16 days. This study was conducted as part of the AltitudeOmics project, described previously in greater detail (218).

METHODS

This study received approval from the University of Oregon, the University of Colorado Denver, and the U.S. Department of Defense. All subjects provided verbal and written informed consent prior to participation and all studies were conducted in accordance with the *Declaration of Helsinki*.

Subject Recruitment and Screening

A complete description of the inclusion/exclusion criteria were published in the project overview paper of this series (218). Briefly, 21 healthy subjects (9 female) recruited from sea level (Eugene, Oregon, 130m, P_B = 749 mm Hg) participated in all aspects of this study and constitute the AltitudeOmics group of subjects in this report. Pertinent to the current report and not described in previous AltitudeOmics publications are the methodologies for determining adequate (≥90% predicted) pulmonary function and diffusion capacity for carbon monoxide parameters and the echocardiographic screening process each subject underwent.

Spirometry, Diffusion Capacity, and Lung Volumes

Baseline pulmonary function was determined using computerized spirometry (MedGraphics, Ultima CardiO_2, St. Paul, MN, USA) according to American Thoracic Society/European Respiratory Society (ATS/ERS) standards (166). Lung diffusion capacity for carbon monoxide (DL_{CO}) was determined by the single-breath, breath hold method according to ATS/ERS standards (119, 152) using the Jones and Meade method for timing (111). Lung volumes and capacities were determined using whole body plethysmography (MedGraphics Elite Plethysmograph, St. Paul, MN, USA) according to ATS/ERS standards (247).

Echocardiographic Screening

All subjects underwent a comprehensive echocardiographic screening process (Philips Sonos 5500, Eindhoven, The Netherlands) by a registered diagnostic cardiac sonographer with >25 yrs of experience (R.D.G.) to ensure subjects were free of cardiac abnormalities or signs of heart disease, as previously conducted by our group (54, 55,

133, 134). Transthoracic saline contrast echocardiography (TTSCE) was used to identify the presence of a PFO or the transpulmonary passage of saline contrast via intrapulmonary arteriovenous anastomoses (IPAVA) as described previously (139). The appearance of ≥1 microbubble(s) in the left heart in any frame during the 20 cardiac cycles following right heart opacification identified subjects as either having a PFO or the transpulmonary passage of saline contrast (68, 159, 163, 198). Delineation between these two sources of left heart contrast results from the timing of contrast appearing in the left heart following right heart opacification, in which a microbubble appearing within ≤3 cardiac cycles is consistent with PFO, while a microbubble appearing after >3 cardiac cycles is consistent with transpulmonary passage (27, 49, 96, 132, 159, 163, 198). Saline contrast injections were performed during normal breathing as well as after provocative maneuvers designed to transiently elevate right atrial pressure and create conditions optimal for detection of PFO (e.g., release of a Valsalva maneuver and after coughing). Multiple injections were performed as necessary when results were equivocal. Each agitated saline contrast injection was scored using a previously published 0-5 bubble scoring system (54, 55, 133, 134, 143, 144). Briefly, bubble scores reflect the quantity and spatial distribution of contrast in the left ventricle in any single frame throughout the 20 cardiac cycles post-right heart opacification; 0 = no bubbles, 1 = 1-3 bubbles, 2 = 4-12 bubbles, 3 = >12 bubbles appearing as a bolus, 4 = >12 bubbles heterogeneously filling the left ventricle, and 5 = >12 bubbles homogeneously filling the left ventricle.

Of the 21 subjects that participated in this study, there were 11 (7 female) subjects with a PFO (PFO+) and 10 (2 female) subjects without a PFO (PFO−). Of note, we originally planned on having an equal number of PFO+ and PFO− subjects, although for

reasons previously described 3 subjects were excluded (218). At baseline, within the PFO+ group, 6 subjects had a bubble score ≥3 upon release of a Valsalva maneuver and 5 subjects had a bubble score of ≤2 upon release of a Valsalva maneuver. It has recently been demonstrated that the degree of left-sided contrast visualized upon release of a Valsalva maneuver in PFO+ subjects correlates to the size of the PFO (64). Accordingly, those with more contrast (i.e., bubble score ≥3) likely have a larger PFO compared to those with less contrast (i.e., bubble score ≤2), and as such there was a range of PFO sizes within our PFO+ group. Within the PFO− group, 6 subjects presented with a trivial degree of transpulmonary passage of contrast (bubble score = 1) at rest breathing room air at SL, and 4 subjects were entirely clear of left-sided contrast during screening. Prior work from our lab has excluded subjects demonstrating transpulmonary passage of contrast at rest due to the unknown significance of this finding. However, considering the circumstances and confines of the current field study based work, we chose to include these subjects. No statistical differences were observed within the PFO− group comparing those with and without the minimal transpulmonary passage of contrast at rest breathing room air at SL.

Acute Normobaric Hypoxia

As part of the preliminary testing at sea level, transthoracic saline contrast echocardiography was performed in the PFO− and PFO+ groups at rest breathing room air and after 20 min of breathing mild hypoxic gas (14 % O_2). Identical to the initial screening procedure, agitated saline contrast injections were performed in subjects reclined at 45° in the left lateral decubitus position. The primary purpose of these measurements in normobaric hypoxia was for an aspect of the project not currently being

reported on; however the secondary purpose pertinent to the current work, was to determine if subjects would have an increase in left-sided contrast at rest breathing mild hypoxic gas compared to room air, as previously demonstrated (134). These studies confirmed that both the PFO− and PFO+ groups in this study had an increase in left-sided contrast breathing normobaric hypoxia.

Timeline

This report presents data collected over 3 experimental study visits: 1) sea level (SL: Eugene, Oregon, 130m, P_B = 749 mm Hg); 2) day 1 at high-altitude (ALT1: Mt. Chacaltaya, Bolivia, 5260m, P_B = 406 mm Hg); and 3) after living at high-altitude for 16 days (ALT16: Mt. Chacaltaya, Bolivia, 5260m, P_B = 406 mm Hg). To provide an acute exposure to 5260m on ALT1, the subjects breathed supplemental oxygen (2 L/min, nasal cannula or mask) during the drive up the mountain. On arrival at 5260m, the first subject immediately began the experimental protocol while the second subject rested while continuing to breathe supplemental oxygen for ~two hours until the first subject had completed the protocol. A complete description of the study timeline was previously published (218).

Subject Instrumentation and Exercise Protocol

A core temperature pill (CorTemp HQInc., Palmetto, FL, USA) was ingested ~5 hrs prior to the start of exercise. Subjects were instrumented with a 20 G radial artery catheter (Arrow International Inc., Reading, PA, USA) under local anesthesia (2% lidocaine) and an 18-22 G intravenous catheter was placed in the antecubital fossa. Subjects rested on an upright stationary cycle ergometer (Velotron Elite, Seattle, WA, USA) for 10 min prior to performing standardized workloads of 70, 100, 130, and 160

Watts for 3 min each. Exercise data are presented as the highest iso-workload achieved within an individual subject across SL, ALT1 and ALT16. For example, subjects may have completed all workloads at SL and ALT16, but only completed 130 W at ALT; in this case the iso-workload reported would be data at 130 W, from each SL, ALT1 and ALT16. TTSCE was performed at rest and during the last min of each 3 min workload with subjects positioned on the cycle ergometer in the forward leaning aerobar position to facilitate obtaining a clear apical, four-chamber view.

Pulmonary Artery Systolic Pressure and Cardiac Output

Following each saline contrast injection, pulmonary artery systolic pressure (PASP) was assessed from the peak velocity of the tricuspid regurgitation using Doppler ultrasound (Sonosite Micromaxx, Bothell, WA, USA) and applied to the modified Bernoulli equation ($4v^2 + P_{RA}$), where v is velocity of the tricuspid regurgitation velocity envelope and P_{RA} is right atrial pressure, according to the guidelines of the American Society for Echocardiography (117, 202, 275). A small volume (<0.5 ml) of air agitated with 3 ml of sterile saline was injected and used to help delineate the tricuspid regurgitation velocity envelope. Cardiac output was calculated with heart rate obtained from the ECG and stroke volume estimates derived from intra-arterial blood pressure tracings obtained via a saline filled transducer (Utah Medical, Salt Lake City, UT, USA) positioned at heart level and attached to the radial artery catheter (19, 219).

Arterial Blood Gases, Body Temperature and Blood Lactate

At rest and at the end of each 3 min submaximal workload, a 3 ml radial artery blood sample was drawn anaerobically over 10-15 sec into a heparinized syringe and rapidly analyzed in duplicate (or triplicate if time permitted) for arterial PO_2 (PaO_2),

arterial PCO_2 ($PaCO_2$), and pH with a blood-gas analyzer calibrated daily with tonometered whole blood (Siemens RAPIDLab 248, Erlangen, Germany). Arterial blood gases were corrected for body temperature (48, 113, 205) based on readings from the ingested core temperature pill. Arterial O_2 saturation (SaO_2) and hemoglobin (Hb) were measured with CO-oximetry (Radiometer OSM3, Copenhagen, Denmark). Hematocrit was analyzed in triplicate at rest and in single measurements for each workload using the microcapillary tube centrifugation method (M24 Centrifuge, LW Scientific, Lawrenceville, GA, USA). Blood lactate was analyzed in duplicate using the Lactate Plus hand held meter and lactate test strips (Nova Biomedical, Waltham, MA, USA).

Calculations

Alveolar PO_2 (PAO_2) was calculated using the ideal gas equation, using temperature corrected $PaCO_2$, and a respiratory quotient (RER) from a 15 sec average of metabolic data corresponding to the time and duration of the arterial blood draw:

$$P_AO_2 = [(P_B - e^{0.05894809 \times T_B + 1.689589}) \times FIO_2] - PaCO_2 \times \left[FIO_2 + \frac{(1 - FIO_2)}{RER}\right]$$

Equation 2.3. Alveolar Gas Equation

where T_B is core body temperature for temperature correction of water vapor pressure, RER is the respiratory exchange ratio ($\dot{V}CO_2/\dot{V}O_2$), and P_B is barometric pressure that was measured daily (Greisinger electronic, GPB 3300). Pulmonary gas exchange efficiency (A-aDO_2) was determined at rest and during exercise as the difference between the temperature corrected PaO_2 and corresponding PAO_2.

Measures of O_2 content were calculated from the standard content equation:

$$O_2\ \text{Content} = \left[1.39 \times \text{Hb} \times \left(\frac{SO_2}{100}\right)\right] + (0.003 \times PO_2)$$

Equation 2.7. Oxygen Content Equation

using an O_2 carrying capacity of 1.39 ml O_2/g Hb and directly measured Hb (g Hb/dL). For arterial O_2 content (CaO_2) SO_2 represents CO-oximetry measured arterial O_2 saturation (SaO_2) and temperature corrected PaO_2. For end-capillary O_2 content ($Cc'O_2$) SO_2 represents the end-capillary O_2 saturation ($Sc'O_2$) calculated from the Kelman equation (114) assuming complete alveolar-capillary O_2 equilibration such that end-capillary PO_2 ($Pc'O_2$) was equal to PAO_2. Mixed venous O_2 content ($C\bar{v}O_2$) was calculated using the Fick principle of mass balance ($\dot{V}O_2 = \dot{Q}_T \times (CaO_2 - C\bar{v}O_2)$) using measured CaO_2, $\dot{V}O_2$, and an estimate of total $\dot{Q}_T$ as described above.

The fraction of venous admixture ($\dot{Q}_{VA}/\dot{Q}_T$) accounting for the entirety of the A-aDO_2 was calculated from the shunt equation using the previously calculated O_2 content values:

$$\frac{Q_{VA}}{Q_T} = \frac{Cc'O_2 - CaO_2}{Cc'O_2 - C\bar{v}O_2}$$

Equation 2.13. Berggren Shunt Equation

Alveolar ventilation ($\dot{V}_A$) was calculated using the measured $\dot{V}CO_2$ and temperature corrected $PaCO_2$:

$$V_A = \frac{(VCO_2 \times 863)}{PaCO_2}$$

Equation 2.1. Alveolar Ventilation

Statistical Analyses

All statistical calculations were made using GraphPad Prism statistical software (v. 5.0d) and significance was set to $p < 0.05$. In both the PFO− and PFO+ groups,

measured and calculated physiologic variables were compared across time points (e.g., SL, ALT1 and ALT16) using a one-way ANOVA. A Newman-Keuls multiple comparison post-hoc test was used to determine specific pairwise differences between groups and time points. Non-parametric analyses (bubble scores) were done using a Kruskal-Wallis one-way ANOVA with a Dunn's multiple comparison post-hoc test. Comparisons were determined *a priori* and performed two times (at rest and during exercise) in the PFO− and PFO+ groups. Differences in measured and calculated variables, between the PFO− and PFO+ groups at rest and during exercise were assessed using an unpaired t-test with Welch's correction. Differences in bubble scores between the PFO− and PFO+ groups at rest and during exercise were assessed using a Mann-Whitney t-test.

RESULTS

Overview

Baseline values for anthropometric, exercise, hematologic and pulmonary function data at SL for the PFO− *(n* = 10) and PFO+ (*n* = 11) groups are presented in **Table 6.1**. Cardiopulmonary data at rest and during exercise for SL, ALT1 and ALT16 for the PFO− and PFO+ groups are presented in **Table 6.2** and **Table 6.3**. The mean iso-workload in the PFO− and PFO+ groups was 150 ± 24 W and 136 ± 28 W, respectively, which was not different between groups. The presentation of results will sequentially describe data collected at rest and during exercise at SL, ALT1 and ALT16 in the PFO− and PFO+ groups.

Table 6.1. Anthropometric, Exercise, Hematologic and Pulmonary Function Data

	PFO−, n=10	PFO+, n=11
Age, yr	21.1 ± 1.4	20.6 ± 1.6
Sex, (female)	2	7
Height, cm	178.4 ± 6.1	173.4 ± 8.8
Weight, kg	71.5 ± 8.4	68.1 ± 9.7
$\dot{V}O_{2peak}$, mL · kg^{-1} · min^{-1}	46.8 ± 7.1	44.0 ± 6.2
Peak power output, W	311 ± 67	268 ± 64
Ferritin, ng · ml^{-1}	61.3 ± 30.6	44.0 ± 32.7
Iron, μg · dL^{-1}	129.5 ± 47.9	134.1 ± 64.1
FVC, L	5.48 ± 0.92	4.73 ± 1.04‡
FVC, %p	100.0 ± 11.0	100.4 ± 11.3
SVC, L	5.61 ± 1.08	5.01 ± 1.18
SVC, %p	102.4 ± 13.5	105.6 ± 11.7
FEV_1, L	4.62 ± 0.60	4.07 ± 0.77‡
FEV_1, %p	101.3 ± 9.0	101.9 ± 7.9
FEV_1/FVC	85.4 ± 9.8	86.4 ± 5.3
FEV_1/FVC, %p	100.9 ± 11.6	100.8 ± 6.1
FEF_{25-75}, L · sec^{-1}	4.79 ± 1.37	4.51 ± 0.84
FEF_{25-75}, %p	100.1 ± 28.5	105.1 ± 15.3
TLC, L_{pleth}	7.16 ± 1.07	6.28 ± 1.33
TLC, %p	104.9 ± 8.2	103.3 ± 11.4
DL_{CO}, mL · min^{-1} · mm Hg^{-1}	43.06 ± 8.74	33.25 ± 10.33‡
DL_{CO}, %p	130.6 ± 21.1	110.1 ± 19.4‡
DL_{CO}/V_A	6.00 ± 0.71	5.61 ± 1.03
DL_{CO}/V_A, %p	124.1 ± 17.5	113.2 ± 21.4

Values are mean ± standard deviation. FVC, forced vital capacity; SVC, slow vital capacity; FEV_1, forced expiratory volume in 1 s; FEF_{25-75}, forced expiratory flow from 25 to 75% of FVC; TLC, total lung capacity; DL_{CO}, diffusion capacity of carbon monoxide; DL_{CO}/V_A, DL_{CO}/alveolar volume; %p, % predicted; ‡ $p <$ 0.05 compared to PFO−.

Table 6.2. Cardiopulmonary and Arterial Blood Gas Data at Rest in the PFO− and PFO+ Groups at Sea level (SL), Acute Hypoxia (ALT1) and After Acclimatization to High-Altitude (ALT16)

	SL		ALT1		ALT16	
	PFO−	PFO+	PFO−	PFO+	PFO−	PFO+
$\dot{V}_E$, L・min^{-1}	14.5 ± 4.7	11.7 ± 3	19.4 ± 4.4	16.7 ± 4.9*	26.2 ± 8.9*	18.7 ± 6.5*‡
$\dot{V}_A$, L・min^{-1}	8.2 ± 3.8	5.9 ± 2.6	12.3 ± 2.7	10.6 ± 4.8*	19.4 ± 7.8*†	12.4 ± 5.1*‡
V_D/V_T	0.42 ± 0.06	0.46 ± 0.06	0.37 ± 0.11	0.42 ± 0.06	0.38 ± 0.16	0.41 ± 0.05
$\dot{V}O_2$, L・min^{-1}	0.34 ± 0.1	0.28 ± 0.14	0.43 ± 0.14	0.34 ± 0.12	0.43 ± 0.06	0.35 ± 0.08‡
$\dot{V}CO_2$, L・min^{-1}	0.32 ± 0.12	0.25 ± 0.11	0.39 ± 0.1	0.32 ± 0.11	0.4 ± 0.11	0.29 ± 0.09‡
RER	0.92 ± 0.08	0.87 ± 0.12	0.93 ± 0.09	0.97 ± 0.09*	0.9 ± 0.07	0.83 ± 0.09†‡
$\dot{V}_E/\dot{V}O_2$	43 ± 5.7	44.5 ± 9.3	47 ± 7.1	51.4 ± 8.4	61.4 ± 15.2*†	53.2 ± 9.6
HR, bpm	76.8 ± 15.1	71.5 ± 12.3	87.3 ± 16.5	89 ± 16.2*	93 ± 16	92 ± 14*
SV, mL	86 ± 18.3	88.2 ± 18.3	90.5 ± 23.1	83.3 ± 13.3	73 ± 16	75 ± 16
$\dot{Q}_T$, L・min^{-1}	6.5 ± 1.6	6.2 ± 1.3	7.7 ± 1.5	7.3 ± 1.4	6.6 ± 1.2	6.9 ± 1.2
PASP, mm Hg	30.4 ± 6.4	24.9 ± 7.3‡	36.6 ± 6.6	31.8 ± 5.1*	34.1 ± 4	31.9 ± 5.6*
CaO_2, ml O_2・dL^{-1}	19.7 ± 1.4	18 ± 1.9‡	14.4 ± 1.2*	13.8 ± 1.7*	20.38 ± 1.91†	17.37 ± 3.2†‡
pH	7.43 ± 0.03	7.42 ± 0.02	7.51 ± 0.02*	7.51 ± 0.03*	7.51 ± 0.03*	7.5 ± 0.03*
HCO_3^-, mmol・L^{-1}	21.98 ± 1.92	22.67 ± 1.2	20.7 ± 1.31	20.82 ± 2.05*	14.4 ± 1.8*†	15.8 ± 1.1*†‡
BE, mmol・L^{-1}	-1.87 ± 1.73	-1.4 ± 0.93	-1.97 ± 1.14	-1.87 ± 1.56	-7.83 ± 1.7*†	-6.71 ± 0.81*†‡
Hct, %	44.5 ± 3	41.1 ± 3.7‡	44.3 ± 3.3	42.4 ± 3.5	51.67 ± 3.21*†	47.23 ± 6.14*‡
Hb, g・dL^{-1}	14.8 ± 1.1	13.6 ± 1.5‡	15 ± 1	13.9 ± 1.5	17.16 ± 1.39*†	15.46 ± 2.37‡
Core Temp, °C	37.1 ± 0.4	37.2 ± 0.4	36.9 ± 0.5	37.1 ± 0.4	37 ± 0.9	37 ± 0.4
Lactate, mmol・L^{-1}	0.98 ± 0.42	0.88 ± 0.37	1.16 ± 0.29	1.26 ± 0.59	1 ± 0.3	1 ± 0.3
n, max	10	11	6	10	9	11

Values are mean ± standard deviation. $\dot{V}_E$, minute ventilation; $\dot{V}_A$, minute ventilation; V_D/V_T, dead space to tidal volume ratio; $\dot{V}O_2$, oxygen consumption; $\dot{V}CO_2$, carbon dioxide production; RER, respiratory exchange ratio; HR, heart rate; SV, stroke volume; $\dot{Q}_T$, cardiac output; PASP, pulmonary artery systolic pressure; CaO_2, arterial oxygen content; pH, arterial pH; HCO_3^-, arterial bicarbonate; BE, arterial base excess; Hct, arterial hematocrit; Hb, arterial hemoglobin; Core Temp, core body temperature. * $p < 0.05$ compared to SL; † $p < 0.05$ compared to ALT1; ‡ $p < 0.05$ compared to PFO−.

Table 6.3. Cardiopulmonary and Arterial Blood Gas Data During Exercise in the PFO− and PFO+ Groups at Sea level (SL), Acute Hypoxia (ALT1) and After Acclimatization to High-Altitude (ALT16)

	SL		ALT1		ALT16	
	PFO−	PFO+	PFO−	PFO+	PFO−	PFO+
$\dot{V}_E$, L · min^{-1}	60.7 ± 9.3	56.2 ± 13.7	101.9 ± 23.5*	106.5 ± 19.6*	122.9 ± 27.2*	118.9 ± 38.3*
$\dot{V}_A$, L · min^{-1}	50 ± 8.3	45.8 ± 11.3	85.9 ± 18.7*	82.5 ± 20.4*	99.6 ± 27.1*	101.8 ± 37.6*
V_D/V_T	0.45 ± 0.05	0.48 ± 0.05	0.42 ± 0.08	0.43 ± 0.11	0.44 ± 0.03	0.44 ± 0.05
$\dot{V}O_2$, L · min^{-1}	2.22 ± 0.37	2 ± 0.47	2.19 ± 0.46	1.94 ± 0.44	2.31 ± 0.48	2.1 ± 0.52
$\dot{V}CO_2$, L · min^{-1}	2.27 ± 0.42	1.97 ± 0.44	2.29 ± 0.52	2.08 ± 0.46	2.25 ± 0.47	2.03 ± 0.45
RER	1.02 ± 0.04	0.99 ± 0.05	1.04 ± 0.05	1.07 ± 0.04*	0.95 ± 0.07*†	0.95 ± 0.06†
$\dot{V}_E/\dot{V}O_2$	27.5 ± 1.7	28.3 ± 3.3	46.5 ± 3.8*	54.1 ± 11.3*‡	53.4 ± 3.7*†	56.2 ± 8*
HR, bpm	139.2 ± 19.8	143.6 ± 13.3	166 ± 12*	163 ± 12*	154 ± 11	156 ± 18
SV, mL	132.3 ± 17.1	113.6 ± 12.8	125 ± 18	116 ± 13	113 ± 19	98 ± 36
$\dot{Q}_T$, L · min^{-1}	18.4 ± 3.5	16.3 ± 2.1	20.8 ± 2.8	19 ± 3*	17.3 ± 2.7	17 ± 1.8
PASP, mm Hg	50.3 ± 5.7	44.1 ± 10.5	53.6 ± 10.9	52.9 ± 10.5	54.5 ± 10.2	57.7 ± 10.2*
CaO_2, ml O_2 · dL^{-1}	20.2 ± 1.6	18.4 ± 1.8‡	14.4 ± 1.18*	13.34 ± 1.81*	17.88 ± 0.85*†	15.47 ± 2.61*†‡
pH	7.36 ± 0.04	7.37 ± 0.02	7.44 ± 0.05	7.42 ± 0.04*	7.42 ± 0.04	7.42 ± 0.04*
HCO_3^-, mmol · L^{-1}	20.69 ± 1.74	21.1 ± 2.13	15.1 ± 1.2*	14 ± 2.7*	11.4 ± 1.3*†	10.8 ± 2.9*†
BE, mmol · L^{-1}	-3.98 ± 2.07	-3.44 ± 2.08	-8.1 ± 1.69*	-9.35 ± 2.92*	-11.89 ± 1.53*†	-12.45 ± 3.17*†
Hct, %	45.4 ± 3	41.5 ± 3.5‡	46.17 ± 4.39	43.51 ± 4.4	52.68 ± 3.47*†	48.03 ± 5.29*†‡
Hb, g · dL^{-1}	15.2 ± 1.2	13.9 ± 1.4‡	15.6 ± 1.19	14.63 ± 1.45	17.38 ± 1.12*†	15.84 ± 2.15*‡
Core Temp, °C	37.2 ± 0.2	37.4 ± 0.4	37 ± 0.3	37.2 ± 0.4	36.8 ± 0.8	37.2 ± 0.5
Lactate, mmol · L^{-1}	2.95 ± 1.52	2.88 ± 1.43	7.2 ± 2.8*	8.8 ± 2.1*	5.6 ± 1.5*	6.9 ± 2.1*†
n, max	6	10	6	10	6	10

Values are mean ± standard deviation. See Table 6.2 for definitions of acronyms and statistical symbols.

Anthropometric, Exercise, Hematologic, and Pulmonary Function Data

No differences were observed between PFO− and PFO+ groups in baseline anthropometric, exercise, or hematologic variables at SL **(Table 6.1)**. The greater number of females in the PFO+ group (n=7) explains the observed differences in absolute pulmonary function values and results from the known differences in absolute lung volumes between males and females (87). However, when the pulmonary function data were expressed as per cent predicted, there were no differences. Of note, preliminary analyses between male and female subjects revealed no differences other than a larger CaO_2 in males as a result of increased Hb across SL, ALT1 and ALT16 (218)

Sea Level (SL)

Pulmonary Gas Exchange Efficiency. Pulmonary gas exchange efficiency (A-aDO_2) in the PFO− and PFO+ groups at rest (**Figure 6.1A**) and during exercise (**Figure 6.1B**) was similar. However, within the PFO+ group, 6 subjects had a resting bubble score ≥3 and 5 subjects had a resting bubble score ≤2 upon release of a Valsalva maneuver. As described in the methods, this has been demonstrated to correlate to the size of the PFO. Accordingly, subjects with a resting bubble score ≥3 (i.e., a larger PFO) had a greater A-aDO_2 (**Figure 6.2A**) and thus a greater calculated venous admixture ($\dot{Q}_{VA}/\dot{Q}_T$) (**Figure 6.2B**) compared to those with a resting bubble score ≤2 (i.e., a smaller PFO) during submaximal exercise at 100, 130 and 160 W.

Figure 6.1. (next page) Pulmonary Gas Exchange and Arterial Blood Gases
*Pulmonary gas exchange efficiency (A and B), alveolar PO_2 (C and D), arterial PO_2 (E and F), arterial PCO_2 (G and H), and arterial O_2 saturation (I and J) for the PFO− and PFO+ groups at rest and during iso-workload exercise at SL, ALT1, and ALT16. Data presented are mean ± standard error (see **Table 6.2** for respective n's), * $p < 0.05$ compared to SL, † $p < 0.05$ compared to ALT1, ‡ $p < 0.05$ compared to the PFO− group.*

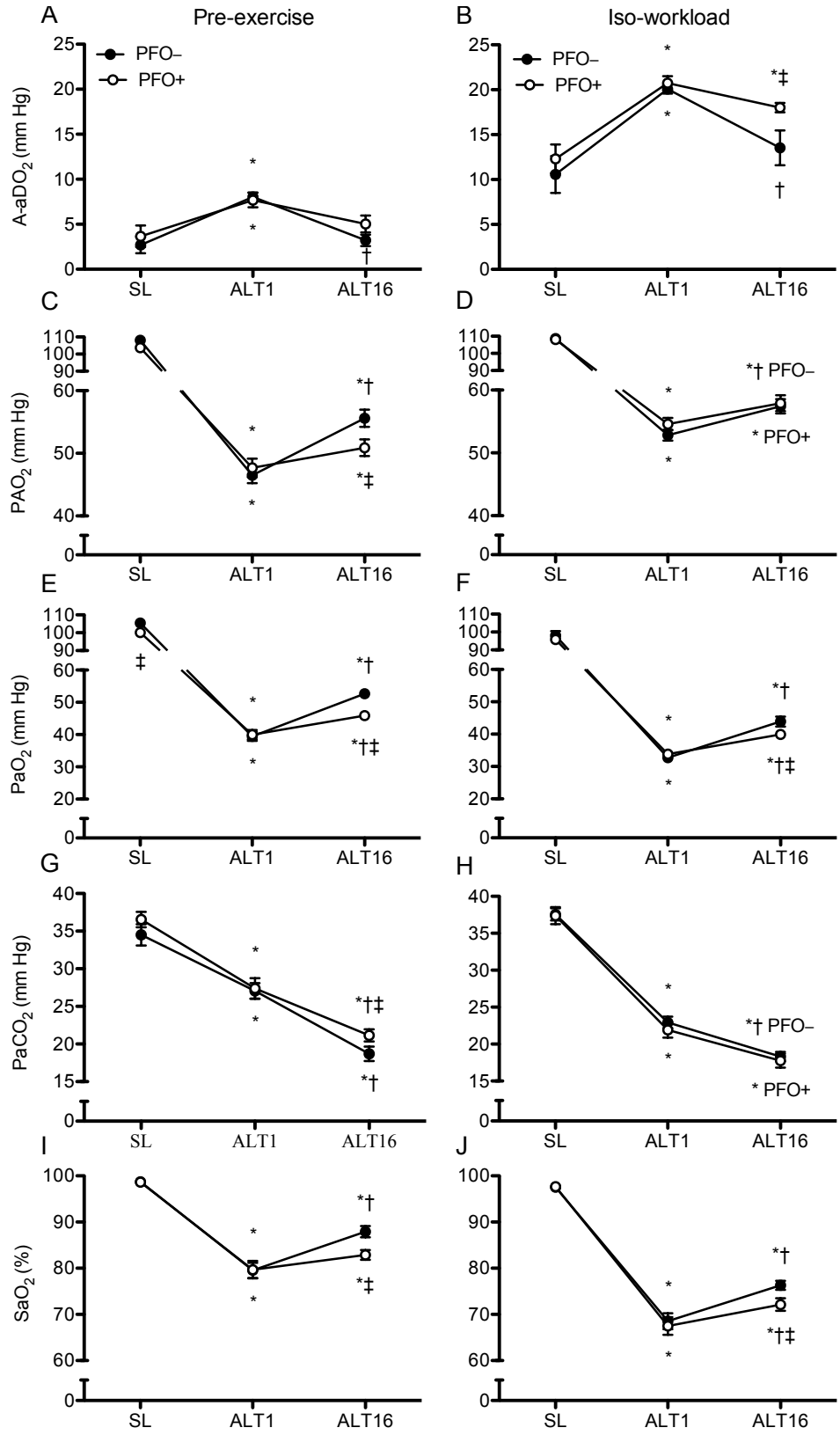
A
Pre-exercise
B
Iso-workload
PFO–
PFO+
A-aDO2 (mm Hg)
C
D
PAO2 (mm Hg)
*† PFO–
* PFO+
E
F
PaO2 (mm Hg)
G
H
PaCO2 (mm Hg)
I
J
SaO2 (%)
SL
ALT1
ALT16

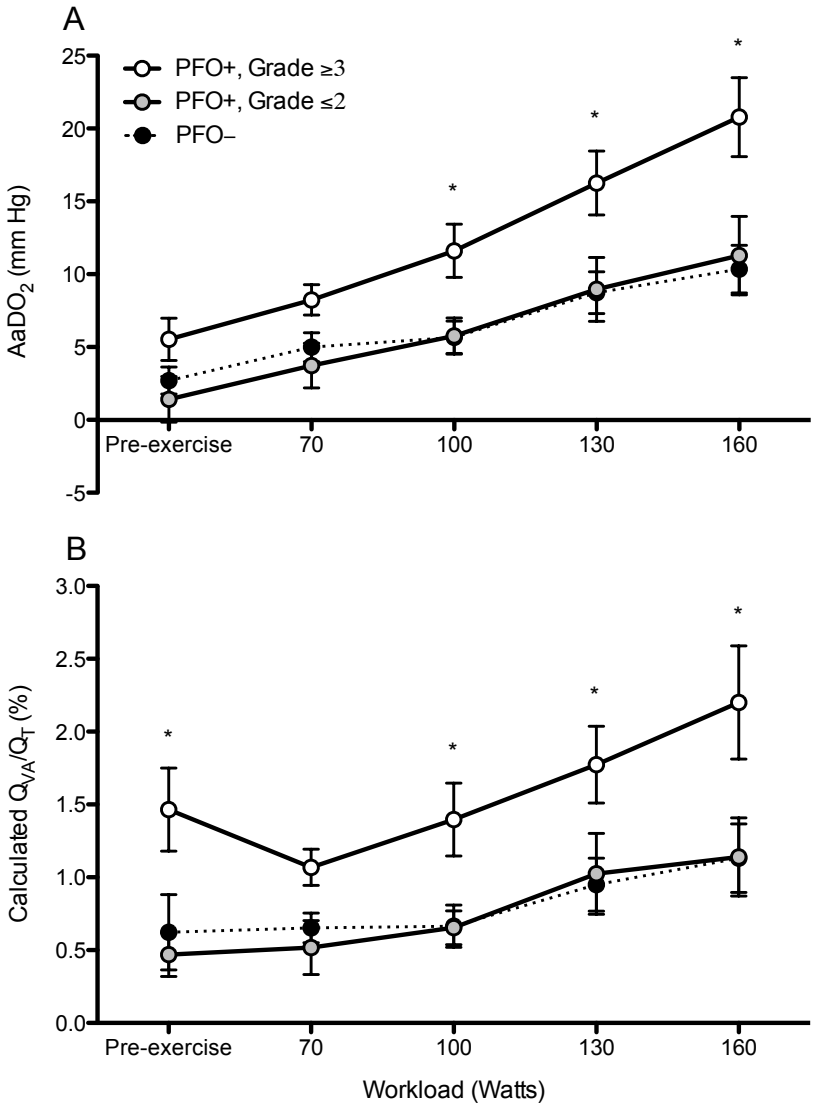

Figure 6.2. Effect of PFO Size on Pulmonary Gas Exchange Efficiency
*Pulmonary gas exchange efficiency (A) and calculated venous admixture (B) at SL at rest and during exercise at 70, 100, 130 and 160 W in the PFO+ group, separated into PFO+ subjects with a resting bubble score of ≤2 upon release of valsalva (shaded circles), and those with a resting bubble score of ≥3 upon release of valsalva (open circles). Filled circles with dashed line represent PFO− subjects and these data are included for comparison only. * $p < 0.05$ compared to PFO+ subjects with a resting bubble score of ≤2.*

Transthoracic Saline Contrast Echocardiography. In both the PFO− and PFO+ groups, bubble scores in the semi-recumbent position at rest increased when breathing 14% O_2 at SL compared to room air, and they were greater in the PFO+ group compared

to the PFO− group when breathing 14% O_2 **(Figure 6.3)**. Bubble scores at rest were qualitatively lower in both the PFO− and PFO+ groups when subjects were upright on the cycle ergometer with a slight forward lean compared to semi-recumbent positioning **(Figure 6.4A)**. This is in agreement with prior work (55, 216) as well as in work reporting bubble scores in subjects at rest breathing 14% O_2 in the semi-recumbent position (134) versus positioned in the upright position with a slight forward lean (54).

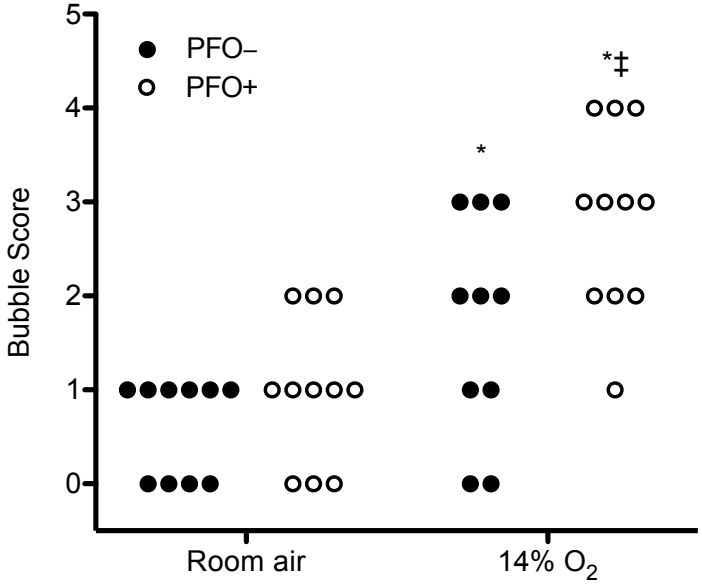

Figure 6.3. Bubble Scores at Rest Breathing Room Air and 14% O_2
*Left-sided contrast (i.e., bubble score) in the PFO− and PFO+ groups in the left lateral decubitus position at rest breathing room air and at rest breathing 14% O_2. Filled circles are PFO− subjects and open circles are PFO+ subjects. * $p < 0.05$ compared to room air, ‡ $p < 0.05$ compared to the PFO− group.*

Acute Ascent to 5260m (ALT1)

Upon arrival to 5260m the cardiopulmonary and respiratory responses between the PFO− and PFO+ groups at rest and during exercise were similar. The A-aDO_2 increased ~2-fold compared to SL in both the PFO− and PFO+ groups at rest **(Figure 6.1A)** and during exercise **(Figure 6.1B)**. Within the PFO+ group the A-aDO_2 increased

to the same extent between those with a resting bubble score ≥3 (i.e., a larger PFO) compared to those with a resting bubble score ≤2 (i.e., a smaller PFO). Similarly, PAO_2, PaO_2, $PaCO_2$, and SaO_2 between the PFO− and PFO+ groups at rest **(Figure 6.1C, E, G, I)** and during exercise **(Figure 6.1D, F, H, J)** were not different. $\dot{V}_E$ and $\dot{V}_A$ were both increased compared to SL in the PFO− and PFO+ groups, and there was no difference in $\dot{V}_E$ or $\dot{V}_A$ between groups **(Table 6.2 and 6.3)**. Additionally, the change in resting $\dot{V}_E$ from SL to ALT1 relative to the change in SaO_2 **(Figure 6.5)** was not different between the PFO− and PFO+ groups. Surprisingly, in both the PFO− and PFO+ groups, bubble scores neither increased at rest nor during exercise at ALT1 compared to SL **(Figure 6.4A and B)**.

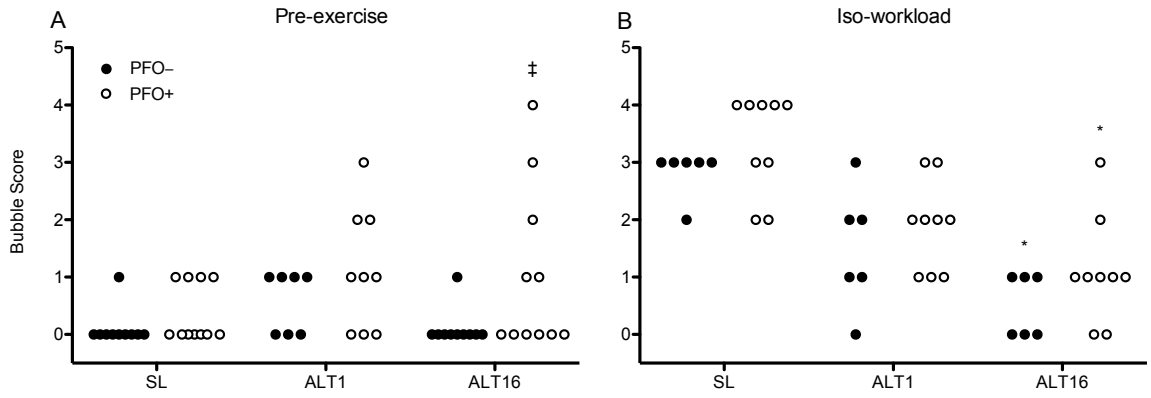

Figure 6.4. Bubble Scores at Rest and During Exercise
*Left-sided contrast (i.e. bubble score) in the PFO− and PFO+ groups when upright and slightly forward leaning at rest (A) and during iso-workload exercise (B) at SL, ALT1, and ALT16. * $p < 0.05$ compared to SL, † $p < 0.05$ compared to ALT1, ‡ $p < 0.05$ compared to the PFO− group.*

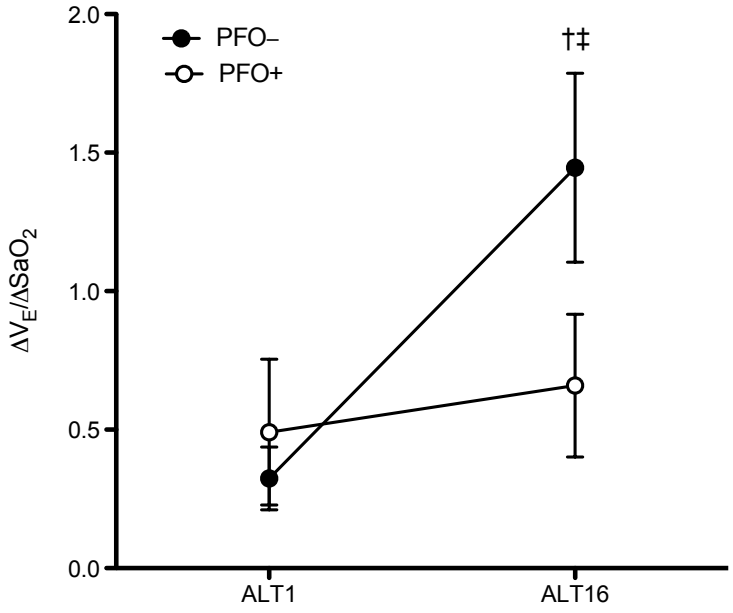

Figure 6.5. Ventilatory Acclimatization
Change in minute ventilation relative to the change in arterial O_2 saturation from SL to ALT1, and from SL to ALT16 in the PFO− and PFO+ groups at rest. Data presented are mean ± standard error. † $p < 0.05$ compared to ALT1, ‡ $p < 0.05$ compared to the PFO− group.

Acclimatization to 5260m (ALT16)

Pulmonary Gas Exchange Efficiency. Unlike the PFO− group, the A-aDO_2 at rest **(Figure 6.1A)** and during exercise **(Figure 6.1B)** in the PFO+ group did not improve (i.e., decrease) compared to ALT1. Furthermore, although there was only a trend for the A-aDO_2 to be greater in the PFO+ group compared to the PFO− group ($p = 0.063$) at rest **(Figure 6.1A)**, the A-aDO_2 was significantly greater in the PFO+ group compared to the PFO− group during exercise **(Figure 6.1B)**. Similar to ALT1, within the PFO+ group there was no difference in the A-aDO_2 between those with a resting bubble score ≥3 (i.e., a larger PFO) compared to those with a resting bubble score ≤2 (i.e., a smaller PFO). This difference in pulmonary gas exchange efficiency between the PFO− and PFO+ groups at ALT16 can also be illustrated by calculating the difference in the total $\dot{Q}_{VA}/\dot{Q}_T$ required

to account for the entire A-aDO_2 for each group between ALT1 and ALT16 **(Figure 6.6)**. From ALT1 to ALT16 at rest, the PFO− group showed a ~21% reduction in calculated $\dot{Q}_{VA}/\dot{Q}_T$, which was greater than the ~13% reduction in the PFO+ group **(Figure 6.6)**. Similarly, from ALT1 to ALT16 during exercise, calculated $\dot{Q}_{VA}/\dot{Q}_T$ in the PFO− group decreased by ~18%, which was also greater than the ~11% decrease in the PFO+ group **(Figure 6.6)**.

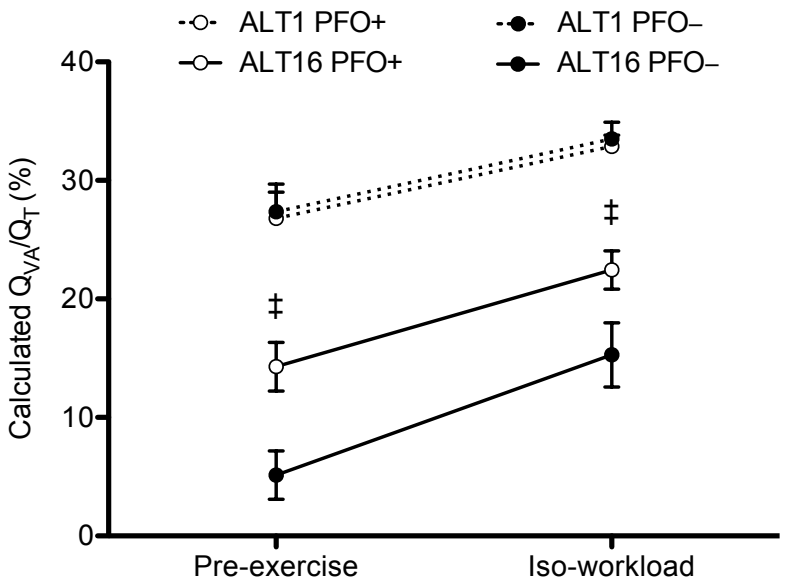

Figure 6.6. Calculated Change in Venous Admixture
Change in minute ventilation relative to the change in arterial O_2 saturation from SL to ALT1, and from SL to ALT16 in the PFO− and PFO+ groups at rest. Data presented are mean ± standard error. † $p < 0.05$ compared to ALT1, ‡ $p < 0.05$ compared to the PFO− group.

Ventilatory Acclimatization and Arterial Blood Gases. Importantly, both the PFO− and PFO+ groups demonstrated a reduction in $PaCO_2$ and an increase in PaO_2 compared to ALT1, consistent with acclimatization to high-altitude **(Figure 6.1E and G)**. That said, the PFO+ group had no improvement in A-aDO_2 from ALT1 to ALT16, and they demonstrated a less pronounced degree of ventilatory acclimatization compared to the

PFO− group. Only the PFO− group increased $\dot{V}_A$ at rest at ALT16 compared to ALT1, and $\dot{V}_A$ was less in the PFO+ group compared to the PFO− group at rest at ALT16 **(Table 6.2)**. Consequently, the PFO+ group had reduced resting PAO_2, PaO_2, SaO_2 and increased $PaCO_2$ compared to the PFO− group **(Figure 6.1C, E, G, I)** at rest at ALT16, and both PAO_2 and SaO_2 had not improved after acclimatization compared to ALT1 **(Figure 6.1C and I)**. This reduced degree of ventilatory acclimatization is also illustrated by the change in resting $\dot{V}_E$ from SL to ALT16 relative to the change in SaO_2 not increasing at ALT16 compared to ALT1 in the PFO+ group **(Figure 6.5)**. This contrasts with the PFO− group who showed an increase in the change in resting $\dot{V}_E$ from SL to ALT16 relative to the change in SaO_2 at ALT16 compared to ALT1 **(Figure 6.5)**.

The difference in $\dot{V}_A$ between the PFO− and PFO+ groups at ALT16 was present only at rest and not during exercise at ALT16. Nevertheless, only the PFO− group increased PAO_2 **(Figure 6.1D)** and decreased $PaCO_2$ **(Figure 6.1H)** during exercise at ALT16 compared to ALT1. Both of the PFO− and PFO+ groups increased PaO_2 and SaO_2 during exercise at ALT16 compared to exercise at ATL1; however, during exercise at ALT16, PaO_2 and SaO_2 in the PFO+ group were lower compared to the PFO− group **(Figure 6.1F and J)**.

Transthoracic Saline Contrast Echocardiography. At rest, bubble scores in the PFO− and PFO+ groups were not different at ALT16 compared to ALT1; however, bubble scores in the PFO+ group were greater than the PFO− group at ALT16 **(Figure 6.4A)**. During exercise, bubble scores in both the PFO− and PFO+ groups remained lower than SL values, and were not reduced compared to ALT1 values.

Hemoglobin and Hematocrit. Hb and Hct were less in the PFO+ group compared to the PFO− group and only the PFO− group increased Hb and Hct compared to ALT1. However, according to unpublished observations (Ryan *et al*., *In Preparation*) by our group, Hb mass increased compared to SL in 19/21 subjects and the 2 subjects who lacked an increase in Hb mass were PFO+ females. Statistical analysis of the PFO+ group without these two subjects shows no differences between the PFO− and PFO+ groups in Hb ($p = 0.20$) or Hct ($p = 0.21$) at ALT16; therefore, in both the PFO− and PFO+ groups Hb and Hct increased compared to ALT1.

DISCUSSION

The primary purpose of this study was to investigate the effect of a PFO on pulmonary gas exchange efficiency at rest and during exercise at sea level (SL), after rapid transport to 5260m (ALT1) and after living at 5260m for 16 days (ALT16) in healthy, PFO− ($n = 10$) and PFO+ ($n = 11$) sea level natives. The novel findings in this study are: 1) pulmonary gas exchange efficiency did not improve at rest or during exercise after acclimatization to 5260m in the PFO+ group; 2) there was a reduced degree of ventilatory acclimatization to 5260m in the PFO+ group; and 3) in contrast to acute normobaric hypoxia, left-sided contrast did not increase during acute hypobaric hypoxia in either of the groups.

Pulmonary Gas Exchange Efficiency in PFO− and PFO+ Subjects at SL

Three distinct factors can impair pulmonary gas exchange efficiency: 1) alveolar ventilation-to-perfusion ($\dot{V}_A/\dot{Q}$) inequality; 2) incomplete end-capillary O_2 diffusion equilibration; and 3) any source of right-to-left shunt [extrapulmonary shunt (e.g. venous

blood from the bronchial and Thebesian circulations), intracardiac shunt (e.g. blood flow through a PFO), and intrapulmonary shunt]. Although this study did not directly assess contributions from $\dot{V}_A/\dot{Q}$ inequality or diffusion limitation, previous work suggests that diffusion limitation represents a minimal contribution to the A-aDO_2 during submaximal exercise ($\dot{V}O_2$ <2.0 L/min) in healthy humans at SL (85, 102, 195, 229, 239) such that the majority of the A-aDO_2 is explained by $\dot{V}_A/\dot{Q}$ inequality and right-to-left shunt. Accordingly, during iso-workload exercise ($\dot{V}O_2$ ~2.0 L/min) in our healthy subject population, at SL $\dot{V}_A/\dot{Q}$ inequality and right-to-left shunt were likely the predominant contributors to the measured A-aDO_2. In both PFO− and PFO+ subjects this would include extrapulmonary shunt, and intrapulmonary shunt, if any. However, subjects in the PFO+ group also have an additional source of shunt, which is intracardiac shunt via the PFO.

Right-to-left blood flow through the PFO is dependent upon right atrial pressure exceeding left atrial pressure, which can occur transiently during the normal respiratory cycle, likely at end inspiration when systemic venous return is augmented by reduced intrathoracic pressure (64, 267). Therefore, during normal respiration, right-to-left blood flow through the PFO would be expected to be intermittent and variable in volume. Although in the current study the A-aDO_2 was not different between the PFO− and PFO+ groups at rest or during exercise at SL, closer inspection of the data and subject characteristics revealed that the size and/or amount of blood flow through the PFO is important. Using TTSCE in PFO+ subjects Fenster *et al*. demonstrated that the degree of left heart contrast (i.e., bubble score) observed upon release of a Valsalva maneuver predicts the size of PFO determined using intracardiac echocardiography (64). According

to these criteria, within the PFO+ group in the current study there were 6 subjects with a bubble score ≥3 at rest upon release of a Valsalva maneuver (i.e., a larger PFO), and 5 subjects with a bubble score ≤2 at rest upon release of a Valsalva maneuver (i.e., a smaller PFO). Although the qualitative assessment of left-heart contrast does not represent a quantitative measure of blood flow, it is intuitive that a larger PFO should permit the passage of a greater volume of blood and thus a greater right-to-left shunt. In support of this idea, the subjects with a larger PFO had an approximately two-fold wider A-aDO_2 at rest and throughout all submaximal workloads at SL compared to those with a smaller PFO **(Figure 6.2A)**. PFO+ subjects with a smaller PFO appear indistinguishable from the PFO− group, which also supports prior work suggesting that bubble scores <2 represent a trivial degree of potential right-to-left shunt (133). Taken together, these data provide rationale for identifying subjects with a PFO when quantifying pulmonary gas exchange efficiency, as the presence of PFO influences the average, and variance of the A-aDO_2 within a given data set.

Pulmonary Gas Exchange Efficiency in PFO− and PFO+ Subjects at ALT1

At 5260m (P_B ~406 mm Hg) inspired PO_2 is lowered to ~75 mm Hg, significantly reducing PAO_2, and reducing the contribution from $\dot{V}_A/\dot{Q}$ inequality on the A-aDO_2 while the contribution of diffusion limitation on the A-aDO_2 increases (183, 184, 255). The effect that a given volume of right-to-left shunt has on the A-aDO_2 is also lessened in hypoxia due to the difference between mixed venous PO_2 ($P\bar{v}O_2$) and PaO_2 becoming less. For this reason, if the shunt fraction via the PFO was constant from SL to ALT1, this additional 0.5-2.0% shunt (as it was calculated to be at SL) would account for between 1-3 mm Hg of the measured A-aDO_2 at ALT1. Therefore, it should not be surprising that at

ALT1 the PFO− and PFO+ groups had similar degrees of pulmonary gas exchange impairment both at rest and during exercise **(Figure 6.2B)**. Additionally, it should not be surprising that within the PFO+ group, there was no difference in the A-aDO_2 between subjects with larger and smaller PFOs corresponding to varying degrees of blood flow through the PFO.

Pulmonary Gas Exchange Efficiency and Ventilatory Acclimatization in PFO− and PFO+ Subjects at ALT16

Acclimatization to hypobaric hypoxia is characterized by a multitude of physiologic adaptations, notably a time-dependent increase in ventilation (250). Compared to acute hypoxia, ventilatory acclimatization helps to increase CaO_2 by increasing PAO_2 and the driving gradient for O_2 diffusion at the alveolar-capillary interface, increasing PaO_2 and therefore, SaO_2. Consequently, compared to acute hypoxia the further increase in $\dot{V}_A$, and therefore PAO_2 with acclimatization would theoretically reduce the relative contributions from $\dot{V}_A/\dot{Q}$ inequality and diffusion limitation while increasing the relative contribution of right-to-left shunt on the A-aDO_2. Indeed, an increase in $\dot{V}_A$ should equate to improved $\dot{V}_A/\dot{Q}$ matching by way of lessening potential disparities in the PO_2 between alveoli (63, 193, 204). Diffusion limitation would theoretically also be reduced compared to ALT1 by way of an increased driving gradient for O_2 diffusion (243), increased $P\bar{v}O_2$, and a potential improvement in diffusing capacity for O_2 (3). Lastly, a given volume of right-to-left shunt would have a greater effect on the A-aDO_2 due to the difference between $P\bar{v}O_2$ and PaO_2 increasing at ALT16 compared to ALT1.

Rest. Accordingly, absence of an increased $\dot{V}_A$ at rest at ALT16 in the PFO+ group may partially explain the absence of a reduction in A-aDO_2 compared to ALT1. The less pronounced degree of ventilatory acclimatization in the PFO+ group corresponded to a lower PAO_2, which, compared to the PFO− group, may increase the relative contribution and potential for $\dot{V}_A/\dot{Q}$ inequality and, particularly diffusion limitation to contribute to the A-aDO_2. Additionally, continued right-to-left shunt via the PFO could have also contributed to the lack of improvement in A-aDO_2 at rest at ALT16. However, the effect of this right-to-left shunt via the PFO, although increased compared to ALT1, would still likely be minimal considering the magnitude of the increase in PaO_2 from ALT1 to ALT16 (40 ± 5 mm Hg at ALT1 vs. 46 ± 3 mm Hg at ALT16). Nevertheless, bubble scores were increased in the PFO+ group at rest at ALT16 and although this neither quantifies blood flow nor strictly reflects blood flow through the PFO, it supports the occurrence of right-to-left shunt via the PFO in the PFO+ group. Conversely, in the PFO− group PaO_2 increased from 40 ± 4 mm Hg at ALT1 to 53 ± 4 mm Hg at ALT16, approximately twice as much as of the PFO+ group ($p = 0.0003$). Importantly, small changes in PaO_2 in this range on the oxygen-hemoglobin dissociation curve correspond to large changes in SaO_2, and thus CaO_2. Indeed, had PaO_2 increased in the PFO+ group to the same degree as it did in the PFO− group, SaO_2 in the PFO+ group would have increased from ~83% to ~88%, corresponding to CaO_2 increasing from ~18 mL O_2/dL blood to ~19 mL O_2/dL blood.

Why the PFO+ group had a lesser degree of ventilatory acclimatization compared to the PFO− group remains unknown, although we speculate that this may actually represent a beneficial response to hypoxia in subjects with an intracardiac right-to-left

shunt (i.e., the PFO+ group). Increasing ventilation and therefore raising PAO_2 would increase PaO_2 in PFO− subjects to a greater extent than PFO+ subjects, due to the continued presence of right-to-left shunt via the PFO. Indeed, perfusion without ventilation defines a right-to-left shunt. Therefore, the metabolic demand associated with increasing ventilation would potentially benefit PFO+ subjects to a lesser degree in terms of raising PaO_2, compared to PFO− subjects. Furthermore, considering pH and temperature were not different between the PFO− and PFO+ groups, the lower V_A in the PFO+ group resulted in a higher $PaCO_2$ and thus, a right-shifted oxygen-hemoglobin dissociation curve. Estimating this shift based off of the calculated P_{50} values using the Hill equation (Hill coefficient = 2.7), the PFO+ group had a higher P_{50} (29.1 ± 0.7 mmHg) compared to the PFO− group (28 ± 1 mmHg), $p = 0.036$ (90). This would facilitate the unloading of O_2 at the tissue, which would be beneficial for PFO+ subjects considering their impaired ability to raise PaO_2 and thus SaO_2, due to right-to-left shunt via the PFO. Interestingly, in animals with an intracardiac right-to-left shunt and in children with cyanotic congenital heart disease, the presence of a right-shifted oxygen-hemoglobin dissociation curve has also been hypothesized to be a possible compensatory mechanism for facilitating O_2 unloading and therefore reducing tissue hypoxia (169, 265).

Exercise. During exercise the A-aDO_2 is greater in acute hypoxia compared to SL and decreases following acclimatization to high-altitude compared to acute hypoxia (13, 28, 47, 150), yet the cause of this subsequent improvement in A-aDO_2 remains speculative. Considering the sample sizes of these prior studies (n = 6-10), statistically we would expect each study to have 2-4 PFO+ subjects, and it is unknown to what extent such

subjects could potentially have influenced the findings in these previous studies. In the current study when the A-aDO_2 data from the PFO− and PFO+ groups is pooled, as previously shown, pulmonary gas exchange efficiency improves following acclimatization to hypobaric hypoxia **(Figure 6.7)**. However, by prospectively identifying PFO− and PFO+ subjects, the current work suggests that this reduction in the A-aDO_2 after acclimatization was not present in the PFO+ subjects in our study. Within the PFO+ group there was no difference in the A-aDO_2 between those with a resting bubble score ≥3 (i.e., a larger PFO) compared to those with a resting bubble score ≤2 (i.e., a smaller PFO). Although, as previously discussed, right-to-left blood flow through the PFO would be expected to intermittent and variable in volume and dependent on a sufficient pressure gradient between the right and left atria. Using pulmonary artery systolic pressure (PASP) as an estimate for this potential pressure gradient, PASP was ~10 mm Hg higher at rest and during exercise at ALT16 in PFO+ subjects with a resting bubble score ≤2 (i.e., a smaller PFO), compared to PFO+ subjects with a resting bubble score ≥3 (i.e., a larger PFO). Thus, despite the "smaller" PFO, these subjects may have had more blood flow through it, such that compared to subjects with a "larger" PFO, differences in the A-aDO_2 were obscured.

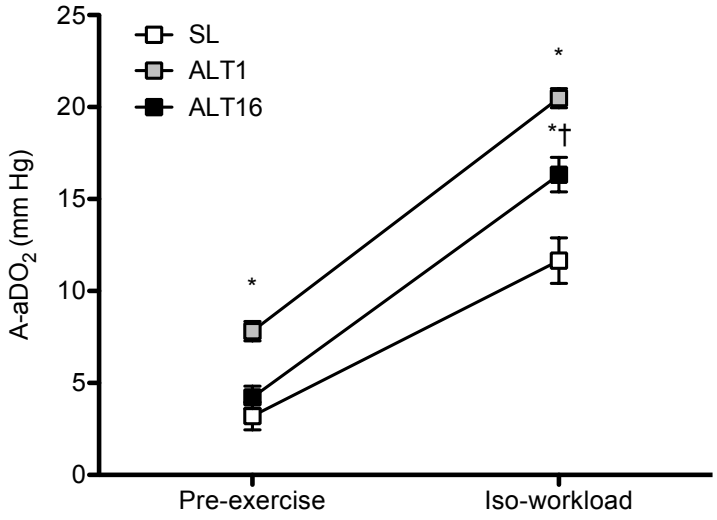

Figure 6.7. Pulmonary Gas Exchange Efficiency, Group
*Pulmonary gas exchange efficiency for the combined group data (i.e., both PFO− and PFO+ groups) at rest and during iso-workload exercise at SL, ALT1, and ALT16. Data presented are mean ± standard error. * $p < 0.05$ compared to SL, † $p < 0.05$ compared to ALT1.*

In contrast to rest, $\dot{V}_A$ and PAO_2 were not different between the PFO− and PFO+ groups during exercise at ALT16. This suggests that contributions from $\dot{V}_A/\dot{Q}$ inequality and diffusion limitation to the A-aDO_2 during exercise may be relatively equal between the PFO− and PFO+ groups. However, while not directly measured, we cannot rule out the possibility that differences between the PFO− and PFO+ groups in terms of $\dot{V}_A/\dot{Q}$ inequality and diffusion limitation existed. Nevertheless, the intracardiac right-to-left shunt via the PFO in the PFO+ group could have also contributed to the lower PaO_2 in the PFO+ group **(Figure 6.1E)**, and therefore, contributed to the lack of improvement in A-aDO_2 compared to ALT1 and significantly greater A-aDO_2 compared to the PFO− group at ALT16 **(Figure 6.1B)**. The calculated volume of venous admixture required to account for the difference in A-aDO_2 during exercise at ALT16 between the PFO− and PFO+ groups was ~7%. This ~7% difference between the PFO− and PFO+ groups

includes all sources of venous admixture, yet this does not preclude the possibility that the intracardiac right-to-left shunt in the PFO+ group was contributing to the lack of improvement in pulmonary gas exchange efficiency expected to occur with acclimatization to high-altitude.

Although our exercise data at ALT16 indicate worse pulmonary gas exchange efficiency in the PFO+ group, this did not translate into differences in functional exercise capacity, that have been described previously (218). However, neither group had an A-aDO_2 >25 mm Hg at this submaximal workload, and therefore it is unlikely that exercise capacity would be limited due to pulmonary gas exchange inefficiency. Alternatively, the lack of functional difference between groups may also be the result of the right-shifted oxygen-hemoglobin dissociation curve that facilitated the unloading of oxygen despite the fact that pulmonary gas exchange efficiency did not improve with acclimatization and ventilatory acclimatization was less than PFO− subjects.

Acclimatization and Left-Sided Contrast in PFO− and PFO+ Subjects

During exercise in healthy humans agitated saline contrast traverses the pulmonary circulation, suggesting an increase in blood flow through large diameter intrapulmonary arteriovenous anastomoses (IPAVA) compared to rest (53, 54, 115, 143, 144, 216). In addition to exercise, acute normobaric hypoxia at rest increases blood flow through IPAVA (134) and combining hypoxia with exercise results in augmented left-sided contrast due increased to blood flow through IPAVA (54, 143). Consistent with previous work (134), normobaric hypoxia (14% O_2) at SL increased left-sided contrast in both the PFO− and PFO+ groups in the supine position **(Figure 6.3)**. However, at ALT1

bubble scores were not different compared to SL, and interestingly, bubble scores at ALT16 were reduced compared to SL **(Figure 6.4)**.

These data are supported by work from Foster *et al*. (67) demonstrating that after 3 weeks of acclimatization to 5050 m only 1/8 PFO− subjects had transpulmonary passage of saline contrast at rest. Yet all 8 PFO− subjects had transpulmonary passage of saline contrast in conditions of acute normobaric hypoxia (10% O_2) in a non-acclimatized state. The current work supports these findings by also demonstrating a reduction in bubble scores in both PFO− and PFO+ subjects, at rest and during exercise, and in both acute hypobaric hypoxia as well as after acclimatization to hypobaric hypoxia **(Figure 6.4)**. The unexpectedly low bubble scores at ALT1 and further reduction in bubble scores at ALT16 are intriguing, and for which there are several possible explanations. Foster *et al*. hypothesized that the reduction in blood flow through IPAVA could be a result of the increase in SpO_2 and decrease in $\dot{Q}_T$ that occurs following acclimatization to high-altitude. It is known that increases in $\dot{Q}_T$ and decreases in SaO_2 are potential mechanisms explaining the increase in blood flow through IPAVA at SL (24, 133, 134). Foster *et al*. also hypothesized that some degree of pulmonary vascular remodeling occurred over the 21 day time span that may contribute to the reduction in blood flow through IPAVA.

Both of these hypotheses imply a time-dependent reduction in blood flow through IPAVA during acclimatization to hypobaric hypoxia, and our data at ALT16 and data from Foster *et al*. at 21 days support this possibility. However, our data at ALT1 suggest that part of this decrease may be due to hypobaria *per se*. All agitated saline contrast injections (i.e., at SL, ALT1 and ALT16) consisted of 3 ml of saline combined with 1 ml of room air. Thus, the ~50% reduction in barometric pressure at 5260m would result in

an ~50% reduction in the absolute moles of gas within the 1 ml volume, although it is unknown to what extent, if any, this would effect microbubble size or time to dissolution. Importantly however, the degree of right-sided contrast was qualitatively not different at ALT1 or ALT16 compared to SL. Nevertheless, this qualitative assessment of right-sided contrast does not preclude the possibility that *in vivo* microbubble dynamics are altered in hypobaric hypoxia. Ultimately, although hypobaria might play a role in the reduction in bubble scores at ALT1, it likely does not explain the further reduction coincident with acclimatization to high-altitude as noted above.

Summary

The current study aimed to assess the impact of a PFO on pulmonary gas exchange efficiency at rest and during exercise at SL, with acute transport to 5260m, and after living at 5260m for 16 days. We identified an improvement in pulmonary gas exchange efficiency with acclimatization to high-altitude similar to previous investigations; however, this finding was not present in PFO+ subjects. The additional source of intracardiac right-to-left shunt in PFO+ subjects may be sufficient to explain their impaired pulmonary gas exchange efficiency at rest and during submaximal exercise compared to PFO− subjects at SL. However, the contribution of this right-to-left shunt to pulmonary gas exchange efficiency is reduced at altitude and may only partially explain the lack of improvement in pulmonary gas exchange efficiency at ALT16. PFO+ subjects demonstrated a less pronounced degree of ventilatory acclimatization to 5260m, concomitant with a greater A-aDO_2 and lower PaO_2 and SaO_2. Although future work is needed to corroborate these findings, we speculate that this reduction in ventilatory acclimatization may be beneficial in PFO+ subjects by limiting the metabolic cost of

hyperventilation, which would not effectively increase PaO_2. Ultimately, a more effective strategy may be to ventilate less, resulting in a right-shifted oxygen-hemoglobin dissociation curve that facilitates O_2 unloading at the tissue when O_2 loading is hindered by the presence of an intracardiac right-to-left shunt.

CHAPTER VII

CONCLUSIONS

MAIN FINDINGS

One of the primary critiques pertaining to the undefined physiologic relevance of blood flow through IPAVA is whether or not this blood flow contributes to pulmonary gas exchange efficiency. Several studies have demonstrated a correlation between increases in blood flow through IPAVA and increases in the A-aDO_2, however no study has demonstrated an increase in blood flow through IPAVA when potential contributions from $\dot{V}_A/\dot{Q}$ inequality and diffusion limitation to the A-aDO_2 are minimized. Accordingly, an experimental paradigm preventing contributions from $\dot{V}_A/\dot{Q}$ inequality and diffusion limitation was employed in Chapter IV, and blood flow through IPAVA was demonstrated to occur at a time when pulmonary gas exchange efficiency became worse. Another primary critique pertaining to the undefined physiologic relevance of blood flow through IPAVA is the undefined mechanistic regulation of these vessels. The experimental paradigm used in Chapter IV also provided a means to pharmacologically increase $\dot{Q}_T$ with and without changes in PASP, and blood flow through IPAVA appears to be increased by increases in $\dot{Q}_T$ independent of changes in PASP.

Similarly, the hyperoxia-mediated reduction in blood flow through IPAVA is another controversial area as this finding suggests, 1) these vessels are regulated opposite to the conventional circulation, and 2) the shunt fraction measured using the 100% O_2 technique when blood flow through IPAVA is not present, may not be equal to the shunt fraction occurring when breathing a FIO_2 <1.0, when blood flow through IPAVA is present. Chapter V pharmacologically targeted the pulmonary vasculature during exercise

breathing a $FIO_2 = 1.0$ and demonstrates that sildenafil, nifedipine, and acetazolamide have no discernable effect using TTSCE on blood flow through IPAVA during exercise breathing a $FIO_2 = 1.0$.

In contrast to the hyperoxia-mediated reduction in blood flow through IPAVA, acute normobaric hypoxia increases blood flow through IPAVA, yet the effect of long-term hypoxia on blood flow through IPAVA remains unknown. This area was investigated by studying human acclimatization to hypobaric hypoxia (5260m) for 16 days, and the data are presented in Chapter VI. It was observed that blood flow through IPAVA is reduced in acute hypobaric hypoxia, and is further reduced following acclimatization to hypobaric hypoxia. Accordingly, these data suggest an effect of hypobaria *per se* on blood flow through IPAVA, yet this does not entirely explain the subsequent reduction in blood flow through IPAVA following acclimatization. Secondarily, in Chapter VI we present data demonstrating the physiologic significance of a PFO, in both the context of pulmonary gas exchange efficiency at rest and during exercise at sea level, and in the context of acclimatization to hypobaric hypoxia.

SUMMARY AND FUTURE DIRECTIONS

Intrapulmonary arteriovenous anastomoses have been unequivocally demonstrated to exist in animal models and in isolated and perfused human lungs using solid microspheres, and convincingly so in healthy humans using ^{99m}Tc-MAA and TTSCE. However, critics remain skeptical of the physiologic relevance of blood flow through IPAVA, primarily because of the undefined contribution of blood flow through IPAVA to pulmonary gas exchange efficiency, and the undefined mechanistic regulation

of blood flow through IPAVA. Furthermore, the classical understanding of pulmonary gas exchange efficiency in healthy humans emphasizes the relative contributions of $\dot{V}_A/\dot{Q}$ inequality and diffusion limitation, while downplaying the relative contribution of right-to-left shunt; because functional gas exchange dependent methods do not detect significant right-to-left shunt.

Accordingly the discrepancy between these two distinctly different approaches to studying the pulmonary circulation and pulmonary gas exchange efficiency may be reconciled in several ways. First, it remains possible that blood flow through IPAVA, although detected using anatomic based methods, participates in some degree of gas exchange and therefore is not a source of *true* shunt and instead is a source of 'venous admixture'. If so, inert gas methods may interpret this blood flow as an area of low $\dot{V}_A/\dot{Q}$, but not below the 0.005 threshold for intrapulmonary right-to-left shunt, or potentially even below the 0.1 threshold for 'low $\dot{V}_A/\dot{Q}$'. Alternatively, non-capillary gas exchange may result in inert gases diffusing out of the blood, prior to reaching IPAVA, and therefore not being retained as evidence of right-to-left shunt. Non-capillary gas exchange has been demonstrated to occur in humans (108, 109, 209) and cats (40) and therefore provides a basis for this concern. Furthermore there exists considerable data demonstrating the exchange of inert gases within the conducting airways and even trachea (220). These data predominantly affect inert gases of high-solubility and high molecular weights (not necessarily sulfur hexafluoride), although these data do suggest the mathematical constraints and theory of the MIGET may be incompletely defined. However, to what extent these potential inaccuracies impact the overall $\dot{V}_A/\dot{Q}$ distribution is unknown. Lastly, the relatively inconsistent data reported from both within a given lab

group, and across different labs, using the MIGET raises the concern that despite the theoretical 'exquisite' sensitivity of the MIGET, in practice it may not be able to detect small but significant shunts such as the PFO which is present in 35-40% of the population. Indeed, all humans have a certain degree of postpulmonary right-to-left shunt via the bronchial and Thebesian circulations of the lungs and heart, respectively, and the MIGET cannot differentiate this postpulmonary shunt from diffusion limitation. Therefore, even at rest the measured A-aDO_2 should *always* exceed the predicted A-aDO_2, yet the reverse is often reported (85, 101, 175, 195, 239), or the two are superimposable (185, 229, 235), leaving no room for postpulmonary shunt. This is a very important distinction, because this suggests the baseline measure does not reflect what one would expect based on the known, and unquestioned presence of postpulmonary right-to-left shunt in all humans. Therefore, the MIGET does not seem to have the sensitivity to detect postpulmonary right-to-left shunt in humans, and thus, raises the question; can the MIGET detect the same volume of intrapulmonary right-to-left shunt in humans during exercise?

Potential support for the MIGET to be capable of detecting small volumes of right-to-left shunt comes from work using the MIGET in healthy subject at rest breathing room air and 100% O_2 (236). In this study 4 healthy young subjects and 5 healthy older subjects were studied. It was shown in young subjects breathing room air that the shunt measured using the MIGET was 0%, which increased in 3 of the 4 young subjects to ~0.5% when breathing 100% O_2. In the older subjects the shunt measured when breathing room air was also 0%, which increased in all 5 subjects to ~3.5% (range = 0.8% – 10.7%) when breathing 100% O_2. These measured values of right-to-left shunt, using the

MIGET, include only intrapulmonary and intracardiac shunt. Intracardiac shunt would also have been present when breathing room air, and thus, the increased shunt detected when breathing 100% O_2 is from an increase in intrapulmonary shunt, which the authors speculated was secondary to atelectasis. In this study the shunt fraction was also measured using the 100% O_2 technique simultaneously with the MIGET. In young subjects the shunt fraction using the MIGET was ~0.5% when breathing 100% O_2, which contrasts with the 100% O_2 technique value of ~4.25%. Similarly, in older subjects the shunt fraction using the MIGET was ~3.5% when breathing 100% O_2, which contrasts with the 100% O_2 technique value of ~8.66%. The measured values of right-to-left shunt using the 100% O_2 technique include intrapulmonary, intracardiac, *and* postpulmonary shunt. The authors speculated that the reason for the consistently larger shunt fractions measured using the 100% O_2 technique was due to the inclusion of postpulmonary shunt, as well as known errors associated with accurately measuring PaO_2 when breathing 100% O_2. The A-aDO_2 in young and older subjects breathing 100% O_2 was ~76 mm Hg and ~133 mm Hg, respectively. Which are markedly higher than previous reports, of ~15 mm Hg at rest breathing 100% O_2 (39) and ~30 mm Hg during exercise breathing 100% O_2 (233). Therefore, it is possible that there were errors in the blood gas measurements, however even if this accounted for half of the difference in shunt fraction, as the authors speculated, the remaining value of ~1.9% in young subjects and ~2.5% in older subjects is then due to postpulmonary shunt. To summarize, these data do provide evidence that the MIGET can detect a small volume of right-to-left shunt in subjects at rest breathing 100% O_2, but does not detect these same volumes of right-to-left shunt in these same subjects at rest breathing room air.

When breathing 100% O_2, the reduction in blood flow through IPAVA that has consistently been demonstrated using anatomic methods, precludes this technique from assuming the measured shunt fraction is the same regardless of the FIO_2. This is of course only if the possibility is entertained that blood flow through IPAVA provides a source of shunt or venous admixture when breathing a FIO_2 <1.0.

Anatomic based methods have the unique strength of quantifying the volume of blood flow through IPAVA in an approach independent of pulmonary gas exchange. While functional gas exchange dependent methods have the unique strength of quantifying gas exchange dependent processes, i.e., $\dot{V}_A/\dot{Q}$ inequality and diffusion limitation. Taken together, it seems appropriate to merge both approaches and investigate pulmonary gas exchange efficiency from a more inclusive view. Nevertheless, before this multi-view approach is reasonable; the aforementioned limitations of the MIGET will need to be addressed. One possibility for addressing, at least in part, this concern would be to measure the A-aDO_2 in subjects with and without a PFO while simultaneously quantifying right-to-left shunt using the MIGET and ^{99m}Tc-MAA. The premise for this is that differences in the A-aDO_2 can be detected in subjects with and without a PFO at rest via arterial blood gas analysis; when diffusion limitation can be excluded from contributing to the A-aDO_2, and potential impairments in $\dot{V}_A/\dot{Q}$ inequality, if present, would likely be similar in subjects with and without a PFO. Right-to-left shunt via the PFO is interpreted by the MIGET as a $\dot{V}_A/\dot{Q}$ ratio of ≤0.005, meaning it is indistinguishable from intrapulmonary right-to-left shunt. Thus, the sensitivity of the MIGET in practice can be assessed through determining whether or not it detects the

additional source of right-to-left shunt via the PFO. This additional source of right-to-left shunt via the PFO should also be quantifiable using ^{99m}Tc-MAA, and through back calculating the required volume of venous admixture to account for the entire A-aDO_2 from the arterial blood gases. There is understandably a certain inherent degree of error associated with each of these measures; nevertheless, this may be an enlightening direction to pursue.

Perhaps the most important next step will be do quantify blood flow through IPAVA during the conditions presented in Chapter IV, and demonstrate an increase in blood flow through IPAVA that can be distinguished from postpulmonary shunt. Currently, we cannot definitively refute the possibility that the increase in A-aDO_2 is entirely due to an increase in postpulmonary shunt, potentially predominantly from Thebesian blood flow. Although our experimental conditions strongly suggest blood flow through IPAVA contributes to pulmonary gas exchange efficiency, quantifying the volume of blood flow through IPAVA using a technique independent of pulmonary gas exchange would lend further support to this conclusion.

Another critical step will be to directly visualize IPAVA, both in healthy humans and in such a way that provides a means to isolate and perfuse these vessels. Visualizing IPAVA in healthy humans may be possible using high-resolution computed tomography, however the challenge will be to balance the effective resolution with the necessary dose of radiation. In the 1950's Tobin and Zariquiey visualized via vascular casting the presence of arteriovenous anastomoses between the pulmonary arterial and venous circulation. However, vinyl vascular casting does not permit the ability after the fact, to isolate and perfuse the vasculature. Isolating IPAVA would permit the ability to perfuse

the vessel and demonstrate it being regulated opposite to the conventional pulmonary circulation. Furthermore, potential molecular mechanisms regulating the vascular tone of IPAVA could be investigated in this preparation.

To come full circle and return to the concluding statement of the *Historical Perspective* in Chapter I (p. 12), the methodological limitations in Haldane's measurement of arterial PO_2 led him to the incorrect conclusion, that the lungs secreted oxygen. Similarly, the methodological limitations of the MIGET, and assumptions regarding the effect of breathing hyperoxia on the pulmonary vasculature, may lead to the incorrect conclusion that right-to-left shunt is not significantly contributing to pulmonary gas exchange efficiency during exercise.

REFERENCES CITED

1. **Abbott OA**, **van Fleit WE**, **Roberto AE**, **Salomone FP**. Studies on the function of the human vagus nerve in various types of intrathoracic disease. *J Thorac Surg* 30: 564–590, 1955.

2. **Abushora MY**, **Bhatia N**, **Alnabki Z**, **Shenoy M**, **Alshaher M**, **Stoddard MF**. Intrapulmonary Shunt Is a Potentially Unrecognized Cause of Ischemic Stroke and Transient Ischemic Attack. *J Am Soc Echocardiogr* 26: 683–690, 2013.

3. **Agostoni P**, **Swenson ER**, **Bussotti M**, **Revera M**, **Meriggi P**, **Faini A**, **Lombardi C**, **Bilo G**, **Giuliano A**, **Bonacina D**, **Modesti PA**, **Mancia G**, **Parati G**, **on behalf of the HIGHCARE Investigators**. High-altitude exposure of three weeks duration increases lung diffusing capacity in humans. *J Appl Physiol* 110: 1564–1571, 2011.

4. **Allemann Y**, **Hutter D**, **Lipp E**, **Sartori C**, **Duplain H**, **Egli M**, **Cook S**, **Scherrer U**, **Seiler C**. Patent foramen ovale and high-altitude pulmonary edema. *JAMA* 296: 2954–2958, 2006.

5. **Asmussen E**, **Nielsen M**. Alveolo-Arterial Gas Exchange at Rest and During Work at Different O2, Tensions. *Acta Physiol Scand* 50: 153–166, 1960.

6. **Aviado DM**, **de Burgh Daly M**, **Lee CY**, **Schmidt CF**. The contribution of the bronchial circulation to the venous admixture in pulmonary venous blood. *J Physiol* 155: 602–622, 1961.

7. **Barcroft SJ**. *Observations Upon the Effect of High Altitude on the Physiological Processes of the Human Body, Carried Out in the Peruvian Andes, Chiefly at Cerro de Pasco*. 1923.

8. **Barker RC**, **Hopkins SR**, **Kellogg N**, **Olfert IM**, **Brutsaert TD**, **Gavin TP**, **Entin PL**, **Rice AJ**, **Wagner PD**. Measurement of cardiac output during exercise by open-circuit acetylene uptake. *J Appl Physiol* 87: 1506–1512, 1999.

9. **Barnes P**, **Liu S**. Regulation of pulmonary vascular tone. *Pharmacological reviews* 47: 87, 1995.

10. **Bartsch P**, **Maggiorini M**, **Ritter M**, **Noti C**, **Vock P**, **Oelz O**. Prevention of high-altitude pulmonary edema by nifedipine. *N Engl J Med* 325: 1284–1289, 1991.

11. **Barzilai B**, **Waggoner AD**, **Spessert C**, **Picus D**, **Goodenberger D**. Two-dimensional contrast echocardiography in the detection and follow-up of congenital pulmonary arteriovenous malformations. *Am J Cardiol* 68: 1507–1510, 1991.

12. **Bates ML**, **Fulmer BR**, **Farrell ET**, **Drezdon A**, **Pegelow DF**, **Conhaim RL**, **Eldridge MW**. Hypoxia recruits intrapulmonary arteriovenous pathways in intact rats but not isolated rat lungs. *J Appl Physiol* 112: 1915–1920, 2012.

13. **Bebout DE**, **Story D**, **Roca J**, **Hogan MC**, **Poole DC**, **Gonzalez-Camarena R**, **Ueno O**, **Haab P**, **Wagner PD**. Effects of altitude acclimatization on pulmonary gas exchange during exercise. *J Appl Physiol* 67: 2286–2295, 1989.

14. **Berggren S**. The oxygen deficit of arterial blood caused by non-ventilating parts of the lung. *Acta Physiol Scand* 4, 1942.

15. **Berk J**, **Hagen J**, **Koo R**, **Beyer W**, **Dochat G**, **Rupright M**, **Nomoto S**. Pulmonary insufficiency caused by epinephrine. *Annals of Surgery* 178: 423, 1973.

16. **Berk J**, **Hagen J**, **Koo R**, **Nomoto S**, **Rupright M**. Pulmonary arteriovenous shunting due to epinephrine. *Horm. Metab. Res.* 5: 65, 1973.

17. **Bert P**. *La pression barométrique*. 1878.

18. **Bhatia N**, **Abushora MY**, **Donneyong MM**, **Stoddard MF**. Determination of the optimum number of cardiac cycles to differentiate intra-pulmonary shunt and patent foramen ovale by saline contrast two- and three-dimensional echocardiography. *Echocardiography* 31: 293–301, 2014.

19. **Bogert LWJ**, **Wesseling KH**, **Schraa O**, **Van Lieshout EJ**, **De Mol BAJM**, **Van Goudoever J**, **Westerhof BE**, **van Lieshout JJ**. Pulse contour cardiac output derived from non-invasive arterial pressure in cardiovascular disease. *Anaesthesia* 65: 1119–1125, 2010.

20. **Bogousslavsky J**, **Garazi S**, **Jeanrenaud X**, **Aebischer N**, **Van Melle G**. Stroke recurrence in patients with patent foramen ovale: the Lausanne Study. Lausanne Stroke with Paradoxal Embolism Study Group. *Neurology* 46: 1301–1305, 1996.

21. **Bohr C**, **Hasselbalch K**, **Krogh A**. Ueber einen in biologischer Beziehung wichtigen Einfluss, den die Kohlensäurespannung des Blutes auf dessen Sauerstoffbindung übt1. *Skandinavisches Archiv für Physiologie* 16: 402–412, 1904.

22. **Bohr C**. Ueber die Lungenathmung. *Skandinavisches Archiv für Physiologie* 2: 236–268, 1891.

23. **Bohr C**. Über die spezifische Tätigkeit der Lungen bei der respiratorischen Gasaufnahme und ihr Verhalten zu der durch die Alveolarwand stattfindenden Gasdiffusion. *Skandinavisches Archiv für Physiologie* 22: 221–280, 1909.

24. **Bryan TL**, **van Diepen S**, **Bhutani M**, **Shanks M**, **Welsh RC**, **Stickland MK**. The effects of dobutamine and dopamine on intrapulmonary shunt and gas exchange in healthy humans. *J Appl Physiol* 113: 541–548, 2012.

25. **Butler BD**, **Hills BA**. The lung as a filter for microbubbles. *J Appl Physiol* 47: 537–543, 1979.

26. **Butler BD**, **Hills BA**. Transpulmonary passage of venous air emboli. *J Appl Physiol* 59: 543–547, 1985.

27. **Cabanes L**, **Coste J**, **Derumeaux G**, **Jeanrenaud X**, **Lamy C**, **Zuber M**, **Mas J-L**. Interobserver and intraobserver variability in detection of patent foramen ovale and atrial septal aneurysm with transesophageal echocardiography. *J Am Soc Echocardiogr* 15: 441–446, 2002.

28. **Calbet JAL**, **Boushel RR**, **Rådegran GG**, **Sondergaard HH**, **Wagner PD**, **Saltin BB**. Why is VO2 max after altitude acclimatization still reduced despite normalization of arterial O2 content? *Am J Physiol Regul Integr Comp Physiol* 284: R304–R316, 2003.

29. **Calbet JAL**, **Lundby C**. Air to muscle O2 delivery during exercise at altitude. *High Alt Med Biol* 10: 123–134, 2009.

30. **Calbet JAL**, **Radegran G**, **Boushel R**, **Sondergaard H**, **Saltin B**, **Wagner PD**. Effect of blood haemoglobin concentration on VO2,max and cardiovascular function in lowlanders acclimatised to 5260 m. *J Physiol* 545: 715–728, 2002.

31. **Calbet JAL**, **Robach P**, **Lundby C**, **Boushel RR**. Is pulmonary gas exchange during exercise in hypoxia impaired with the increase of cardiac output? *Appl Physiol Nutr Metab* 33: 593–600, 2008.

32. **Canfield RE**, **Rahn H**. Arterial-Alveolar N2 Gas Pressure Differences Due to Ventilation-Perfusion Variations. *J Appl Physiol* 10: 165–172, 1957.

33. **Capen RLR**, **Wagner WW**. Intrapulmonary blood flow redistribution during hypoxia increases gas exchange surface area. *J Appl Physiol* 52: 1575–1580, 1982.

34. **Cardús J**, **Burgos F**, **Diaz O**, **Roca J**, **Barbera JA**, **Marrades RM**, **Rodriguez-Roisin R**, **Wagner PD**. Increase in pulmonary ventilation-perfusion inequality with age in healthy individuals. *Am. J. Respir. Crit. Care Med.* 156: 648–653, 1997.

35. **Casey DP**, **Joyner MJ**. Local control of skeletal muscle blood flow during exercise: Influence of available oxygen. *J Appl Physiol* 111: 1527–1538, 2011.

36. **Christie A**. Normal closing time of the foramen ovale and the ductus arteriosus: an anatomic and statistical study. *Archives of Pediatrics & Adolescent Medicine* 40: 323–326, 1930.

37. **Coceani F**, **Kelsey L**, **Seidlitz E**. Occurrence of endothelium-derived relaxing factor--nitric oxide in the lamb ductus arteriosus. *Can. J. Physiol. Pharmacol.* 72: 82–88, 1994.

38. **Coceani F**, **Olley PM**. The response of the ductus arteriosus to prostaglandins. *Can. J. Physiol. Pharmacol.* 51: 220–225, 1973.

39. **Cole R**, **Bishop J**. Effect of varying inspired O2 tension on alveolar-arterial O2 tension difference in man. *J Appl Physiol* 18: 1043, 1963.

40. **Conhaim R**, **Staub N**. Reflection spectrophotometric measurement of O2 uptake in pulmonary arterioles of cats. *J Appl Physiol* 48: 848–856, 1980.

41. **Conkin J**, **Bedahl SR**, **Van Liew HD**. A computerized databank of decompression sickness incidence in altitude chambers. *Aviat Space Environ Med* 63: 819–824, 1992.

42. **Currie PJ**, **Seward JB**, **Chan KL**, **Fyfe DA**, **Hagler DJ**, **Mair DD**, **Reeder GS**, **Nishimura RA**, **Tajik AJ**. Continuous wave Doppler determination of right ventricular pressure: a simultaneous Doppler-catheterization study in 127 patients. *J Am Coll Cardiol* 6: 750–756, 1985.

43. **Dalton J**. On the Constitution of the Atmosphere. *Philosophical Transactions of the Royal Society of London* 116: 174–188, 1826.

44. **Dalton J**. Doctrines of the Circulation. [Online]. *Henry C. Lea's Son & Co.* 1884. https://play.google.com/books/reader?id=3h4IAAAAIAAJ&printsec=frontcover&output=reader&authuser=0&hl=en&pg=GBS.PA18 [8 May. 1884].

45. **Dantzker DR**, **Wagner PD**, **West JB**. Instability of lung units with low VA/Q ratios during O2 breathing. *J Appl Physiol* 38: 886–895, 1975.

46. **de Jong N**, **Cate Ten FJ**, **Lancée CT**, **Roelandt JR**, **Bom N**. Principles and recent developments in ultrasound contrast agents. *Ultrasonics* 29: 324–330, 1991.

47. **Dempsey JA**, **Reddan WG**, **Birnbaum ML**, **Forster HV**, **Thoden JS**, **Grover RF**, **Rankin J**. Effects of acute through life-long hypoxic exposure on exercise pulmonary gas exchange. *Respir Physiol* 13: 62–89, 1971.

48. **Dempsey JA**, **Wagner PD**. Exercise-induced arterial hypoxemia. *J Appl Physiol* 87: 1997–2006, 1999.

49. **Di Tullio M**, **Sacco R**, **Gopal A**, **Mohr J**, **Homma S**. Patent foramen ovale as a risk factor for cryptogenic stroke. *Ann Intern Med* 117: 461, 1992.

50. **Di Tullio M**, **Sacco R**, **Venketasubramanian N**, **Sherman D**, **Mohr J**, **Homma S**. Comparison of diagnostic techniques for the detection of a patent foramen ovale in stroke patients. *Stroke* 24: 1020, 1993.

51. **Douglas CG**, **Haldane JS**, **Henderson Y**, **Schneider EC**, **Webb GB**, **Richards J**. Physiological Observations Made on Pike's Peak, Colorado, with Special Reference to Adaptation to Low Barometric Pressures. *Philosophical Transactions of the Royal Society of London. Series B* 203: 185–318, 1913.

52. **Douglas CG**, **Haldane JS**. Investigations by the carbon monoxide method on the oxygen tension of arterial blood. *Skandinavisches Archiv für Physiologie* 25: 169–182, 1911.

53. **Eldridge MW**, **Dempsey JA**, **Haverkamp HC**, **Lovering AT**, **Hokanson JS**. Exercise-induced intrapulmonary arteriovenous shunting in healthy humans. *J Appl Physiol* 97: 797–805, 2004.

54. **Elliott JE**, **Choi Y**, **Laurie SS**, **Yang X**, **Gladstone IM**, **Lovering AT**. Effect of initial gas bubble composition on detection of inducible intrapulmonary arteriovenous shunt during exercise in normoxia, hypoxia, or hyperoxia. *J Appl Physiol* 110: 35–45, 2011.

55. **Elliott JE**, **Nigam SM**, **Laurie SS**, **Beasley KM**, **Goodman RD**, **Hawn JA**, **Gladstone IM**, **Chesnutt MS**, **Lovering AT**. Prevalence of left heart contrast in healthy, young, asymptomatic humans at rest breathing room air. *Respiratory Physiology & Neurobiology* 188: 71–78, 2013.

56. **Ellsworth ML**, **Ellis CG**, **Goldman D**, **Stephenson AH**, **Dietrich HH**, **Sprague RS**. Erythrocytes: oxygen sensors and modulators of vascular tone. *Physiology (Bethesda)* 24: 107–116, 2009.

57. **Ellsworth ML**, **Sprague RS**. Regulation of blood flow distribution in skeletal muscle: role of erythrocyte-released ATP. *J Physiol* 590: 4985–4991, 2012.

58. **Emmanouilides GC**, **Moss AJ**, **Duffie ER**, **Adams FH**. Pulmonary arterial pressure changes in human newborn infants from birth to 3 days of age. *J Pediatr* 65: 327–333, 1964.

59. **Enghoff H**. Volumen Inefficax. Bemerkungen zur Frage des schadlichen Raumes. *Upsala Laekarefoeren. Foerh.* 44: 191–218, 1938.

60. **Epstein PS**, **Plesset MS**. On the Stability of Gas Bubbles in Liquid-Gas Solutions. *J Chem Phys* 18: 5, 1950.

61. **Escourrou P**, **Johnson DG**, **Rowell LB**. Hypoxemia increases plasma catecholamine concentrations in exercising humans. *J Appl Physiol* 57: 1507–1511, 1984.

62. **Evans JW**, **Wagner PD**. Limits on VA/Q distributions from analysis of experimental inert gas elimination. *J Appl Physiol* 42: 889–898, 1977.

63. **Felici M**, **Filoche M**, **Sapoval B**. Diffusional screening in the human pulmonary acinus. *J Appl Physiol* 94: 2010–2016, 2003.

64. **Fenster BE**, **Curran-Everett D**, **Freeman AM**, **Weinberger HD**, **Kern Buckner J**, **Carroll JD**. Saline Contrast Echocardiography for the Detection of Patent Foramen Ovale in Hypoxia: A Validation Study Using Intracardiac Echocardiography. *Echocardiography* 31: 420–427, 2013.

65. **Forster RE**. Exchange of Gases Between Alveolar Air and Pulmonary Capillary Blood: Pulmonary Diffusing Capacity. *Physiol Rev* 37: 391–452, 1957.

66. **Forwand SA**, **Landowne M**, **Follansbee JN**, **Hansen JE**. Effect of acetazolamide on acute mountain sickness. *N Engl J Med* 279: 839–845, 1968.

67. **Foster GE**, **Ainslie PN**, **Stembridge M**, **Day TA**, **Bakker A**, **Samuel J E Lucas**, **Lewis NCS**, **MacLeod DB**, **Lovering AT**. Resting pulmonary haemodynamics and shunting: a comparison of sea-level inhabitants to high altitude Sherpas. *J Physiol* 592: 1397–1409, 2014.

68. **Freeman JA**, **Woods TD**. Use of saline contrast echo timing to distinguish intracardiac and extracardiac shunts: failure of the 3- to 5-beat rule. *Echocardiography* 25: 1127–1130, 2008.

69. **Gale GE**, **Torre-Bueno JR**, **Moon RE**, **Saltzman HA**, **Wagner PD**. Ventilation-perfusion inequality in normal humans during exercise at sea level and simulated altitude. *J Appl Physiol* 58: 978–988, 1985.

70. **Gan K**, **Nishi I**, **Chin I**, **Slutsky A**. On-line determination of pulmonary blood flow using respiratory inert gas analysis. *Biomedical Engineering, IEEE Transactions on* 40: 1250–1259, 1993.

71. **Gao Y**, **Raj JU**. Regulation of the pulmonary circulation in the fetus and newborn. *Physiol Rev* 90: 1291–1335, 2010.

72. **Genovesi MG**, **Tierney DF**, **Taplin GV**, **Eisenberg H**. An intravenous radionuclide method to evaluate hypoxemia caused by abnormal alveolar vessels. Limitation of conventional techniques. *Am Rev Respir Dis* 114: 59–65, 1976.

73. **Germonpre P**, **Dendale P**, **Unger P**, **Balestra C**. Patent foramen ovale and decompression sickness in sports divers. *J Appl Physiol* 84: 1622–1626, 1998.

74. **Gjedde A**. Diffusive insights: on the disagreement of Christian Bohr and August Krogh at the Centennial of the Seven Little Devils. *Adv Physiol Educ* 34: 174–185, 2010.

75. **Glazier JB**, **Hughes JM**, **Maloney JE**, **West JB**. Measurements of capillary dimensions and blood volume in rapidly frozen lungs. *J Appl Physiol* 26: 65–76, 1969.

76. **Glenny R**. Teaching ventilation/perfusion relationships in the lung. *Advan in Physiol Edu* 32: 192, 2008.

77. **González-Alonso J**. ATP as a mediator of erythrocyte-dependent regulation of skeletal muscle blood flow and oxygen delivery in humans. *J Physiol* 590: 5001–5013, 2012.

78. **Gramiak R**, **Shah PM**, **Kramer DH**. Ultrasound cardiography: contrast studies in anatomy and function. *Radiology* 92: 939–948, 1969.

79. **Gramiak R**, **Shah PM**. Echocardiography of the aortic root. *Invest Radiol* 3: 356–366, 1968.

80. **Groves BM**, **Reeves JT**, **Sutton JR**, **Wagner PD**, **Cymerman A**, **Malconian MK**, **Rock PB**, **Young PM**, **Houston CS**. Operation Everest II: elevated high-altitude pulmonary resistance unresponsive to oxygen. *J Appl Physiol* 63: 521–530, 1987.

81. **Hacievliyagil SS**, **Gunen H**, **Kosar FM**, **Sahin I**, **Kilic T**. Prevalence and clinical significance of a patent foramen ovale in patients with chronic obstructive pulmonary disease. *Respir Med* 100: 903–910, 2006.

82. **Hagen P**, **Scholz D**, **Edwards W**. Incidence and size of patent foramen ovale during the first 10 decades of life: an autopsy study of 965 normal hearts. *Mayo Clinic Proc* 59: 17, 1984.

83. **Haldane J**, **Smith JL**. The Oxygen Tension of Arterial Blood. *J Physiol* 20: 497–520, 1896.

84. **Haldane J**. A Method of Detecting and Estimating Carbonic Oxide in Air. *J Physiol* 18: 463–469, 1895.

85. **Hammond MD**, **Gale GE**, **Kapitan KS**, **Ries A**, **Wagner PD**. Pulmonary gas exchange in humans during exercise at sea level. *J Appl Physiol* 60: 1590–1598, 1986.

86. **Hammond MD**, **Gale GE**, **Kapitan KS**, **Ries A**, **Wagner PD**. Pulmonary gas exchange in humans during normobaric hypoxic exercise. *J Appl Physiol* 61: 1749–1757, 1986.

87. **Hankinson JLJ**, **Odencrantz JRJ**, **Fedan KBK**. Spirometric reference values from a sample of the general U.S. population. *Am. J. Respir. Crit. Care Med.* 159: 179–187, 1999.

88. **Hansen JE**, **Vogel JA**, **Stelter GP**, **Consolazio CF**. Oxygen uptake in man during exhaustive work at sea level and high altitude. *J Appl Physiol* 23: 511–522, 1967.

89. **Harder DR**, **Narayanan J**, **Birks EK**, **Liard JF**, **Imig JD**, **Lombard JH**, **Lange AR**, **Roman RJ**. Identification of a putative microvascular oxygen sensor. *Circ Res* 79: 54–61, 1996.

90. **Hill AV**. The possible effects of the aggregation of the molecules of haemoglobin on its dissociation curves. *J Physiol* 22: 208–210, 1910.

91. **Hills BA**, **Butler BD**. Size distribution of intravascular air emboli produced by decompression. *Undersea Biomed Res* 8: 163–170, 1981.

92. **Himelman R**, **Stulbarg M**, **Kircher B**, **Lee E**, **Kee L**, **Dean N**, **Golden J**, **Wolfe C**, **Schiller N**. Noninvasive evaluation of pulmonary artery pressure during exercise by saline-enhanced Doppler echocardiography in chronic pulmonary disease. *Circulation* 79: 863, 1989.

93. **Hlastala M**, **Lamm W**, **Karp A**, **Polissar N**, **Starr I**, **Glenny R**. Spatial distribution of hypoxic pulmonary vasoconstriction in the supine pig. *J Appl Physiol* 96: 1589, 2004.

94. **Hlastala MP**, **Farhi LE**. Absorption of gas bubbles in flowing blood. *J Appl Physiol* 35: 311–316, 1973.

95. **Hlastala MP**, **Van Liew HD**. Influence of bubble size and blood perfusion on absorption of gas bubbles in tissues. *Respir Physiol* 7: 111–121, 1969.

96. **Hlastala MP**, **Van Liew HD**. Absorption of in vivo inert gas bubbles. *Respir Physiol* 24: 147–158, 1975.

97. **Hlastala MP**. Multiple inert gas elimination technique. *J Appl Physiol* 56: 1–7, 1984.

98. **Homma S**, **Sacco R**. Patent foramen ovale and stroke. *Circulation* 112: 1063, 2005.

99. **Homma S**, **Sacco RL**, **Di Tullio MR**, **Sciacca RR**, **Mohr JP**, **Mohr JP**. Effect of medical treatment in stroke patients with patent foramen ovale: patent foramen ovale in Cryptogenic Stroke Study. *Circulation* 105: 2625–2631, 2002.

100. **Hopkins SR**, **Belzberg AS**, **Wiggs BR**, **McKenzie DC**. Pulmonary transit time and diffusion limitation during heavy exercise in athletes. *Respir Physiol* 103: 67–73, 1996.

101. **Hopkins SR**, **Gavin TP**, **Siafakas NM**, **Haseler LJ**, **Olfert IM**, **Wagner H**, **Wagner PD**. Effect of prolonged, heavy exercise on pulmonary gas exchange in athletes. *J Appl Physiol* 85: 1523–1532, 1998.

102. **Hopkins SR**, **McKenzie DC**, **Schoene RB**, **Glenny RW**, **Robertson HT**. Pulmonary gas exchange during exercise in athletes. I. Ventilation-perfusion mismatch and diffusion limitation. *J Appl Physiol* 77: 912–917, 1994.

103. **Hopkins SR**, **Olfert IM**, **Wagner PD**. Point:Counterpoint: Exercise-induced intrapulmonary shunting is imaginary vs. real. *J Appl Physiol* 107: 993–994, 2009.

104. **Hsia CC**, **Herazo LF**, **Ramanathan M**, **Claassen H**, **Fryder-Doffey F**, **Hoppeler H**, **Johnson RL**. Cardiopulmonary adaptations to pneumonectomy in dogs. III. Ventilatory power requirements and muscle structure. *J Appl Physiol* 76: 2191–2198, 1994.

105. **Hsia CC**, **Herazo LF**, **Ramanathan M**, **Johnson RL**, **Wagner PD**. Cardiopulmonary adaptations to pneumonectomy in dogs. II. VA/Q relationships and microvascular recruitment. *J Appl Physiol* 74: 1299–1309, 1993.

106. **Hsia CC**, **Herazo LF**, **Ramanathan M**, **Johnson RL**. Cardiopulmonary adaptations to pneumonectomy in dogs. IV. Membrane diffusing capacity and capillary blood volume. *J Appl Physiol* 77: 998–1005, 1994.

107. **Imray CH**, **Pattinson KT**, **Myers S**, **Chan CW**, **Hoar H**, **Brearey S**, **Collins P**, **Wright AD**. Intrapulmonary and Intracardiac Shunting With Exercise at Altitude. *Wilderness & Environmental Medicine* 19: 199–204, 2008.

108. **Jameson A**. Diffusion of gases from alveolus to precapillary arteries. *Science* 139: 826–828, 1963.

109. **Jameson A**. Gaseous diffusion from alveoli into pulmonary arteries. *J Appl Physiol* 19: 448–456, 1964.

110. **Johnson BD**, **Beck KC**, **Proctor DN**, **Miller J**, **Dietz NM**, **Joyner MJ**. Cardiac output during exercise by the open circuit acetylene washin method: comparison with direct Fick. *J Appl Physiol* 88: 1650–1658, 2000.

111. **Jones R**, **Meade F**. A theoretical and experimental analysis of anomalies in the estimation of pulmonary diffusing capacity by the single breath method. *Exp Physiol* 46: 131–143, 1961.

112. **Jonk AM**, **van den Berg IP**, **Olfert IM**, **Wray DW**, **Arai T**, **Hopkins SR**, **Wagner PD**. Effect of acetazolamide on pulmonary and muscle gas exchange during normoxic and hypoxic exercise. *J Physiol* 579: 909–921, 2007.

113. **Kelman G**, **Nunn J**. Nomograms for correction of blood Po2, Pco2, pH and base excess for time and temperature. *J Appl Physiol* 21: 1484–1490, 1966.

114. **Kelman G**. Digital computer subroutine for the conversion of oxygen tension into saturation. *J Appl Physiol* 21: 1375–1376, 1966.

115. **Kennedy JM**, **Foster GE**, **Koehle MS**, **Potts JE**, **Sandor GGS**, **Potts MT**, **Houghton KM**, **Henderson WR**, **Sheel AW**. Exercise-induced intrapulmonary arteriovenous shunt in healthy women. *Respiratory Physiology & Neurobiology* 181: 8–13, 2012.

116. **Kerut EK**, **Norfleet WT**, **Plotnick GD**, **Giles TD**. Patent foramen ovale: a review of associated conditions and the impact of physiological size. *J Am Coll Cardiol* 38: 613–623, 2001.

117. **Kircher BJ**, **Himelman RB**, **Schiller NB**. Noninvasive estimation of right atrial pressure from the inspiratory collapse of the inferior vena cava. *Am J Cardiol* 66: 493–496, 1990.

118. **Kizer J**, **Devereux R**. Patent foramen ovale in young adults with unexplained stroke. *N Engl J Med* 353, 2005.

119. **Knudson RJ**, **Kaltenborn WT**, **Knudson DE**, **Burrows B**. The single-breath carbon monoxide diffusing capacity. Reference equations derived from a healthy nonsmoking population and effects of hematocrit. *Am Rev Respir Dis* 135: 805–811, 1987.

120. **Kovacs G**, **Olschewski A**, **Berghold A**, **Olschewski H**. Pulmonary vascular resistances during exercise in normal subjects: a systematic review. *Eur Respir J* 39: 319–328, 2012.

121. **Krogh A**, **Krogh M**. On the Tensions of Gases in the Arterial Blood. *Skandinavisches Archiv für Physiologie* 23: 179–192, 1910.

122. **Krogh A**, **Krogh M**. On the Rate of Diffusion of Carbonic Oxide into the Lungs of Man. *Skandinavisches Archiv für Physiologie* 23: 236–247, 1910.

123. **Krogh A**. On the Oxygen-Metabolism of the Blood. *Skandinavisches Archiv für Physiologie* 23: 193–199, 1910.

124. **Krogh A**. On the Mechanism of the Gas-Exchange in the Lungs of the Tortoise. *Skandinavisches Archiv für Physiologie* 23: 200–216, 1910.

125. **Krogh A**. On the Combination of Hæmoglobin with mixtures of Oxygen and Carbonic Oxide. *Skandinavisches Archiv für Physiologie* 23: 217–223, 1910.

126. **Krogh A**. Some Experiments on the Invasion of Oxygen and Carbonic Oxide into Water. *Skandinavisches Archiv für Physiologie* 23: 224–235, 1910.

127. **Krogh A**. On the Mechanism of the Gas-Exchange in the Lungs. *Skandinavisches Archiv für Physiologie* 23: 248–278, 1910.

128. **Krogh M**. The diffusion of gases through the lungs of man. *J Physiol* 49: 271–300, 1915.

129. **Kunert M**, **Roman R**, **Alonso-Galicia M**, **Falck J**, **Lombard J**. Cytochrome P-450 ω-hydroxylase: a potential O2 sensor in rat arterioles and skeletal muscle cells. *Am J Physiol Heart Circ Physiol* 280: H1840, 2001.

130. **La Gerche A**, **MacIsaac A**, **Burns A**, **Mooney D**, **Inder W**, **Voigt J**, **Heidbüchel H**, **Prior D**. Pulmonary transit of agitated contrast is associated with enhanced pulmonary vascular reserve and right ventricular function during exercise. *J Appl Physiol* 109: 1307, 2010.

131. **Lalande S**, **Yerly P**, **Faoro V**, **Naeije R**. Pulmonary vascular distensibility predicts aerobic capacity in healthy individuals. *J Physiol* 590: 4279–4288, 2012.

132. **Lamy C**. Clinical and Imaging Findings in Cryptogenic Stroke Patients With and Without Patent Foramen Ovale: The PFO-ASA Study. *Stroke* 33: 706–711, 2002.

133. **Laurie SS**, **Elliott JE**, **Goodman RD**, **Lovering AT**. Catecholamine-induced opening of intrapulmonary arteriovenous anastomoses in healthy humans at rest. *J Appl Physiol* 113: 1213–1222, 2012.

134. **Laurie SS**, **Yang X**, **Elliott JE**, **Beasley KM**, **Lovering AT**. Hypoxia-induced intrapulmonary arteriovenous shunting at rest in healthy humans. *J Appl Physiol* 109: 1072, 2010.

135. **Lechat P**, **Mas JL**, **Lascault G**, **Loron PH**, **Theard M**, **Klimczac M**, **Drobinski G**, **Thomas D**, **Grosgogeat Y**. Prevalence of Patent Foramen Ovale in Patients with Stroke. *N Engl J Med* 318: 1148–1152, 1988.

136. **Light RB**, **Ali J**, **Breen P**, **Wood LD**. The pulmonary vascular effects of dopamine, dobutamine, and isoproterenol in unilobar pulmonary edema in dogs. *J. Surg. Res.* 44: 26–35, 1988.

137. **Lilienthal JL**, **Riley RL**. An experimental analysis in man of the oxygen pressure gradient from alveolar air to arterial blood during rest and exercise at sea level and at altitude. *Am J Physiol* 147: 199–216, 1946.

138. **Loeppky JA**, **Caprihan A**, **Altobelli SA**, **Icenogle MV**, **Scotto P**, **Vidal Melo MF**. Validation of a two-compartment model of ventilation/perfusion distribution. *Respiratory Physiology & Neurobiology* 151: 74–92, 2006.

139. **Lovering AT**, **Goodman RD**. Detection of Intracardiac and Intrapulmonary Shunts at Rest and During Exercise Using Saline Contrast Echocardiography. *Applied Aspects of Ultrasonography in Humans*.

140. **Lovering AT**, **Haverkamp HC**, **Eldridge MW**. Responses and Limitations of the Respiratory System to Exercise. *Clin. Chest Med.* 26: 439–457, 2005.

141. **Lovering AT**, **Haverkamp HC**, **Romer LM**, **Hokanson JS**, **Eldridge MW**. Transpulmonary passage of 99mTc macroaggregated albumin in healthy humans at rest and during maximal exercise. *J Appl Physiol* 106: 1986–1992, 2009.

142. **Lovering AT**, **Laurie SS**, **Elliott JE**, **Beasley KM**, **Yang X**, **Gust CE**, **Mangum TS**, **Goodman RD**, **Hawn JA**, **Gladstone IM**. Normal pulmonary gas exchange efficiency and absence of exercise-induced arterial hypoxemia in adults with bronchopulmonary dysplasia. *J Appl Physiol* 115: 1050–1056, 2013.

143. **Lovering AT**, **Romer LM**, **Haverkamp HC**, **Pegelow DF**, **Hokanson JS**, **Eldridge MW**. Intrapulmonary shunting and pulmonary gas exchange during normoxic and hypoxic exercise in healthy humans. *J Appl Physiol* 104: 1418–1425, 2008.

144. **Lovering AT**, **Stickland MK**, **Amann M**, **Murphy JC**, **O'Brien MJ**, **Hokanson JS**, **Eldridge MW**. Hyperoxia prevents exercise-induced intrapulmonary arteriovenous shunt in healthy humans. *J Physiol* 586: 4559–4565, 2008.

145. **Lovering AT**, **Stickland MK**, **Amann M**, **O'Brien MJ**, **Hokanson JS**, **Eldridge MW**. Effect of a patent foramen ovale on pulmonary gas exchange efficiency at rest and during exercise. *J Appl Physiol* 110: 1354–1361, 2011.

146. **Lovering AT**, **Stickland MK**, **Kelso AJ**, **Eldridge MW**. Direct demonstration of 25- and 50-μm arteriovenous pathways in healthy human and baboon lungs. *Am J Physiol Heart Circ Physiol* 292: H1777–81, 2007.

147. **Lozo M**, **Lojpur M**, **Madden D**, **Lozo P**, **Banic I**, **Dujic Z**. The effects of nitroglycerin, norepinephrine and aminophylline on intrapulmonary arteriovenous anastomoses in healthy humans at rest. *Respiratory Physiology & Neurobiology* (2014). doi: 10.1016/j.resp.2014.04.007.

148. **Luft UC**, **Loeppky JA**, **Mostyn EM**. Mean alveolar gases and alveolar-arterial gradients in pulmonary patients. *J Appl Physiol* 46: 534–540, 1979.

149. **Lumb A**. *Nunns Applied Respiratory Physiology, 6th Edition*. Elsevier, 2005.

150. **Lundby C**, **Calbet JAL**, **van Hall G**, **Saltin B**, **Sander M**. Pulmonary gas exchange at maximal exercise in Danish lowlanders during 8 wk of acclimatization to 4,100 m and in high-altitude Aymara natives. *Am J Physiol Regul Integr Comp Physiol* 287: R1202–8, 2004.

151. **Lynch JP**, **Mhyre JG**, **Dantzker DR**. Influence of cardiac output on intrapulmonary shunt. *J Appl Physiol* 46: 315–321, 1979.

152. **Macintyre N**, **Crapo R**, **Viegi G**, **Johnson D**, **Van der Grinten C**, **Brusasco V**, **Burgos F**, **Casaburi R**, **Coates A**, **Enright P**. Standardisation of the single-breath determination of carbon monoxide uptake in the lung. *Eur Respir J* 26: 720, 2005.

153. **Mak S**, **Egri Z**, **Tanna G**, **Colman R**, **Newton G**. Vitamin C prevents hyperoxia-mediated vasoconstriction and impairment of endothelium-dependent vasodilation. *Am J Physiol Heart Circ Physiol* 282: H2414, 2002.

154. **Manier G**, **Castaing Y**. Influence of cardiac output on oxygen exchange in acute pulmonary embolism. *Am Rev Respir Dis* 145: 130–136, 1992.

155. **Maren TH**. Carbonic anhydrase: chemistry, physiology, and inhibition. *Physiol Rev* 47: 595–781, 1967.

156. **Marriott K**, **Manins V**, **Forshaw A**, **Wright J**, **Pascoe R**. Detection of Right-to-Left Atrial Communication Using Agitated Saline Contrast Imaging: Experience with 1162 Patients and Recommendations for Echocardiography. *J Am Soc Echocardiogr* 26: 96–102, 2013.

157. **Mas J-L**, **Arquizan C**, **Lamy C**, **Zuber M**, **Cabanes L**, **Derumeaux G**, **Coste J**. Recurrent cerebrovascular events associated with patent foramen ovale, atrial septal aneurysm, or both. *N Engl J Med* 345: 1740–1746, 2001.

158. **McMullan DM**, **Hanley FL**, **Cohen GA**, **Portman MA**, **Riemer RK**. Pulmonary arteriovenous shunting in the normal fetal lung. *J Am Coll Cardiol* 44: 1497–1500, 2004.

159. **Meerbaum S**. *Principles of echo contrast. In Advances in Echo Imaging Using Contrast Enhancement.* Kluwer Academic, 1993.

160. **Meier B**, **Kalesan B**, **Mattle HP**, **Khattab AA**, **Hildick-Smith D**, **Dudek D**, **Andersen G**, **Ibrahim R**, **Schuler G**, **Walton AS**, **Wahl A**, **Windecker S**, **Jüni P**, **Jüni P**. Percutaneous closure of patent foramen ovale in cryptogenic embolism. *N Engl J Med* 368: 1083–1091, 2013.

161. **Mekjavic IB**, **Rempel ME**. Determination of esophageal probe insertion length based on standing and sitting height. *J Appl Physiol* 69: 376–379, 1990.

162. **Melsom MN**, **Flatebø T**, **Nicolaysen G**. Hypoxia and hyperoxia both transiently affect distribution of pulmonary perfusion but not ventilation in awake sheep. *Acta Physiol Scand* 166: 151–158, 1999.

163. **Meltzer RS**, **Sartorius OE**, **Lancée CT**, **Serruys PW**, **Verdouw PD**, **Essed CE**, **Roelandt J**. Transmission of ultrasonic contrast through the lungs. *Ultrasound in Med & Biol* 7: 377–384, 1981.

164. **Meltzer RS**, **Tickner EG**, **Popp RL**. Why do the lungs clear ultrasonic contrast? *Ultrasound in Med & Biol* 6: 263–269, 1980.

165. **Messé SR**, **Silverman IE**, **Kizer JR**, **Homma S**, **Zahn C**, **Gronseth G**, **Kasner SE**, **Kasner SE**. Practice parameter: recurrent stroke with patent foramen ovale and atrial septal aneurysm: report of the Quality Standards Subcommittee of the American Academy of Neurology. *Neurology* 62: 1042–1050, 2004.

166. **Miller MR**, **Hankinson J**, **Brusasco V**, **Burgos F**, **Casaburi R**, **Coates A**, **Crapo R**, **Enright P**, **van der Grinten CPM**, **Gustafsson P**, **Jensen R**, **Johnson DC**, **Macintyre N**, **McKay R**, **Navajas D**, **Pedersen OF**, **Pellegrino R**, **Viegi G**, **Wanger J**. Standardisation of spirometry. *Eur Respir J* 26: 319–338, 2005.

167. **Miyata N**, **Roman R**. Role of 20-hydroxyeicosatetraenoic acid (20-HETE) in vascular system. *Journal of Smooth Muscle Research* 41: 175–193, 2005.

168. **Moon R**, **Camporesi E**, **Kisslo J**. Patent foramen ovale and decompression sickness in divers. *Lancet* 333: 513–514, 1989.

169. **Morse M**, **Cassels DE**, **Holder M**, **Numajiri F**, **O'Connell E**. The position of the oxygen dissociation curve of the blood in cyanotic congenital heart disease. *Journal of Clinical Investigation* 29: 1098, 1950.

170. **Muthalif M**, **Benter I**, **Karzoun N**, **Fatima S**, **Harper J**, **Uddin M**, **Malik K**. 20-Hydroxyeicosatetraenoic acid mediates calcium/calmodulin-dependent protein kinase II-induced mitogen-activated protein kinase activation in vascular smooth muscle cells. *Proc Natl Acad Sci USA* 95: 12701, 1998.

171. **Niden A**, **Aviado D**. Effects of pulmonary embolism on the pulmonary circulation with special reference to arteriovenous shunts in the lung. *Circ Res* 4: 67–73, 1956.

172. **Nomoto S**, **Berk J**, **Hagen J**, **Koo R**. Pulmonary anatomic arteriovenous shunting caused by epinephrine. *Archives of Surgery* 108: 201, 1974.

173. **Norris HC**, **Mangum TS**, **Duke JW**, **Straley TB**, **Hawn JA**, **Goodman RD**, **Lovering AT**. Exercise- and hypoxia-induced blood flow through intrapulmonary arteriovenous anastomoses is reduced in older adults. *J Appl Physiol*. 2014.

174. **Oelz O**, **Ritter M**, **Jenni R**, **Maggiorini M**, **Waber U**, **Vock P**, **Bärtsch P**. Nifedipine for high altitude pulmonary oedema. *Lancet* 334: 1241–1244, 1989.

175. **Olfert IM**, **Balouch J**, **Kleinsasser A**, **Knapp A**, **Wagner H**, **Wagner PD**, **Hopkins SR**. Does gender affect human pulmonary gas exchange during exercise? *J Physiol* 557: 529–541, 2004.

176. **Olszowka AJ**. Can VA/Q distributions in the lung be recovered from inert gas retention data? *Respir Physiol* 25: 191–198, 1975.

177. **Ostrowski AM**. *Solutions of equations and systems of equations.* New York and London, 1970.

178. **Ozcan Ozdemir A**, **Tamayo A**, **Munoz C**, **Dias B**, **David Spence J**. Cryptogenic stroke and patent foramen ovale: clinical clues to paradoxical embolism. *Journal of the Neurological Sciences* 275: 121–127, 2008.

179. **Parker B**, **Andresen D**, **Smith J**. Observations on Arteriovenous Communications in Lungs of Dogs. *Experimental Biology and Medicine* 98: 306, 1958.

180. **Patten BM**. The closure of the foramen ovale. *American Journal of Anatomy* 48: 19–44, 1931.

181. **Patten BM**. Developmental defects at the foramen ovale. *Am J Pathol* 14: 135, 1938.

182. **Piiper J**, **Scheid P**. Respiration: alveolar gas exchange. *Annu Rev Physiol* 33: 131–154, 1971.

183. **Piiper J**, **Scheid P**. Model for capillary-alveolar equilibration with special reference to O2 uptake in hypoxia. *Respir Physiol* 46: 193–208, 1981.

184. **Piiper J**, **Scheid P**. Comparison of diffusion and perfusion limitations in alveolar gas exchange. *Respir Physiol* 51: 287–290, 1983.

185. **Podolsky A**, **Eldridge MW**, **Richardson RS**, **Knight DR**, **Johnson EC**, **Hopkins SR**, **Johnson DH**, **Michimata H**, **Grassi B**, **Feiner J**, **Kurdak SS**, **Bickler PE**, **Severinghaus JW**, **Wagner PD**. Exercise-induced V_A/Q inequality in subjects with prior high-altitude pulmonary edema. *J Appl Physiol* 81: 922–932, 1996.

186. **Prinzmetal M**, **Ornitz E**. Arterio-venous anastomoses in liver, spleen, and lungs. *Am J Physiol* 152: 48–52, 1947.

187. **Rahn H**, **Fenn W**. *A graphical analysis of the respiratory exchange: The O_2 CO_2 diagram.* Washington DC: Am Physiol Soc, 1955.

188. **Rahn H**, **Stroud RC**, **Tobin CE**. Visualization of arterio-venous shunts by cinefluorography in the lungs of normal dogs. *Experimental Biology and Medicine* 80: 239, 1952.

189. **Raisinghani A**, **DeMaria AN**. Physical principles of microbubble ultrasound contrast agents. *Am J Cardiol* 90: 3J–7J, 2002.

190. **Ranoux D**, **Cohen A**, **Cabanes L**, **Amarenco P**, **Bousser M**, **Mas J**. Patent foramen ovale: is stroke due to paradoxical embolism? *Stroke* 24: 31, 1993.

191. **Rasanen J**, **Wood DC**, **Weiner S**, **Ludomirski A**, **Huhta JC**. Role of the Pulmonary Circulation in the Distribution of Human Fetal Cardiac Output During the Second Half of Pregnancy. *Circulation* 94: 1068–1073, 1996.

192. **Ravin M**, **Epstein R**, **Malm J**. Contribution of thebesian veins to the physiologic shunt in anesthetized man. *J Appl Physiol* 20: 1148, 1965.

193. **Reeves J**, **Dempsey J**, **Grover R**. Pulmonary circularion during exercise. *Lung biology in health and disease* 38: 107–133, 1989.

194. **Rennotte MT**, **Reynaert M**, **Clerbaux T**, **Willems E**, **Roeseleer J**, **Veriter C**, **Rodenstein D**, **Frans A**. Effects of two inotropic drugs, dopamine and dobutamine, on pulmonary gas exchange in artificially ventilated patients. *Intensive Care Med* 15: 160–165, 1989.

195. **Rice AJ**, **Thornton AT**, **Gore CJ**, **Scroop GC**, **Greville HW**, **Wagner H**, **Wagner PD**, **Hopkins SR**. Pulmonary gas exchange during exercise in highly trained cyclists with arterial hypoxemia. *J Appl Physiol* 87: 1802–1812, 1999.

196. **Riley R**, **Cournand A**. Ideal alveolar air and the analysis of ventilation-perfusion relationships in the lungs. *J Appl Physiol* 1: 825–847, 1949.

197. **Robin E**, **Laman P**, **Goris M**, **Theodore J**. A shunt is (not) a shunt is (not) a shunt. *Am Rev Respir Dis* 115: 553, 1977.

198. **Roelandt J**. Contrast echocardiography. *Ultrasound in Med & Biol* 8: 471–492, 1982.

199. **Rosenzweig DY**, **Hughes JM**, **Glazier JB**. Effects of transpulmonary and vascular pressures on pulmonary blood volume in isolated lung. *J Appl Physiol* 28: 553–560, 1970.

200. **Roughton FJ**, **Forster RE**. Relative importance of diffusion and chemical reaction rates in determining rate of exchange of gases in the human lung, with special reference to true diffusing capacity of pulmonary membrane and volume of blood in the lung capillaries. *J Appl Physiol* 11: 290–302, 1957.

201. **Rubanyi G**, **Vanhoutte P**. Superoxide anions and hyperoxia inactivate endothelium-derived relaxing factor. *Am J Physiol Heart Circ Physiol* 250: H822, 1986.

202. **Rudski LG**, **FASE WWL**, **Afilalo J**, **Hua L**, **Handschumacher MD**, **Chandrasekaran K**, **Solomon SD**, **Louie EK**, **Schiller NB**. Guidelines for the Echocardiographic Assessment of the Right Heart in Adults: A Report from the American Society of Echocardiography. *J Am Soc Echocardiogr* 23: 685–713, 2010.

203. **Saltin B**, **Grover RF**, **Blomqvist CG**, **Hartley LH**, **Johnson RL**. Maximal oxygen uptake and cardiac output after 2 weeks at 4,300 m. *J Appl Physiol* 25: 400–409, 1968.

204. **Sapoval B**, **Filoche M**, **Weibel ER**. Smaller is better--but not too small: A physical scale for the design of the mammalian pulmonary acinus. *Proc Natl Acad Sci USA* 99: 10411–10416, 2002.

205. **Severinghaus J**. Blood gas calculator. *J Appl Physiol* 21: 1108–1116, 1966.

206. **Shimoda LA**, **Luke T**, **Sylvester JT**, **Shih HW**, **Jain A**, **Swenson ER**. Inhibition of hypoxia-induced calcium responses in pulmonary arterial smooth muscle by acetazolamide is independent of carbonic anhydrase inhibition. *Am J Physiol Lung Cell Mol Physiol* 292: L1002–L1012, 2006.

207. **Simonneau G**, **Escourrou P**, **Duroux P**, **Lockhart A**. Inhibition of hypoxic pulmonary vasoconstriction by nifedipine. *N Engl J Med* 304: 1582–1585, 1981.

208. **Sirsi M**, **Bucher K**. Studies on arteriovenous anastomoses in the lungs. *Experientia* 9: 217–218, 1953.

209. **Sobol B**, **Bottex G**, **Emirgil C**, **Gissen H**. Gaseous diffusion from alveoli to pulmonary vessels of considerable size. *Circ Res* 13: 71–79, 1963.

210. **Soliman A**, **Shanoudy H**, **Liu J**, **Russell DC**, **Jarmukli NF**. Increased prevalence of patent foramen ovale in patients with severe chronic obstructive pulmonary disease. *J Am Soc Echocardiogr* 12: 99–105, 1999.

211. **Spies C**, **Wong M**. Patent foramen ovale and cryptogenic stroke: a complex neuro-cardio-vascular problem. *Expert Rev Cardiovasc Ther* 7: 1455–1467, 2009.

212. **Staub NC**, **Bishop JM**, **Forster RE**. Velocity of O_2 uptake by human red blood cells. *J Appl Physiol* 16: 511–516, 1961.

213. **Staub NC**, **Bishop JM**, **Forster RE**. Importance of diffusion and chemical reaction rates in O2 uptake in the lung. *J Appl Physiol* 17: 21–27, 1962.

214. **Stickland MK**, **Lindinger MI**, **Heigenhauser GJF**, **Hopkins SR**. Pulmonary Gas Exchange and Acid-Base Balance During Exercise. John Wiley & Sons, Inc. Hoboken, NJ, USA: John Wiley & Sons, Inc, 2013.

215. **Stickland MK**, **Lovering AT**, **Eldridge MW**. Exercise-induced arteriovenous intrapulmonary shunting in dogs. *Am J Respir Crit Care Med* 176: 300–305, 2007.

216. **Stickland MK**, **Welsh RC**, **Haykowsky MJ**, **Petersen SR**, **Anderson WD**, **Taylor DA**, **Bouffard M**, **Jones RL**. Intra-pulmonary shunt and pulmonary gas exchange during exercise in humans. *J Physiol* 561: 321–329, 2004.

217. **Stout RL**, **Wessel HU**, **Paul MH**. Pulmonary blood flow determined by continuous analysis of pulmonary N_2O exchange. *J Appl Physiol* 38: 913–918, 1975.

218. **Subudhi AW**, **Bourdillon N**, **Bucher J**, **Davis C**, **Elliott JE**, **Eutermoster M**, **Evero O**, **Fan J-L**, **Houten SJ-V**, **Julian CG**, **Kark J**, **Kark S**, **Kayser B**, **Kern JP**, **Kim SE**, **Lathan C**, **Laurie SS**, **Lovering AT**, **Paterson R**, **Polaner DM**, **Ryan BJ**, **Spira JL**, **Tsao JW**, **Wachsmuth NB**, **Roach RC**. AltitudeOmics: The Integrative Physiology of Human Acclimatization to Hypobaric Hypoxia and Its Retention upon Reascent. *PLoS ONE* 9: e92191, 2014.

219. **Sugawara J**, **Tanabe T**, **Miyachi M**, **Yamamoto K**, **Takahashi K**, **Iemitsu M**, **Otsuki T**, **Homma S**, **Maeda S**, **Ajisaka R**, **Matsuda M**. Non-invasive assessment of cardiac output during exercise in healthy young humans: comparison between Modelflow method and Doppler echocardiography method. *Acta Physiol Scand* 179: 361–366, 2003.

220. **Swenson ER**, **Robertson HT**, **Polissar NL**, **Middaugh ME**, **Hlastala MP**. Conducting airway gas exchange: diffusion-related differences in inert gas elimination. *J Appl Physiol* 72: 1581–1588, 1992.

221. **Swenson ER**. Carbonic anhydrase inhibitors and ventilation: a complex interplay of stimulation and suppression. *Eur Respir J* 12: 1242–1247, 1998.

222. **Swenson ER**. Carbonic anhydrase inhibitors and hypoxic pulmonary vasoconstriction. *Respiratory Physiology & Neurobiology* 151: 209–216, 2006.

223. **Teplick R**, **Snider MT**, **Gilbert JP**. A comparison of continuous and discrete foreign gas VA/Q distributions. *J Appl Physiol* 49: 684–692, 1980.

224. **Teppema LJ**, **Balanos GM**, **Steinback CD**, **Brown AD**, **Foster GE**, **Duff HJ**, **Leigh R**, **Poulin MJ**. Effects of acetazolamide on ventilatory, cerebrovascular, and pulmonary vascular responses to hypoxia. *Am. J. Respir. Crit. Care Med.* 175: 277–281, 2007.

225. **Tobin CE**, **Zariquiey MO**. Arteriovenous shunts in the human lung. *Proc Soc Exp Biol Med* 75: 827–829, 1950.

226. **Tobin CE**, **Zariquiey MO**. Some observations on the blood supply of the human lung. *Medical radiography and photography* 29: 9–18, 1953.

227. **Tobin CE**. The bronchial arteries and their connections with other vessels in the human lung. *Surg Gynecol Obstet* 95: 741–750, 1952.

228. **Tobin CE**. Arteriovenous shunts in the peropheral pulmonary circulation in the human lung. *Thorax* 21: 197–204, 1966.

229. **Torre-Bueno JR**, **Wagner PD**, **Saltzman HA**, **Gale GE**, **Moon RE**. Diffusion limitation in normal humans during exercise at sea level and simulated altitude. *J Appl Physiol* 58: 989–995, 1985.

230. **Tristani-Firouzi M**, **Reeve HL**, **Tolarova S**, **Weir EK**, **Archer SL**. Oxygen-induced constriction of rabbit ductus arteriosus occurs via inhibition of a 4-aminopyridine-, voltage-sensitive potassium channel. *J Clin Invest* 98: 1959–1965, 1996.

231. **Tsujino T**, **Shima A**. The behaviour of gas bubbles in blood subjected to an oscillating pressure. *J Biomech* 13: 407–416, 1980.

232. **Vidal Melo MF**, **Loeppky JA**, **Caprihan A**, **Luft UC**. Alveolar ventilation to perfusion heterogeneity and diffusion impairment in a mathematical model of gas exchange. *Comput. Biomed. Res.* 26: 103–120, 1993.

233. **Vogiatzis I**, **Zakynthinos S**, **Boushel R**, **Athanasopoulos D**, **Guenette JA**, **Wagner H**, **Roussos C**, **Wagner PD**. The contribution of intrapulmonary shunts to the alveolar-to-arterial oxygen difference during exercise is very small. *J Physiol* 586: 2381–2391, 2008.

234. **Wagner PD**, **Araoz MM**, **Boushel RR**, **Calbet JAL**, **Jessen BB**, **Rådegran GG**, **Spielvogel HH**, **Søndegaard HH**, **Wagner HH**, **Saltin BB**. Pulmonary gas exchange and acid-base state at 5,260 m in high-altitude Bolivians and acclimatized lowlanders. *J Appl Physiol* 92: 1393–1400, 2002.

235. **Wagner PD**, **Gale GE**, **Moon RE**, **Torre-Bueno JR**, **Stolp BW**, **Saltzman HA**. Pulmonary gas exchange in humans exercising at sea level and simulated altitude. *J Appl Physiol* 61: 260–270, 1986.

236. **Wagner PD**, **Laravuso RB**, **Uhl RR**, **West JB**. Continuous distributions of ventilation-perfusion ratios in normal subjects breathing air and 100 per cent O2. *J Clin Invest* 54: 54–68, 1974.

237. **Wagner PD**, **Naumann PF**, **Laravuso RB**. Simultaneous measurement of eight foreign gases in blood by gas chromatography. *J Appl Physiol* 36: 600–605, 1974.

238. **Wagner PD**, **Saltzman HA**, **West J**. Measurement of continuous distributions of ventilation-perfusion ratios: theory. *J Appl Physiol* 36: 588–599, 1974.

239. **Wagner PD**, **Sutton JR**, **Reeves JT**, **Cymerman A**, **Groves BM**, **Malconian MK**. Operation Everest II: pulmonary gas exchange during a simulated ascent of Mt. Everest. *J Appl Physiol* 63: 2348–2359, 1987.

240. **Wagner PD**, **West JB**. Effects of diffusion impairment on O 2 and CO 2 time courses in pulmonary capillaries. *J Appl Physiol* 33: 62–71, 1972.

241. **Wagner PD**. A general approach to the evaluation of ventilation-perfusion ratios in normal and abnormal lungs. *Physiologist* 20: 18–25, 1977.

242. **Wagner PD**. Diffusion and chemical reaction in pulmonary gas exchange. *Physiol Rev* 57: 257–312, 1977.

243. **Wagner PD**. Influence of mixed venous PO_2 on diffusion of O_2 across the pulmonary blood: gas barrier. *Clinical Physiology* 2: 105–115, 1982.

244. **Wagner PD**. The lungs during exercise. *Physiology (Bethesda)* 2: 6–10, 1987.

245. **Wagner PD**. Impairment of gas exchange in liver cirrhosis. *Eur Respir J* 8: 1993–1995, 1995.

246. **Wagner PD**. The multiple inert gas elimination technique (MIGET). *Intensive Care Med* 34: 994–1001, 2008.

247. **Wanger J**, **Clausen JL**, **Coates A**, **Pedersen OF**, **Brusasco V**, **Burgos F**, **Casaburi R**, **Crapo R**, **Enright P**, **van der Grinten CPM**, **Gustafsson P**, **Hankinson J**, **Jensen R**, **Johnson D**, **Macintyre N**, **McKay R**, **Miller MR**, **Navajas D**, **Pellegrino R**, **Viegi G**. Standardisation of the measurement of lung volumes. *Eur Respir J* 26: 511–522, 2005.

248. **Webster MW**, **Chancellor AM**, **Smith HJ**, **Swift DL**, **Sharpe DN**, **Bass NM**, **Glasgow GL**. Patent foramen ovale in young stroke patients. *Lancet* 2: 11–12, 1988.

249. **Weibel ER**. Morphological basis of alveolar-capillary gas exchange. *Physiol Rev* 53: 419–495, 1973.

250. **Weil JV**. Ventilatory control at high altitude. *Compr Physiol*. 1986.

251. **Weir E**, **Obreztchikova M**, **Vargese A**, **Cabrera J**, **Peterson D**, **Hong Z**. Mechanisms of oxygen sensing: a key to therapy of pulmonary hypertension and patent ductus arteriosus. *Br J Clin Pharmacol* 155: 300–307, 2008.

252. **Weir EK**, **López-Barneo J**, **Buckler KJ**, **Archer SL**. Acute oxygen-sensing mechanisms. *N Engl J Med* 353: 2042–2055, 2005.

253. **West J**. Invited review: Pulmonary capillary stress failure. *J Appl Physiol* 89: 2483–2489, 2000.

254. **West JB**, **Schoene RB**, **Milledge JS**. *High Altitude Medicine and Physiology, 4th Edition*. Hodder Arnold, 2007.

255. **West JB**, **Wagner PD**. Predicted gas exchange on the summit of Mt. Everest. *Respir Physiol* 42: 1–16, 1980.

256. **West JB**. Ventilation-perfusion inequality and overall gas exchange in computer models of the lung. *Respir Physiol* 7: 88–110, 1969.

257. **West JB**. Man at extreme altitude. *J Appl Physiol* 52: 1393–1399, 1982.

258. **West JB**. Ibn al-Nafis, the pulmonary circulation, and the Islamic Golden Age. *J Appl Physiol* 105: 1877–1880, 2008.

259. **West JB**. The physiological legacy of the Fenn, Rahn, and Otis school. *AJP: Lung Cellular and Molecular Physiology* 303: L845–L851, 2012.

260. **Whipp BJ**, **Wasserman K**. Alveolar-arterial gas tension differences during graded exercise. *J Appl Physiol* 27: 361–365, 1969.

261. **Whyte MK**, **Peters AM**, **Hughes JM**, **Henderson BL**, **Bellingan GJ**, **Jackson JE**, **Chilvers ER**. Quantification of right to left shunt at rest and during exercise in patients with pulmonary arteriovenous malformations. *Thorax* 47: 790–796, 1992.

262. **Wilkinson M**, **Fagan D**. Postmortem demonstration of intrapulmonary arteriovenous shunting. *Arch Dis Child* 65: 435–437, 1990.

263. **Williams MH**, **Zohman LR**, **Bertrand CA**. Effect of atropine on the pulmonary circulation during rest and exercise in patients with chronic airway obstruction. *Diseases of the Chest* 37: 597–601, 1960.

264. **Windecker S**, **Wahl A**, **Chatterjee T**, **Garachemani A**, **Eberli F**, **Seiler C**, **Meier B**. Percutaneous closure of patent foramen ovale in patients with paradoxical embolism: long-term risk of recurrent thromboembolic events. *Circulation* 101: 893, 2000.

265. **Wood SC**. Effect of O_2 affinity on arterial PO_2 in animals with central vascular shunts. *J Appl Physiol* 53: 1360–1364, 1982.

266. **Woods TD**, **Harmann L**, **Purath T**, **Ramamurthy S**, **Subramanian S**, **Jackson S**, **Tarima S**. Small-and moderate-size right-to-left shunts identified by saline contrast echocardiography are normal and unrelated to migraine headache. *Chest* 138: 264, 2010.

267. **Woods TD**, **Patel A**. A critical review of patent foramen ovale detection using saline contrast echocardiography: when bubbles lie. *J Am Soc Echocardiogr* 19: 215–222, 2006.

268. **Yamazaki F**. Hyperoxia attenuates endothelial-mediated vasodilation in the human skin. *The Journal of Physiological Sciences* 57: 81–84, 2007.

269. **Yang WJ**, **Echigo R**, **Wotton DR**, **Hwang JB**. Experimental studies of the dissolution of gas bubbles in whole blood and plasma. I. Stationary bubbles. *J Biomech* 4: 275–281, 1971.

270. **Yang WJ**, **Echigo R**, **Wotton DR**, **Hwang JB**. Experimental studies of the dissolution of gas bubbles in whole blood and plasma. II. Moving bubbles or liquids. *J Biomech* 4: 283–288, 1971.

271. **Yang WJ**, **Echigo R**, **Wotton DR**, **Ou JW**, **Hwang JB**. Mass transfer from gas bubbles to impinging flow of biological fluids with chemical reaction. *Biophys J* 12: 1391–1404, 1972.

272. **Yang WJ**, **Liang CY**. Dynamics of dissolution of gas bubbles or pockets in tissues. *J Biomech* 5: 321–332, 1972.

273. **Yang WJ**. Dynamics of gas bubbles in whole blood and plasma. *J Biomech* 4: 119–125, 1971.

274. **Yeh MP**, **Gardner RM**, **Adams TD**, **Yanowitz FG**. Computerized determination of pneumotachometer characteristics using a calibrated syringe. *J Appl Physiol* 53: 280–285, 1982.

275. **Yock PG**, **Popp RL**. Noninvasive estimation of right ventricular systolic pressure by Doppler ultrasound in patients with tricuspid regurgitation. *Circulation* 70: 657–662, 1984.